

A Comprehensive Evaluation of a new Direct
Amplification System (PowerPlex[®] 18D)
in Forensic DNA Profiling

by

Casie Parish-Fisher

A thesis submitted in partial fulfilment for the requirements for the degree of
Doctor of Philosophy at the University of Central Lancashire

March 2016

STUDENT DECLARATION FORM

*I declare that while registered as a candidate for the research degree, I have not been a registered candidate or enrolled student for another award of the University or other academic or professional institution

*I declare that no material contained in the thesis has been used in any other submission for an academic award and is solely my own work

Signature of Candidate Casie Parish-Fisher

Type of Award **Doctor of Philosophy**

School **Forensic and Applied Sciences**

ABSTRACT

Short tandem repeat typing is the primary method of DNA identification used in the field of forensic science. Over the past several years the need to improve on this method has moved to the forefront of research. Due to the increasing number of criminal cases and the substantial backlogs most laboratories are facing, it is vital to evaluate methods which can produce quality DNA profiles in a fast and reliable manner. Direct amplification, also referred to as direct PCR, is one alternative method that has been proposed to address this issue. Direct amplification allows for the generating of DNA profiles without using the DNA isolation process. While direct PCR would reduce processing time and resources, it is unknown if this technique would be able to generate a robust full or partial profile from samples which could be collected from scenes of crime. Often crime scene personnel must use visualization techniques, either in powder or chemical form, in order to see and collect biological evidence for submission to a crime laboratory.

In order to evaluate if direct PCR is a feasible solution a comparative study between a direct PCR kit and standard DNA profiling practices was undertaken using mock crime scene type samples. Samples of this nature include surfaces which have been exposed to fingerprint powders and whole blood which has been chemically enhanced for visualization. PowerPlex[®] 18D, a direct amplification system, and PowerPlex[®] 16HS, an extraction-based method, were used to produce the profiles. An assessment of the kits aimed to critically evaluate and compare how the direct amplification kit performs on samples which have been exposed to powder and chemical processing for visual enhancement. This will be done by reviewing two types of samples; epithelial cells which have been exposed the fingerprint powders (black, magnetic and white) and whole blood which has been exposed to chemicals (luecocrystal violet, amido black and ninhydrin).

Samples subjected to direct amplification using PowerPlex[®] 18D generated DNA profiles with greater peak heights when compared to the extraction-based method. The peak balances for heterozygous loci were also higher and more full profiles were generated with direct amplification than with the extraction method. The amount of DNA retrieved from each substrate also varied even though the same amounts of starting material were deposited, proving that the type of substrate can affect the retrieval of DNA.

Epithelial cell samples were most successful when processed with white powder. Magnetic powder samples also yielded a positive result when using direct amplification which was not expected as in previous data magnetic powder samples have not been successful. Whole blood samples which were processed with amido black produced profiles with lower overall peak heights when compared to the two other chemical processes. This could be attributed to the rinse step which is required when working with amido black. Ninhydrin was the most successful of the chemicals in generating full, good quality profiles.

TABLE OF CONTENTS

Title	Page No.
Chapter 1: Introduction	1
1.1 Deoxyribonucleic Acid (DNA)	1
1.2 Diversity within the Human Genome	3
1.3 DNA Isolation	9
1.4 Amplification	10
1.4.1 Amplification Process	12
1.4.2 Direct Amplification	14
1.4.3 Components of a Direct Amplification	15
1.5 STR Analysis	16
1.5.1 Current Technologies used for STR-based DNA Profiling	16
1.5.2 Development of Electropherograms by Capillary Electrophoresis	19
1.6 Forensic Type Samples	21
1.6.1 Factors Affecting the Development of a DNA Profile	21
1.6.2 Contact Surfaces	22
1.6.3 Biological Samples	22
1.6.3.1 Skin Epithelial Cells	23
1.6.3.1.1 Fingerprint Enhancement Techniques	24
1.6.3.1.2 Powder Processing	24
1.6.3.2 Blood	27
1.6.3.2.1 Chemical Enhancement	27
1.6.3.2.1.1 Amino-reactive Dyes	30
1.6.3.2.1.2 Protein Dyes	30
1.6.3.2.1.3 Haem-reactive Dyes	31

Title	Page No.
1.7 The Project	32
1.7.1 Working Hypothesis	32
1.7.2 Project Aims	32
Chapter 2: Materials and Methods	34
2.1 Quality Management	34
2.2 Enhancement Products	34
2.2.1 Latent Fingerprint Powders	34
2.2.2 Chemical Enhancement Techniques	35
2.3 Substrates for Forensic Samples	35
2.4 Collection and preparation of samples	35
2.4.1 Collection of Buccal Samples	35
2.4.2 Population Selection	36
2.4.3 Collection of Buccal cells from Saliva for Powder Study	36
2.4.3.1 Epithelial Cell Dilutions (Limit of Detection)	37
2.4.3.2 Preparation of Epithelial Cells Recovered from Substrates	37
2.4.4 Collection of Blood Samples for Simulated Forensic Samples	38
2.4.4.1 Blood Dilutions (Limit of Detection)	38
2.4.4.2 Preparation of Human Blood Samples on Substrates	38
2.5 Profiling of Human DNA	39
2.5.1 Extraction of human DNA	39
2.5.1.1 DNA extraction of Omni Swabs	39
2.5.1.2 DNA extraction from Cotton Swabs	40
2.5.1.3 DNA extraction of Blood Samples	40
2.5.2 Pre-treatment of Direct Amplification Samples	41
2.5.3 Quantification of DNA using NanoDrop 2000	41

Title	Page No.
2.5.4 Haematocrit Counts	41
2.5.4.1 Staining of Epithelial Cells	42
2.5.5 Controls	42
2.5.6 Amplification of Promega® PowerPlex® 16HS and PowerPlex® 18D	43
2.5.6.1 Amplification with Promega® PowerPlex® 16HS	43
2.5.6.1.1 Amplification at full volume reactions (25µl)	43
2.5.6.1.2 Amplification at reduced reaction volume (12.5µl)	43
2.5.6.2 Amplification with Promega® PowerPlex® 18D	44
2.5.6.2.1 Amplification at full volume reactions (25µl)	44
2.5.6.2.2 Amplification at reduced reaction volume (12.5µl)	44
2.5.7 Fragment analysis by capillary electrophoresis	45
2.5.7.1 Preparation of samples for CE	45
2.5.7.2 Sample analysis using the Genetic Analyser	45
2.5.7.3 Analysis of DNA profiles	46
2.6 Results of Analysis	47
2.7 Statistical Analysis	48
Chapter 3: Sensitivity Study –Reduced Volume and Dilution Determination-	49
3.1 Overview	49
3.2 Experimental Design	50
3.2.1 Evaluation of Full (25 µl) and Half (12.5 µl) Reactions using Decreasing Amounts of DNA Template	50
3.2.2 Sensitivity of Epithelial Cell Samples	51
3.2.3 Sensitivity of Blood Samples	53

Title	Page No.
3.3 Results	54
3.3.1 Results of Reduced Volume on PCR Products	54
3.3.2 Results of Epithelial Based Samples	64
3.3.3 Results for Whole Blood Samples	69
3.3.4 Controls	74
3.4 Discussion	74
3.4.1 Reduced Volume Reactions (12.5µl)	74
3.4.2 Epithelial Cell Samples	75
3.4.3 Whole Blood Samples	76
Chapter 4: Concordance Study	78
4.1 Overview	78
4.2 Experimental Design	80
4.3 Results and Discussion	80
4.3.1 Evaluation of Concordance	80
4.3.2 Peak Height Assessment	80
4.3.3 Variant Alleles	83
4.3.4 CSF1PO	84
4.3.5 Allele Frequencies	85
4.4 Discussion	85
4.4.1 CSF1PO	86

Title	Page No.
Chapter 5: Evaluations of Epithelial Cell Samples Processed with Powder	87
5.1 Overview	87
5.2 Experiential Design	89
5.3 Results	89
5.3.1 Assessment of Profile Quality	91
5.3.2 Comparison of Individual Factors	99
5.3.1.1 Evaluation of CSF1PO	107
5.4 Discussion	107
Chapter 6: Preliminary Evaluation of Blood Enhancement Samples	110
6.1 Overview	110
6.2 Experimental Design	112
6.3 Results and Discussion	113
6.3.1 Luecocrystal Violet (LCV)	113
6.3.1.1 Heterozygous Peak Height Balance	127
6.3.1.1.1 Evaluation of CSF1PO	128
6.3.1.2 Stutter and other Artefacts	139
6.3.2 Amido Black	139
6.3.2.1 Heterozygous Peak Height Balance	150
6.3.2.1.1 Evaluation of CSF1PO	151
6.3.2.2 Stutter and other Artefacts	161
6.3.3 Ninhydrin	162
6.3.3.1 Heterozygous Peak Height Balance	167
6.3.3.1.1 Evaluation of CSF1PO	177

Title	Page No.
6.3.3.2 Stutter and other Artefacts	177
6.3.4 Collective Evaluation of All Chemicals	177
6.3.4.1 Chemicals	177
6.3.4.2 Dilutions	178
6.3.4.3 Substrates	179
6.3.4.4 Human Identification Kits	180
6.4 Discussion	181
6.4.1 Substrates	182
6.4.2 Chemicals	183
Chapter 7: General Discussion	185
7.1 Overview of the Study and Main Outcomes	185
7.2 Application of Direct Amplification for Forensic Casework	188
7.3 Crime Scene Personnel	189
7.4 Future Work	189
7.5 Conclusion	191
References	190

Title	Page No.
Appendices	221
Appendix 1: Material and Equipment Used	222
Appendix 2: Reagent Preparation	225
Appendix 3: DNA Raw Data	226
Appendix 4: Human DNA profiles	227
Appendix 5: Partial Profile Generated using Promega® PowerPlex® 16HS	229
Appendix 6: Consent Forms	231
Appendix 7: NanoDop® Results of Extracted Samples for the Concordance Study	236
Appendix 8: Summary of Loci in PowerPlex® 16HS and PowerPlex® 18D	243
Appendix 9: Allele Frequency and Comparison Charts	244

FIGURES AND TABLES

Chapter 1:

- Figure 1.1: Diagram of a DNA molecule (Ingram, 2007).
- Figure 1.2: A DNA sample taken from a crime scene is compared with DNA samples from three different suspects utilizing VNTRs to create the bands on the gel. If a suspects DNA profile matches the crime scene sample, then the evidence recovered from the crime scene came from that suspect. Conversely, if the DNA profiles do not match, then the evidence cannot have come from the suspect. Suspect 2 and the crime scene sample match (outlined in yellow); therefore, the sample from the crime scene is positively identified as coming from Suspect 2 (Leja, 2010).
- Figure 1.3: Figure 1.3: Examples of a short tandem repeat sequence using the CSF1PO [AGAT repeat sequence]. A.) Homozygous example with 9 repeating units and B.) Heterozygous example with 9 and 6 repeating units. C.) Electropherogram output which would be representative of the samples generated from A and B.
- Figure 1.4: Microsatellite sequence variation results from the gain and loss of single repeat units or a single nucleotide. This occurs when there is a brief dissociation of the replicating DNA strands followed by misaligned re-association (Ellegren, 2004).
- Figure 1.5: A single nucleotide polymorphism is a change in the genetic code of an individual where a single nucleotide (1) is replaced by another nucleotide (2) in the DNA sequence (Kucukkal et al., 2014).
- Table 1.1: Components of PCR reaction mix (Butler, 2005).
- Figure 1.6: Schematic of the DNA amplification process. 1.) The double-stranded DNA molecule is separated into two

single strands using heat. 2.) The temperature is then lowered to allow the oligonucleotide primers (shown in blue) to anneal to the target areas on the single-stranded DNA. 3.) The temperature is increased in order for DNA polymerase to produce a complete copy of the target DNA region (Reece et al., 2010).

Table 1.2: A summary of loci which are available in different commercially available kits. The colour represents the dye attached to their respective primer.

Figure 1.7: Configuration of the (A) Promega PowerPlex[®]16HS and (B) PowerPlex[®]18D kits demonstrating the fluorescent dye colour labels and relative PCR product size ranges for each of the loci present. (Source: Promega Corporation)

Figure 1.8: Allelic ladder which represents alleles in PowerPlex[®]18D. The same alleles are present in PowerPlex[®]16HS with the exception of D21338 and D19S433 which are not present in this kit. Green bars contain the loci names. The red triangles along the baseline represent the size range where alleles for a specific locus are called and the boxes below the baseline represent the allele call for that specific peak. The X-axis numerical values indicate the fragment size in base pair number.

Figure 1.9: Electropherogram demonstrating a DNA profile generated utilizing PowerPlex[®]18D. The profile displays positive control 2800M. The grey boxes label each of the loci present in the STR kit and the boxes under each of the peaks are the allele call(s) for that specific peak with the designated locus. The X-axis numerical values indicate the base pair number and the Y-axis the RFU (relative fluorescent unit) values (Source: Promega Corporation).

Table 1.3: Fingerprint powders used for enhancement of nonporous and semi-porous surfaces.

Table 1.4: Chemical enhancement methods used for visualization of blood.

Figure 1.10: The chemical structure of ninhydrin. (The structure was generated using eMolecules (Gubernator et al., 2015).

Figure 1.11: The chemical structure of amido black. (The structure was generated using eMolecules (Gubernator et al., 2015).

Figure 1.12: The chemical structure of leucocrystal violet. (The structure was generated using eMolecules (Gubernator et al., 2015).

Chapter 2:

Table 2.1: Chemical enhancement techniques and their corresponding substrates.

Table 2.2: Promega® PowerPlex® 16HS cycling conditions for a 32 cycle program

Table 2.3 Promega® PowerPlex® 18D cycling conditions for a 27 cycle program.

Table 2.4: Conditions for the electrophoresis run.

Table 2.5: Parameters for the analysis of PCR fragments when utilizing the ABI 3500 and GeneMapper *ID-X* software.

Table 2.6: Parameters for the analysis of PCR fragments when utilizing the ABI 3130 and GeneMapper *v3.2* software for analysis.

Chapter 3:

Table 3.1: Known genetic profile for 2800M.

Table 3.2: Known genetic profile for epithelial cell sample.

Table 3.3: Known genetic profile for whole blood sample.

Table 3.4 Results showing the minimum, maximum and average peak heights, the profile type, total PCR product and PCR concentration for the various dilutions of 2800M amplified using whole (25µl) and half (12.5µl) reactions with and PowerPlex® 16HS. The values are averages of three replicates.

Table 3.5: Results showing the minimum, maximum and average

peak heights, the profile type, total PCR product and PCR concentration for the various dilutions of 2800M amplified using whole (25µl) and half (12.5µl) reactions with and PowerPlex® 18D. The values are averages of three replicates.

Figure 3.1: Charts which depict heterozygous loci ratios at different concentrations when amplified at (Top) 25µl and (Bottom) 12.5µl with PowerPlex® 16HS. The red line indicates the 0.70 Hb threshold for the heterozygous peak balance. Samples displayed are based on three replicates.

Figure 3.2: Charts which depict heterozygous loci ratios at different concentrations when amplified at (Top) 25µl and (Bottom) 12.5µl with PowerPlex® 18D. The red line indicates the 0.70 Hb threshold for the heterozygous peak balance. Samples displayed are based on three replicates.

Figure 3.3: Graphs demonstrating the variation in the heterozygous peak balance ratio (Hb) for the amplification of the 25µl (green circles) and 12.5µl (blue diamonds) reactions for PowerPlex® 16HS for each individual loci. The red line indicates the 0.70 threshold for the heterozygous peak balance.

Figure 3.4: Graphs demonstrating the variation in the heterozygous peak balance ratio (Hb) for the amplification of the 25µl (green circles) and 12.5µl (blue diamonds) reactions for PowerPlex® 18D for each individual loci. The red line indicates the 0.70 threshold for the heterozygous peak balance.

Table 3.6: Results showing the minimum, maximum and average peak heights, the profile type, total PCR product and PCR concentration for the various dilutions of epithelial cells amplified at 12.5µl with PowerPlex® 16HS and PowerPlex® 18D. The values are averages of three replicates.

Figure 3.5: Heterozygous loci peak height ratios for epithelial cells at different dilutions when amplified at 12.5µl with (Top) PowerPlex® 16HS and (Bottom) PowerPlex® 18D. The red line indicates the 0.70 Hb threshold for the heterozygous peak balance. Samples displayed are based on three replicates.

Figure 3.6: Electropherograms displaying DNA profiles generated with epithelial cells at x2 dilution using (1) PowerPlex® 16HS (RFU 20,000) and (2) PowerPlex® 18D (RFU 5,000). The x-axis represents relative fluorescent units (RFU) and the y-axis fragment size in base pairs.

Figure 3.7: Electropherograms displaying DNA profiles generated with epithelial cells at x10 dilution using (1) PowerPlex® 16HS (RFU 9,500) and (2) PowerPlex® 18D (RFU 5,000). The x-axis represents relative fluorescent units (RFU) and the y-axis fragment size in base pairs.

Table 3.7: Results showing the minimum, maximum and average peak heights, the profile type, total PCR product and PCR concentration for the various dilutions of whole blood amplified at 12.5µl with PowerPlex® 16HS and PowerPlex® 18D. The values are averages of three replicates.

Figure 3.8: Heterozygous loci peak height ratios for whole blood samples at different dilutions when amplified at 12.5µl with (Top) PowerPlex® 16HS and (Bottom) PowerPlex® 18D. The red line indicates the 0.70 Hb threshold for the heterozygous peak balance. Samples displayed are based on three replicates.

Figure 3.9: Electropherograms displaying full profiles generated with whole blood cells at a x2 dilution using (1) PowerPlex® 16HS (RFU 20,000) and PowerPlex® 18D (RFU 10,000). The x-axis represents relative fluorescent units (RFU) and the y-axis fragment size in base pairs.

Figure 3.10: Electropherograms displaying full profiles generated with whole blood cells at a x10 dilution using (1) PowerPlex® 16HS (RFU 20,000) and PowerPlex® 18D (RFU 2,500). The x-axis represents relative fluorescent units (RFU) and the y-axis fragment size in base pairs.

Chapter 4:

Table 4.1: Loci within Promega® PowerPlex® 16HS and Promega® PowerPlex® 18D kits, their chromosome location, repeat category and motif, and primer sequences.

Figure 4.1: Bar graph representation of the average peak heights (in RFU) by locus for 150 profiles generated using the standard extraction method and profiled using PowerPlex® 16HS. Error bars represent the standard deviation.

Figure 4.2: Bar graph representation of the average peak heights (in RFU) by locus for 150 profiles generated using the standard extraction method and profiled using PowerPlex® 18D. Error bars represent the standard deviation.

Figure 4.3: Bar graph representation of the average heterozygous peak height balance ratio by locus for 50 profiles generated for the *Mexican* population using both PowerPlex® 16HS and PowerPlex® 18D. The red line indicates the 0.70 Hb threshold for the heterozygous peak balances. Error bars represent the standard deviation.

Figure 4.4: Bar graph representation of the average heterozygous peak height balance ratio by locus for 50 profiles generated for the *Caucasian* population using both PowerPlex® 16HS and PowerPlex® 18D. The red line indicates the 0.70 Hb threshold for the heterozygous peak balances. Error bars represent the standard deviation.

Figure 4.5: Bar graph representation of the average heterozygous peak height balance ratio by locus for 50 profiles generated for the *African American* population using both PowerPlex® 16HS and PowerPlex® 18D. The red line indicates the

0.70 Hb threshold for the heterozygous peak balances. Error bars represent the standard deviation.

Table 4.2: Microvariant (MV) and off ladder (OL) alleles produced in both PowerPlex[®] 16HS and PowerPlex[®] 18D kits.

Table 4.3: CSF1PO peak balance ratios for profiles containing allele 9 for PowerPlex[®] 16HS and PowerPlex[®] 18D.

Chapter 5:

Figure 5.1: (A) Example of a fibre-glass brush used for powder processing (Evident, 2015). (B) Example of a magnetic wand with a 'bulb' of powder at the end of the wand (Arrowhead Forensics, 2015). This 'bulb' acts as the brush when processing a surface.

Figure 5.2: Photographs of white and black laminate which exhibit developed epithelial deposits with standard black powder, magnetic flake and white powder (left to right, respectively) for samples A and B with a x2 dilution. Row 1 depicts sample A which was analysed with PowerPlex[®] 16HS. Row 2 depicts sample A which was analysed with PowerPlex[®] 18D. Row 3 depicts sample B which was analysed with PowerPlex[®] 16HS. Row 4 depicts sample B which was analysed with PowerPlex[®] 18D.

Figure 5.3: A diagrammatic representation of the quality of the profiles obtained from the PowerPlex[®] 16HS (left) and PowerPlex[®] 18D (right) kits. Different dilutions (x1, x2, x10) of the two DNA samples (A and B) were processed in triplicate using standard black powder and amplified with PowerPlex[®] 16HS and PowerPlex[®] 18D. Green squares indicate that the full correct alleles were observed for those loci. Yellow squares represent one allele drop out. Red squares represent loci where both expected alleles are missing.

Figure 5.4: A diagrammatic representation of the quality of the profiles obtained from the PowerPlex[®] 16HS (left) and PowerPlex[®] 18D (right) kits. Different dilutions (x1, x2, x10) of the two DNA samples (A and B) were processed in triplicate using magnetic flake powder and amplified with PowerPlex[®] 16HS and PowerPlex[®] 18D. Green squares indicate that the full correct alleles were observed for those loci. Yellow squares represent one allele drop out. Red squares represent loci where both expected alleles are missing.

Figure 5.5: A diagrammatic representation of the quality of the profiles obtained from the PowerPlex[®] 16HS (left) and PowerPlex[®] 18D (right) kits. Different dilutions (x1, x2, x10) of the two DNA samples (A and B) were processed in triplicate using white powder and amplified with PowerPlex[®] 16HS and PowerPlex[®] 18D. Green squares indicate that the full correct alleles were observed for those loci. Yellow squares represent one allele drop out. Red squares represent loci where both expected alleles are missing.

Table 5.1: Results for profiles generated with PowerPlex[®] 16HS showing the minimum, maximum and average peak heights, the profile type, total PCR product and PCR concentration for the various dilutions of samples A and B, amplified using half (12.5µl) reactions, and processed with the 3 powders (black, magnetic, and white). The values are averages of three replicates.

Table 5.2: Table 5.2: Results for profiles generated with PowerPlex[®] 18D showing the minimum, maximum and average peak heights, the profile type, total PCR product and PCR concentration for the various dilutions of samples A and B, amplified using half (12.5µl) reactions, and processed with the 3 powders (black, magnetic, and white). The

values are averages of three replicates.

Figure 5.6: (1) Electropherogram of sample B processed with black powder, x1 dilution and analysed with PowerPlex® 16HS on a scale of 560 RFU. (2) Electropherogram of sample B processed with black powder, x1 dilution and analysed with PowerPlex® 18D on a scale of 1050 RFU. The x-axis represents relative fluorescent units (RFU) and the y-axis fragment size in base pairs.

Figure 5.7: (1) Electropherogram of sample B processed with magnetic flake powder, x2 dilutions and analysed with PowerPlex® 16HS on a scale of 100 RFU. (2) Electropherogram of sample B processed with magnetic flake powder, x2 dilution and analysed with PowerPlex® 18D on a scale of 900 RFU. The x-axis represents relative fluorescent units (RFU) and the y-axis fragment size in base pairs.

Figure 5.8: Variation in the average total PCR product (RFU) between the powders and dilutions processed with PowerPlex® 16HS. Error bars represent the standard deviation. No samples with a x10 dilution produced a profile for any of the powders.

Figure 5.9: Variation in the average total PCR product (RFU) between the powders and dilutions processed with PowerPlex® 18D. Error bars represent the standard deviation.

Figure 5.10: Variation in the average total PCR product (RFU) between the dilutions and kits utilized to process the powder samples. Error bars represent the standard deviation.

Figure 5.11: Variation of the average total PCR product (RFU) between the powders and kits utilized to process the powder samples. Error bar represent the standard deviation.

Figure 5.12: Peak height ratios of the various heterozygous loci present in both samples A and B processed with *black powder* and

analysed with PowerPlex[®] 16HS. The red line indicates the 0.70 Hb threshold for the heterozygous peak balances. Blue diamond symbols represent x1 dilutions, green diamonds represent x2 dilutions, and orange diamonds represent x10 dilution samples.

Figure 5.13: Peak height ratios of the various heterozygous loci present in both samples A and B processed with *black powder* and analysed with PowerPlex[®] 18D. The red line indicates the 0.70 Hb threshold for the heterozygous peak balances. Blue diamond represent x1 dilutions, green diamonds represent x2 dilutions and the orange diamonds x10 dilution samples.

Figure 5.14: Peak height ratios of the various heterozygous loci present in both samples A and B processed with *magnetic flake* and analysed with PowerPlex[®] 16HS. The red line indicates the 0.70 Hb threshold for the heterozygous peak balances. Blue diamond symbols represent x1 dilutions, green diamonds represent x2 dilutions, and orange diamonds represent x10 dilution samples.

Figure 5.15: Peak height ratios of the various heterozygous loci present in both samples A and B processed with *magnetic flake* and analysed with PowerPlex[®] 18D. The red line indicates the 0.70 Hb threshold for the heterozygous peak balances. Blue diamond represent x1 dilutions, green diamonds represent x2 dilutions and the orange diamonds x10 dilution samples.

Figure 5.16: Peak height ratios of the various heterozygous loci present in both samples A and B processed with *white powder* and analysed with PowerPlex[®] 16HS. The red line indicates the 0.70 Hb threshold for the heterozygous peak balances. Blue diamond symbols represent x1 dilution, green diamonds represent x2 dilutions, and orange diamonds represent x10 dilution samples.

Figure 5.17: Peak height ratios of the various heterozygous loci present in both samples A and B processed with *white powder* and analysed with PowerPlex[®] 18D. The red line indicates the 0.70 Hb threshold for the heterozygous peak balances. Blue diamond represent x1 dilutions, green diamonds represent x2 dilutions and the orange diamonds x10 dilution samples.

Chapter 6:

Figure 6.1: Graph displaying the average PCR product concentration (RFU/ μ l) for each kit, PowerPlex[®] 16HS and PowerPlex[®] 18D, for all samples processed using LCV (purple bars) and for all samples processed with no chemical enhancement (grey bars). The error bars represent the standard deviations for each of the kits.

Figure 6.2: A diagrammatic representation of the quality of the profiles obtained from the PowerPlex[®] 16HS (left) and PowerPlex[®] 18D (right) kits. Different dilutions (x1, x2, and x10) of the two samples (A and B) were processed in triplicate using *LCV on Plastic* and amplified with PowerPlex[®] 16HS and PowerPlex[®] 18D. Green squares indicate that the full correct alleles were observed for that locus. Yellow squares represent one allele drop out. Red squares represent loci where both expected alleles are missing.

Figure 6.3: A diagrammatic representation of the quality of the profiles obtained from the PowerPlex[®] 16HS (left) and PowerPlex[®] 18D (right) kits. Different dilutions (x1, x2, and x10) of the two samples (A and B) were processed in triplicate using *LCV on Tile* and amplified with PowerPlex[®] 16HS and PowerPlex[®] 18D. Green squares indicate that the full correct alleles were observed for that locus. Yellow squares represent one allele drop out. Red

squares represent loci where both expected alleles are missing.

Figure 6.4: A diagrammatic representation of the quality of the profiles obtained from the PowerPlex[®] 16HS (left) and PowerPlex[®] 18D (right) kits. Different dilutions (x1, x2, and x10) of the two samples (A and B) were processed in triplicate using *LCV on Raw Wood* and amplified with PowerPlex[®] 16HS and PowerPlex[®] 18D. Green squares indicate that the full correct alleles were observed for that locus. Yellow squares represent one allele drop out. Red squares represent loci where both expected alleles are missing.

Figure 6.5: A diagrammatic representation of the quality of the profiles obtained from the PowerPlex[®] 16HS (left) and PowerPlex[®] 18D (right) kits. Different dilutions (x1, x2, and x10) of the two samples (A and B) were processed in triplicate using *LCV on Lead* and amplified with PowerPlex[®] 16HS and PowerPlex[®] 18D. Green squares indicate that the full correct alleles were observed for that locus. Yellow squares represent one allele drop out. Red squares represent loci where both expected alleles are missing.

Figure 6.6: A diagrammatic representation of the quality of the profiles obtained from the PowerPlex[®] 16HS (left) and PowerPlex[®] 18D (right) kits. Different dilutions (x1, x2, and x10) of the two samples (A and B) were processed in triplicate using *LCV on Laminate* and amplified with PowerPlex[®] 16HS and PowerPlex[®] 18D. Green squares indicate that the full correct alleles were observed for that locus. Yellow squares represent one allele drop out. Red squares represent loci where both expected alleles are missing.

Figure 6.7: A diagrammatic representation of the quality of the profiles obtained from the PowerPlex[®] 16HS (left) and PowerPlex[®] 18D (right) kits. Different dilutions (x1, x2, and x10) of the two samples (A and B) were processed in triplicate using *LCV on Gypsum* and amplified with PowerPlex[®] 16HS and PowerPlex[®] 18D. Green squares indicate that the full correct alleles were observed for that locus. Yellow squares represent one allele drop out. Red squares specify loci where both expected alleles are missing.

Figure 6.8: A diagrammatic representation of the quality of the profiles obtained from the PowerPlex[®] 16HS (left) and PowerPlex[®] 18D (right) kits. Different dilutions (x1, x2, and x10) of the two samples (A and B) were processed in triplicate using *LCV on Glass* and amplified with PowerPlex[®] 16HS and PowerPlex[®] 18D. Green squares indicate that the full correct alleles were observed for that locus. Yellow squares represent one allele drop out. Red squares represent loci where both expected alleles are missing.

Table 6.1: Results for LCV profiles using PowerPlex[®] 16HS showing the minimum, maximum and average peak heights, the profile type, total PCR product and PCR concentration for the various dilutions of samples A and B, amplified using half (12.5µl) reactions, and processed on various substrates. The values are averages of three replicates.

Table 6.2: Results for LCV profiles using PowerPlex[®] 18D showing the minimum, maximum and average peak heights, the profile type, total PCR product and PCR concentration for the various dilutions of samples A and B, amplified using half (12.5µl) reactions, and processed on various substrates. The values are averages of three replicates.

Figure 6.9: Average PCR product concentration (RFU/µl) for each kit,

PowerPlex[®] 16HS and PowerPlex[®] 18D, for all samples processed using LCV (purple bars) and for all samples processed with no chemical enhancement (grey bars). The error bars represent the standard deviations for each of the dilutions.

Figure 6.10 (A-G): The average PCR product concentration in (RFU/ μ l) by dilution for samples processed with no chemicals and samples processed with LCV on A) glass, B) gypsum, C) laminate, D) lead, E) plastic, F) raw wood, and G) tile. The error bars represent the standard deviations for each of the dilutions and processed/unprocessed sample averages.

Figure 6.11: (Top) Peak height ratios for *CSFIPO* produced for various substrates when analysed with PowerPlex[®] 16HS. (Bottom) Peak height ratios for *CSFIPO* produced for various substrates when analysed with PowerPlex[®] 18D. All three replicates of each sample (A and B) for each dilution are represented.

Figure 6.12: Figure 6.12: (Top) Peak height ratios for *D13S317* produced for various substrates when analysed with PowerPlex[®] 16HS. (Bottom) Peak height ratios for *D13S317* produced for various substrates when analysed with PowerPlex[®] 18D. All three replicates of each sample (A and B) for each dilution are represented.

Figure 6.13: Figure 6.13: (Top) Peak height ratios for *D18S51* produced for various substrates when analysed with PowerPlex[®] 16HS. (Bottom) Peak height ratios for *D18S51* produced for various substrates when analysed with PowerPlex[®] 18D. All three replicates of each sample (A and B) for each dilution are represented.

Figure 6.14: Figure 6.14: (Top) Peak height ratios for *D21S11* produced for various substrates when analysed with PowerPlex[®] 16HS. (Bottom) Peak height ratios for

D2IS11 produced for various substrates when analysed with PowerPlex® 18D. All three replicates of each sample (A and B) for each dilution are represented.

Figure 6.15: Figure 6.15: (Top) Peak height ratios for *D3S1358* produced for various substrates when analysed with PowerPlex® 16HS. (Bottom) Peak height ratios for *D3S1358* produced for various substrates when analysed with PowerPlex® 18D. All three replicates of each sample (A and B) for each dilution are represented.

Figure 6.16: Figure 6.16: (Top) Peak height ratios for *D7S820* produced for various substrates when analysed with PowerPlex® 16HS. (Bottom) Peak height ratios for *D7S820* produced for various substrates when analysed with PowerPlex® 18D. All three replicates of each sample (A and B) for each dilution are represented.

Figure 6.17: (Top) Peak height ratios for *FGA* produced for various substrates when analysed with PowerPlex® 16HS. (Bottom) Peak height ratios for *FGA* produced for various substrates when analysed with PowerPlex® 18D. All three replicates of each sample (A and B) for each dilution are represented.

Figure 6.18: Figure 6.18: (Top) Peak height ratios for Penta E produced for various substrates when analysed with PowerPlex® 16HS. (Bottom) Peak height ratios for Penta E produced for various substrates when analysed with PowerPlex® 18D. All three replicates of each sample (A and B) for each dilution are represented.

Figure 6.19: Combined dye electropherogram displaying (1) sample A (Glass, x1) processed with PowerPlex® 16HS displayed at 500 RFU. Combined dye electropherogram displaying (2) sample A (Glass, x1) processed with PowerPlex® 18D displayed at 15000 RFU.

Figure 6.20: Sample A, x1 dilution (left) and processed with

PowerPlex® 16HS. Sample A, x1 dilution (right) processed with PowerPlex® 18D.

Figure 6.21: Electropherograms demonstrating profiles produced with PowerPlex® 16HS and 18D. (1) Sample A, x1 dilution and processed with PowerPlex® 16HS on lead. (2) Sample A, x1 dilution and processed with PowerPlex® 18D on lead. The x-axis represents relative fluorescent units (RFU) and the y-axis fragment size in base pairs.

Figure 6.22: The average PCR product concentration (RFU/μl) for each kit, PowerPlex® 16HS and PowerPlex® 18D, for all samples processed using amido black and for all samples processed with no chemical enhancement. The error bars represent the standard deviations for each of the kits.

Figure 6.23: A diagrammatic representation of the quality of the profiles obtained from the PowerPlex® 16HS (left) and PowerPlex® 18D (right) kits. Different dilutions (x1, x2, and x10) of the two samples (A and B) were processed in triplicate using *Amido Black on Plastic* and amplified with PowerPlex® 16HS and PowerPlex® 18D. Green squares indicate that the full correct alleles were observed for that locus. Yellow squares represent one allele drop out. Red squares represent loci where both expected alleles are missing.

Figure 6.24: A diagrammatic representation of the quality of the profiles obtained from the PowerPlex® 16HS (left) and PowerPlex® 18D (right) kits. Different dilutions (x1, x2, and x10) of the two samples (A and B) were processed in triplicate using *Amido Black on Tile* and amplified with PowerPlex® 16HS and PowerPlex® 18D. Green squares indicate that the full correct alleles were observed for that locus. Yellow squares represent one allele drop out. Red squares represent loci where both expected alleles are missing.

Figure 6.25: A diagrammatic representation of the quality of the profiles obtained from the PowerPlex® 16HS (left) and PowerPlex® 18D (right) kits. Different dilutions (x1, x2, and x10) of the two samples (A and B) were processed in triplicate using *Amido Black on Lead* and amplified with PowerPlex® 16HS and PowerPlex® 18D. Green squares indicate that the full correct alleles were observed for that locus. Yellow squares represent one allele drop out. Red squares represent loci where both expected alleles are missing.

Figure 6.26: A diagrammatic representation of the quality of the profiles obtained from the PowerPlex® 16HS (left) and PowerPlex® 18D (right) kits. Different dilutions (x1, x2, and x10) of the two samples (A and B) were processed in triplicate using *Amido Black on Laminate* and amplified with PowerPlex® 16HS and PowerPlex® 18D. Green squares indicate that the full correct alleles were observed for that locus. Yellow squares represent one allele drop out. Red squares represent loci where both expected alleles are missing.

Figure 6.27: A diagrammatic representation of the quality of the profiles obtained from the PowerPlex® 16HS (left) and PowerPlex® 18D (right) kits. Different dilutions (x1, x2, and x10) of the two samples (A and B) were processed in triplicate using *Amido Black on Glass* and amplified with PowerPlex® 16HS and PowerPlex® 18D. Green squares indicate that the full correct alleles were observed for that locus. Yellow squares represent one allele drop out. Red squares represent loci where both expected alleles are missing.

Table 6.3: Results for Amido Black profiles using PowerPlex® 16HS showing the minimum, maximum and average peak heights, the profile type, total PCR product and PCR

concentration for the various dilutions of samples A and B, amplified using half (12.5 μ l) reactions, and processed on various substrates. The values are averages of three replicates.

Table 6.4: Results for Amido Black profiles using PowerPlex[®] 18D showing the minimum, maximum and average peak heights, the profile type, total PCR product and PCR concentration for the various dilutions of samples A and B, amplified using half (12.5 μ l) reactions, and processed on various substrates. The values are averages of three replicates.

Figure 6.28: The average PCR product concentration (RFU/ μ l) for each kit, PowerPlex[®] 16HS and PowerPlex[®] 18D, for all samples processed using amido black (green bars) and for all samples processed with no chemical enhancement (grey bars). The error bars represent the standard deviations for each of the dilutions.

Figure 6.29 (A-E): The average PCR product concentration in (RFU/ μ l) by dilution for samples processed with no chemicals and samples processed with amido black on A) Glass, B) Laminate, C) Lead, D) Plastic, and E) Tile. The error bars represent the standard deviations for each of the dilutions and processed/unprocessed sample averages.

Figure 6.30: (Top) Peak height ratios for *CSFIPO* produced for various substrates processed with amido black and analysed with PowerPlex[®] 16HS. (Bottom) Peak height ratios for *CSFIPO* produced for various substrates processed with amido black and analysed with PowerPlex[®] 18D. All three replicates of each sample (A and B) for each dilution are represented.

Figure 6.31: (Top) Peak height ratios for *D13S317* produced for various substrates processed with amido black and analysed with PowerPlex[®] 16HS. (Bottom) Peak height

ratios for *D13S317* produced for various substrates processed with amido black and analysed with PowerPlex® 18D. All three replicates of each sample (A and B) for each dilution are represented.

Figure 6.32: (Top) Peak height ratios for *D18S51* produced for various substrates processed with amido black and analysed with PowerPlex® 16HS. (Bottom) Peak height ratios for *D18S51* produced for various substrates processed with amido black and analysed with PowerPlex® 18D. All three replicates of each sample (A and B) for each dilution are represented.

Figure 6.33: (Top) Peak height ratios for *D21S11* produced for various substrates processed with amido black and analysed with PowerPlex® 16HS. (Bottom) Peak height ratios for *D21S11* produced for various substrates processed with amido black and analysed with PowerPlex® 18D. All three replicates of each sample (A and B) for each dilution are represented.

Figure 6.34: (Top) Peak height ratios for *D3S1358* produced for various substrates processed with amido black and analysed with PowerPlex® 16HS. (Bottom) Peak height ratios for *D3S1358* produced for various substrates processed with amido black and analysed with PowerPlex® 18D. All three replicates of each sample (A and B) for each dilution are represented.

Figure 6.35: (Top) Peak height ratios for *D7S820* produced for various substrates processed with amido black and analysed with PowerPlex® 16HS. (Bottom) Peak height ratios for *D7S820* produced for various substrates processed with amido black and analysed with PowerPlex® 18D. All three replicates of each sample (A and B) for each dilution are represented.

Figure 6.36: (Top) Peak height ratios for *FGA* produced for various

substrates processed with amido black and analysed with PowerPlex[®] 16HS. (Bottom) Peak height ratios for *FGA* produced for various substrates processed with amido black and analysed with PowerPlex[®] 18D. All three replicates of each sample (A and B) for each dilution are represented.

Figure 6.37: (Top) Peak height ratios for *Penta E* produced for various substrates processed with amido black and analysed with PowerPlex[®] 16HS. (Bottom) Peak height ratios for *Penta E* produced for various substrates processed with amido black and analysed with PowerPlex[®] 18D. All three replicates of each sample (A and B) for each dilution are represented.

Figure 6.38: Electropherograms of (1) Sample B (x1, Laminate) processed with PowerPlex[®] 16HS and displayed at 2000RFU. (2) Sample B (x1, Laminate) processed with PowerPlex[®] 18D and displayed at 20000RFU. The y-axis shows the relative fluorescent units (RFU) and x-axis numbers indicate the fragment size in base pairs.

Figure 6.39: (Left) Sample A prepared with x1 dilution on lead and processed with amido black. This sample was processed with PowerPlex[®] 16HS. (Right) Sample A prepared with x2 dilution on lead and processed with amido black. This sample was processed with PowerPlex[®] 18D.

Figure 6.40: Graph displaying the average PCR product concentration (RFU/ μ l) for each kit, PowerPlex[®] 16HS and PowerPlex[®] 18D, for all samples processed using ninhydrin and for all samples processed with no chemical enhancement. The error bars represent the standard deviations for each of the kits.

Figure 6.41: A diagrammatic representation of the quality of the profiles obtained from the PowerPlex[®] 16HS (left) and PowerPlex[®] 18D (right) kits. Different dilutions (x1, x2,

and x10) of the two samples (A and B) were processed in triplicate using Ninhydrin on Raw Wood and amplified with PowerPlex[®] 16HS and PowerPlex[®] 18D. Green squares indicate that the full correct alleles were observed for that locus. Yellow squares represent one allele drop out. Red squares represent loci where both expected alleles are missing.

Figure 6.42: A diagrammatic representation of the quality of the profiles obtained from the PowerPlex[®] 16HS (left) and PowerPlex[®] 18D (right) kits. Different dilutions (x1, x2, and x10) of the two samples (A and B) were processed in triplicate using Ninhydrin on Gypsum and amplified with PowerPlex[®] 16HS and PowerPlex[®] 18D. Green squares indicate that the full correct alleles were observed for that locus. Yellow squares represent one allele drop out. Red squares represent loci where both expected alleles are missing.

Table 6.5: Results for Ninhydrin profiles using PowerPlex[®] 16HS showing the minimum, maximum and average peak heights, the profile type, total PCR product and PCR concentration for the various dilutions of samples A and B, amplified using half (12.5µl) reactions, and processed on various substrates. The values are averages of three replicates.

Table 6.6: Results for Ninhydrin profiles using PowerPlex[®] 18D showing the minimum, maximum and average peak heights, the profile type, total PCR product and PCR concentration for the various dilutions of samples A and B, amplified using half (12.5µl) reactions, and processed on various substrates. The values are averages of three replicates.

Figure 6.43: The average PCR product concentration (RFU/µl) for each kit, PowerPlex[®] 16HS and PowerPlex[®] 18D, for all

samples processed using ninhydrin and for all samples processed with no chemical enhancement. The error bars represent the standard deviations for each of the dilutions.

Figure 6.44: (Top) Peak height ratios for *CSFIPO* produced for various substrates processed with ninhydrin and analysed with PowerPlex[®] 16HS. (Bottom) Peak height ratios for *CSFIPO* produced for various substrates processed with ninhydrin and analysed with PowerPlex[®] 18D. All three replicates of each sample (A and B) for each dilution are represented.

Figure 6.45: (Top) Peak height ratios for *D13S317* produced for various substrates processed with ninhydrin and analysed with PowerPlex[®] 16HS. (Bottom) Peak height ratios for *D13S317* produced for various substrates processed with ninhydrin and analysed with PowerPlex[®] 18D. All three replicates of each sample (A and B) for each dilution are represented.

Figure 6.46: (Top) Peak height ratios for *D18S51* produced for various substrates processed with Ninhydrin and analysed with PowerPlex[®] 16HS. (Bottom) Peak height ratios for *D18S51* produced for various substrates processed with Ninhydrin and analysed with PowerPlex[®] 18D. All three replicates of each sample (A and B) for each dilution are represented.

Figure 6.47: (Top) Peak height ratios for *D21S11* produced for various substrates processed with Ninhydrin and analysed with PowerPlex[®] 16HS. (Bottom) Peak height ratios for *D21S11* produced for various substrates processed with Ninhydrin and analysed with PowerPlex[®] 18D. All three replicates of each sample (A and B) for each dilution are represented.

- Figure 6.48: (Top) Peak height ratios for *D3S1358* produced for various substrates processed with Ninhydrin and analysed with PowerPlex[®] 16HS. (Bottom) Peak height ratios for *D3S1358* produced for various substrates processed with Ninhydrin and analysed with PowerPlex[®] 18D. All three replicates of each sample (A and B) for each dilution are represented.
- Figure 6.49: (Top) Peak height ratios for *FGA* produced for various substrates processed with Ninhydrin and analysed with PowerPlex[®] 16HS. (Bottom) Peak height ratios for *FGA* produced for various substrates processed with Ninhydrin and analysed with PowerPlex[®] 18D. All three replicates of each sample (A and B) for each dilution are represented.
- Figure 6.50: Figure 6.50: (Top) Peak height ratios for *D7S820* produced for various substrates processed with Ninhydrin and analysed with PowerPlex[®] 16HS. (Bottom) Peak height ratios for *D7S820* produced for various substrates processed with Ninhydrin and analysed with PowerPlex[®] 18D. All three replicates of each sample (A and B) for each dilution are represented.
- Figure 6.51: Figure 6.51: (Top) Peak height ratios for *Penta E* produced for various substrates processed with Ninhydrin and analysed with PowerPlex[®] 16HS. (Bottom) Peak height ratios for *Penta E* produced for various substrates processed with Ninhydrin and analysed with PowerPlex[®] 18D. All three replicates of each sample (A and B) for each dilution are represented.
- Figure 6.52: Electropherograms demonstrating the two profiles generated from sample A (x1, Gypsum). (Top) The profile generated with PowerPlex[®] 16HS. (Bottom) The profile generated with PowerPlex[®] 18D.

- Figure 6.53: Average of the total PCR products for each of the chemicals used as enhancements for the substrates in this project. Error bars represent the standard deviations for each of the chemicals.
- Figure 6.54: Average of the total PCR products for all of the chemicals used as enhancements for the substrates without regard to kit or specific chemical. Error bars represent the standard deviations for each of the dilutions.
- Figure 6.55: The total PCR concentrations for all substrates: glass, gypsum, laminate, lead, plastic, raw wood, and tile without regard to kit or chemical. Error bars represent the standard deviation.
- Figure 6.56 Total PCR concentrations for both kits, PowerPlex[®] 16HS and PowerPlex[®] 18D. Error bars represent the standard deviations for the total PCR concentration.

Appendix:

- A1.1 Materials and Equipment
- A4.1 Known genetic profiles used throughout the project.
- A5.1 PowerPlex[®] 16HS partial profiles from concordance study.
- A7.1 Quantitation using NanoDrop 2000 for extracted samples from concordance study.
- A8.1 A short summary of all the loci used in both kits for the course of this project.
- A9.1 Allele frequency charts for African American, Caucasian and Mexican populations.
- A9.2 Allele frequency comparison charts for data generated in A9.1

ACKNOWLEDGMENTS

When I began this project almost six years ago I never realized what a passion and sense of commitment a project of this nature could have on a person. I also didn't realize the amount of people who would touch my life and become a part of me just as this work has.

First, I would like to express my gratitude to my supervisor Dr. Sibte Hadi who gave me the opportunity to do a PhD in forensic genetics and to work on an interesting and challenging project. His supervision allowed me to be pushed farther than I ever dreamed I could go. Although we did not always see eye-to-eye I feel his passion for teaching and drive to push his students to do their best is unparalleled. I will forever be thankful to you for helping me become the person I am today.

I am also thankful to the other supervisors on my committee: Dr. William Goodwin for giving your kind words and sound advice and Dr. Sulatha Dwaraka for your leadership and the opportunity to work in your laboratory. Dr. Lisa Goering, I definitely would not have made it without you. Thank you for being my daily support system in the states, for keeping me going all these years and seeing me through until the very, very end. And finally to Dr. David Horton without your mentorship and constant example of academic excellence I would have never started the journey to complete my PhD. You will all always hold a special place in my heart for pushing me to accomplish this goal and walking through the entire journey with me.

I would like to acknowledge Dr. James Derr and Dr. Xiaomin Cai and all the people at the Department of Veterinary Pathobiology, College of Veterinary Medicine and Biomedical Sciences at Texas A&M University. Without opening your doors and allowing me to work your laboratory my project could not have been completed. Also, to Dr. Ashley Hall from the University of Nebraska, thank you for your assistance and willingness to help with the project.

I would also like to acknowledge Brady Mills, Karl Morton, and Gary Molina from the Texas Department of Public Safety. This project was born out of my work in the CODIS laboratory at the department. Your support for the project over the past few years has been unwavering and I am grateful to you all.

A special acknowledgement to St. Edward's University and, specifically, to Sister Donna Jurick; Dean of Behavioural and Social Sciences- Dr. Brenda Valance; former Dean of Natural Sciences- Dr. Thomas Mitzel; Vice President of Academic Affairs Dr. Mary Boyd and current Chair of the Department of Criminal Justice and Forensic Science, Tina Miranda, JD. It was a difficult task to complete this work and maintain the program of Forensic Science, however, with your financial support and encouraging words this project was able to be completed.

I would have not progressed through the years if it was not for Prof. Jai Singh, our Director of Study, who constantly monitored the development of the project and made sure things were progressing in a timely manner.

Throughout this project I have had to opportunity to see true friendship in action. Emily, I will be forever grateful for your friendship and helping me get to the finish line with this work. Nathalie, thank you for your constant support and encouragement in completing my project, I appreciate you more than you will ever know. Claire and Cat, I would have not made it through the final summer without your help and support. Lauren, I would not have been able to complete all my work without your help. To Christine and Cele, for always being there regardless of the time of day or night when things weren't going well, you girls always had my back and were there to support me. Sarah, I really appreciated your help and patience as I navigated through the digital challenges of this project. Without your help I am not sure it would be in one piece.

I owe a special thank you to the UCLAN Master's students in the summer of 2014. It was a pleasure getting to know you all and thank you for sharing your time and laughter as we finished up our projects. I also want to send a special thank you to my teaching assistances, Katie, Olivia, Austin and Jessica, for all your help during the semesters when I was traveling to the UK and writing. With your help I was able to make it through the semesters without any major tragedies.

I have heard that once in an ordinary life, love can give you a fairy tale. I am truly blessed to have found my husband Chris who is my fairy tale. Thank you for loving me unconditionally and supporting me through the ups and downs of this project. I could have never finished without you. I love you more than you will ever know.

I would like to thank my parents and my little brother, who without your love and financial support I would have never been able to complete this. Your words of encouragement and prayers have gotten me where I am today. I love you all very much.

Finally I would like to thank the people who are working scenes of crime and in laboratories to help further the field of forensic science. You are truly the unsung heroes and inspiration behind this project. Without your scientific voice, crimes may remain unsolved and many victims voices unheard. I only hope this work will aid you in your quest to seek the truth.

A mari usque ad mare...Many 'Thanks' to you all!

--Casie Parish-Fisher, MSc. (DNA Profiling)

CHAPTER 1.

INTRODUCTION

DNA profiling has attained an important position among the tools used for criminal and civil casework since the first 'DNA fingerprint' was generated using restriction fragment length polymorphisms (RFLPs) by Sir Alec Jeffreys in 1984 (Jeffreys et al., 1985a). In 1985, polymerase chain reaction (PCR) was introduced by Kary Mullis and the Cetus Corporation (Mullis et al., 1987). The development of PCR allowed for the enzymatic replication of a specific region of DNA using minute amounts of biological sample (Saiki et al., 1985; Mullis et al., 1987). By the early 1990s, short tandem repeats (STRs) became the standard genetic markers to generate DNA profiles (Lygo et al., 1994). STR technology is easy to implement, robust, works with trace amounts of DNA and can be utilized for different types of casework samples (Butler, 2005). The evolution of multiplex STR kits has been rapid and it continues to evolve and change as new methodologies and technologies are introduced. Recently direct PCR has been introduced to the field of forensic science (Wang et al., 2009; Yang et al., 2007a; Yang et al., 2007b). This means that DNA profiles can be generated directly from the different types of samples without the need of DNA extraction. One such kit is Powerplex[®] 18D, which has been developed by Promega[®] Technologies (Oostdik et al., 2013). As all new techniques need to be rigorously tested in the forensic sector, this comparative study aims to develop DNA profiles from surfaces which have been processed with field techniques employing treatments such as fingerprint powders and blood enhancement chemicals using a commonly used kit (PowerPlex[®] 16HS) and a direct amplification kit (Powerplex[®] 18D).

1.1 Deoxyribonucleic Acid (DNA)

Deoxyribonucleic acid (DNA) is found in nucleated cells in the human body. The DNA molecule contains genetic information which is the information needed for the development and function of an organism (Butler, 2005; Klug and Cummings, 2003). DNA is a polynucleotide meaning it is a nucleic acid built by linking mononucleotides (Klug and Cummings, 2003). A single nucleotide is composed of a phosphate group,

nitrogenous base and a ribose pentose sugar (Klug and Cummings, 2003; Watson and Crick, 1935). For the DNA molecules, the C-2' position of the sugar is occupied by a hydrogen atom, hence making up the deoxynucleotide. The phosphate group of one nucleotide is found on the C-5' of the 2'-deoxyribose sugar molecule and this reacts to the –OH group on the C-3' of the neighbouring nucleotide to form a phosphodiester bond (Mathews et al., 2000). The nucleotides are composed of four different nitrogenous bases. Purines, adenine (A) and guanine (G), are nine-member double-rings while pyrimidines, cytosine (C) and thymine (T), are six-member single-rings (Mathews et al., 2000; Watson and Crick, 1935). The nucleo-bases are bound to the structure at the C-1' position (Klug and Cummings, 2003). This formation differs from ribonucleic acid (RNA) which contains a hydroxyl group at the same C-2' position of the sugar in DNA and also replaces thymine (T) with uracil (U) in order to execute the blueprint laid out by the DNA molecule (Klug and Cummings, 2003).

The configuration of a DNA molecule is in the form of a double helix (Watson, 1935). It is formed when complementary, anti-parallel chains of nucleotides bond to one another and coil around a central axis forming a right-handed double helix (Klug and Cummings, 2003; Mathews et al., 2000). Complementary pairing of the nucleo-bases, (A) to (T) and (C) to (G) provides the hydrogen bonds necessary for the chemical stability of the structure (Klug and Cummings, 2003). Adenine (A) pairing with thymine (T) produces a double hydrogen bond while cytosine (C) pairing with guanine (G) produces a triple hydrogen bond. The sugar-phosphate “backbone” of the helix is hydrophilic allowing both parts to interact with water (Klug and Cummings, 2003). The phosphate group is negatively charged giving the overall DNA molecule a negative charge. The nitrogenous base pairs, which are hydrophobic, are layered horizontally within the structure and protected from contact with water (Klug and Cummings, 2003). (Figure 1.1)

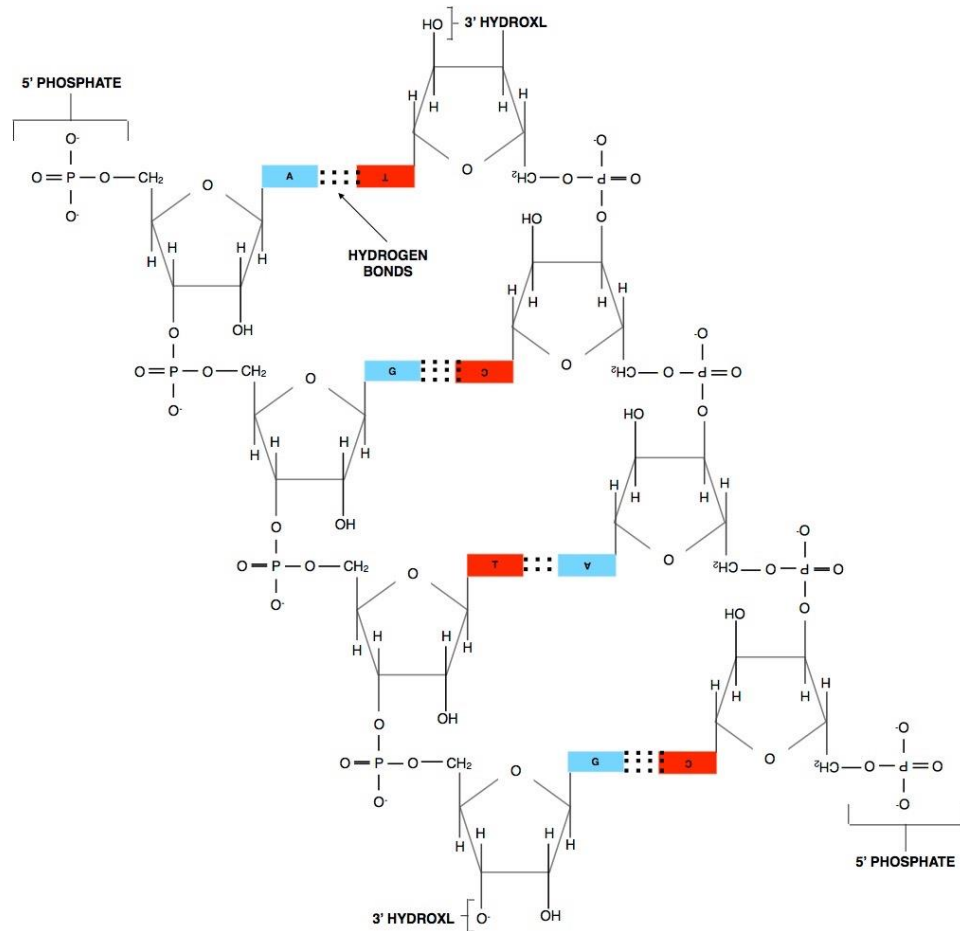


Figure 1.1: Diagram of a DNA molecule (Ingram, 2007).

1.2 Diversity within the Human Genome

Diversity within the human genome allows for various techniques to be used in forensic and paternity based cases by identifying individuals based on their genetic makeup. The whole human genome is represented by 22 pairs of chromosomes, two sex chromosomes and mitochondrial DNA. Sex is determined by the XY-sex determining system where XX is found in females and XY in males, the Y chromosome being dominantly male sex determining. The human gene usually analysed to determine sex of a sample in forensic based cases is the amelogenin locus. During PCR amplification using a single primer pair, fragments of different lengths are generated depending on whether the person is male or female. The sequence on the X chromosome is shorter by 6bp when compared to the Y chromosome allele; thus a female would produce a single peak on an electropherogram while a male would exhibit two peaks (Akane, 1998; Buel et al., 1995).

Located on each of the chromosomes are two distinct sequence classes, coding regions and non-coding regions. Coding regions are areas which are transcribed, called genes. Genes make up approximately 2% of the human genome. Genes can be classified as protein coding and non-protein coding. Protein coding genes are made up of exons and introns. Exons contain protein coding-regions of the gene and are retained in the final mature messenger RNA (mRNA). Introns are intervening sequences that are removed by RNA splicing. Non-coding regions have an important function as well including sequences important for the regulation of the transcription and translation of the protein-coding sequences. The regulatory function of a gene is influenced by multiple stretches of DNA located both in close proximity and far from the actual gene and translated region of mRNA. Just as protein-coding genes can contain genetic variation, non-coding regions can also show variability. They include differences in VNTRs, *variable number tandem repeats*; STRs, *short tandem repeats*; and SNPs, *single nucleotide polymorphisms*.

Tandem repeats occur in DNA sequences when two or more nucleotides are repeated directly next to each other for a number of times. Variable number tandem repeats (VNTRs), also referred to as minisatellites, can be seen as variable number sequences of tandem repeats within the human genome. VNTR individual repeat units range from 10-100bp long. In 1985, Alec Jeffreys developed the first DNA profile by understanding and utilizing the sequences and patterns of VNTRs that are specific to an individual's genomic profile (Jeffreys et al., 1985b; Jeffreys et al., 1985c). A match probability is determined by the rarity of the alleles presented in the profile. Each allelic marker within a specific locus has a frequency with which it occurs in the population and by evaluating the combined frequency a match probability can then be generated. The VNTR markers were found to be highly discriminating, giving a match probability lower than 3×10^{-11} (Jeffreys et al., 1985c). The visualization of these VNTRs required the use of restriction enzymes which cleaved the regions of DNA surrounding the VNTRs. This technique was termed restriction fragment length polymorphism (RFLP). Gel electrophoresis was used to separate the DNA fragments by molecular weight and the gel fragments were transferred to a nitrocellulose membrane using Southern blotting and identified via a radio-labelled DNA probe. Multi-locus DNA probes detect sets of 15-20 variable fragments per individual ranging from 3.5 to 20kb in size and single locus probe detects a single hypervariable locus using high stringency hybridization (Roewer, 2013). The

various sizes of bands located on the gel represent the varying fragment sizes obtained from one individual making them unique identifiers (Figure 1.2). While this methodology was promising, it required a large amount of DNA (>100ng), was labour intensive and required a large amount of time to conduct (Meyers 1995).

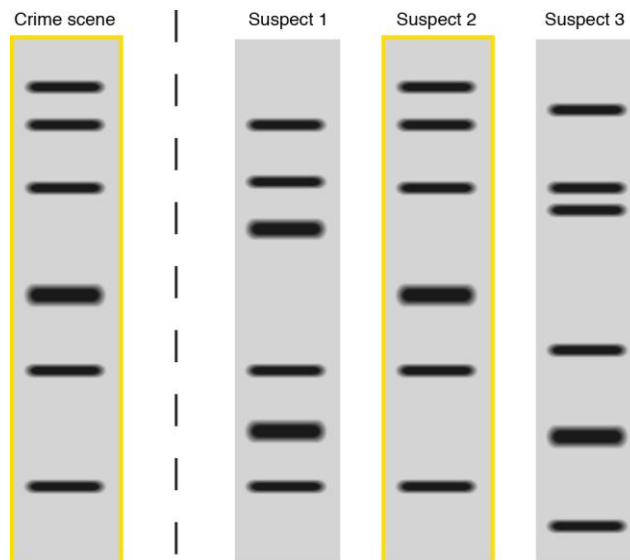


Figure 1.2: A DNA sample taken from a crime scene is compared with DNA samples from three different suspects utilizing VNTRs to create the bands on the gel. If a suspects DNA profile matches the crime scene sample, then the evidence recovered from the crime scene came from that suspect. Conversely, if the DNA profiles do not match, then the evidence cannot have come from the suspect. Suspect 2 and the crime scene sample match (outlined in yellow); therefore, the sample from the crime scene is positively identified as coming from Suspect 2 (Leja, 2010).

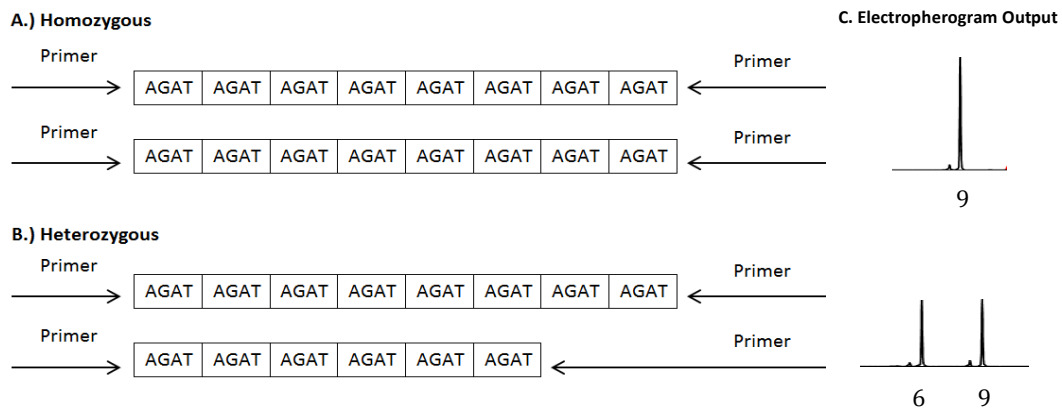


Figure 1.3: Examples of a short tandem repeat sequence using the CSF1PO [AGAT repeat sequence]. A.) Homozygous example with 9 repeating units and B.) Heterozygous example with 9 and 6 repeating units. C.) Electropherogram output which would be representative of the samples generated from A and B.

STRs, short tandem repeats, are microsatellites which usually contain 2 to 6bp repeat sequences (Figure 1.3) (Kotte-Marchant and Davis, 2012). Like VNTRs, they are highly discriminating and have a low mutation rate (10^{-3} per generation) (Brinkmann et al., 1998; Shriver et al., 1995; Weber and Wong, 1993; Butler, 2005). Mutations within STR loci occur slowly over time (rates are in the order of 1-5 mutations per 1,000 allele transfers) and are thought to occur because of replication slippage or defective DNA replication repair (Figure 1.4) (Nadir, 1996; Ellegren, 2004; Butler, 2005). STRs were targeted to build commercial DNA kits due to their ability to be multiplexed and their utility in amplifying small amounts of biological samples (Lander et al., 2001). Studies to use STRs as genetic markers began with the UK Forensic Science Service (FSS) in the early 1990s (Butler, 2005). The United States' Federal Bureau of Investigation, Royal Canadian Mounted Police, and other European laboratories also contributed to the early efforts to develop a multiplex kit for forensic purposes (Butler, 2005). During the efforts to develop kits for forensic use, a number of loci were identified. Initially kits could amplify three to four loci used with silver staining methods and, in a matter of a couple of years, expanded to over fifteen STRs which use multi-coloured fluorescent tags (Butler, 2005). Most of the loci used for forensic testing are tetranucleotide repeats, meaning they contain a four-base repeating sequence. Tetranucleotides are used more often as the four-base spread in the alleles makes closely spaced heterozygotes easier to resolve during capillary electrophoresis. Tetranucleotides are also more common than penta- and hexanucleotides in the human genome; however, these are still considered for possible implementation into commercial STR kits. Di- and trinucleotides are not used

as the stutter peak, a peak which appears one or more repeat unit less than the true allele due to strand slippage during PCR, may present exhibit itself with a peak height 30% or higher when compared to the true peak and would make it difficult to determine if it is in fact a true allele or stutter product. Displaying peaks of this nature would make it difficult to interpret sample mixtures. Characteristics of these loci include amplifiability using polymerase chain reaction (PCR); high heterozygosity; predictable length of alleles (Ruitberg et al., 2001); and the ability to multiplex the loci in one reaction. To date, there are more than 20,000 tetranucleotide STR loci which have been characterized in the human genome and there may be more than one million depending on the method used to count the loci (Collins et al., 2003).

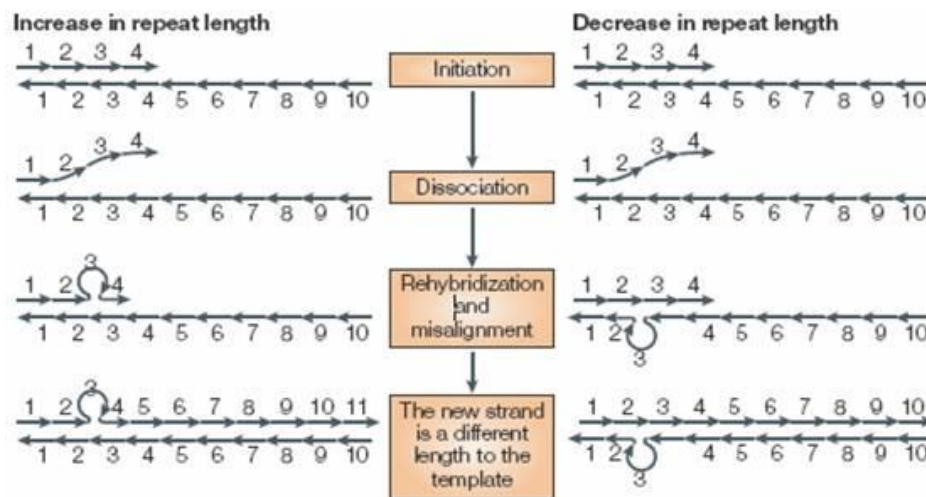


Figure 1.4: Microsatellite sequence variation results from the gain and loss of single repeat units or a single nucleotide. This occurs when there is a brief dissociation of the replicating DNA strands followed by misaligned re-association (Ellegren, 2004).

SNPs, single nucleotide polymorphisms, are single base variants between individuals at a specific point in the human genome (Figure 1.5) (Morin et al., 2004). Between any two individuals there are likely to be millions of SNPs which become yet another tool one could use to differentiate between individuals (Divne et al., 2005). Because SNPs are single nucleotides they have been targeted in the use of highly degraded samples where long flanking regions for primers used in standard amplification may not exist or be degraded so the extent that adhering to the region is not possible (Budowle and Van Daal, 2008). However, due to the loci being bi-allelic, 50-80 SNPs are required to obtain the discriminating power of a typical STR-based system (Budowle and Van Daal, 2008;

Chakraborty et al., 1999; Divne and Allen 2005; Morin et al., 2004). The mutation rate of SNPs, on average 1 in 10^{-8} per nucleotide per generation, is much lower than those of STRs (Durrett and Limic, 2001; Nachman and Crowell, 2000). This makes them particularly useful when complex kinship analysis or parentage testing is required.

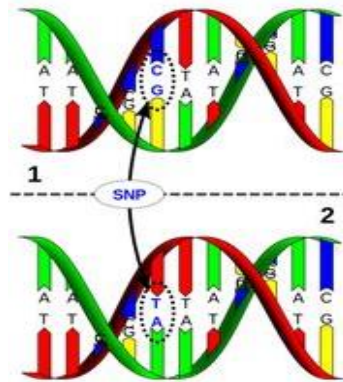


Figure 1.5: A single nucleotide polymorphism is a change in the genetic code of an individual where a single nucleotide (1) is replaced by another nucleotide (2) in the DNA sequence (Kucukkal et al., 2014).

Another type of DNA which exists in a cell is mitochondrial DNA, mtDNA. Mitochondria is found in abundance in the human body and are predominately known for their production of adenosine triphosphate (ATP) which is the energy currency cells need to function. Unlike nuclear DNA, mtDNA comes from the cytoplasm of an oocyte that contributes to the formation of the zygote, and thus it is of maternal origin. It is found in abundance within cells (>1000 copies) which makes mtDNA a viable option when dealing with highly degraded samples and when standard STR analysis fails. Mitochondrial DNA is a circular molecule that is 16,569bp long and does not contain intron sequences (Anderson et al., 1981; Levin et al., 1999). Mitochondrial DNA is passed through the maternal line and may not be able to individualize persons but can provide a family association. For forensic purposes, the focus is on two hypervariable regions that are specifically targeted in the mtDNA molecule, HV1 and HV2, as they are highly polymorphic noncoding regions (Budowle et al., 2003; Holland and Parsons, 1999; Wilson et al., 1995). While mtDNA does not produce an individualized profile, it can establish familial linkage which can be useful in missing and unidentified person's cases. Once these regions have been sequenced, the data are compared to the Cambridge Reference Sequence (CRS), the variants reported and then an association may be made (Bandelt et al., 2014).

1.3 DNA Isolation

DNA isolation, also referred to as extraction, is the process of separating genomic DNA from cellular proteins and other molecules (Butler, 2005). Failure to remove other cellular debris can inhibit the PCR and data analysis. Numerous kits are available on the market for genomic DNA extraction.

Organic extraction, also referred to as phenol-chloroform extraction, involves the serial addition of several chemicals in order to recover high-molecular-weight double-stranded DNA (Butler, 2005). To begin the process sodium dodecylsulfate (SDS) and Proteinase K are added to a tube containing the biological sample in order to break down the proteins that protect the DNA molecule (Vandenberg et al., 1997). Then phenol-chloroform and isoamyl alcohol are added to the sample in order to separate the proteins from the DNA. The sample is then placed in a centrifuge to separate the unwanted proteins and cellular debris from the DNA (Mason, 2015; Vandenberg et al., 1997). The resulting product is double-stranded DNA molecules which can then be used for further analysis. This process was primarily used during RFLP analysis as it is the most effective way to obtain high molecular weight DNA (Comey et al., 1994). However, it is time-consuming, especially when dealing with a large number of samples, involves hazardous chemicals (phenol is highly corrosive and can cause severe chemical burns), involves transferring the sample between multiple tubes which elevates the risk of error or contamination, and could aid in the loss of overall DNA sample quantity (Butler, 2005; Montpetit et al., 2005).

FTA cards (formerly Whatman, now part of the GE Healthcare Life Sciences, Pittsburgh, PA) are commonly used today to isolate DNA (FTA/FTA Elute Sample Collection Cards and Kits: Product Information, 2011). The cards work by having the biological material spotted onto the chemically coated paper where the cells are lysed and protected from degradation and bacterial growth (Vandenberg et al., 1997; Wang et al., 2009). A small punch can be utilized to extract the stain from the paper and placed into a tube for washing. The bound DNA is then released using a FTA Purification Reagent to remove the haem and other inhibitors. The cleaned punch can then be added to the PCR mix for amplification (Vandenberg et al., 1997; Wang et al., 2009). This type of method is primarily used for its ease of collection, ability to be shipped without coolant/ refrigerant

shipping containers, and its ability to be placed in long-term storage at room temperature when used with blood and saliva samples (Butler, 2005).

Another approach commonly used today is solid-phase extraction. There are various methods which utilize a substrate such as silica particles to bind DNA in an automated process (Montpetit et al., 2005; Shewale and Liu 2014). Solid-phase extraction kits allow for rapid and efficient purification of nuclear DNA located within the sample (Tan et al., 2009). They are designed to isolate genomic DNA from blood samples, buccal swabs and several other sample medium types after exposure to a lysate solution using selective binding to silica-based membranes in the presence of chaotropic salts (Shewale and Liu, 2014). Through a series of washes and spins, the nuclear DNA is purified and eluted in a low salt elution buffer until further processing. There are several commercially available products for this purpose. QIAGEN[®], Inc. developed QIAmp[®] spin columns to isolate the DNA (Greenspoon et al., 1998; Scherczinger et al., 1997), while DNA IQ, marketed by Promega[®], utilizes the same silica-based DNA binding and elution chemistries but uses silica-coated paramagnetic resin (Bowden et al., 2011; Frégeau et al., 2010).

The techniques for DNA isolation have progressed over the years to compensate for need to increase throughput and efficiency in casework laboratories (Montpetit et al., 2005). Many of these processes can be aided with liquid handling systems (such as TECAN liquid handling robotics, Männedorf, Switzerland) or automated DNA extraction machines (such as the Promega Maxwell[®]16 and Qiagen BioRobotEZ1), but the extraction step still takes time to process (Davis et al., 2012; Frégeau et al., 2010; Lindner et al., 2011; Morf et al., 2011; Silva et al., 2013; Stangegaard et al., 2009). While these processes have assisted in helping to reduce backlogs, the maintenance and overall purchase costs of the robotics are a concern when considering the budgets of some laboratories.

1.4 Amplification

The process of amplification is the act of replicating or copying a target portion of the DNA sequence until the desired concentration is achieved for analysis. Polymerase chain reaction allows such amplification (Nishimura et al., 2000). This replication is achieved by preparing PCR reaction mix and combining it with a sample of the DNA.

The PCR reaction contains several components which aid in the amplification process (Table 1.1).

Table 1.1: Components of PCR reaction mix (Butler, 2005).

Reagent	Typical Concentration
<i>Tris-HCL, pH 8.3</i>	10 mM
<i>Magnesium chloride</i>	1.2-2.5mM
<i>Potassium chloride</i>	50mM
<i>Deoxynucleotide triphosphate (dNTPs)</i>	200µM each dATP, dTTP, dCTP, dGTP
<i>DNA Polymerase, thermal stable (Taq and TaqGold- most common)</i>	0.5-2.5U
<i>Bovine serum albumin (BSA)</i>	100µg/mL
<i>Primers</i>	0.1-1.0µM
<i>Template DNA</i>	1-10ng genomic DNA

Each component of the PCR reaction mix plays an important role in the replication process.

The ‘reaction buffer’ generally comes as a single commercially produced solution which provides the optimal pH and monovalent salt environment for the target reaction. Each individual component can also be purchased which allows the user to have more control over the conditions present in specific reactions. The ‘reaction buffer’ usually contains Tris-HCL, potassium chloride and sometimes magnesium chloride (MgCl₂) (Integrated DNA Technologies, 2011; Butler, 2005). Depending on the product purchased, magnesium chloride may be separate from the ‘reaction buffer’. Magnesium chloride, additionally, influences the interaction between the primers and the DNA template and is essential for polymerase action to occur. Low concentrations of MgCl₂ may help to stabilize interaction of the primers and their intended primer binding site on the DNA template; however, too low of a concentration may yield a low PCR product since magnesium chloride is need in order for polymerase reactions to occur. High concentrations of MgCl₂ may yield nonspecific binding and/or erroneous PCR product formation (Butler, 2005; Shewale and Liu, 2014).

Bovine serum albumin (BSA) is a PCR additive which can help to increase the yield of the PCR products produced. BSA is believed to aid in the relief of inhibition effects seen in the replication process (Department of Environmental Sciences, 2004; Ralser et al., 2006). It is an optional component and not included in all reaction mixes.

Deoxynucleotide triphosphates (dNTPs) are the building blocks of the DNA template which is being replicated (Butler, 2005; Department of Environmental Sciences, 2004). The addition of dNTPs allows for the synthesizing of DNA for the polymerase enzyme (Shewale and Liu, 2014). An equal concentration of dATP, dTTP, dGTP, and dCTPs are necessary to ensure accuracy during the replication process.

DNA polymerase is used to build the complementary strand to the single-stranded DNA template by using the nucleotides present in the reaction. Almost all PCR reactions employ a heat-stable polymerase which is derived from heat-loving organisms referred to as thermophiles (ABI Life Technologies, 2011; Butler, 2005; Shewale and Liu, 2014). *Taq*DNA Polymerase was originally isolated from the bacterium *Thermus aquaticus* and is commonly used in commercial DNA kits (Gelfand et al., 1989; Tindall and Kunkel, 1988).

DNA primers, oligonucleotides, are short single-stranded DNA molecules that flank the target region to be repeated during the amplification process (Mitsuhashi et al., 1996; Ralser et al., 2006; Robertson and Walsh-Weller, 1998). They can be used in a single capacity where a forward and reverse primer targets a single location on the DNA strand; however, advances in the amplification technique allow for ‘multiplexing’. Multiplex PCR uses multiple sets of forward and reverse primers to target multiple locations along the DNA strand in a single PCR reaction. They are generally 15-30 nucleotides in length and are not complementary to themselves or to any other primers in the multiplex (Gill et al., 1997). This helps to avoid primer dimers and hairpin formations during the amplification process (Vallone and Butler, 2004).

PCR products are a vital component in developing a DNA profile from a small sample using capillary electrophoresis (Yang et al., 2007; Saferstein, 2005). The development of commercialized STR multiplex kits and automated machines has made the process easier.

1.4.1 Amplification Process

Amplification is enzymatic process by which the target regions within the DNA molecule are replicated repeatedly in order to increase the amount of a specific DNA sequence (Butler, 2005). It is carried out using thermal cycling which is a series of heating and cooling cycles conducted on a thermo cycler machine (Mullis, 1987; Mullis and Faloona, 1987). Generally, there are three steps in the cycling process -

denaturation, annealing, and elongation (Figure 1.6). Denaturation completely denatures the target DNA making it single stranded and opening it up for the complementary sequences of the primers (Integrated DNA Technologies, 2011; Robertson and Walsh-Weller, 1998). This is generally conducted at around 94°-95°C for 30 seconds to one minute. Annealing allows the primers to adhere to the target areas that are being replicated. Annealing temperatures fluctuate based on the composition of the primers (Integrated DNA Technologies, 2011; Department of Environmental Sciences, 2004). For the purposes of this project, 60°C was optimal. Elongation occurs in the last step of the process where the temperature is elevated to approximately 70-72°C (Integrated DNA Technologies, 2011; Department of Environmental Sciences, 2004). At this point DNA polymerase is at its optimal temperature and it extends the primers using dNTPs to create a complementary strand. The cycles are then repeated. The number of cycles is dependent on the type of samples being processed and the optimal cycling parameters for the kit being used. With each heating cycle, the number of copies of the target DNA theoretically doubles thus exponentially growing the amount of target DNA.

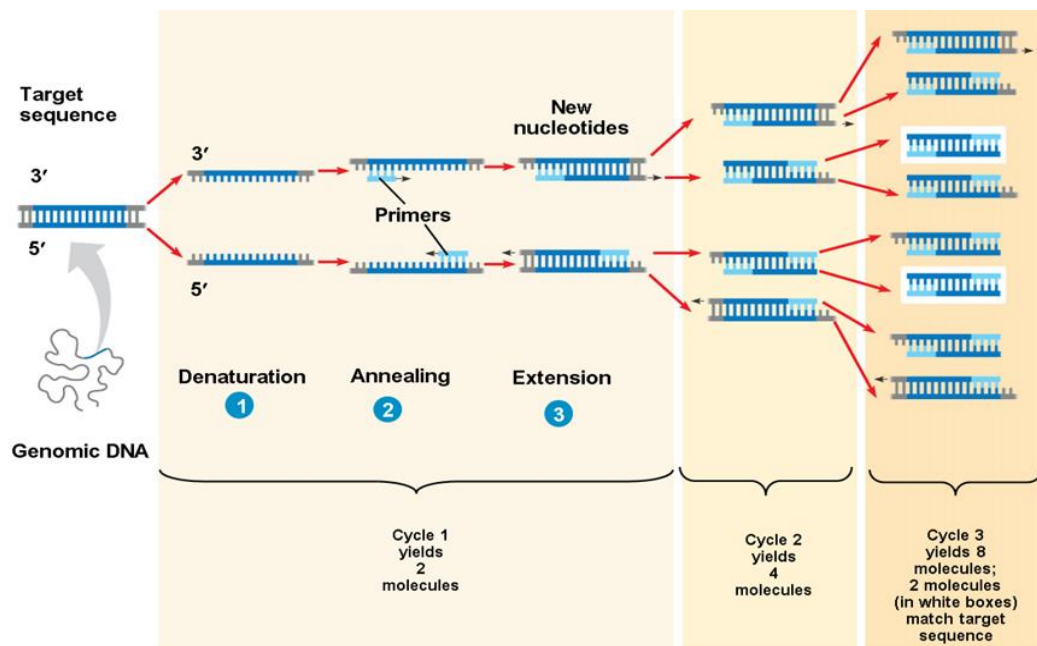


Figure 1.6: Schematic of the DNA amplification process. 1.) The double-stranded DNA molecule is separated into two single strands using heat. 2.) The temperature is then lowered to allow the oligonucleotide primers (shown in blue) to anneal to the target areas on the single-stranded DNA. 3.) The temperature is increased in order for DNA polymerase to produce a complete copy of the target DNA region (Reece et al., 2010).

1.4.2 Direct Amplification

Over the past several years, scientists have been working to eliminate the DNA isolation step which was once thought absolutely necessary for profile development (Morata et al., 1998; Akane et al., 1994; Park et al., 2008). New developments in direct amplification technology suggest that the step may not be as important as once conceived (Mercier et al., 1990).

The concept of eliminating the DNA isolation step is not new; however, it really became an area of focus in the field of forensic science in the early 2000s. While the theory of direct amplification is relatively sound, blood samples in low quantity seem to be highly problematic. Blood contains numerous inhibitors which must be taken into account such as haem (Akane et al., 1994), and immunoglobulin in human plasma (Al-Soud and Radstrom, 2001). Denaturing reagents and detergents previously used in the isolation step also yield a number of problems during the amplification process (Burckhardt, 1994). In the early 1990s Mercier et al.(1990), reported that whole blood samples, both fresh and frozen, could be amplified without extraction, or any other alternate form of purification, by heating and cooling the sample three times prior to beginning the replication process. In 1994, a technique using a microwave treatment successfully amplified non-purified whole blood and hair shaft samples. In 2007, BioQuest Inc. from Seoul, South Korea, released a novel buffer system which not only eliminated the extraction process but using a patented buffer, AnyDirect, also improved PCR replication and overall profile quality (Yang et al., 2007). The AnyDirect buffer system was the first of its kind to be placed on the market for consumers. Successful direct amplification using the AnyDirect Buffer was not limited to whole blood but also included obtaining profiles from Arabidopsis leaves (Yang et al., 2007) and chicken DNA (Bailes et al., 2006). In the fall of 2009, Applied Biosystems released its first direct amplification kit internationally, Identifiler[®] Direct (ABI Product Overview, 2010). In May of 2010, the FBI approved this application as the first direct amplification system for database and paternity testing laboratories (Genomeweb, 2010). In June of 2011, PowerPlex[®] 18D, Promega's direct amplification system, was approved by NIST for database and familial relationship testing. To date, neither kit has been approved for casework samples.

1.4.3 Components of a Direct Amplification

While the exact components of the newly optimized commercial kits for extracted samples and direct PCR are unknown, there are publications which may offer insight into the possible elements of their composition.

In March of 2010, DNA Polymerase Technology Inc. published a paper regarding novel mutants of Taq polymerase (Zhang et al., 2010). OmniTaq (Taq-22), a double mutant of Taq polymerase, is an enzyme which is resistant to the inhibitory effects of blood, soil, crude soil extracts, and some food media (Zhang et al., 2010). It is extremely sensitive and able to amplify trace amounts of DNA very quickly. Omni KlenTaq LA (Klen-taq-10) is a triple mutant of the KlenTaq polymerase which makes the enzyme resistant to the same inhibitory effects as OmniTaq with the inclusion of fluorescent dyes (Kermekchiev et al., 2009). The 'long accurate' option of the Omni KlenTaq LA is also available and allows for amplification of longer products with higher fidelity and accuracy (Kermekchiev et al., 2009). Clontech Laboratories, part of Takara Biotech Company, has also released 'Terra™ PCR direct polymerase' which is a novel enzyme developed for direct amplification from tissue samples, crude extracts, and dirty templates. The utility of these novel alterations to Taq polymerase are especially notable in regards to whole blood samples which have often been a source of contention for the DNA analyst because of the inhibition displayed due to haemoglobin which can copurify with DNA (Akane et al., 1994). This ultimately leads to the inactivation of the DNA polymerase, nonbinding primers, and/or degradation of the target DNA rendering these samples non-viable for development of a partial or full profile (Al-Soud and Radstrom, 2001). As blood is a common biological fluid found in scenes of crime, this is an area of weakness within older multiplex kits.

PCR enhancers may also aid in the robustness of the newly configured kits. Dimethyl sulfoxide, tetramethylxene, betaine, and homoectoine have all been documented as chemicals which can have positive effects on PCR (Bachman et al., 1990; Schnoor et al., 2004; Zhang et al., 2010). Also, an increase in magnesium chloride and bovine serum albumin (BSA) concentration have been suggested as other alternatives for the increase in strong profiles generated from the new kits (vanOorschot et al., 2010).

1.5 STR Analysis

1.5.1 Current Technologies used for STR-based DNA Profiling

The development of commercial multiplex kits for human identification involves the amplification of several STR loci within one reaction tube also referred to as multiplexing. This allows for gathering maximum information from the small amount of DNA and reduces processing times. The STR loci within the commercial kits range in size from 100-600 base pairs depending on the specific loci contained in the kit. Loci with alleles that fall in similar base pair size ranges have been given a different dye colour in order to avoid overlapping.

Several multiplex STR kits have been validated for forensic and DNA databasing such as Applied Biosystems® AmpFℓSTR® SGM Plus® (Cotton, 2000), Applied Biosystems® AmpFℓSTR® Profiler Plus® (Frank et al., 2001; Frégeau et al., 2003; Holt et al., 2002), Applied Biosystems® AmpFℓSTR® Cofiler® (Holt et al., 2002; LaFountain et al., 2001; Moretti et al., 2001), Applied Biosystems® AmpFℓSTR® Identifiler® (Boon et al., 2006; Collins et al., 2004), Promega® PowerPlex® 16 System (Krenke et al., 2002). While these kits are the foundation of forensic and databasing work, advancements in STR technology have recently introduced several new kits. The new kits involve new optimized master mixes to help overcome inhibition, direct amplification for increased efficiency and an increased number of loci in order to harmonize loci across multiple jurisdictions as well as increase discrimination capacity when loci drop-out occurs such as in degraded samples or when analysing mixtures (Gill et al., 2006). These kits include, but are not limited to, Promega® PowerPlex® 18D (Myers et al., 2012; Vallone et al., 2011), Applied Biosystems® AmpFℓSTR® IdentifilerDirect™ (Mulero et al., 2008), Applied Biosystems® AmpFℓSTR® NGM™ (ABI: Life Technologies, 2011; Barbaro et al., 2011a, Barbaro et al., 2011b). Table 1.2 displays loci information for the kits as well as dye colours.

DNA amplification using commercial multiplex kits contains primers which are labelled with different fluorophores, allowing the sample to be reproduced while distinguishing between different loci. Again, a table depicting various kits with their corresponding loci and dye colours are located in Table 1.2. After amplification, a small portion of the amplicon is mixed with an internal lane standard, or ILS. The ILS is a solution consisting of different known fragment sizes which is tagged with its own dye, different

from any used during PCR. Internal lane standards which are commonly used by Applied Biosystems™ are GeneScan™ 500 which is labelled with ROX™ and is red in colour and GeneScan™ 600 which is labelled with LIZ, generally orange in colour from Applied Biosystems. Promega® kits generally contain ILS600 which is red in colour and CC5 ILS500 which is orange. The fragments are then separated by size and colour by capillary electrophoresis, CE, and detected by laser-induced fluorescence (Applied Biosystems, 2005; Beale, 1998; Budowle et al., 1997; Butler, 2004; Landers et al., 1996; Lazaruk et al., 1998; Slater et al., 2003).

Promega PowerPlex® 16HS and PowerPlex® 18D were used throughout the course of this work. PowerPlex® 16HS contains 15 loci plus amelogenin, and detects using four fluorescent dyes (Figure 1.7A). The internal lane standard for this kit is ILS600 which is displayed in red. PowerPlex® 18D contains 17 loci plus amelogenin, and detects using four fluorescent dyes (Figure 1.7B). The internal lane standard for this kit is CC5 ILS500 which is displayed in orange. A full list of the loci, size range of the allelic ladder and the number of repeats for each locus used in the two kits (Promega® PowerPlex® 16HS and Promega® PowerPlex® 18D) are located in Appendix 8.

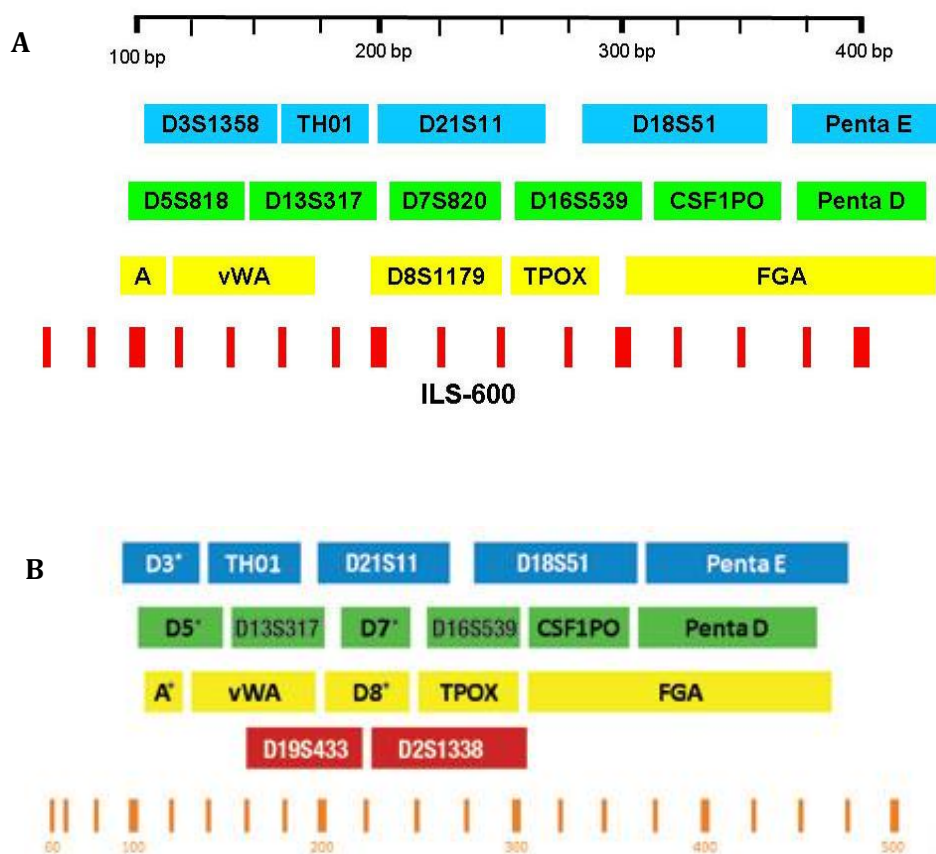


Figure 1.7: Configuration of the (A) Promega PowerPlex®16HS and (B) PowerPlex®18D kits demonstrating the fluorescent dye colour labels and relative PCR product size ranges for each of the loci present. (Source: Promega Corporation)

1.5.2 Development of Electropherograms by Capillary Electrophoresis

During the migration of the sample through the capillary, the fluorophore attached to the 5' end of the amplified fragment is excited and light of a particular wavelength is emitted. This emitted wave is separated by colour by the prism and a multi-coloured electropherogram is then generated for analysis. Software, generally GeneMapper® ID or IDx, is used to analyse the raw data generated from the genetic analyser.

Fragments are compared to an allelic ladder which is run in conjunction with the samples. Figure 1.8 shows the allelic ladder for PowerPlex® 18D. The ladder is the same for PowerPlex® 16HS except loci D21338 and D19S433 are not present. All common alleles for each locus are present in the allelic ladder. The sample fragments in combination with the allelic ladder peaks allow for the assignment of alleles for each

peak present in the profile (Butler, 2005). A typical electropherogram showing a DNA profile generated using Promega's PowerPlex® 16HS is demonstrated in Figure 1.9.

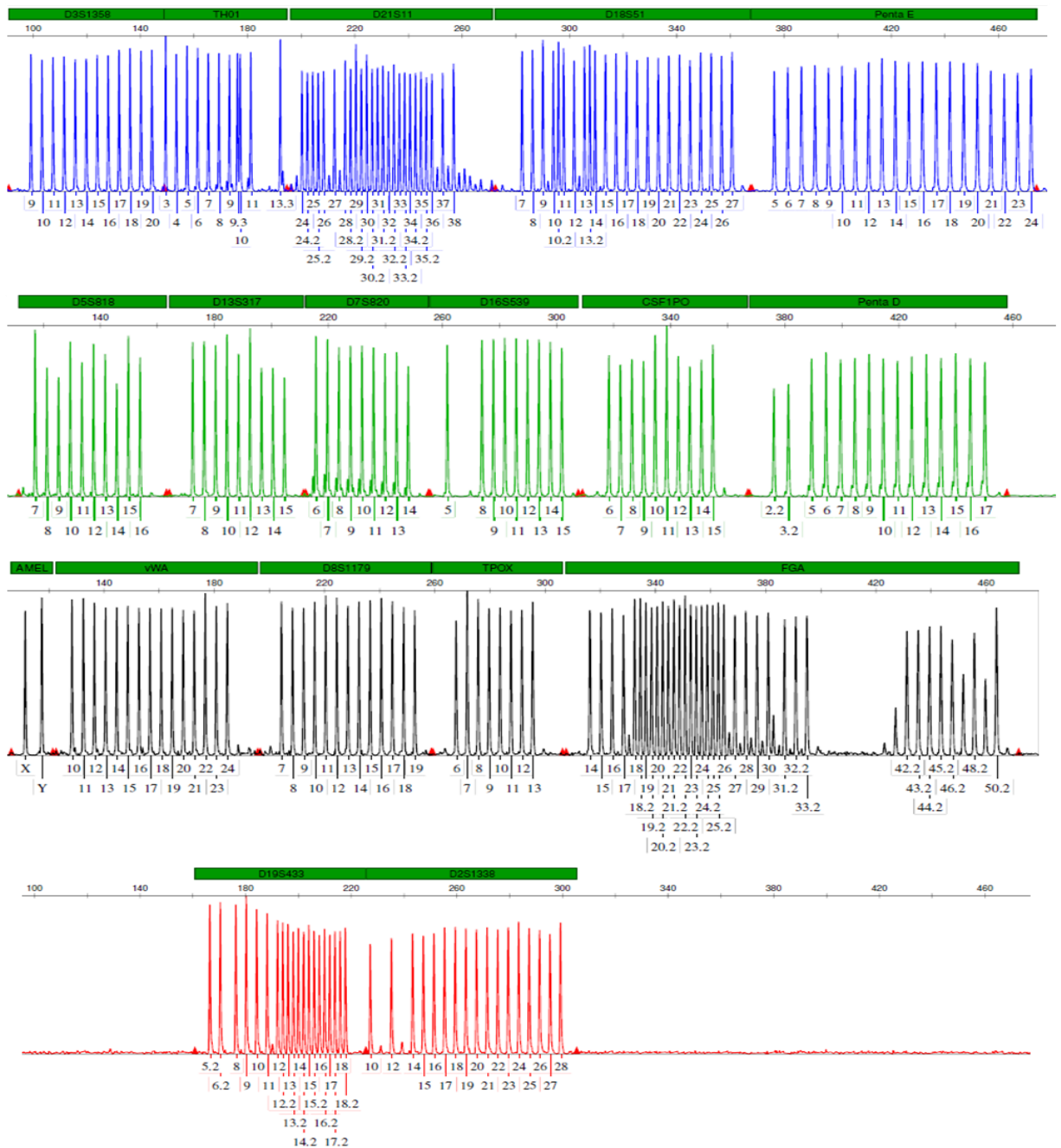


Figure 1.8: Allelic ladder which represents alleles in PowerPlex® 18D. The same alleles are present in PowerPlex® 16HS with the exception of D21338 and D19S433 which are not present in this kit. Green bars contain the loci names. The red triangles along the baseline represent the size range where alleles for a specific locus are called and the boxes below the baseline represent the allele call for that specific peak. The X-axis numerical values indicate the fragment size in base pair number.

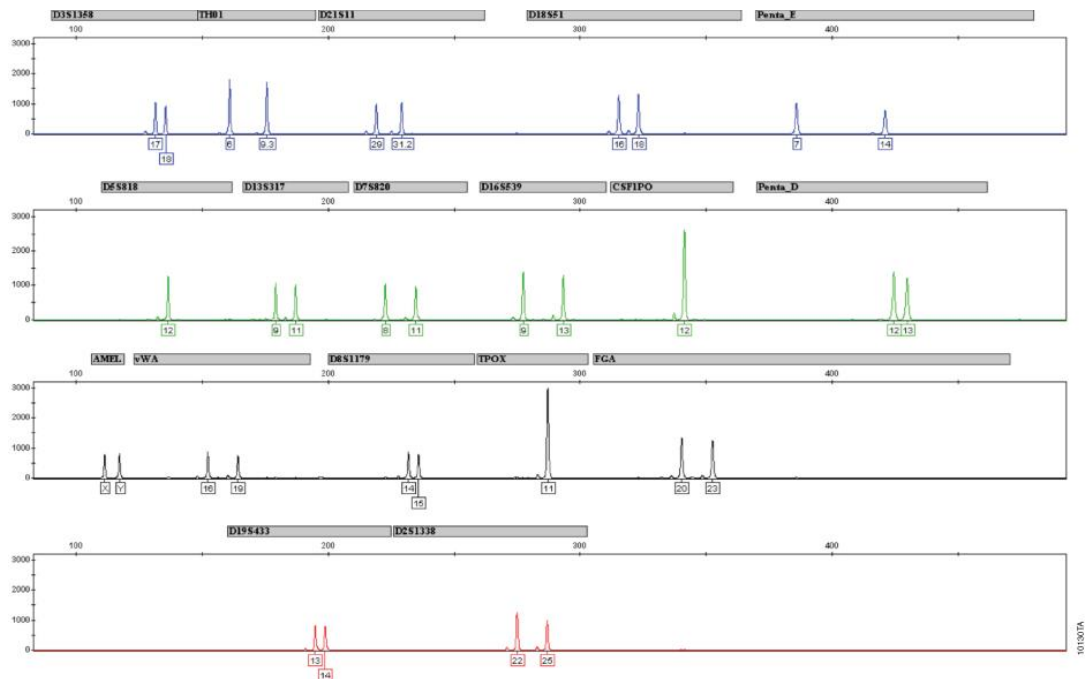


Figure 1.9: Electropherogram demonstrating a DNA profile generated utilizing PowerPlex® 18D. The profile displays positive control 2800M. The grey boxes label each of the loci present in the STR kit and the boxes under each of the peaks are the allele call(s) for that specific peak with the designated locus. The X-axis numerical values indicate the base pair number and the Y-axis the RFU (relative fluorescent unit) values (Source: Promega Corporation).

1.6 Forensic Type Samples

A DNA profile can be generated using almost any biological material containing nucleated cells. These can vary from bodily fluids, to soft tissue, to bone. A reference profile allows for the comparison of such samples and enables statistical evaluation of the forensic sample's source of origin.

1.6.1 Factors Affecting the Development of a DNA Profile

There are many external aspects to take into consideration when developing a viable DNA profile for comparison. Environmental considerations such as ultraviolet light, extreme temperatures, humidity, bacterial growth, and acidity can cause the sample to degrade and therefore limit the chance of obtaining a profile (McNally et al., 1989).

Crimes which involve more than one person such as sexual assaults can also complicate the evaluation of the DNA provided. Also, first responders and investigators may compromise and contaminate biological evidence if proper safety precautions are not

observed. This may lead to more complex samples which may not be resolved down to the original, or single, source of the DNA.

When working scenes of crime, techniques to process biological samples may also be required. The use of powders for latent fingerprints or enhancement chemicals for blood, semen, saliva, etc. is common practice to further visualize the evidence which can then be collected for analysis and identification. It is important to understand how these powders and chemicals can affect the production of a DNA profile further downstream from the crime scene collection.

1.6.2 Contact Surfaces

Surface characteristics play an important part in determining the processing or enhancement technique needed within a specific scene of a crime. The basic types of surfaces encountered at a scene are:

- Porous (Gardner, 2012): paper, cardboard, raw wood
- Semi Porous (Lennard, 2007): glossy paper, wax paper, plasticized cardboard
- Nonporous Smooth (Gardner, 2012): painted/varnished wood, plastics, glass, metal
- Nonporous Rough (Gardner, 2012): leather, vinyl, textured surfaces such as countertops
- Special Conditions (Gardner, 2012): adhesive tapes, human skin, latent blood prints

Other factors which must be considered are temperature of the substrate, electrostatic forces on the receptive surfaces, and the degree of wetness on the surface (Gardner, 2012; Lennard, 2007). When possible the entire item should be collected for processing in a sterile laboratory environment.

1.6.3 Biological Samples

Biological evidence consists of samples recovered from scenes of crime that are of unknown origin. They may be in the form of hair, tissue, bones, teeth, and blood or other bodily fluids. Although this type of evidence is not always visible, almost all scenes do contain biological evidence. Locard's Exchange Principle first stated in 1910 by criminologist Edmond Locard, states that when an object contacts another object, there is an exchange of material between the two objects. This is the foundation of the transfer of evidentiary material within a crime scene or whilst in the act of committing a crime. The four most common types of samples recovered from a crime scene and received by

forensic laboratories for the development of DNA profiles are blood, semen, epithelial cells and hair follicles (Goodwin et al., 2007).

1.6.3.1 Skin Epithelial Cells

Dermal epithelial cells account for approximately 16% of a person's total body weight (Camden, 2009). These are shed constantly and can also be deposited through skin surface/item interaction. Epithelial cell samples are generally collected from surface swabbing in crime scenes, suspects or as reference samples through the use of swabs. Fingerprints are also a good source of epithelial cells. When a person touches an object during a crime, fingerprint patterns consisting of amino acids, proteins, salts, and epithelial cells can be transferred to the surface and left behind at the scene. While fingerprints are common at scenes, it may be difficult to develop a DNA profile from the trace amount of cells deposited and this is dependent upon the perpetrator's ability to 'shed' cells from their body.

The determination of a person's ability to 'shed' has been heavily debated and reported within scientific articles. The varied quantities of DNA collected from individuals from touched objects could be due to the different amounts of DNA shed from each individuals (vanOorschot and Jones, 1997). The first thorough investigation of this concept came from Lowe et al who defined the level of shedders as 'good' and 'poor' based on the number of alleles recovered after a plastic tube was held at various time intervals and after hand washing (Lowe et al., 2002). It has been indicated that that there is more variation in the amount of DNA deposited between individuals than the variation of deposit between the same individuals' left and right hands (Meakin and Jamieson, 2013; Bright and Petricevic, 2004). Further studies have revealed that individuals and their respective hands could exhibit different 'shedder' types on different days thus leading to the belief that the label of shedder type may be too narrow and does not take into account other factors which may affect the deposition of DNA (Meakin and Jamieson, 2013). The complexity of the shedding process and the differences in the interaction between the dermal surfaces and the touched surfaces has also cast doubts on consistent shedder status of individuals (Quinones and Daniel, 2012).

1.6.3.1.1 Fingerprint Enhancement Techniques

Fingerprint enhancement techniques are routinely used at crime scenes. Powder processing or chemical enhancements may be utilized to better visualize or increase the detail of latent or blood evidence that is faintly visible, or latent. Enhancement can increase the value of evidence when bloodstain patterns, finger and palm prints, footwear impressions, tool/weapon impressions, etc. are suspected at the scene of crime.

1.6.3.1.2 Powder Processing

The utilization of powder to develop latent friction ridge impressions dates back to the late 19th century. Friction ridge skin can be found on the palms of hands, fingers, and the soles of feet. The purpose of the powder is to enhance the ridges of the friction ridge skin deposit which is unique to each individual and can be used for identification.

The adhesion of powders to fingerprint residue is accomplished by a pressure deficit mechanism (Thomas, 1978). When a powder particle is moist only on its lower side during the sweat deposit, the bottom of the curvature of the meniscus then causes a pressure deficit inside the droplet, causing the particulate to adhere (Sodhi and Kaur, 2001; Thomas, 1978). The electrostatic attraction between the sweat residue and the powder particles, resulting due to frictional charges, also plays a small role in adhesion (Thomas, 1978).

The adherence of the processing powder to the ridges depends on the size and shape of the particles that compose the formulation. Small, fine particles adhere more easily than large, coarse ones. Generally powders are formulated with either very fine, rounded particles (about 1 μm in diameter) or of fine flake particles (about 10 μm in diameter) (Wilshire, 1996).

Powder processing is conducted on nonporous surfaces where the moisture and oil, residual from the sweat and natural secretion of a depositor, is located. Once a latent print surface has been identified the powder is applied mechanically using a glass-fibre or camel hair brush. The powder binds to the ridge pattern of the fingerprint and is collected through photography and/or lifting with an adhesive medium such as tape.

Fingerprint powder composition has varied greatly since its first use. These powders can be broken down into three broad categories: standard, metallic, and luminescent. Standard powder is composed of a resinous polymer and a colorant which yields contrast to the surface for visualization. Metallic powders contain a resinous polymer, pulverized metal and a colorant. These are less messy than the standard powders but their use is limited due to their metallic property which enables them to bind to metal surfaces, coating the fingerprint pattern. Luminescent powder is composed of natural or synthetic organic compound derivatives which when exposed to ultraviolet or laser light illuminate the print with fluorescence or phosphorescence. The advantage of luminescent powders is their ability to be viewed under alternative wavelengths of light which helps to neutralize multi-coloured backgrounds.

Table 1.3 lists the powders used during the course of this project. Luminescent powders were not used due to the need of an alternative light source and barrier filters for viewing and a single-reflex camera to document the developed fingerprint.

Table 1.3: Fingerprint powders used for enhancement of nonporous and semi-porous surfaces.

	Name	Chemical Components*	Shape / Size
White Powder Formulations			
	Haddonite White	Titanium Dioxide 67% Kaolin 16.5% French Chalk 16.5% OR Titanium Dioxide 33.3% Basic Lead Carbonate 33.3% Gum Arabic 33.3%	Granular Shape
	Lanconide	Zinc Sulfide Zinc Oxide Barium Sulfate Titanium Dioxide Bismuth Oxychloride Calcium Carbonate	
	White Tempera	Titanium Dioxide Starch	
Black Powder Formulations			
	Black Powder	Graphite Charcoal Lamp Black Photocopier Toners Anthocene Other Ingredients**	Granular Shape
	Dactyl Black and Haddonite Black	Lamp Black 70% Graphite 20% Gum Acacia 10%	
	Dragon's Blood Variation***	Lamp Black 25% Rosin 25% Oxide 50%	
	Grey	Mercury 25% Chalk 50% Gum Acacia 25% OR Lead carbonate 87.5% Gum Acacia 12.5%	
Metallic Powder Formulation			
	Dual Component: 1. Magnetic Iron Carrier 2. Non-Magnetic Flake Developer	Chalk or Talc Bronze Gold Aluminum Metal Stearic Acid	1. Spherical Iron Carrier: 50µm diameter 2. Granular Flake Developer: 10µm-20 µm diameter

* Can include filler material, which is commonly fine to medium mesh pumice; volcanic rock rich in silica and is lightweight.

** Other ingredients include: Lycopodium powder, Lead, Mercury, Copper, Cadmium, Silicon, Titanium and Bismuth

*** Dragon's Blood is powered rosin from the *Daemonorops draco* plant.

1.6.3.2 Blood

Blood is the most common biological fluid found at scenes of crimes (Virkler and Lednev, 2009). Blood is a complex fluid which consists of plasma, which is proteinaceous solution containing proteins, amino acids, salts, and different cells. These are red blood cells (erythrocytes), white blood cells (leukocytes), and platelets (thrombocytes) (Bleay et al., 2012; Bossers et al., 2011). Erythrocytes and thrombocytes lack a nucleus, leaving the leukocytes as the only source of nuclear DNA in the blood (Bleay et al., 2012).

Detection of blood at a crime scene can vary from visualization through the human eye to using a chemical enhancement which may or may not need an alternative light source. Over the past few decades a variety of chemicals have been made available for forensic use. Each chemical is advantageous for a variety of reasons. Whether by substrate, reaction colour, reaction mechanism or ability to fluoresce, there should be an optimum chemical for one to select when processing any substrate found or submitted as evidence to a laboratory for processing. Table 1.4 lists the most commonly reported chemical enhancement methods, mechanisms for development, preferred surface type, reaction colour and fluorescence details.

1.6.3.2.1 Chemical Enhancement

Chemical enhancement is a reaction of compounds to various components of a stain which is indicative of the presence of a biological secretion. These chemicals generally fall into one of the following categories: amino-reactive compounds, protein dyes, or haem-reactive chemicals.

Table 1.4: Chemical enhancement methods used for visualization of blood.

Chemical	Common Name	Sensitivity	Reaction Colour	Fluorescence	Wavelength/ Lenses-Glasses	Surface Type	Reference
Acid Violet 17	Coomassie Violet	Proteins	Purple	No	N/A	Porous and Nonporous	(Champod et al., 2004; Sears et al., 2001)
Acid Yellow 7	Brilliant Sulfoflavin	Proteins	Yellow	Yes	400-490/ yellow or orange	Nonporous	(Marchant and Tague, 2007; Stoilovic and Lennard, 2010)
Acid Black 1	Amido Black	Proteins	Dark blue	No	N/A	Porous and Nonporous	(Bevel and Gardner, 2008; Bossers et al., 2011; Cullen et al., 2010; Farrugia et al., 2010; Sears and Prizeman, 2000)
Acid Blue 83	Coomassie Blue	Proteins	Dark blue	No	N/A	Porous and Nonporous	(Blakesley and Boezi, 1977; Volker et al., 1985)
<i>Multiple Chemicals: Crocein scarlet 7B, Coomassie brilliant blue, Glacial acetic acid, Trichloroacetic acid</i>	Crowl's Double Stain	Proteins	Red	No	N/A	Nonporous	(Bossers et al., 2011; Frégeau et al., 2000)
Acid Violet 19	Hungarian Red (Acid Fuchsin)	Proteins	Red	Yes	515-560/ red	Nonporous	(Bossers et al., 2011; Frégeau et al., 2000)
1,8-diazafluoren-9-one	DFO	Amino Acids	Purple	Yes	495-550/ red or orange	Porous and Nonporous	(Lennard, 2001; Sears et al., 2005; Theeuwen et al., 1998)
1,2-indanedione	IND	Amino Acids	Yellow	Yes	515-570/ red or orange	Porous	(Hauze et al., 1998 ; Wallace-Kunkel et al., 2007; Weisner et al., 2001)
Ninhydrin	Nin	Amino Acids	Purple	No	N/A	Porous	(Bossers et al., 2011; Cullen et al., 2010; Frégeau et al., 2000; Grubwieser et al., 2008)

<i>Multiple Chemicals</i> <i>**Luminol based</i>	Bluestar®	Haem	Dark blue	Yes	Chemiluminescent	Nonporous	(Dilbeck, 2006; Cullen et al., 2010; Farrugia et al., 2010; Tobe et al., 2007)
Diaminobenzidine	DAB	Haem	Brown	No	N/A	Porous and Nonporous	(Lennard, 2001; 2007)
Fluorescein	None	Haem	Yellow	Yes	420-485/ orange and yellow	Nonporous	(Sears and Prizeman, 2000; Barni et al., 2007)
4,4',4''-Methylidynetris(N,N-dimethylaniline)	Leucocrystal Violet (LCV)	Haem	Purple	No	N/A	Porous and Nonporous	(Cullen et al., 2010; Farrugia et al., 2010)
3-Aminophthalhydrazide	Luminol	Haem	Blue/Green	Yes	Chemiluminescent	Nonporous	(Barni et al., 2007; Tobe et al., 2007)
Ortho-toluidine	O-tol	Haem	Blue	No	N/A	Nonporous	(Frégeau et al., 2000)
Tetramethylbenzidine	TMB	Haem	Blue/Green	No	N/A	Nonporous	(Garner et al., 1976)
Titanium dioxide	TiO ₂	Haem	White	No	N/A	Nonporous	(Bergeron, 2003; Wade, 2002)

1.6.3.2.1.1 Amino-reactive Dyes

Amino acids are an abundant class of chemical compounds found in latent finger and blood prints (James et al., 2005). The substrates which react with amino-reactive chemicals may be reacting to the terminal amino acid groups on proteins and peptides, as well as the free amino acids found in plasma (Bossers et al., 2011; Farrugia et al., 2013; Lee and Gaensslen, 2001). Human sweat has been widely reported in scientific literature as containing a large amount of amino acids, varying in type and concentration (Jelly et al., 2009). Since the concentration and profile of amino acids fluctuate, it is important that the chemicals used to enhance these types of evidentiary items be non-specific amino-sensitive reagents (James et al., 2005). This allows for greater availability and a higher probability of enhancement. Amino-reactive chemicals can be used on porous surfaces, raw wood and as an enhancement for latent blood prints (Bleay et al., 2012; IAI, 2012). A wide range of chemicals has been proposed with the most conventional ones being ninhydrin (Figure 1.10), 1,8-diazafluoren-9-one (DFO), and 1,2-indanedione (IND). DFO and IND are fluorescent chemicals and require the use of an alternative light source for visualization (Bleay et al., 2012; IAI, 2012).

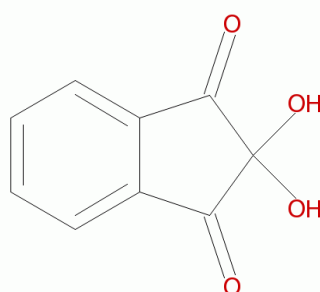


Figure 1.10: The chemical structure of ninhydrin. (The structure was generated using eMolecules (Gubernator et al., 2015).

1.6.3.2.1.2 Protein Dyes

Dyes that bind to the cationic groups of proteins are referred to as “protein reactive dyes” (Bossers et al., 2011; Farrugia et al., 2011; James et al., 2005). The negative charge of the sulfonate group within the dye is attracted to the positive charge of the proteins found within blood under moderately acidic conditions (Bossers et al., 2011). Thus, most formulations of these chemicals often contain an acidic component, such as citric acid, acetic acid, or sulfosalicylic acid (SSA). Acid Yellow 7, coomassie blue, hungarian red

(acid fuchsin), and amido black are among the most popular dyes used in forensic laboratories (Bleay et al., 2012; Praska and Langenburg, 2013). Amido black is the most versatile of the protein dye chemicals as it can be dissolved in a number of solvents including water and citric acid; water, ethanol, and acetic acid; and acetic acid and methanol (Figure 1.11). It also performs well on nonporous surfaces.

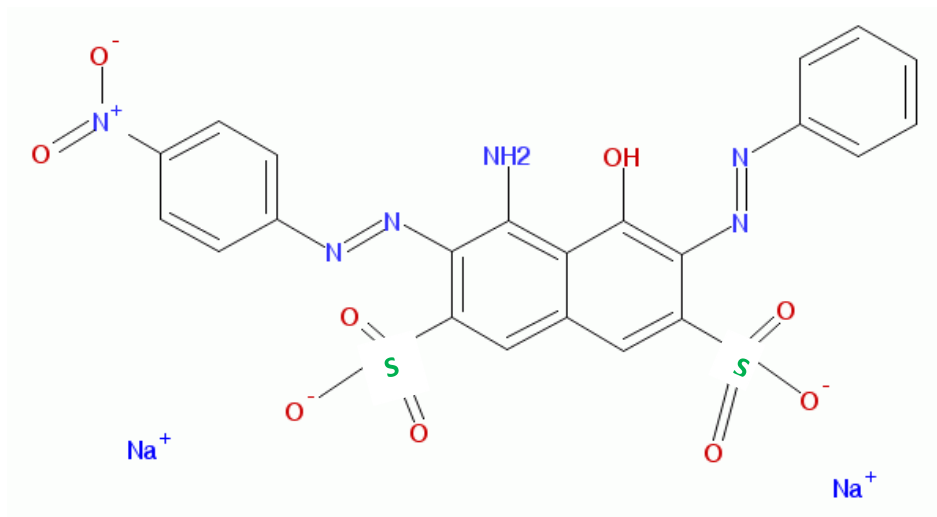


Figure 1.11: The chemical structure of amido black. (The structure was generated using eMolecules (Gubernator et al., 2015).

1.6.3.2.1.3 Haem-reactive Dyes

Haemoglobin is an oxygen-transporting protein with a molecule size of about 65,000 daltons (Cotter, 2001). Haemoglobin make up about 95% of the dry weight (mass) of the red blood cell (Scott and White Hospital, 2013; Cotter, 2001). The active site on the haemoglobin structure is an iron atom which is coordinated in a porphyrin macrocycle (Wirstam et al., 1999). Haem catalyses oxidation reactions; the chemicals within this category begin as colourless and convert to colour once the reaction has taken place. These chemicals do have a limitation in that they are not human specific and will react to the blood of any species. Leucocrystal violet (Figure 1.12) is one of the more popular chemicals used in the class of solutions (Bossers et al., 2011; Praska and Langenburg, 2013). It yields a purple/blue reaction when it encounters the haemoglobin in blood.

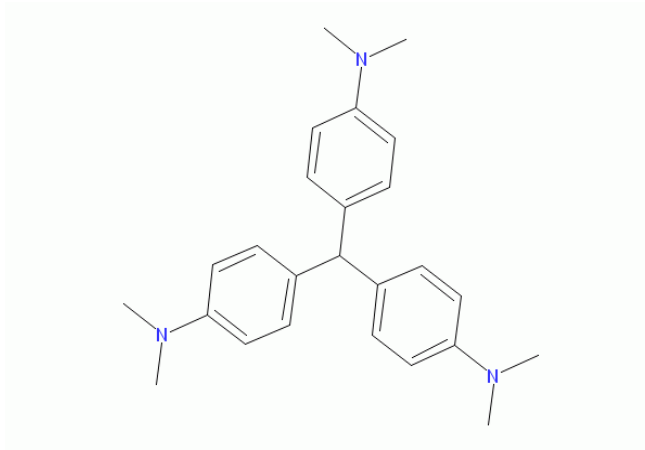


Figure 1.12: The chemical structure of leucocrystal violet. (The structure was generated using eMolecules (Gubernator et al., 2015)).

1.7 The Project

The aim of this project is the evaluation of a direct amplification system (PowerPlex[®] 18D) in forensic samples, specifically blood and epithelial cells, which have been exposed enhancement techniques. These techniques include powder enhancement for epithelial cell samples and chemical processing for whole blood samples.

1.7.1 Working hypothesis:

- Direct amplification systems will be accurate and surpass the efficiency of the current DNA profiling methods.
- The direct amplification system will be effective in providing accurate DNA profiles when used on evidentiary samples which have been processed using other forensic processing techniques (i.e. Powder Processing, Amido Black, Leucocrystal Violet, and Ninhydrin).

1.7.2 Project Objectives

1. To process and evaluate epithelial cell samples and whole blood samples at various dilutions in order to determine the limit-of-detection for the enhanced samples used during this project.
2. To conduct a concordance study with 150 samples to show that both PowerPlex[®] 16HS and PowerPlex[®] 18D produce concordant alleles for all 150 samples.
3. To process and comparatively analyse epithelial cell samples under various dilutions which have been placed on a nonporous laminate surface and exposed to one of three powder types- black powder, magnetic flake, or white powder.

These samples will be processed with both PowerPlex® 16HS and PowerPlex® 18D.

4. To process and comparatively analyse whole blood samples under various dilutions which have been placed on one of seven substrates (gypsum, glass, tile, lead, plastic, raw wood or laminate) and enhanced with one of three chemicals (leucocrystal violet, amido black or ninhydrin).

CHAPTER 2.

MATERIALS AND METHODS

The following section describes the methodologies used during this project. It also details the experiments which were carried out. A list of materials and equipment employed during this project is given in *Appendix 1*.

2.1 Quality Management

Good laboratory practices were employed throughout the course of this project to ensure the reliability, consistency, and quality of the samples and the integrity of chemicals used. Lab coats and disposable gloves were worn throughout the procedure in order to reduce the chance of contamination. Surfaces and equipment were thoroughly cleaned with 2% (v/v) bleach solution and lightly rinsed with deionized water before preparing the samples. All samples were prepared using dedicated pipettes with sterile filter tips to prevent cross-contamination. For each PCR run, both positive and negative controls were conducted to ensure success of the PCR run and to check for possible contamination issues.

Prior to collecting any samples this project was approved through the Institutional Review Board at St. Edward's University and received ethical approval through the University of Central Lancashire. A risk assessment is also on file at the University of Central Lancashire. All samples obtained from individuals during the course of this research were collected following a written consent which was approved by both universities. A copy of both consent forms can be found in *Appendix 6*.

2.2 Enhancement Products

2.2.1 Latent Fingerprint Powders

Latent fingerprint powders were purchased from an approved forensic vendor as indicated in the *Appendix 1*. The powders used for this experiment were standard black powder, magnetic flake, and standard white powder. These powders were selected due to their availability and widespread usage in the field of latent fingerprint processing.

2.2.2 Chemical Enhancement Techniques

Amido black (acid black 1), leucocrystal violet (LCV), and ninhydrin were purchased from approved forensic vendors as indicated in *Appendix 1*. The recipes for each prepared solution can be found in *Appendix 2*.

2.3 Substrates for Forensic Samples

White and black laminate were chosen for the powder-based samples in order to show maximum contrast with the powder colour which was being used for that specific sample and dilution.

The substrates used for the chemical processes were white laminate (12in x 12in carrara marble), tile (Value White Wall Tile 150mm x 150mm), glass (Microscope slide), metal (lead), plastic (acetate sheets), gypsum board and raw wood. These substrates were selected based on their usage as substrates in other publications regarding DNA analysis. Metal (lead), gypsum board and raw wood have also been noted as samples which have produced little to no profile when using standard DNA analysis techniques (Spear et al., 2002).

Each substrate was cleaned with a 2% (v/v) bleach solution and placed in the cross-linker for 30 minutes.

2.4 Collection and preparation of samples

2.4.1 Collection of Buccal Swabs

Fifty buccal swab samples from each population (Caucasian, Black, and Mexican-American), were collected using sterile OmniSwabs (Whatman[®]). Each unrelated person submitted two samples, one for each kit used during the concordance study. The swabs were placed in a 2.25 inch x 3.5 inch coin envelope (Quality Parks Products) to dry and were stored at 4°C until used. Both samples were consumed during the experiment.

2.4.2 Population Selection

The populations selected for this study were Mexican, African American and U.S. Caucasian. The Mexican population was to be the primary focus while the African American and U.S. Caucasian populations were used as a base population for the study.

The Mexican population has a huge impact on the state of Texas. While generally accepted as part of the Hispanic population, the Mexican population is largely from the northern part of Mexico which, as history indicates, was occupied by the Olmec, Maya, Teotihuacan, Toltec, and Aztec Indians prior to Spanish conquest in the mid-1500s (Philip, 2010). With a shared border and growing instability in the Mexican government, migration to the US from Mexico is a common occurrence. According to the Census Bureau's American Community Survey, approximately 29.2 million, or 13.7% of the US population, is Mexican American and lives in the United States as legal US citizens (Farley and Alba, 2002). It is estimated that there are an additional 12-20 million undocumented immigrants currently living in the US (Farley and Alba, 2002; History of Illegal Immigration in the U.S., 2009). There are roughly 24 million people living in the state of Texas as of 2009; 36.9% of these are Mexican Americans (Pew Hispanic Center, 2009). A comparative look at the allelic frequencies, the power of discrimination (PD), and power of exclusion (PE) between the Hispanic database and Native American database initially was to be reviewed with regard to the Mexican samples which would traditionally be reported using the Hispanic database. However, due to the limited amount of reagents allotted for this thesis, the original population study was not carried out. The samples were used as concordance between the two commercial DNA kits used during the course of this work for the mock crime scene samples.

2.4.3 Collection of Buccal cells from Saliva for Powder Study

In order to eliminate the inconsistency between fingerprint deposits left by individuals on surfaces, either by depletion or shedder status, a decision was made to use 'cleaned' epithelial cells obtained from cheek swabs in order to provide a consistent deposit of cells for powder development. Buccal swabs were collected from two unrelated individuals using sterile OmniSwabs (Whatman®). These swabs are in addition to the

concordance study samples discussed in 2.4.1.. Each swab was placed into a 1.5ml tube containing 200µl of PBS 1X solution and vortexed vigorously for 1 minute. The swab was removed from the tube and spun at 12,000rpm for 1 minute. The supernatant was removed from the tube leaving the remaining buccal “pellet” which was suspended again in 200µl of PBS solution by vortexing vigorously. This process was repeated twice to remove the amylase from the saliva leaving the buccal cells (McClintock 2014).

2.4.3.1 Epithelial Cell Dilutions (Limit of Detection)

A buccal swab was taken from an individual in accordance with the protocol outlined in Section 2.4.2. The sample was diluted using the following ratios: x2, x10, x50, x100, x150 and x200 with amplification grade water (Frégeau et al., 2000). DNA was extracted using the *QIAamp*[®] DNA Mini extraction kit. A second set of samples was prepared for direct amplification with the same dilutions and pre-treated with Swab Solution[™]. They were then amplified in triplicate using the half-reaction protocols for Promega[®] PowerPlex[®] 16HS and Promega[®] PowerPlex[®] 18D, respectively (Section 2.5.5).

2.4.3.2 Preparation of Epithelial Cells Recovered from Substrates

Laminate flooring tiles were obtained in two colours, black and white. These were used as the substrates for this experiment. Each flooring tile was cut into roughly 1.5-2 inch squares and cleaned with deionized water and 2% (v/v) bleach solution then UV irradiated in a cross-linker for 30 minutes before use. Once the substrates were prepared, 3 samples were created for each individual utilizing 20µl of the x10 epithelial cell dilution: small stains were created on the laminate flooring tiles and the area that the stain encompassed was circled with a black permanent marker. The samples were allowed to dry for 24 hours in a dry secure area. After the stains dried, standard black powder and magnetic black powder were applied to the white laminate squares and the white standard powder was applied to the black laminate squares. Each of the squares was photographed and labelled. Once the photographs were complete, each square was swabbed individually using the dual swab technique. The samples were amplified in

triplicate for the autosomal STR kits being tested, Promega® PowerPlex® 16HS and Promega® PowerPlex® 18D.

2.4.4 Collection of Blood Samples for Simulated Forensic Samples

Two samples of human blood were collected from 2 unrelated individuals using Vacuette® EDTA tubes by a licensed registered nurse. The samples were labelled “BIOHAZARD” and stored at 4°C.

2.4.4.1 Blood Dilutions (Limit of Detection)

A whole blood sample was drawn from an individual in accordance with the protocol outlined in Section 2.4.4. The blood was then diluted with distilled water at the following ratios: x2, x10, x50, x100, x150 and x200 (Frégeau et al., 2000). The DNA was then extracted from the blood samples using the Qiagen DNA extraction method as described in Section 2.5.1. Samples were then amplified in triplicate using the Promega® PowerPlex® 16HS kit.

A second set of samples was prepared with the same dilutions and pre-treated with Swab Solution (Section 2.5.2). They were then subjected to amplification using the Promega® PowerPlex® 18D. Each sample was amplified in triplicate.

2.4.4.2 Preparation of Human Blood Samples on Substrates

Approximately 20µl of x1 blood was applied to various substrates and lightly spread using a thin glass spatula. The substrates listed in Section 2.3 were selected based on their common occurrence at crime scenes, and as substrates which had been previously processed without enhancement chemicals using a direct amplification system (Frégeau et al., 2000; Swaran and Welch, 2012). All were prepared in triplicate. The x1 blood samples were then diluted to x2 and x10, respectively. The substrate preparation process was repeated for the x2 and x10 dilutions. All surfaces were photographed prior to exposure to blood enhancement chemicals. All samples were allowed to dry for 24 hours prior to processing.

After the 24 hour period, samples to be enhanced with amido black (acid black 1) were sprayed with the chemical and allowed to process for 1 minute. Once the processing was complete, the substrates were then rinsed with amplification grade water and

allowed to dry at room temperature. Gypsum wood and raw wood were not used with this chemical as amido black is not suitable for porous substrates due to the rinse step.

All selected samples developed with leucocrystal violet (LCV) were exposed to the chemical via spray. Once a reaction was visualized as the stain turned purple, no further chemical was deposited. Since LCV does not have a rinse step, all substrates selected for this study were processed.

Samples to be processed with ninhydrin were sprayed with the chemical and left to dry overnight. No heat was applied to the sample. ninhydrin is only used on porous surfaces; therefore, only gypsum wood and raw wood were processed using the chemical.

Table 2.1 details each chemical and the substrates which were processed. All developed blood enhanced stains were then photographed again to document the reaction of the chemical and swabbed using the double swab method (Sweet et al., 1997).

Table 2.1: Chemical enhancement techniques and their corresponding substrates.

Chemical (Name Abbreviation)	Substrates
Leucocrystal Violet (LCV)	Tile, Plastic, Lead, Glass, Laminate, Gypsum Board, Raw Wood
Amido Black (AB)	Tile, Plastic, Lead, Glass, Laminate
Ninhydrin (NIN)	Gypsum Board, Raw Wood

2.5 Profiling of Human DNA

2.5.1 Extraction of human DNA

2.5.1.1 DNA extraction of Omni Swabs

Extraction of buccal swabs was conducted using the *QIAamp*[®] DNA Mini kit in accordance with the manufacturer's recommended procedure and utilizing all solutions supplied with the kit (Qiagen, 2011). Each swab was placed into a sterile, 2ml micro centrifuge tube and 600µl of 1X PBS was added. Samples were then briefly mixed by vortexing and quickly centrifuged. The swabs were then removed and discarded. 20µl of Proteinase K and 600µl of Buffer AL were added to each of the tubes. The samples were mixed by vortexing and briefly centrifuged. The samples were allowed to

incubate at 56°C for 10 minutes. Following incubation, 600µl of 100% (v/v) ethanol was added to each of the tubes, which were mixed again and quickly centrifuged to remove any droplets which may be present in the cap of the tube.

A QIAGEN® Spin Column was placed in a correspondingly labelled collection tube and approximately 700µl of the sample mixture was added to the spin column. Each sample was centrifuged at 8,000rpm for 1 min and the contents located at the bottom of the collection tube were discarded. This step was repeated until the entire sample mixture had been filtered. Each QIAGEN® Spin Column was then transferred to a clean 2ml tube and 500µl of Wash Buffer AW1 was then added to the column. The column was centrifuged at 8,000rpm for 1 min. The contents in the collection tube were discarded. The column was placed into a clean collection tube. 500µl of Wash Buffer AW2 was added to the column and centrifuged at 8,000rpm for 1 minute at room temperature.

Each of the sample columns was finally placed in a sterile labelled 1.5 ml microcentrifuge tube. 100µl of Buffer AE was added to the column. The sample was allowed to incubate at room temperature for 1 minute and then centrifuged at 8,000rpm for 1 minute. All samples were stored at 4°C until use.

2.5.1.2 DNA extraction from Cotton Swabs

Extraction from cotton swabs was carried out as described in section 2.5.1.1 with the following modification: Buffer AL and Ethanol were both reduced to 400µl (Qiagen, 2011).

2.5.1.3 DNA extraction of Blood Samples

Extraction of buccal swabs was conducted using the *QIAamp*® DNA Mini kit (Qiagen) in accordance with the manufacturer's recommended procedure (Qiagen, 2011). For each sample, 20µl of Proteinase K was added to a sterile labelled 2ml microcentrifuge tube. 200µl of each whole blood sample was then added to each tube. Where the sample was less than 200µl, PBS was added to the sample for a final volume of 200µl.

Again, the extraction procedure was carried out as described in section 2.5.1.1 with the following modification: Buffer AL and Ethanol were both reduced to 200µl.

2.5.2 Pre-treatment of Direct Amplification Samples

Samples which were processed using the direct amplification protocol were pre-treated with Swab Solution™ (Promega® 2013) according to the manufacturer's recommendations (Promega Corporation, 2015). Each swab was placed in a 1.5ml tube with 500µl of Swab Solution™ (Promega® 2013). The tubes were then incubated at 70 °C for 30 min. Samples were stored at 4 °C.

2.5.3 Quantification of DNA using NanoDrop 2000

Extracted human biological samples were quantified using the NanoDrop 2000 (Thermo Fisher Scientific). The NanoDrop 2000 is a spectrophotometer which measures the absorption of light at specific wavelengths by biological molecules; absorption is expressed in nanometres (Thermo Fisher Scientific, 2009). Purification of the samples through DNA extraction is a necessity when working with nucleic acid samples in order to ensure accurate results. Generally, nucleic acids have absorbance maxima at 260 nm and proteins at 280 nm, and absorbance is proportional to the total concentration of the molecule. 1µl of extracted DNA solution was placed on the receptor and the concentration and quality of the sample assessed using the nucleic acid concentration (derived from the absorbance at 260 nm) and the 260/280 ratio (Thermo Fisher Scientific, 2010). A ratio of 1.8 is generally accepted as 'pure' DNA (Thermo Fisher Scientific, 2007; Thermo Fisher Scientific, 2009). Ratios significantly higher or lower could indicate the presence of phenol, proteins, or other contaminants. A blank was run after every ten samples to ensure a proper reading but this is not reflected in the list of data.

2.5.4 Haematocrit Counts

For the mock forensic samples that were not extracted, the two blood samples and two epithelial samples were quantified using haematocrit counts. Haematocrit counts were necessary in order to approximate the amount of DNA in each sample. As the samples were amplified in their raw state, i.e. not extracted and purified, the use of the NanoDrop 2000 (Thermo Fisher Scientific) was not possible. A microscope slide specifically designed for haematocrit counting was cleaned with 97% (v/v) ethanol and rinsed with deionized water. The slide was then allowed to dry at room temperature. Both epithelial cell samples were then diluted x10, placed on the slide and stained using

hematoxylin and eosin for visualization. A cell count was then conducted. Each sample was counted in triplicate and the average of the cells taken in order to quantify each sample.

2.5.4.1 Staining of Epithelial Cells

Ehrlich's haematoxylin and eosin (H&E) was used to stain the epithelial cells in order for them to be counted. This method was used to stain the nuclei within cells blue. The red blood cells, cytoplasm, and connective tissue which were also present were stained red/pink. The protocol and staining supplies were obtained from the University of Central Lancashire laboratory technician. The recipes for the solutions as dictated in the instruction sheet can be found in *Appendix 2* (Avwioro, 2011). As described in section 2.5.4, the slides were allowed to dry and Ehrlich's haematoxylin was applied and the sample exposed for 15 minutes. After 15 minutes, the slide was gently rinsed with distilled water then again with Scott's tap water for 3 minutes. (Scott's tap water is a blueing reagent designed for histology and cytology.) The slide was then stained with alcoholic eosin for 3 minutes. After 3 minutes, an absolute alcohol rinse was applied to dehydrate the sample. The stain was mounted by placing a small drop of a glue-like substance (histomount) to the stain and then a clear cover slide was placed over the stain.

2.5.5 Controls

Negative control samples were conducted using PBS 1X, blank swabs, and the Swab Solution. Extraction negatives were conducted with each set of extracted samples. Positive controls were conducted and analysed with each amplification run using Promega[®] 2800M positive control for both direct amplification and extracted samples.

For all substrates processed with chemicals (i.e. tile, plastic, lead, glass, laminate, gypsum board, raw wood), a positive control was conducted by placing each of the samples on the substrate and swabbing without any chemical processing.

Commercial internal lane standards with known fragment sizes were used with all samples analysed for this project. Internal lane standard ILS600, was run with all samples analysed with PowerPlex[®] 16HS. CC5 ILS500, internal lane standard, was run

with every sample analysed with PowerPlex[®] 18D. Multiple allelic ladders were run with each plate of samples placed on the genetic analyser. A ladder correctly identifying all alleles above the minimum threshold was used for analysis and identification of alleles. All samples were analysed at a 50 RFU threshold.

2.5.6 Amplification using Promega[®] PowerPlex[®] 16HS and PowerPlex[®] 18D

Throughout the project, human DNA was amplified using the human identification kits Promega[®] PowerPlex[®] 16HS and Promega[®] PowerPlex[®] 18D.

2.5.6.1 Amplification with Promega[®] PowerPlex[®] 16HS

2.5.6.1.1 Amplification at full volume reactions (25µl)

Full volume reactions were run at 25µl. Samples were prepared as described by the manufacturer, with 5µl of the Promega[®] PowerPlex[®] 16HS Master Mix, 2.5µl Promega[®] PowerPlex[®] 16HS Primer Mix, 15.5µl nuclease-free water and 2µl of DNA.

2.5.6.1.2 Amplification at reduced reaction volume (12.5µl)

Reduced volume reactions were run at 12.5µl. Samples were prepared as described by the manufacturer using half of the stated volumes, i.e. 2.5µl of the Promega[®] PowerPlex[®] 16HS Master Mix, 1.25µl Promega[®] PowerPlex[®] 16HS Primer Mix, 8.25µl nuclease-free water and 1µl of DNA. The following table (Table 2.2) describes of the cycling parameters used.

Table 2.2: Promega® PowerPlex® 16HS cycling conditions for a 32 cycle program.

PCR Stages	Temperature	Time	
Initial Incubation	96 °C	2 min	
Denaturation	94 °C	30 sec	} 10 Cycles
Amplification	60 °C	30 sec	
Extension	70 °C	45 sec	
Denaturation	90 °C	30 sec	} 22 Cycles
Amplification	60 °C	30 sec	
Extension	70 °C	45 sec	
Final Incubation	60 °C	30 min	
Hold	4 °C	∞	

2.5.6.2 Amplification with Promega® Powerplex® 18D

Promega® PowerPlex® 18D is a direct amplification system which is being tested for its concordance against an already used kit as well as its robustness when using forensic based samples.

2.5.6.2.1 Amplification at full reaction volume (25µl)

Amplification of human DNA with the Promega® PowerPlex® 18D human identification kit was carried out as described by the manufacturer. For each reaction, 5µl of Promega® PowerPlex® 18D Master Mix 5X (the Master Mix included *AmpliTaq* Gold), 5µl of Promega® PowerPlex 18d® 5X Primer Mix and 13µl of Promega® PowerPlex® 18D nuclease-free water were mixed with 2µl of human DNA. Together with the DNA samples, the appropriate positive and negative controls were prepared.

2.5.6.2.2 Amplification at reduced reaction volume (12.5µl)

Half volume, 12.5µl amplification reaction with Promega® PowerPlex® 18D human identification kit was carried out using 2.5µl of Promega® PowerPlex® 18D Master Mix 5X (the Master Mix included *AmpliTaq* Gold), 2.5µl of Promega® PowerPlex® 18D 5X

Primer Mix and 6.5µl of Promega® PowerPlex® 18D nuclease-free water, mixed with 1µl of human DNA for a final volume of 12.5µl. Together with the DNA samples, the appropriate positive and negative controls were prepared. Samples were then vortexed, spun down and amplified using the conditions outlined in Table 2.3.

Table 2.3 Promega® PowerPlex® 18D cycling conditions for a 27 cycle program.

PCR Stages	Temperature	Time	
Initial Incubation	96 °C	2 min	
Denaturation	94 °C	10 secs	} 27 Cycles
Amplification	60 °C	1 min	
Final Incubation	60 °C	20 min	
Hold	4 °C	∞	

2.5.7 Fragment analysis by capillary electrophoresis

This section describes the analysis of PCR products by capillary electrophoresis (CE) with the ABI Prism® 3130 and 3500.

2.5.7.1 Preparation of samples for CE

Amplified PCR products, allelic ladders and CE blanks were prepared in tubes by mixing 1µl of the sample with 9.5µl of Hi-Di formamide and 0.5µl of either ILS 600™ for Promega® PowerPlex® 16HS or CC5 ILS 500 for Promega® PowerPlex® 18D to give a total volume of 11.0µl. Tubes were then vortexed, centrifuged, covered with septa, and denatured at 94 °C for 2 min. After denaturation, tubes were immediately transferred onto ice and allowed to stand for 5 min before being loaded onto the instrument.

2.5.7.2 Sample analysis using the Genetic Analyser

Electrophoresis was performed on the ABI Prism® 3130 or 3500 machine through POP-6™ polymer using a 50 cm capillary and Running Buffer (1X). The position of each sample was entered onto the sample sheet and the appropriate dye for the internal standard was selected.

2.5.7.3 Analysis of DNA profiles

Results were analysed using GeneMapper[®] ID v3.2 or *ID-X*. Parameters for the analysis of the PCR products were those described in Table 2.4. The analysis range and the size call range were defined for each run. All other factors were kept constant. The CE blank was used to define the internal standard for each run.

Table 2.4: Conditions for the electrophoresis run.

Parameters	Value
Injection time	5 s
Injection voltage	15 kV
Run Voltage	15 kV
Temperature	60 °C
Run Time	30 min

Table 2.5: Parameters for the analysis of PCR fragments when utilizing the ABI 3500 and GeneMapper *ID-X* software.

Parameter	Value
Analysis Range	Variable
Size Call Range	Variable
Data Processing	None
Size Calling Method	Local Southern
Peak Detection	50 RFU
Baselining	251 pts
Min Peak Half Width	2 pts
Polynomial Degree	3 pts
Peak Window Size	19 pts
Peak Window Size Slope Threshold for peak start / end	0-0

Table 2.6: Parameters for the analysis of PCR fragments when utilizing the ABI 3130 and GeneMapper v3.2 software for analysis.

Parameter	Value
Analysis Range	Variable
Size Call Range	Variable
Data Processing	None
Size Calling Method	Local Southern
Peak Detection	30 RFU
Baselining	251 pts
Min Peak Half Width	2 pts
Polynomial Degree	3 pts
Peak Window Size	19 pts
Peak Window Size Slope Threshold for peak start / end	0-0

2.6 Analysis of results

All the data presented are summaries of the raw data obtained. The raw data are referenced in the *Appendix 3*, while the actual values can be found on the complementary CD attached to this report in the folder called *Data*. The genotypes of the human DNA that were used throughout the various studies can be found in *Appendix 4*.

Tables of results represent a summary of raw data, and in most cases DNA profiles are expressed in terms of minimum, maximum and average peak heights and profile type. *Minimum peak height* is the peak height of the allele showing the lowest RFU which meets the analysis parameters; *maximum peak height* is the peak height of the allele showing the highest RFU which meets the analysis parameters; *average peak height* is the average RFU of all the alleles in a profile. *Peak height ratios* express the balance of the heterozygous peaks which are present at a specific locus in a percentage.

The profile types describe the type of profile obtained i.e. full profile (FP), partial profile (PP) and no profile (NP). In case of PP, the number of loci completely

genotyped is indicated utilizing replicates and the “2 of 3” system to determine each of the called loci. A locus was considered complete if all the expected alleles in the loci were identified.

2.7 Statistical analysis

In order to investigate differences between the samples, statistical analysis was done on peak heights (RFU) of replicates. Calculation of averages and standard deviation (s.d.) were carried out using Excel 2010. MiniTab v17 was used to perform statistical analysis such as *one-way ANOVA* with $\alpha=0.05$. Table of results for the statistical analyses are referenced in the relevant chapters and in *Appendix 3*. Minitab projects were created for each area where statistical analysis occurred. The actual outputs of the calculations can be found in the complementary CD attached to the report under the folder *Data*. Each area of analysis has a dedicated folder. For example, data for the chemicals is referenced under the folder labelled (*Data Chemicals*).

CHAPTER 3.

SENSITIVITY STUDY

-REDUCED VOLUME AND DILUTION DETERMINATION-

3.1 Overview

Human identification kits such as Promega's PowerPlex[®] 16 have been optimized for forensic use. This type of kit allows for the amplification of a small amount DNA to be replicated with multiple loci that contain fluorescently labeled primers. PCR products can then be processed on an automated generic analyzer which provides a faster development of DNA profiles (Krenke et al., 2002; Spathis and Lum, 2008). Further research and development of the components within human identification kits have led to the production of products which are even more tolerant to PCR inhibitors and some can even be used in a 'direct' manner which skips the extraction and quantitation steps previously needed for development of DNA profiles (Oostdik et al., 2013; Ensenberger et al., 2013).

Promega's PowerPlex[®] 16HS was the first in the list of Promega's products to contain the improved master mix. The kit still contains Taq DNA polymerase and the same primers and dyes as the previous version of PowerPlex[®] 16 (Ensenberger et al., 2010). The optimized mater mix allows for the kit to overcome common PCR inhibitors seen in forensic type samples. PowerPlex[®] 18D followed in 2010 as a human identification system specifically designed for direct amplification. PowerPlex[®] 18D can be used with extracted samples; however, the validation confirms the optimization of the kit was based direct sample and utilizing extracted samples is not recommended (Oostdik et al., 2011 and 2013). The validation also discusses the components of the kit which contain primers from two kits currently on the market (discussed further in *Chapter 4*), DNA polymerase and optimized magnesium concentrations within the reaction mix.

The manufacturer recommendations for full volume reactions with both Promega's PowerPlex[®] 16HS and PowerPlex[®] 18D were to utilize 25µl for a final DNA concentration of 0.5-1.0 ng/µl. Lower DNA concentrations have been noted to develop

full profiles but the frequency of imbalanced peaks and allele drop also increased. The utilization of a 25 μ l reaction is not cost effective for this work; therefore, in order to maximize resources available, the PCR reaction mix was reduced by half, 12.5 μ l. Published data for both kits indicate that reduced volume reactions are achievable and produce reliable results (Oostdik et al., 2013; Hoffman and Fenger, 2010). The first part of this chapter aims to confirm the published information regarding the effects of reducing the PCR volume.

This project aims to conduct a comparative preliminary evaluation of Promega's PowerPlex[®] 16HS and PowerPlex[®] 18D in order to determine if direct amplification was a viable option for forensic samples which have been exposed to various processing techniques. While these samples are usually found in very minute concentrations, it was the goal to evaluate the products with an adequate amount of DNA to determine if inhibition of the enhancement materials were apparent. During the course of this project two sample types were used, epithelial cells and whole blood. The amount of DNA which can be yielded from each of these sample types differs based in the individual (Raymond et al., 2009; Sewell et al., 2008; Compté et al., 2015). It was imperative to find dilutions which gave a full genetic profile above the 50 RFU threshold in order to move forward with the enhancement of the substrates.

The primary goals for this chapter were to,

1. Determine if half reaction volumes are a viable option for this work;
2. Identify the dilutions which produce a full profile above the 50 RFU threshold when processing samples composed of epithelial cells;
3. Identify the dilutions which produce a full profile above the 50 RFU threshold when processing samples composed of whole blood.

3.2 Experimental Design

3.2.1 Evaluation of Full (25 μ l) and Half (12.5 μ l) Reactions using Decreasing Amounts of DNA Template

Amplification of human control DNA 2800M was carried out utilizing both kits at full (25 μ l) and half (12.5 μ l) reactions to explore the effect of reducing the PCR volume on the quality of DNA profiles generated and on the sensitivity of the assay. Different amounts of standard human DNA (0.06 ng, 0.13 ng, 0.25 ng, 0.5 ng, 1 ng and 2 ng) were amplified in (standard) 25 μ l reactions and (reduced) 12.5 μ l reactions and analyzed on ABI 3500 as described in Chapter 2, Section 2.5.7.3. Each sample type was prepared

in triplicate. The raw data can be found in *Output Data*. ANOVA statistical analysis was conducted to evaluate the difference between volume groups as well as the two kits.

The amplification of the standard human DNA 2800M with PowerPlex[®] 16HS gave a profile with twelve heterozygous and three homozygous loci and an XY for amelogenin. PowerPlex[®] 18D gave the same profile with an additional two heterozygous loci, D19 and D2, respectively. The allele calls for each locus can be seen in Table 3.1. The effect on the amplification efficiency and assay sensitivity were evaluated using peak heights and /allele drop-out. These were used to monitor the variation in amplification efficiencies between the different PCR volumes at constant DNA concentration.

Table 3.1: Known genetic profile for 2800M.

<i>Locus</i>	<i>Allele Call</i>
D3S1358	17,18
TH01	6, 9.3
D21S11	29, 31.2
D18S51	16, 18
Penta E	7, 14
D5S818	12
D13S317	9, 11
D7S820	8,11
D16S539	9, 13
CSF1PO	12
Penta D	12, 13
Amel	X, Y
vWA	16, 19
D8S1179	14,15
TPOX	11
FGA	20,23
D19S433	13,14
D2S1338	22,25

3.2.2 Sensitivity of Epithelial Cell Samples

One sample containing epithelial cells was prepared using the procedure outlined in section 2.4.3.1 for amplification. A comparative analysis using both kits in a series of sample dilutions was used to aid in determining the amount of retrievable DNA from

the epithelial cell samples. Dilutions were carried out at x2, x10, x50, x100, x150 and x200. Half volume reactions of 12.5µl were used for all samples. The sample was quantified using a cell count described in 2.5.4. Each sample type was prepared in triplicate.

The amplification of the sample with PowerPlex® 16HS gave a profile with eight heterozygous and six homozygous loci and an XX for amelogenin. PowerPlex® 18D gave the same profile with additional homozygous and heterozygous loci, D19 and D2, respectively. The allele calls for each locus can be seen in Table 3.2. The effect on the amplification efficiency and assay sensitivity were evaluated using peak heights and allele drop-out. These were used to monitor the variation in amplification between the different PCR volumes.

Table 3.2: Known genetic profile for epithelial cell sample.

<i>Locus</i>	<i>Allele Call</i>
D3S1358	17, 18
TH01	7
D21S11	30.2, 32.2
D18S51	14, 19
Penta E	7, 17
D5S818	11
D13S317	11, 13
D7S820	8, 10
D16S539	11
CSF1PO	10, 11
Penta D	12
Amel	X
vWA	14
D8S1179	12
TPOX	11
FGA	22, 24
D19S433	15
D2S1338	17, 25

3.2.3 Sensitivity of Blood Samples

One sample which contained whole blood in an EDTA tube was prepared using the procedure outline in 2.4.4.1. A comparative analysis using both kits in a series of sample dilutions was used, as in the epithelial cell samples, to aid in determining the amount of retrievable DNA from the whole blood samples. Dilutions were carried out at x2, x10, x50, x100, x150 and x200.

The amplification of the single sample with PowerPlex® 16HS gave a profile with eight heterozygous and six homozygous loci and an XX for amelogenin. PowerPlex® 18D gave the same profile with two additional heterozygous loci, D19 and D2, respectively. The allele calls for each locus can be seen in Table 3.3. The effect on the amplification efficiency and assay sensitivity were evaluated in the same manner as the epithelial cells in section 3.2.2. These were used to monitor the variation in the amplification between the different PCR volumes.

Table 3.3: Known genetic profile for whole blood sample.

<i>Locus</i>	<i>Allele Call</i>
D3S1358	17, 18
TH01	7
D21S11	30.2, 32.2
D18S51	14, 19
Penta E	7, 17
D5S818	11
D13S317	11, 13
D7S820	8, 10
D16S539	11
CSF1PO	10, 11
Penta D	12
Amel	X
vWA	14
D8S1179	12
TPOX	11
FGA	22, 24
D19S433	15
D2S1338	17, 25

3.3 Results

3.3.1 Results of Reduced Volume on PCR Product

Using both PowerPlex® 16HS and PowerPlex® 18D, amplification of human DNA (2800M) was carried out in decreasing reaction volumes to examine the effects of reducing the PCR volume on the quality of the DNA profiles which were generated. Reactions were carried out for both kits using 25µl and 12.5µl total reaction volumes for varying amount of DNA input; 0.06 ng, 0.13 ng, 0.25 ng, 0.5 ng, 1 ng, and 2 ng. All samples were run in triplicate. The raw data can be found in *Output Data*. ANOVA statistical analysis was conducted to evaluate the difference between volume groups as well as the two kits.

The PCR product concentration and total PCR product were used to evaluate the efficiency of the amplifications at lower volumes for both kits. The total PCR product (in RFU) is calculated by summing the peak heights for all alleles for each of the samples at a specific volume. The total PCR product is then divided by the final volume in order to obtain the PCR product concentration (in RFU/µl) (Gaines et al., 2002). The total PCR product and PCR product concentration can be seen in Tables 3.4 for PowerPlex® 16HS and 3.5 for PowerPlex® 18D.

It was observed that as the final DNA concentration was lowered the peak height averages and maxima were also decreased for both kits. This was to be expected as the concentration of target DNA was being reduced. The difference in concentration of the total PCR for both kits was not statistically significant when evaluating full versus half reactions [$F(1, 10) = 2.53$, $p\text{-value} = 0.143$]. The half volume reactions in most cases gave a higher final PCR product concentration. Tables 3.4 and 3.5 reflect the data generated from PowerPlex® 16HS and PowerPlex® 18D in regards to full versus half reactions. The quality of a DNA profile is assessed a number of ways including the evaluation of heterozygous peak height balance (peak height ratio or heterozygote balance (Hb) calculation), level of stutter, and other artefacts such as spikes, dye blobs, and pull-ups which can all interfere with the interpretation of the profile. Overall, the peaks which were generated with the amplification standard (2800M) were of good quality. Split peaks were noted in profiles generated with 2.0 ng of DNA at the 12.5µl reaction volume and 2.0 ng at the 25µl reaction volume. On occasion spikes, sharp peaks which are very intense and appear equally in all dye channels, were also seen in the data; however, upon reinjection these peaks were no longer visible.

A key factor in assessing the effect of profile quality is determining the heterozygous peak balance (Hb), which is the ratio of the two peaks in each heterozygous locus. This is calculated by dividing the allele with the lower peak height by the allele with the higher peak height (Fourney et al., 2004; Kelly et al., 2012). For the purpose of this project, peak height was assessed since single-source samples were used and ≥ 0.70 set as the threshold for acceptable heterozygous peak balance (Hb) (Gill et al., 1997).

This gives a value ranging from 0 to 1 with 1 representing peaks of equal height (Fourney et al., 2004; Gill et al., 1997). Hb values which are lower than 0.70 indicate peak imbalance. Figure 3.4 depicts heterozygous loci which were processed with PowerPlex[®] 16HS in full and half reaction volumes. Figure 3.5 depicts heterozygous loci which were processed with PowerPlex[®] 18D in both full and half reactions. Figure 3.3 compares the peak height ratios from each of the volumes for individual heterozygous loci processed with PowerPlex[®] 16HS. Figure 3.4 compares the peak height ratios from each of the volumes for individual heterozygous loci processed with PowerPlex[®] 18D.

Overall the samples with the lowest DNA concentrations, ones which fell below 0.01 ng, were below the 0.70 Hb limit more often than samples with higher concentrations. When comparing the two kits, PowerPlex[®] 16HS gave a larger number of peak imbalances than PowerPlex[®] 18D (Figures 3.1 and 3.2). PowerPlex[®] 18D when processed with a total volume reaction of 25 μ l failed to produce any samples over the Hb limit of 0.70 when using DNA concentrations of 0.01 ng and 0.005 ng. The 12.5 μ l samples were slightly more successful with several samples processed with 0.01 ng were observed above the limit. The correct allele calls for the known profile (2800M) were produced for all developed samples.

Table 3.4: Results showing the minimum, maximum and average peak heights, the profile type, total PCR product and PCR concentration for the various dilutions of 2800M amplified using whole (25µl) and half (12.5µl) reactions with and PowerPlex® 16HS. The values are averages of three replicates.

Volume (in µl)	DNA added (in ng)	Final [DNA] (in ng/µl)	Profile Properties				Total PCR product (in RFU)	PCR product concentration (in RFU/µl)
			Max PH	Min PH	Average PH	Profile Type		
12.5	0.06	0.0025	--	--	--	NP	--	--
	0.13	0.005	977 (s.d. 134.1)	64 (s.d. 4.04)	243.9	FP	19509 (s.d. 1375.0)	1560.72 (s.d. 125.0)
	0.25	0.01	1313 (s.d. 161.1)	66 (s.d. 37.0)	403.1	FP	34667 (s.d. 1125.7)	2773.4 (s.d. 102.3)
	0.5	0.02	4540 (s.d. 802.4)	287 (s.d. 91.3)	1065.3	FP	92681 (s.d. 9951.6)	7414.5 (s.d. 1065.3)
	1.0	0.04	3428 (s.d. 1200.8)	152 (s.d. 110.7)	1205.7	FP	104910 (s.d. 12014.2)	8392.8 (s.d. 1092.2)
	2.0	0.08	12591 (s.d. 1593.4)	1254 (s.d. 739)	5416.8	FP	471258 (s.d. 31314.2)	37700.6 (s.d. 2846.7)
25	0.06	0.005	113 (s.d. 40.3)	50 (s.d. 4.6)	80.0	PP1	1921 (s.d. 410.6)	76.8 (s.d. 37.3)
	0.13	0.01	461 (s.d. 129)	50 (s.d. 5.5)	119.0	PP13	8808 (s.d. 392.3)	325.3 (s.d. 35.7)
	0.25	0.02	1019 (s.d. 261.6)	50 (s.d. 1.5)	200.1	FP	17411 (s.d. 492.8)	696.4(s.d. 44.8)
	0.5	0.04	1365 (s.d. 147.6)	109 (s.d. 36.3)	407.6	FP	35464 (s.d. 1145)	1418.6 (s.d. 104.1)
	1.0	0.08	3069 (s.d. 218.3)	293 (s.d. 82.1)	886.2	FP	77103 (s.d. 1147.0)	3084.1 (s.d. 104.1)
	2.0	0.16	8010 (s.d. 898.8)	955 (s.d. 377.7)	3157.3	FP	274688 (s.d. 8948.3)	10987.52 (s.d. 1047.8)

Table 3.5: Results showing the minimum, maximum and average peak heights, the profile type, total PCR product and PCR concentration for the various dilutions of 2800M amplified using whole (25µl) and half (12.5µl) reactions with and PowerPlex® 18D. The values are averages of three replicates.

Volume (in µl)	DNA added (in ng)	Final [DNA] (in ng/µl)	Profile Properties				Total PCR product (in RFU)	PCR product concentration (in RFU/µl)
			Max PH	Min PH	Average PH	Profile Type		
12.5	0.06	0.0025	105 (s.d. 60.6)	105 (s.d. 60.2)	105	NP	105 (s.d. 0)	8.4 (s.d. 5.5)
	0.13	0.005	338 (s.d. 54.2)	100 (s.d. 4.93)	150.5	PP5	1425 (s.d. 231.5)	114 (s.d. 45.4)
	0.25	0.01	559 (s.d.91)	102 (s.d. 1.15)	205.25	PP8	14208 (s.d. 845.9)	1136.6 (s.d. 55.4)
	0.5	0.02	1035 (s.d. 89.2)	102 (s.d. 8.4)	293.93	PP16	37238 (s.d. 3035.2)	2979.0 (s.d. 152.9)
	1.0	0.04	2902 (s.d. 441.1)	110 (s.d. 19.5)	638.35	FP	86728 (s.d. 4099.9)	6938.2 (s.d. 247.1)
	2.0	0.08	4473 (s.d. 873.4)	108 (s.d. 45.3)	1112.64	FP	110151 (s.d. 8725.4)	8812 (s.d. 793.2)
25	0.06	0.005	218 (s.d. 109.1)	102 (s.d. 63.7)	144	PP1	688 (s.d. 301.6)	27.52 (s.d. 27.4)
	0.13	0.01	213 (s.d. 48.5)	100 (s.d. 19.2)	127.44	PP2	1147 (s.d. 350.9)	45.9 (s.d. 31.9)
	0.25	0.02	550 (s.d. 141.0)	105 (s.d. 1.5)	186.2	PP2	4097 (1365.7)	163.9 (s.d. 86)
	0.5	0.04	439 (s.d. 64.8)	102 (s.d. 11)	180.12	PP10	8465 (s.d. 495.8)	338.6 (s.d. 45.7)
	1.0	0.08	1794 (s.d. 396.3)	101 (s.d. 11.9)	405.05	PP16	35239 (s.d. 2360.2)	1409.6 (214.6)
	2.0	0.16	3612 (s.d. 1012.5)	111 (s.d. 6.2)	718.14	FP	71096 (s.d. 12632.1)	2843.8 (s.d. 774.6)

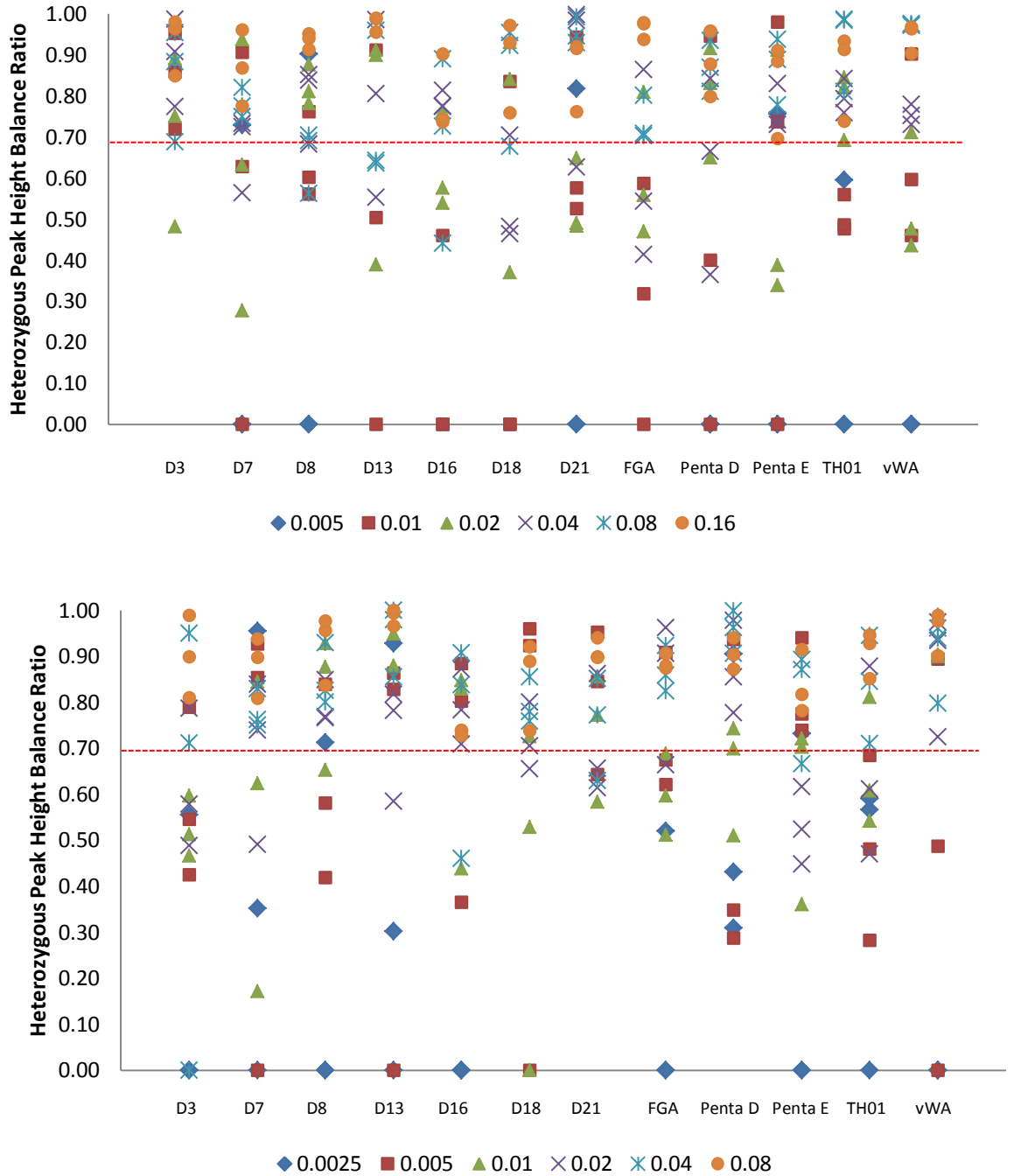


Figure 3.1: Charts which depict heterozygous loci ratios at different concentrations when amplified at (Top) 25µl and (Bottom) 12.5µl with PowerPlex® 16HS. The red line indicates the 0.70 Hb threshold for the heterozygous peak balance. Samples displayed are based on three replicates.

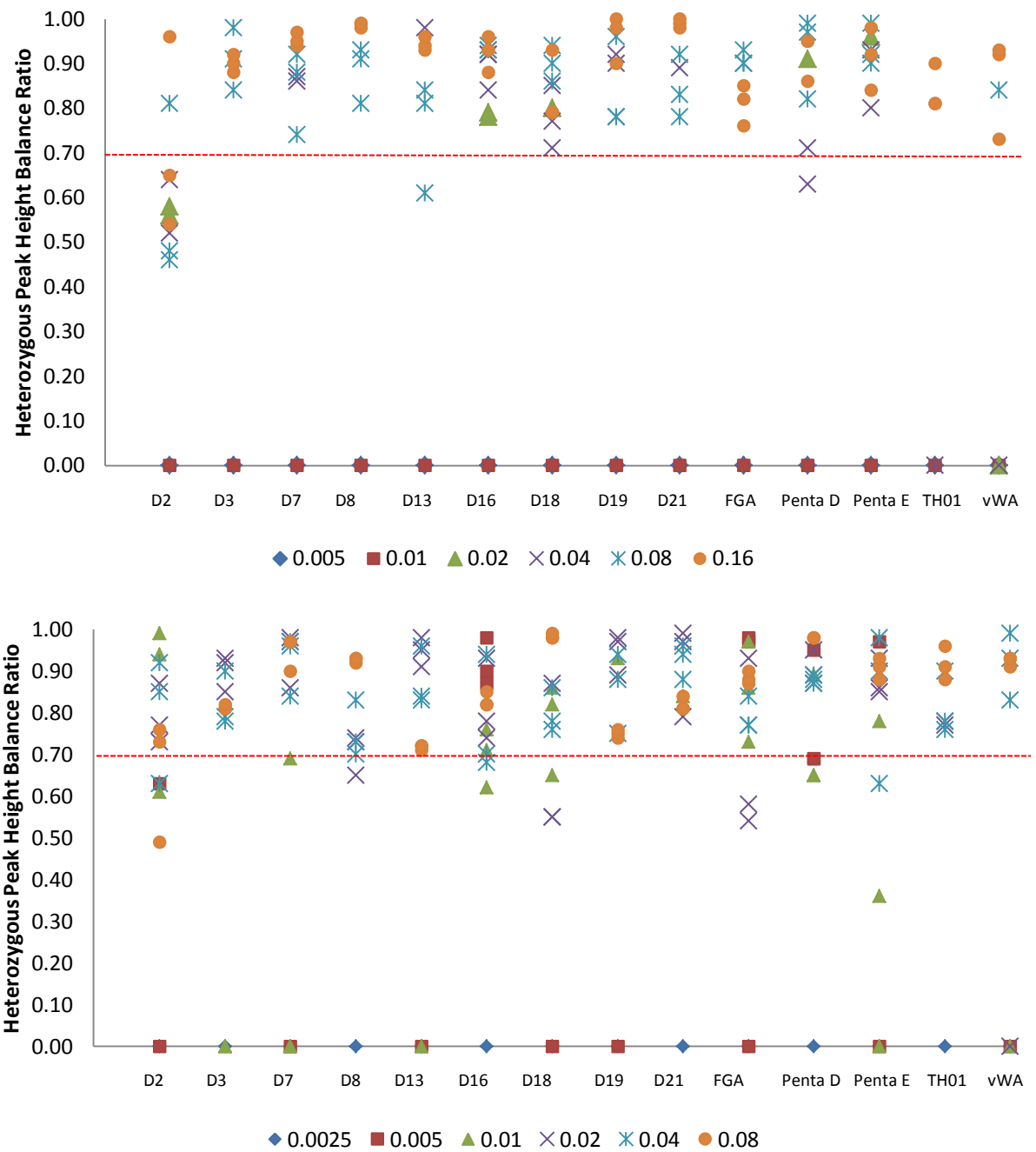
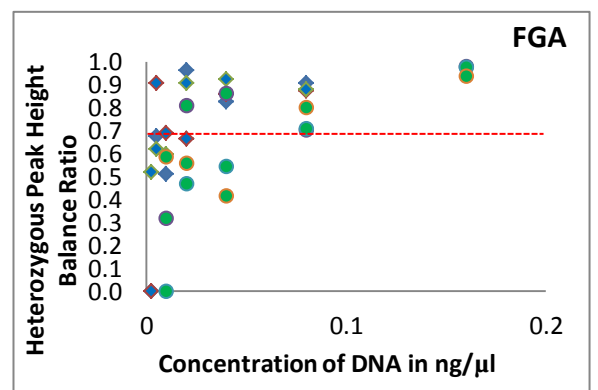
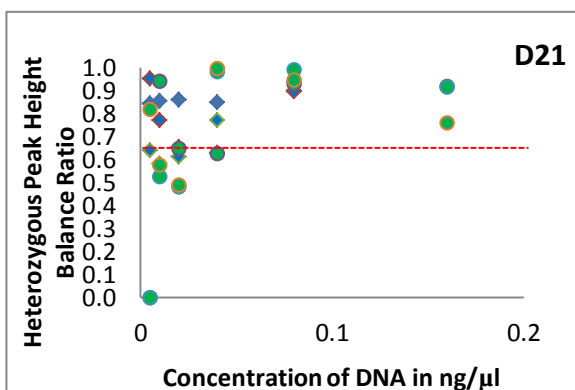
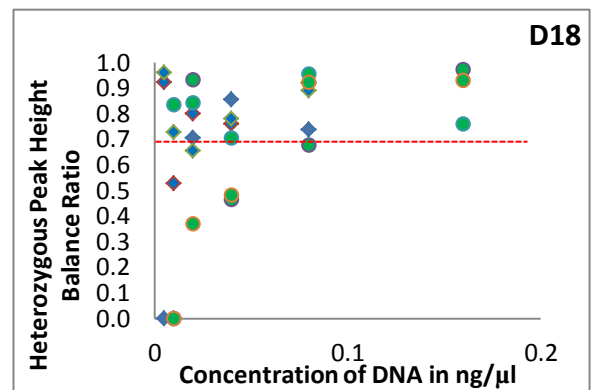
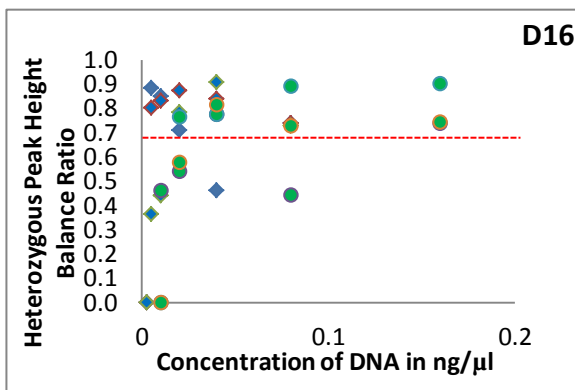
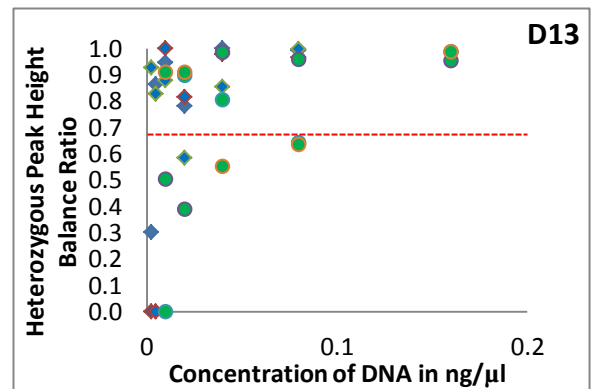
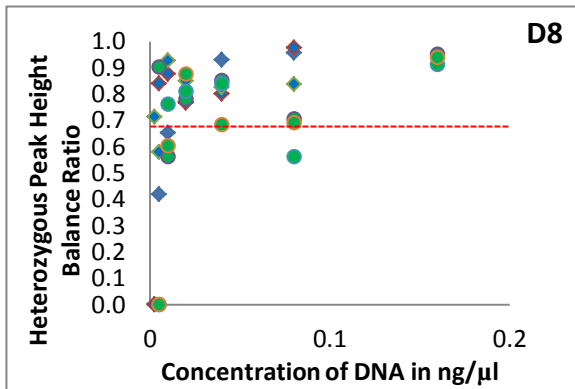
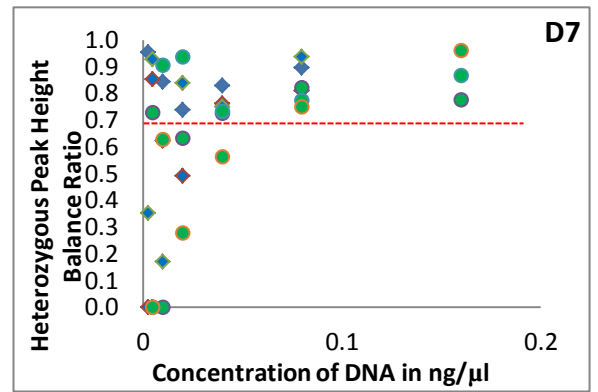
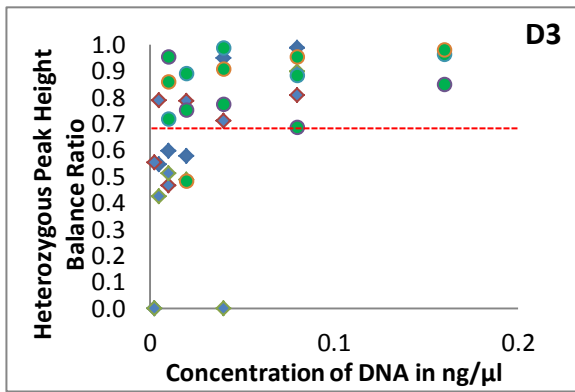


Figure 3.2: Charts which depict heterozygous loci ratios at different concentrations when amplified at (Top) 25µl and (Bottom) 12.5µl with PowerPlex® 18D. The red line indicates the 0.70 Hb threshold for the heterozygous peak balance. Samples displayed are based on three replicates.



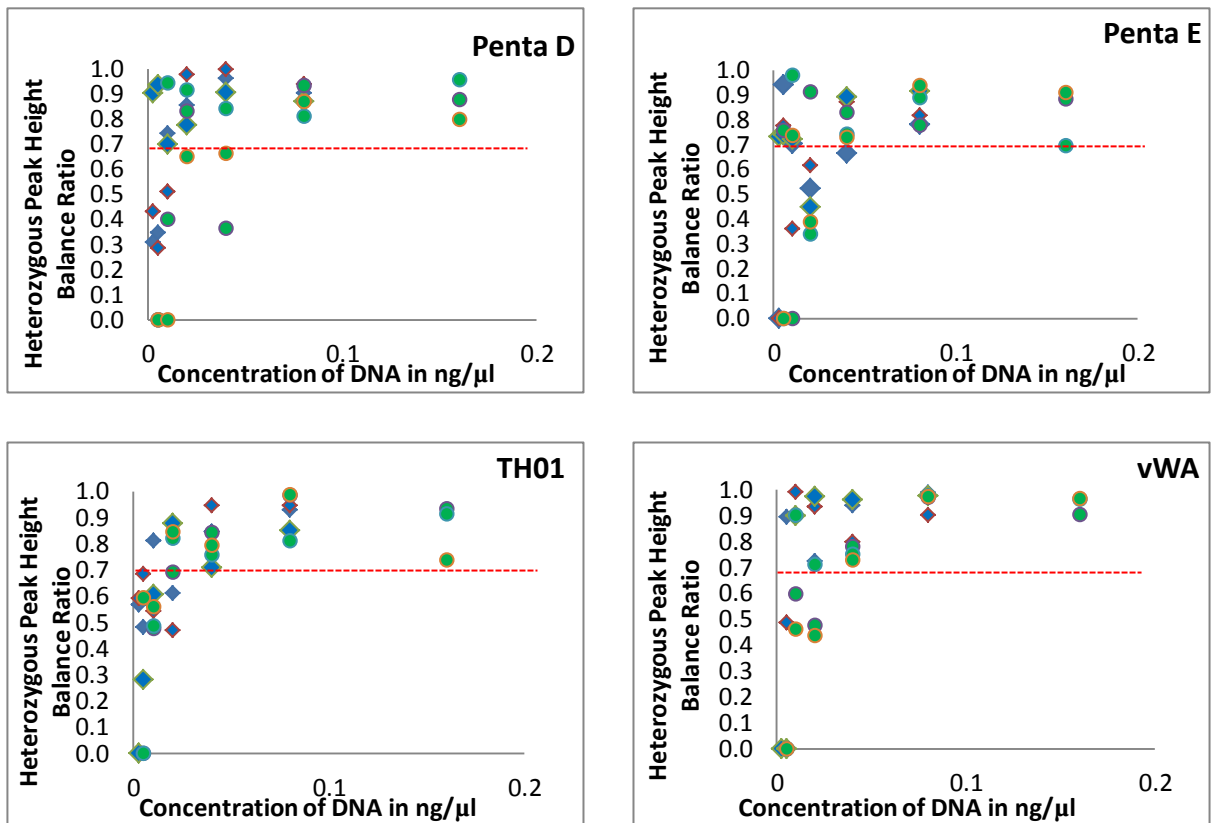
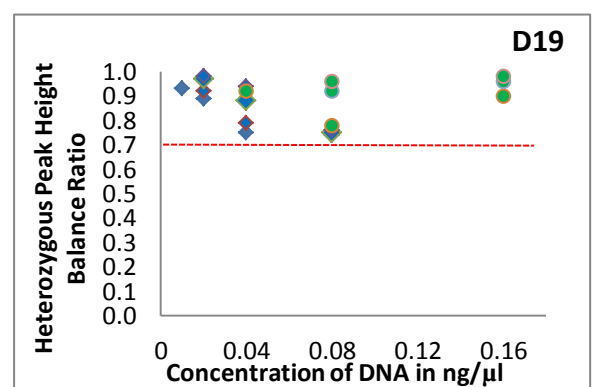
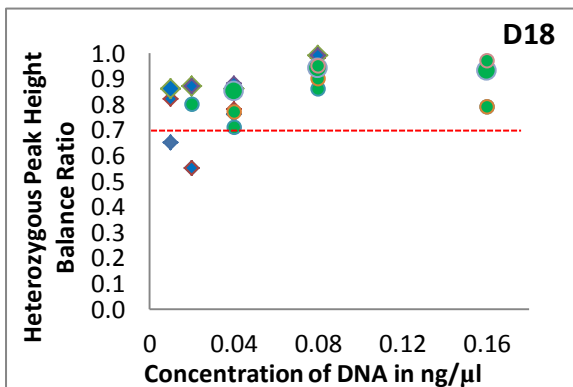
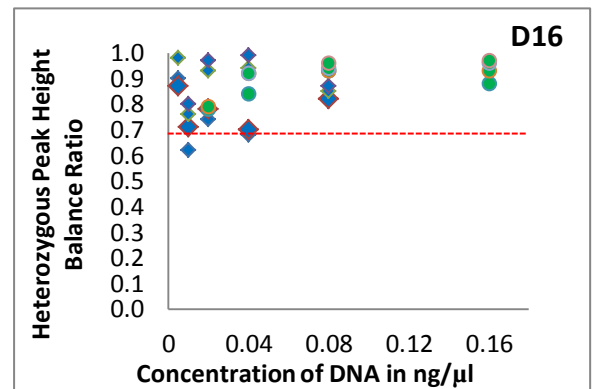
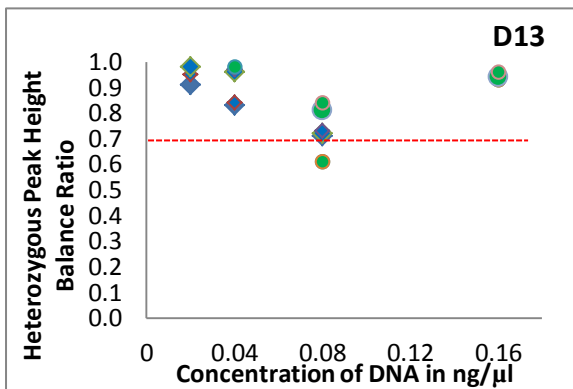
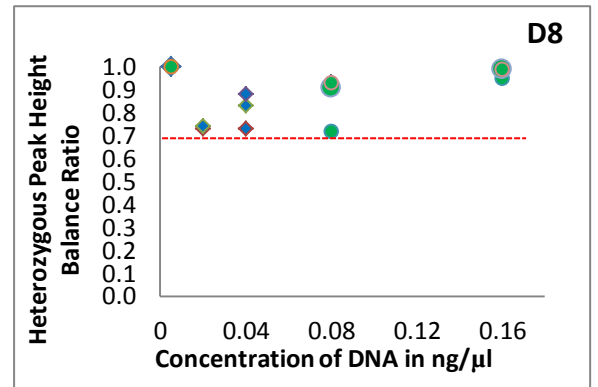
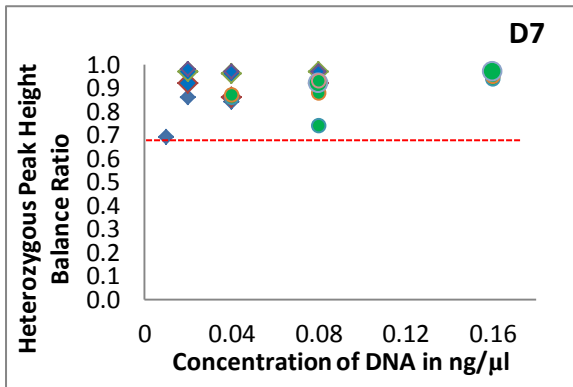
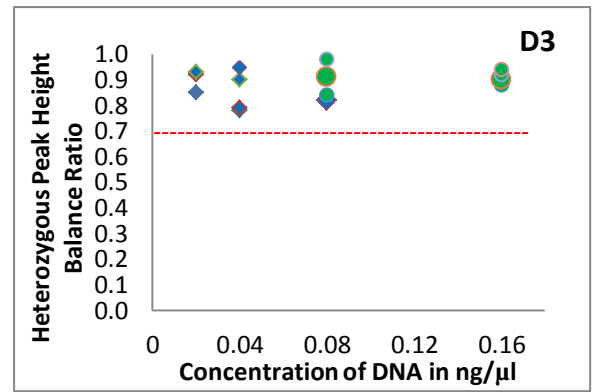
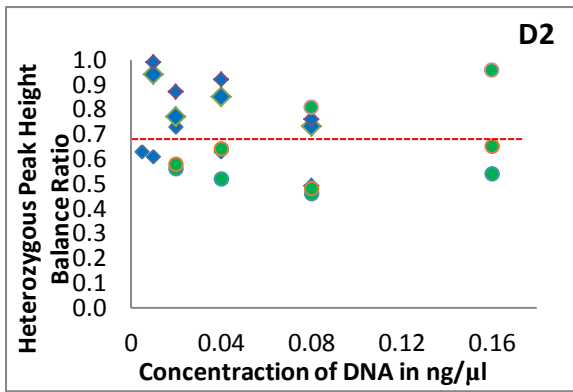


Figure 3.3: Graphs demonstrating the variation in the heterozygous peak balance ratio (Hb) for the amplification of the 25μl (green circles) and 12.5μl (blue diamonds) reactions for PowerPlex® 16HS for each individual loci. The red line indicates the 0.70 threshold for the heterozygous peak balance.

For PowerPlex® 16HS, D3S1358, Penta D, Penta E and TH01 were observed to have the most imbalanced peaks when analysed with a total volume of 25μl. D2 and Penta D also struggled to maintain peak height balances above the threshold when processed with 12.5μl reactions (Figure 3.3). In PowerPlex® 18D, D2S1338 was observed to go below the threshold more often than any other locus (Figure 3.4). This trend was observed in both reaction volumes.

Peak height ratios for 12.5μl reactions were more variable than those observed with the full volume. DNA concentrations which were above 0.04 ng reflected good peak balance for both volumes tested. Lowering the concentrations adversely affected the quality of the peak balance.



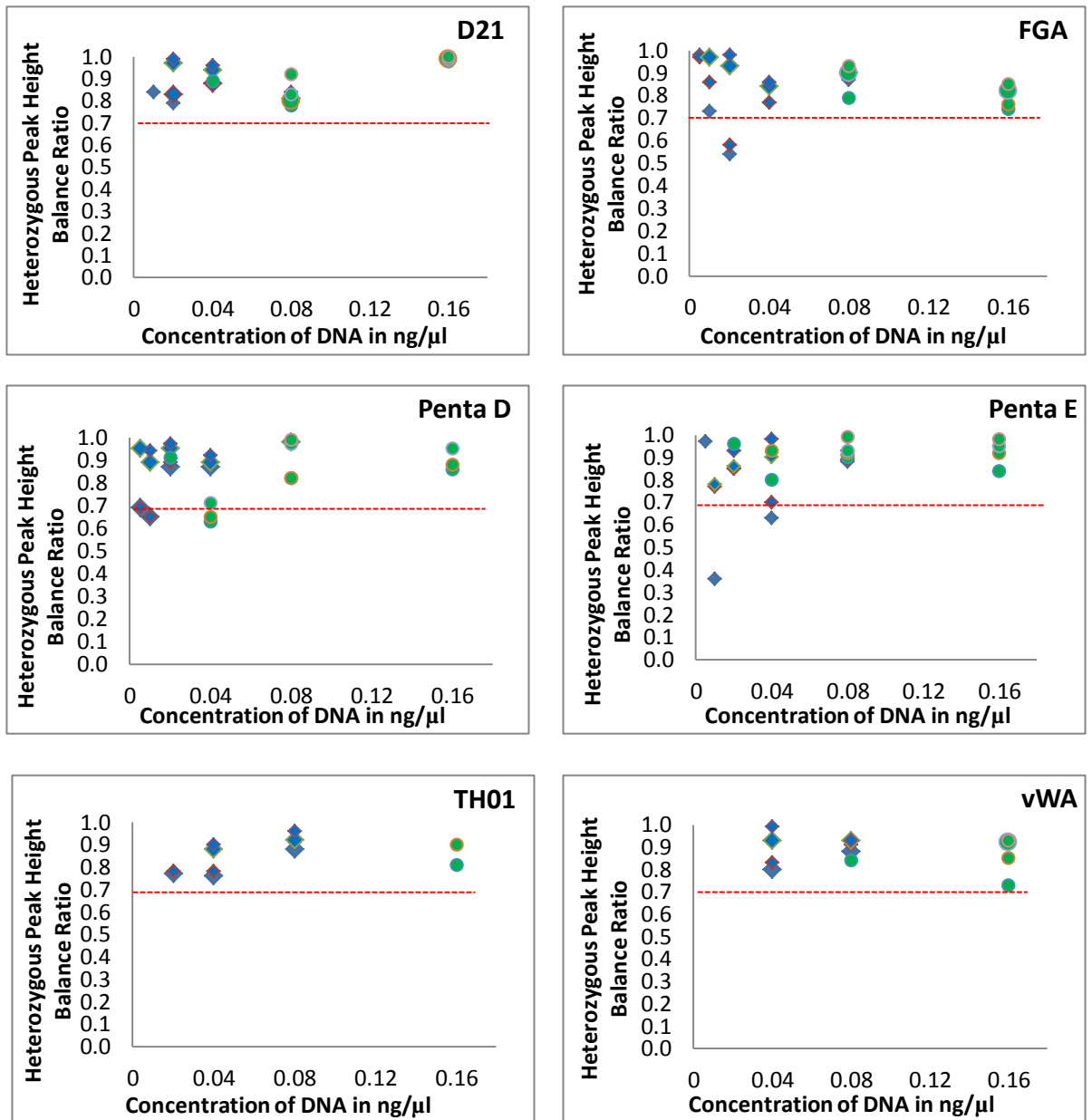


Figure 3.4: Graphs demonstrating the variation in the heterozygous peak balance ratio (Hb) for the amplification of the 25μl (green circles) and 12.5μl (blue diamonds) reactions for PowerPlex® 18D for each individual loci. The red line indicates the 0.70 threshold for the heterozygous peak balance.

3.3.2 Results of Epithelial Based Samples

Epithelial cell samples were produced in triplicate in order to determine the dilutions to be used for the powder enhancement study (Chapter 5). Samples were evaluated based on a 50 RFU threshold and dilutions which produced a low but consistent result for both kits were selected for use in further studies. Low but consistent means the peak heights for the samples were close or at 50 RFU but not below this threshold for the triplicate sample. For the samples in Table 3.6, dilutions x2 and x10 were observed to give full profiles above the threshold for PowerPlex® 16HS. PowerPlex® 18D was more successful in that it was able to generate a full profile for samples x2, x10, and x50. However, since the x50 dilutions in the PowerPlex® 16HS samples only produced a partial profile, the dilutions used for the powder study were the x2 and x10 dilutions only.

While full profiles were generated for the x2 and x10 dilutions, overall peak height balance was observed more in PowerPlex® 18D and of the 18 samples ran 12 displayed loci which were above the 0.70 Hb threshold (Figure 3.5 (Bottom)). PowerPlex® 16HS showed strong homozygous peaks which elevated the peak height totals and overall PCR product concentration date, however, of the 18 samples only 9 displayed loci which were above the 0.70 Hb threshold (Figure 3.5 (Top)). Figure 3.6 displays electropherograms generated from both PowerPlex® 16HS and PowerPlex® 18D using x2 dilutions. Figure 3.7 displays electropherograms generated from both PowerPlex® 16HS and PowerPlex® 18D using x10 dilutions. When evaluating these numbers statistically, there was not found be a significant difference between the dilutions or the kits (p-values below 0.05) (*Output Data*). The correct allele calls for the known epithelial cell sample were produced for all developed samples.

Table 3.6: Results showing the minimum, maximum and average peak heights, the profile type, total PCR product and PCR concentration for the various dilutions of epithelial cells amplified at 12.5 μ l with PowerPlex[®] 16HS and PowerPlex[®] 18D. The values are averages of three replicates.

Kit	Dilution	Profile Properties				Total PCR product (in RFU)	PCR product concentration (in RFU/ μ l)
		Max PH	Min PH	Average PH	Profile Type		
PP16HS	x2	29725 (s.d. 10605.2)	71 (s.d. 665.4)	4976.1	FP	358283 (s.d. 23589.0)	28662 (s.d. 2144.5)
	x10	4522 (s.d. 753.4)	146 (s.d. 104)	1263.7	FP	90986 (s.d. 4409.7)	7278.9 (s.d. 400.9)
	x50	1179 (s.d. 401.9)	50 (s.d. 4.9)	242.6	PP12	12856 (s.d. 2685.4)	1028.3 (s.d. 244.1)
	x100	1150 (s.d. 133.7)	50 (s.d. 15.4)	240.1	PP8	10563 (s.d. 602.9)	845.0 (s.d. 54.8)
	x150	277 (s.d. 93.8)	50 (s.d. 7.1)	116.4	PP3	2794 (s.d. 468.2)	223.5 (s.d. 42.6)
	x200	245 (s.d. 92.0)	50 (s.d. 7.5)	114.8	PP2	1607 (s.d. 362.5)	128.6 (s.d. 33.0)
PP18D	x2	3988 (s.d. 619.1)	676 (s.d. 142.2)	1632.8	FP	132253 (s.d. 6773.8)	10580.2 (s.d. 615.8)
	x10	1654 (s.d. 335.9)	120 (s.d. 113.9)	542.5	FP	43946 (s.d. 3785.6)	3515.7 (s.d. 344.1)
	x50	409 (s.d. 193.3)	52 (s.d. 11.0)	169.6	FP	13567 (s.d. 1351.1)	1085.4 (s.d. 11.0)
	x100	256 (s.d. 28.3)	50 (s.d. 9)	110.8	PP16	6867 (s.d. 411.4)	549.4 (s.d. 37.4)
	x150	296 (s.d. 20.0)	52 (s.d. 3.5)	135.0	PP17	10123 (s.d. 472.0)	809.8 (s.d. 42.9)
	x200	160 (s.d. 28.4)	50 (s.d. 7.2)	76.0	PP6	2432 (s.d. 403.0)	194.6 (s.d. 36.6)

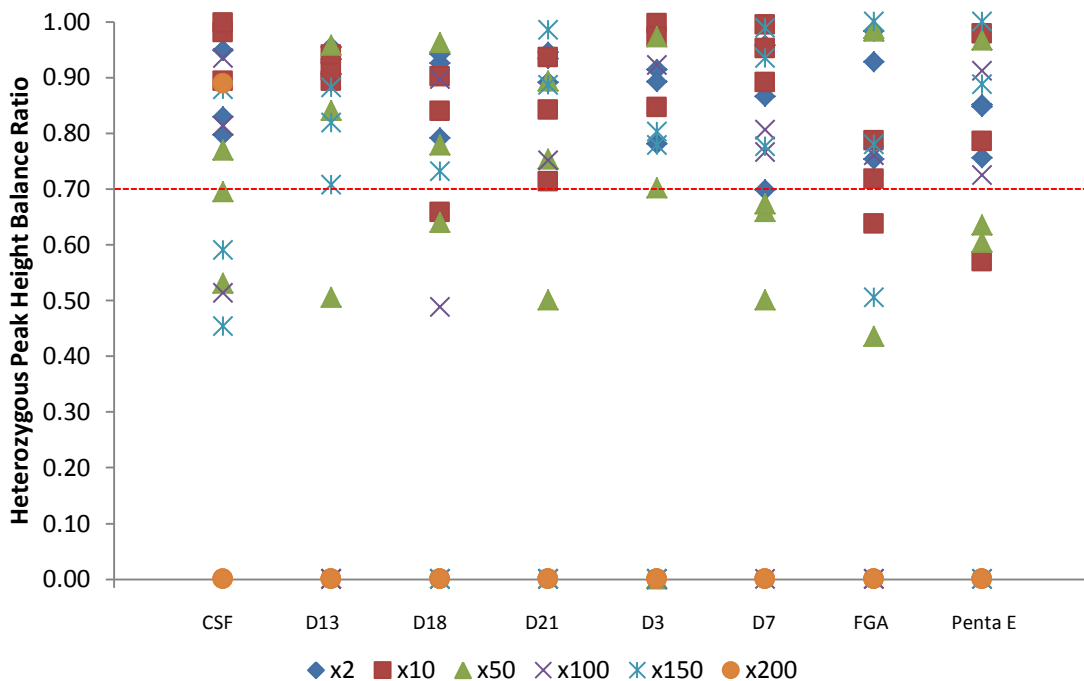
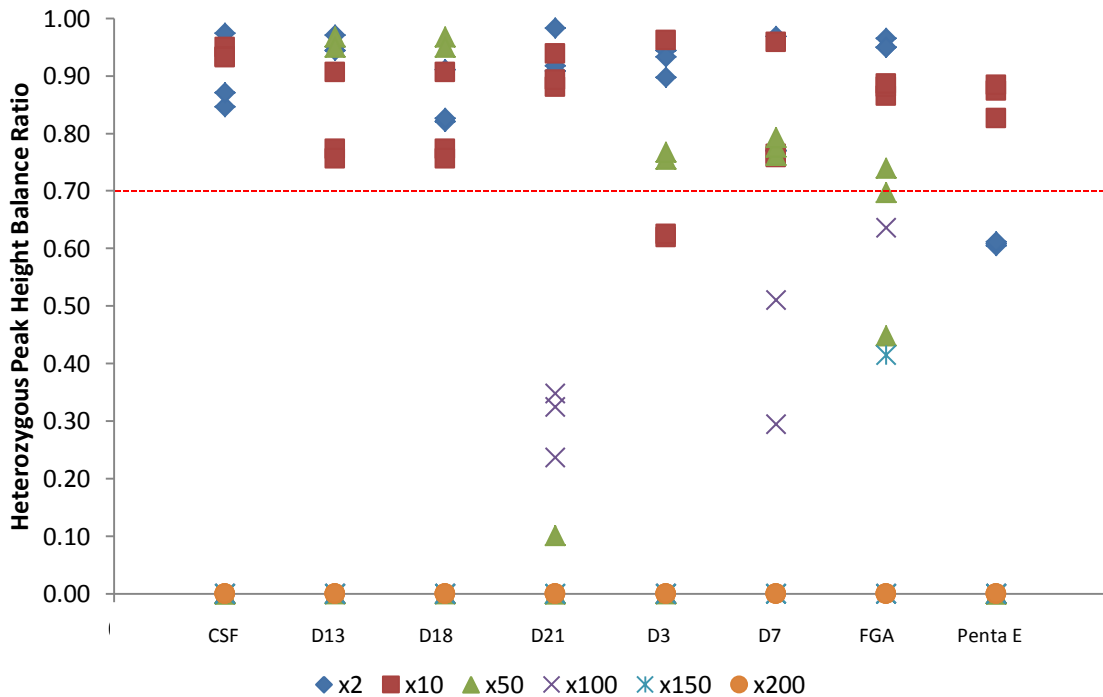


Figure 3.5: Heterozygous loci peak height ratios for epithelial cells at different dilutions when amplified at 12.5 μ l with (Top) PowerPlex[®] 16HS and (Bottom) PowerPlex[®] 18D. The red line indicates the 0.70 Hb threshold for the heterozygous peak balance. Samples displayed are based on three replicates.

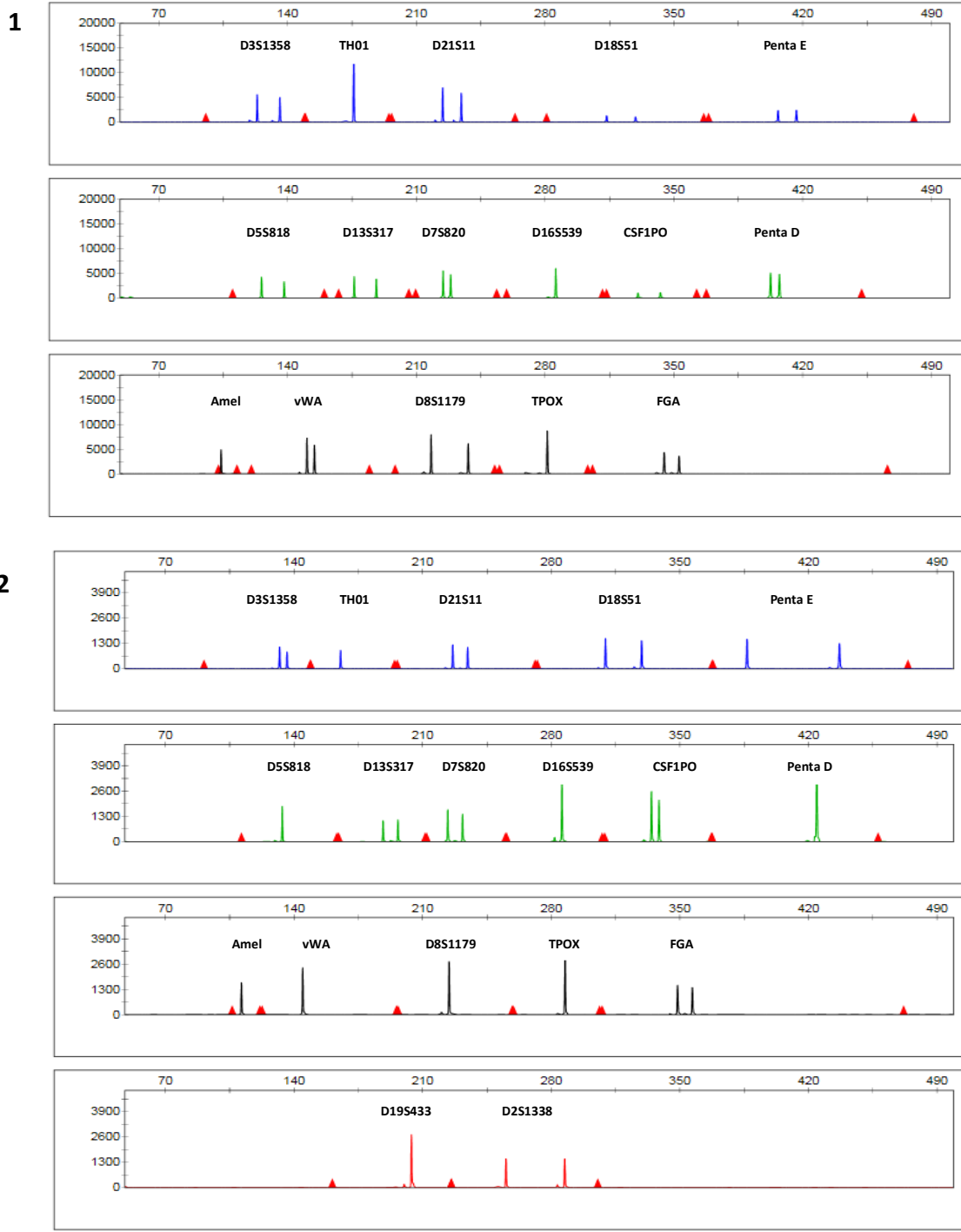
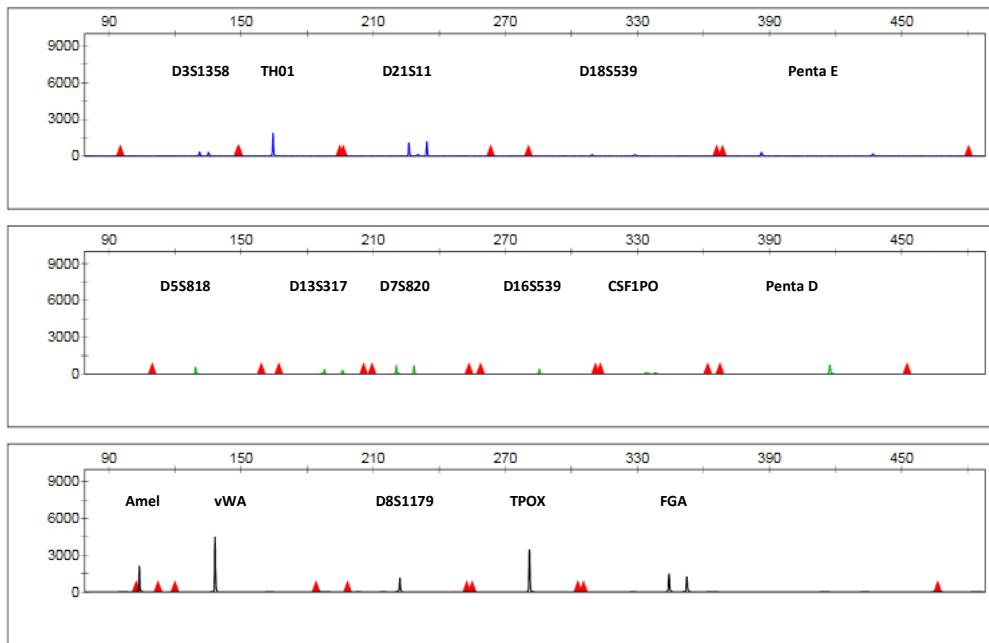


Figure 3.6: Electropherograms displaying DNA profiles generated with epithelial cells at x2 dilution using (1) PowerPlex[®] 16HS (RFU 20,000) and (2) PowerPlex[®] 18D (RFU 5,000). The x-axis represents relative fluorescent units (RFU) and the y-axis fragment size in base pairs.

1



2

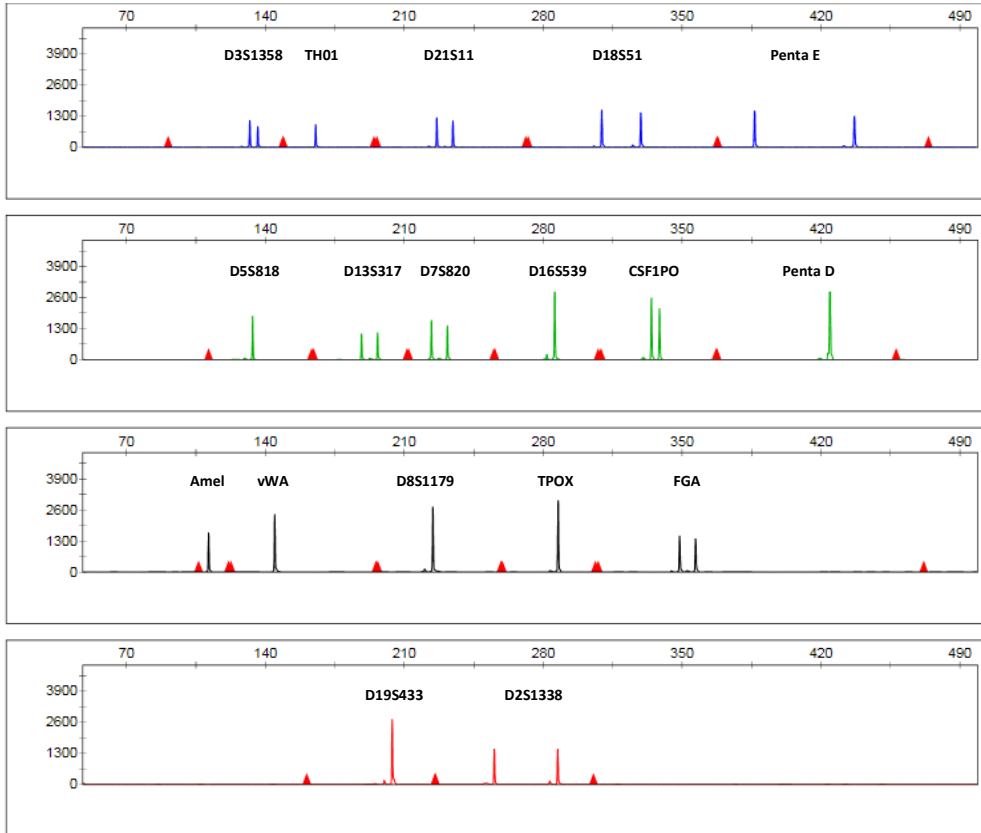


Figure 3.7: Electropherograms displaying DNA profiles generated with epithelial cells at x10 dilution using (1) PowerPlex[®] 16HS (RFU 9,500) and (2) PowerPlex[®] 18D (RFU 5,000). The x-axis represents relative fluorescent units (RFU) and the y-axis fragment size in base pairs.

3.3.3 Results for Whole Blood Samples

Whole blood samples were produced in triplicate in order to determine the dilutions to be used for the chemical enhancement study (Chapter 6). Samples were evaluated based on a 50 RFU threshold and dilutions which produced a low but consistent result for both kits were selected for use in further studies. Low but consistent means the peak heights for the samples were close or at 50 RFU but not below this threshold for the triplicate sample. For the samples in Table 3.7, all dilutions were observed to give full profiles above the threshold for PowerPlex® 16HS. PowerPlex® 18D was not as successful in that it was only able to generate a full profile for samples x2 and x10.

While full profiles were generated on for the x2 and x10 dilutions using PowerPlex® 18D , overall peak height balance was observed more in PowerPlex® 18D and of the 9 samples displaying profiles, the majority of the heterozygous loci showed alleles above the 0.70 Hb threshold(Figure 3.8 (Bottom)). PowerPlex® 16HS showed strong homozygous peaks which elevated the peak height totals and overall PCR product concentration date, however, of the 18 samples only 9 displayed loci which were above the 0.70 Hb threshold (Figure 3.8 (Top)). Figure 3.9 displays electropherograms generated from both PowerPlex® 16HS and PowerPlex® 18D using x2 dilutions. Figure 3.10 displays electropherograms generated from both PowerPlex® 16HS and PowerPlex® 18D using x10 dilutions. When evaluating these numbers statistically, there was not found be a significant difference between the dilutions or the kits (p-values below 0.05) (*Output Data*). The correct allele calls for the known whole blood sample were produced for all developed samples.

Table 3.7: Results showing the minimum, maximum and average peak heights, the profile type, total PCR product and PCR concentration for the various dilutions of whole blood amplified at 12.5µl with PowerPlex® 16HS and PowerPlex® 18D. The values are averages of three replicates.

Kit	Dilution	Profile Properties				Total PCR product (in RFU)	PCR product concentration (in RFU/µl)
		Max PH	Min PH	Average PH	Profile Type		
PP16HS	x2	32293 (s.d. 1818.1)	244 (s.d. 490.1)	6761.6	FP	567977 (s.d. 19716.1)	45438.2 (s.d. 1792.4)
	x10	17664 (s.d. 1043.0)	901 (s.d. 204.6)	4907.0	FP	412187 (s.d.137395.7)	32975.0 (s.d. 194.8)
	x50	11740 (s.d. 1270.2)	794 (s.d. 181.2)	3395.7	FP	285241 (s.d. 12898.4)	22819.3 (s.d. 1172.6)
	x100	5709 (s.d. 713.9)	334 (s.d. 145.2)	2068.0	FP	173710 (s.d. 9437.0)	13896.8 (s.d. 857.9)
	x150	9599 (s.d. 1644.7)	628 (s.d. 108.1)	2851.1	FP	239491 (s.d. 7728.4)	19159.3 (s.d. 702.6)
	x200	7063 (s.d. 860.2)	345 (s.d. 156.8)	2147.5	FP	180392 (s.d. 4392.4)	14431.4 (s.d. 399.3)
PP18D	x2	440 (s.d. 40.2)	51 (s.d. 4.7)	152.1	FP	12320 (s.d. 336.7)	328.5 (s.d. 26.9)
	x10	1449 (s.d. 222.5)	158 (s.d. 98.7)	543.0	FP	29323 (s.d. 4580.1)	7819 (s.d. 366.4)
	x50	2365 (s.d. 132.1)	56 (s.d.516.8)	1230.3	PP6	54133 (s.d. 9170.4)	4330.6 (s.d. 733.6)
	x100	--	--	--	NP	--	--
	x150	--	--	--	NP	--	--
	x200	--	--	--	NP	--	--

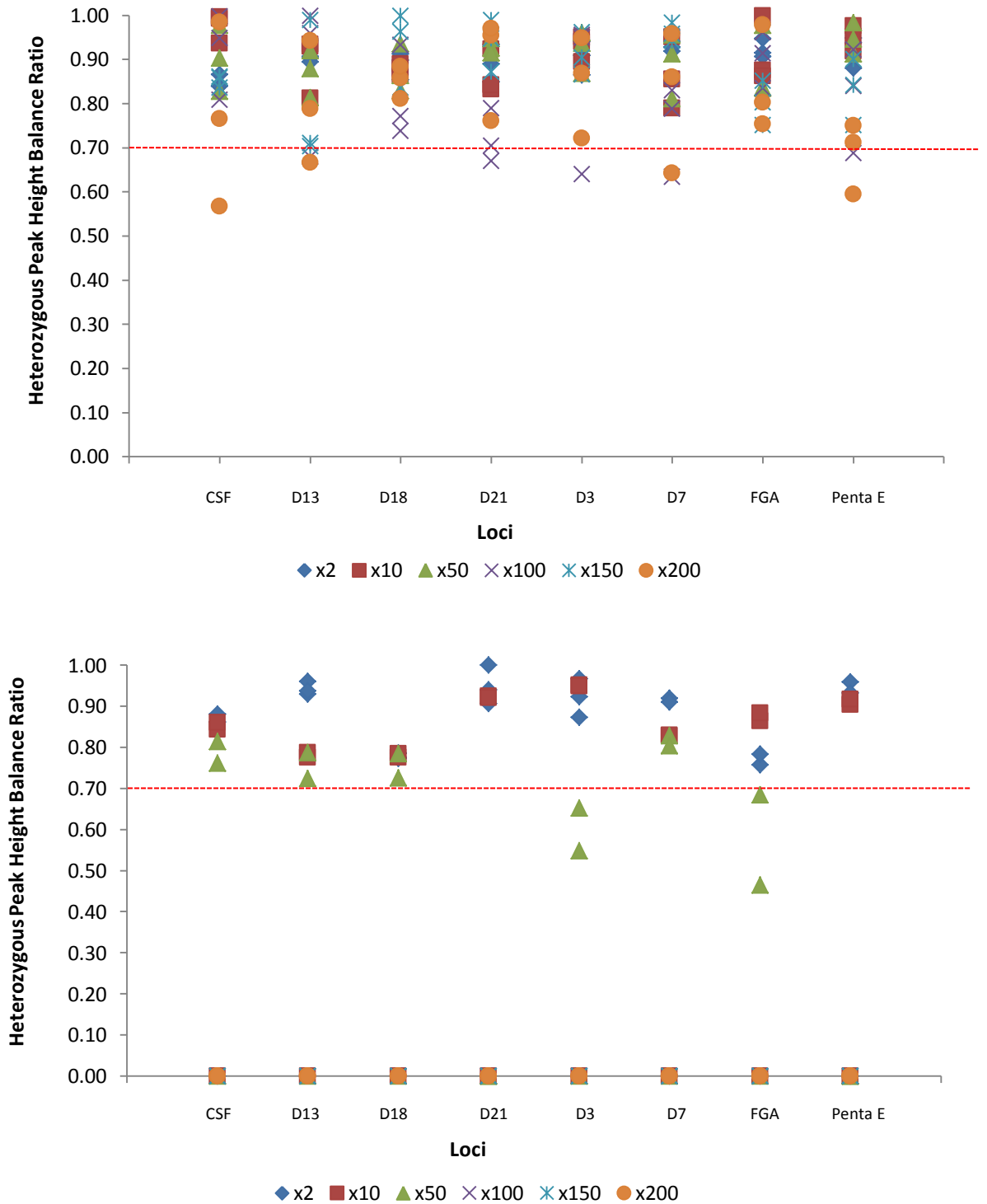


Figure 3.8: Heterozygous loci peak height ratios for whole blood samples at different dilutions when amplified at 12.5 μ l with (Top) PowerPlex[®] 16HS and (Bottom) PowerPlex[®] 18D. The red line indicates the 0.70 Hb threshold for the heterozygous peak balance. Samples displayed are based on three replicates.

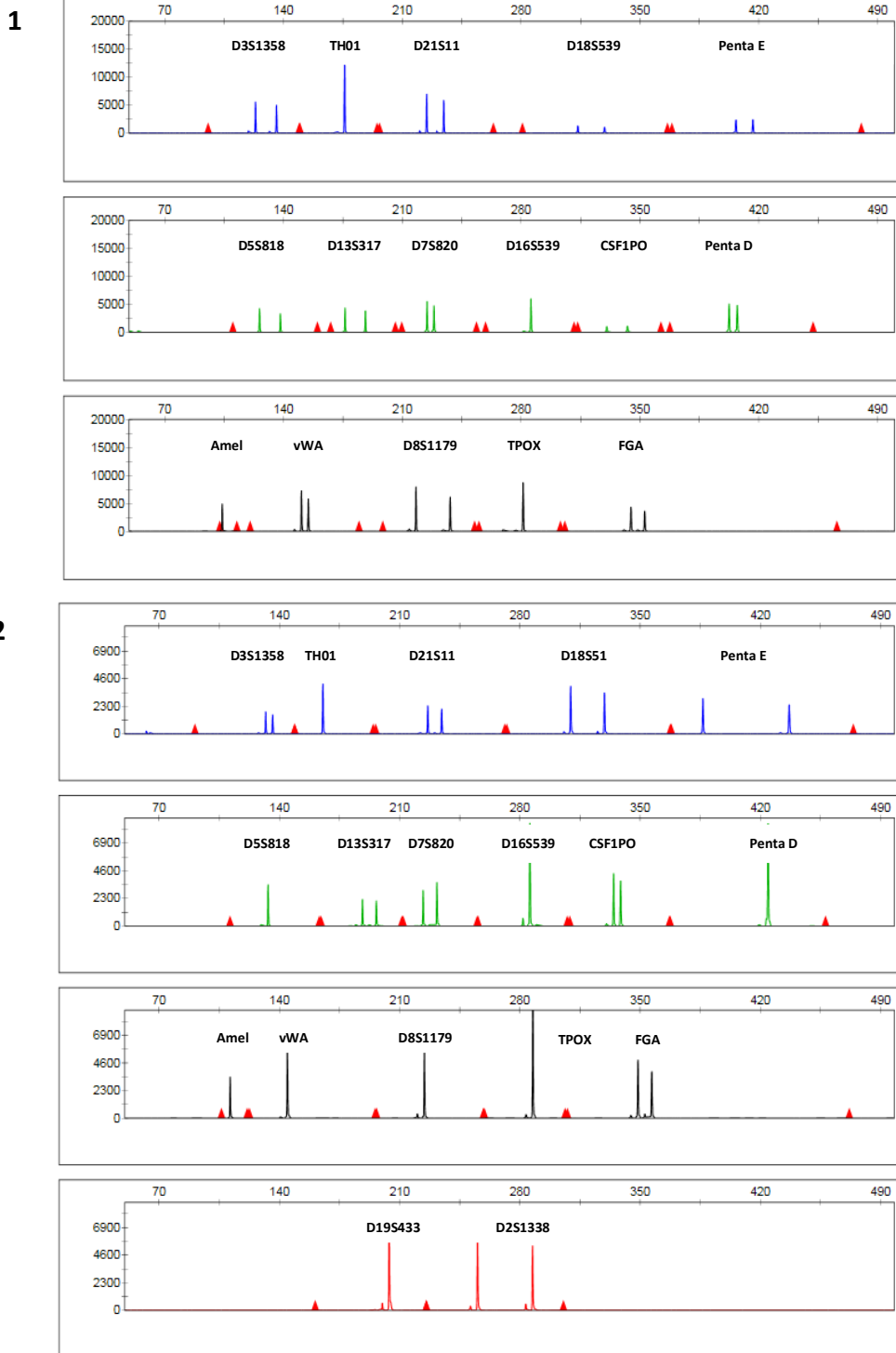
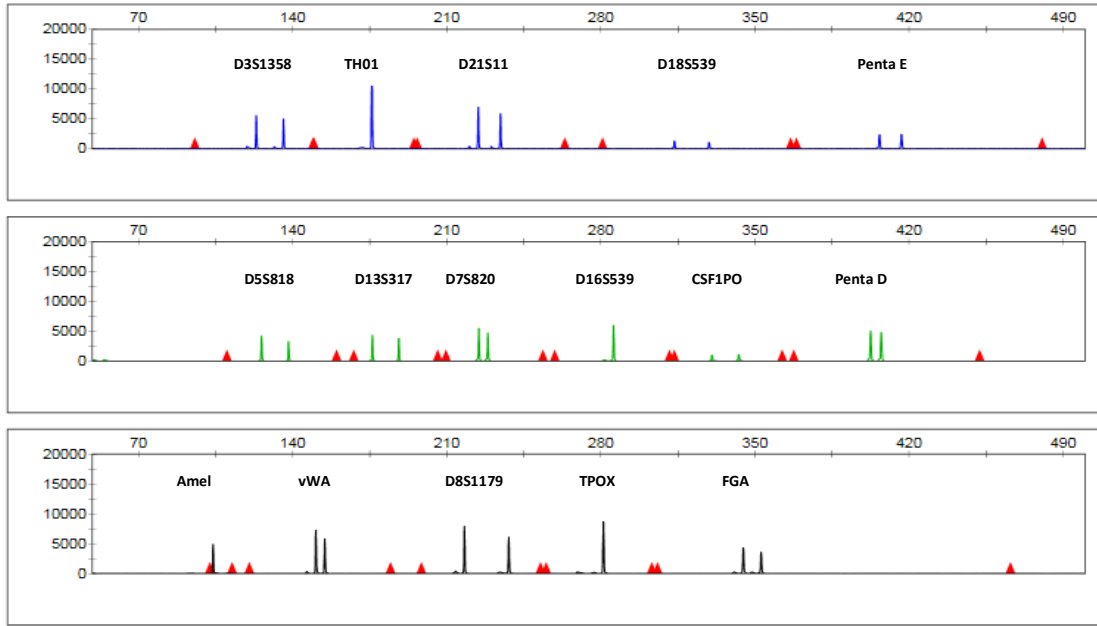


Figure 3.9: Electropherograms displaying full profiles generated with whole blood cells at a x2 dilution using (1) PowerPlex[®] 16HS (RFU 20,000) and PowerPlex[®] 18D (RFU 10,000). The x-axis represents relative fluorescent units (RFU) and the y-axis fragment size in base pairs.

1



2

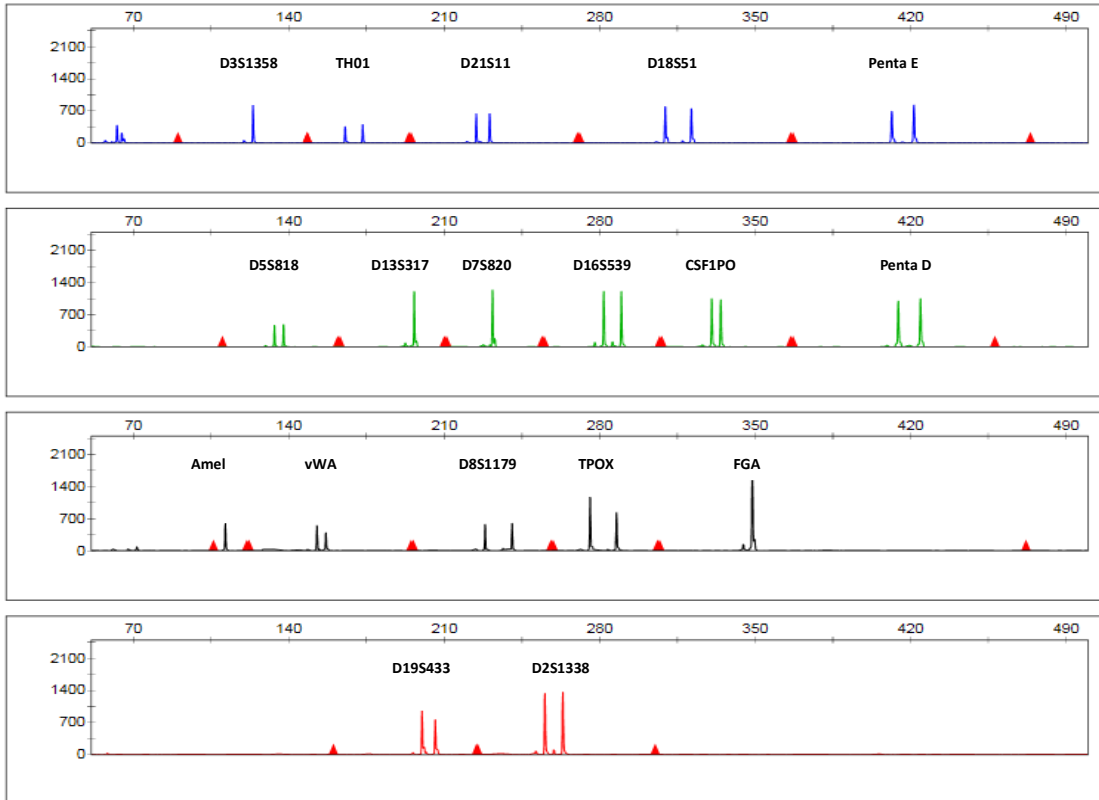


Figure 3.10: Electropherograms displaying full profiles generated with whole blood cells at a x10 dilution using (1) PowerPlex[®] 16HS (RFU 20,000) and PowerPlex[®] 18D (RFU 2,500). The x-axis represents relative fluorescent units (RFU) and the y-axis fragment size in base pairs.

3.3.4 Controls

Commercial internal lane standards with known peak sizes were used with all samples processed for this project. Internal lane standard, ILS600, was run with all samples analysed with PowerPlex[®] 16HS. CC5 ILS500, internal lane standard, was run with every sample analysed with PowerPlex[®] 18D. Multiple allelic ladders were run with each plate of samples placed on the genetic analyser. A ladder correctly identifying all alleles above the minimum threshold was used for analyse and identification of alleles. All samples were analysed at a 50 RFU threshold.

3.4 Discussion

3.4.1 Reduced Volume Reactions (12.5µl)

The amplification of DNA with PowerPlex[®] 16HS and 18D at a reduced volume was found to have a positive effect on the sensitivity and cost efficiency of the amplifications.

PowerPlex[®] 16HS yielded full profiles for all DNA input above 0.13 ng at a 12.5µl reaction. Reaction volumes of 25µl produced full profiles in samples above 0.25 ng and a partial profile with 0.13 ng (PP13) and 0.06 ng (PP1) of DNA. No profiles were generated for samples with 0.06 ng of DNA for reactions with a total volume of 12.5µl. PCR product concentrations (RFU/µl) and the average peak heights for the profiles generated were higher when evaluating 12.5µl reactions than with 25µl. These results are consistent with the data generated by Hoffman and Fenger (2010) for PowerPlex[®] 16 which reported ideal half reaction input DNA to be between 0.25-1 ng. The half reactions were slightly more successful with PowerPlex[®] 16HS than were reflected in the PowerPlex[®] 16 as input DNA at 0.13 ng produced a full profile. This could be due in part to the enhanced buffer system included in PowerPlex[®] 16HS (Ensenberger et al., 2010; Hoffman and Fenger, 2010).

Heterozygous peak balance (Hb) for samples generated with PowerPlex[®] 16HS proved to be almost equal when looking at full (45% below threshold) versus half reactions (50%) across all dilutions and heterozygous loci. This was slightly lower than values presented in the validation studies; however, decreasing amounts of DNA were not evaluated in this study (Ensenberger et al., 2010).

PowerPlex[®] 18D yielded full profiles for DNA input at 2.0 ng and 1 ng with a 12.5µl reaction. Reaction volumes of 25µl produced only full profiles in samples with 2.0 ng of DNA. Partial profiles were generated at all other input DNA volumes, except for 0.06 ng where no profile was generated. PCR product concentrations (RFU/µl) were higher when evaluating 12.5µl reactions than with 25µl. While PowerPlex[®] 18D was not as successful in producing full profiles; however, higher peak heights and more loci were present in the 12.5µl reactions than with the 25µl. This is possibly due to the direct amplification materials which are typically cruder than purified samples and often include inhibitors from the raw DNA sample (Oostdik et al., 2013). It has been noted that adding the same amount of direct amplification material recommended for a full reaction into a reduced reaction volume can negatively impact performance; however, the developmental validation showed reaction volumes $\geq 12.5 \mu\text{l}$ produced reliable full profiles (Oostdik et al., 2013).

Heterozygous peak balance (Hb) for samples generated with PowerPlex[®] 18D proved to be almost equal when looking at full (45% below threshold) versus half reactions (50%) across all dilutions and heterozygous loci. This was slightly lower than values presented in the validation studies; however, decreasing amounts of DNA were not evaluated in this study (Ensenberger et al., 2010).

Across both kits, the amplification products produced exceeds those reported in the validation studies of both kits (Ensenberger et al., 2010; Hoffman and Fenger, 2010; Oostdik et al., 2013). For the purpose of this project, the study showed the validity of the 12.5 µl volumes for the amplification of human DNA and properly characterise the profiles. For studies in this thesis, all amplifications were carried out at 12.5µl.

3.4.2 Epithelial Cell Samples

Epithelial cell samples produced full profiles with PowerPlex[®] 16HS using the x2 and x10 dilutions. Partial profiles were produced with the remaining dilutions tested. The x200 dilution contained the lowest total PCR product (1607 RFU) and provided a partial profile containing 2 loci.

PowerPlex[®] 18D produced profiles for dilutions x2, x10 and x50. Partial profiles which contained all but one and two loci, respectively, were obtained for x100 and x150 dilutions. Profiles at the x200 dilution again gave the lowest total PCR product peak heights (2432

RFU) and a partial profile of 6 loci. The ability of PowerPlex® 18D to perform better than PowerPlex® 16HS could be due in part to the enhanced buffer system included in PowerPlex® 18D (Ensenberger et al., 2010; Hoffman and Fenger, 2010). The PowerPlex® 18D system was also optimized for direct amplification and contains components that can overcome inhibition without the washing or purification step generally needed for STR profiling. The elimination of this step also allows for the retention of more of the deposited sample.

Dilutions x2 and x10 were consistent in both kits and the x10 dilution yielded a profile with low RFUs and fairly balanced peaks. These dilutions were utilized on the laminate substrate for exposure to powder processing.

3.4.3 Whole Blood Samples

For the whole blood samples, PowerPlex® 16HS was more successful than PowerPlex® 18D. PowerPlex® 16HS produced full profiles at all dilutions. This result is consistent with what one would expect to see as the PowerPlex® 16HS samples are extracted, removing inhibitors and other components which may interfere with the STR profiling process. The total PCR product (in RFU) and total PCR concentration (in RFU/ μ l) exhibited a decreasing pattern of numerical values as the sample became more diluted and less DNA template was present in the sample. This was to be expected as the amount of biological material is reducing the higher the dilution goes.

The whole blood samples processed with PowerPlex® 18D were not treated except with the SwabSolution™ prior to amplification; therefore, all the components of the whole blood were still present in the sample. Again, the total PCR product (in RFU) and total PCR concentration (in RFU/ μ l) exhibited a decreasing pattern of numerical values as the sample became more diluted and less DNA template was present in the sample.

PowerPlex® 18D produced profiles for dilutions x2 and x10. A partial profile which contained 6 loci was produced at the x50 dilution. Profiles at the x100, x150, and x200 dilutions produced no profile. The highest value of PCR concentration was also observed at the x10 dilution (7819 RFU/ μ l).

The whole blood samples were much stronger than the epithelial cell samples generated in section 3.4.2. This is possibly due to the blood samples containing $>2\text{ng}/\mu\text{l}$ for each sample which is greater than the epithelial cell samples which contained $<1\text{ng}/\mu\text{l}$ for each sample generated.

Dilutions x2 and x10 were consistent in both kits and the x10 dilution yielded a profile with low RFUs and fairly balanced peaks. These dilutions were utilized on all substrates for exposure to chemical enhancements.

CHAPTER 4.

CONCORDANCE STUDY

The following section describes the evaluation of the concordance of Promega® PowerPlex® 16HS and Promega® PowerPlex® 18D human identification systems.

4.1 Overview

As DNA databases and crime laboratories expand their use of multiplex human identification kits, evaluation of concordance regarding specific autosomal STR products can help identify incorrect or null alleles present in a dataset due to primer binding site mutations. Since these multiplex kits can be composed of different primer sequences, such examination may identify problems regarding discordant alleles.

A significant degree of confidence was placed on the two kits used for this study as both kits are products of Promega® Corporation and have been tested repeatedly for concordance (Budowle et al., 2011). PowerPlex® 16HS contains the same unchanged primer pairs included in PowerPlex® 16 (Ensenberger et al. 2010). PowerPlex® 18D is composed of primers from PowerPlex® 16 which include amelogenin, Penta D, Penta E, and the 13 core CODIS loci and D2S1338 and D19S433 from the PowerPlex® ESI System (Hill et al. 2011; Oostdik et al., 2013).

Table 4.1 lists all of the loci from PowerPlex® 16HS and PowerPlex® 18D, their chromosome locations, repeat category and motif, as well as the published forward and reverse primers. Further details of each of the loci can be found in Appendix 8.

The purpose of this experiment is to

1. Demonstrate the profiles generated with Promega® PowerPlex® 16HS and Promega® PowerPlex® 18D human identification systems are concordant;
2. Identify any discordance if reflected in the data;
3. Discuss any microvariants/off-ladder alleles which may be present in samples;
4. Create allele frequency and comparison charts from samples used in this study and produced with both Promega® PowerPlex® 16HS and Promega® PowerPlex® 18D .

Table 4.1: Loci within Promega® PowerPlex® 16HS and Promega® PowerPlex® 18D kits, their chromosome location, repeat category and motif, and primer sequences.

STR Loci ¹	Chromosomal Location	Category; Repeat Motif	Primer Sequences (F) Forward, (R) Reverse
D2S1338	2q35	Compound; TGCC/TTCC	<i>Primer sequences proprietary to Applied Biosystems®².</i>
D3S1358	3p21.31	Compound; TCTA/TCTG	(F) ACTGCAGTCCAATCTGGGT (R) ATGAAATCAACAGAGGCTTGC
D5S818	5q23.2	Simple; AGAT	(F) GGTGATTTTCTCTTTGGTATCC (R) AGCCACAGTTTACAACATTTGTATCT
D7S820	7q21.11	Simple; GATA	(F) ATGTTGGTCAGGCTGACTATG (R) GATTCCACATTTATCCTCATTGAC
D8S1179	8q24.13	Compound; TCTA/TCTG	(F) ATTGCAACTTATATGTATTTTTGTATTTCATG (R) ACCAAATTGTGTTCATGAGTATAGTTTC
D13S317	13q31.1	Simple; TATC	(F) ATTACAGAAGTCTGGGATGTGGAGGA (R) GGCAGCCCAAAAAGACAGA
D16S539	16q24.1	Simple; GATA	(F) GGGGGTCTAAGAGCTTGTA AAAAAG (R) GTTTGTGTGTGCATCTGTAAGCATGTATC
D18S51	18q21.33	Simple; AGAA	(F) TTCTTGAGCCAGAAAGGTTA (R) ATTCTACCAGCAACAACACAAATAAAC
D19S433	19q12	Compound; AAGG/TAGG	<i>Primer sequences proprietary to Applied Biosystems®.</i>
D21S11	21q21.1	Complex; TCTA/TCTG	(F) ATATGTGAGTCAATTCCCAAG (R) TGTATTAGTCAATGTTCTCCAGAGAC
FGA	4q31.3; Alpha fibrinogen, 3 rd Intron	Compound; CTTT/TTCC	(F) GGCTGCAGGGCATAACATTA (R) ATTCTATGACTTTGCGCTTCAGGA
TH01	11p15.5; Tyrosine Hydroxylase, 1 st Intron	Simple; TCAT	(F) GTGATTCCCATTGGCCTGTTC (R) ATTCCTGTGGGCTGAAAAGCTC
vWA	12p13.31; vonWillebrand Factor, 40 th Intron	Compound; TCTA/TCTG	(F) GCCCTAGTGGATGATAAGAATAATCAGTATGTG (R) GGACAGATGATAAATACATAGGATGGATGG
Penta E	15q26.2	Simple; AAAGA	(F) ATTACCAACATGAAAGGGTACCAATA (R) TGGGTTATTAATTGAGAAAACCTCCTTACAATTT
Penta D	21q22.3	Simple; AAAGA	(F) GAAGGTCTGAAGCTGAAGTG (R) ATTAGAATTCTTTAATCTGGACACAAG
TPOX	2p25.3; Thyroid peroxidase, 10 th Intron	Simple; AATG	(F) GCACAGAACAGGCACTTAGG (R) CGCTCAAACGTGAGGTTG
CSF1PO	5q33.1; c-fms proto-oncogene, 6 th Intron	Simple; AGAT	(F) CCGGAGGTAAAGGTGTCTTAAAGT (R) ATTCCTGTGTGACAGACCCTGTT ³

¹ D2S1338 and D19S433 are in **bold** to represent the 2 additional loci in PowerPlex® 18D.

² Applied Biosystems is now Life Technologies.

³ Red 'G' represents the C→T single nucleotide polymorphism (SNP) at the end of the CSF1PO reverse primer which could result in the drop/imbalance of allele 9.

4.2 Experimental Design

150 buccal swabs were collected using sterile OmniSwabs (Whatman[®]) from unrelated individuals from three different populations as detailed in Section 2.4.2. Each person sampled supplied two swabs, one for analysis using standard extraction procedures and the other for direct amplification. The samples were processed once with Promega[®] PowerPlex[®] 16HS and once with Promega[®] PowerPlex[®] 18D (no replicates). All extracted samples were quantitated using the NanoDrop 2000. The data can be seen in Appendix 7. Cell counts were not conducted for the direct amplification samples for this portion of the project.

4.3 Results

4.3.1 Evaluation of Concordance

Concordance evaluations for Promega[®] PowerPlex[®] 16HS and Promega[®] PowerPlex[®] 18D were performed by comparing the two sets of typing results with each other. Since these multiplex kits are composed of the same primer sequences, it is expected to yield comparable results with the absence of null and discordant alleles. Of the 150 samples profiled with 16HS, 110 produced full profiles, 28 partial profiles and 12 exhibited no profiles. PowerPlex[®] 18D produced full profiles for all 150 samples. Of the full and partial profiles detected, all allele calls were harmonious between the two kits. (A list of the partial profiles from PowerPlex[®] 16HS can be found in Appendix 5.)

4.3.2 Peak Height Assessment

Peak height data could not be directly compared since the two kits were run on two different genetic analyser platforms. The PowerPlex[®] 16HS data (for this study alone) were produced on an ABI 3130 Genetic Analyser while the PowerPlex[®] 18D data generated on an ABI 3500 Genetic Analyser. According to documentation from Thermo Fisher Scientific, the “3500 series data has approximately 4x RFU dynamic range increase over the 31XX platforms”. Figures 4.1 and 4.2 represent the average peak height data sets for all concordance samples processed using PowerPlex[®] 16HS and 18D, respectively. D2S1338 and D19S433 are represented on the direct amplification figure only as they are only present in the PowerPlex[®] 18D kit.

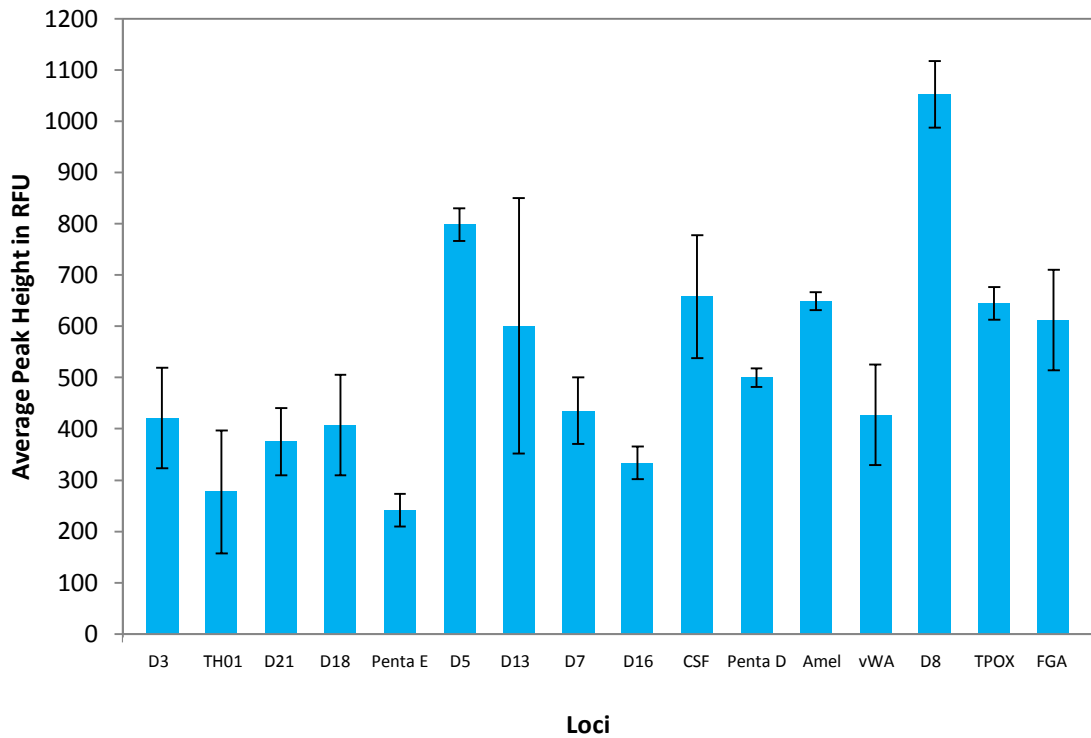


Figure 4.1: Bar graph representation of the average peak heights (in RFU) by locus for 150 profiles generated using the standard extraction method and profiled using PowerPlex® 16HS. Error bars represent the standard deviation.

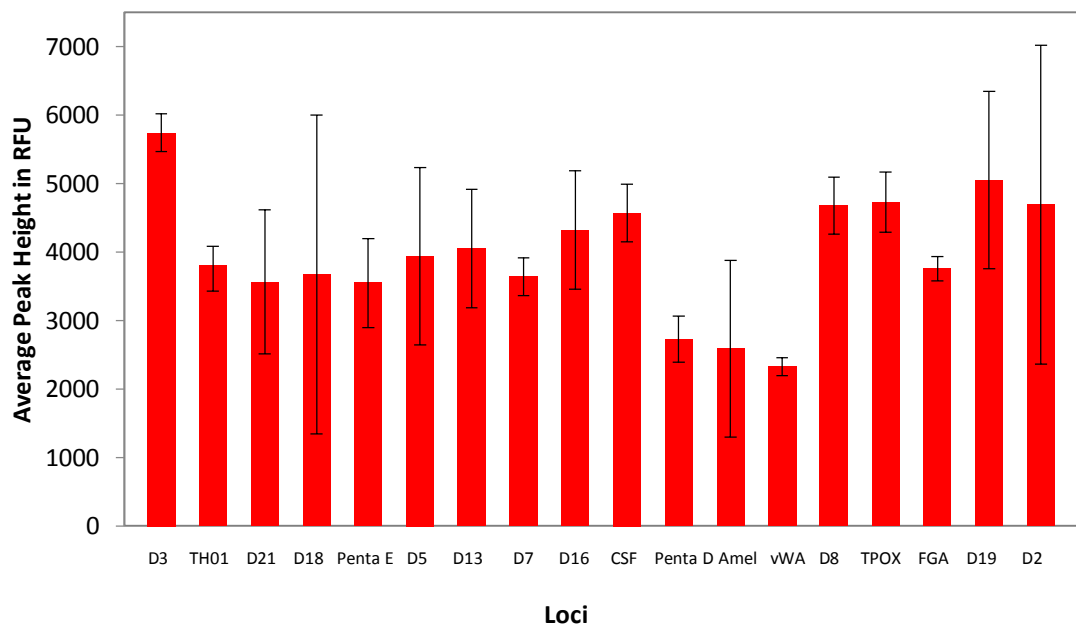


Figure 4.2: Bar graph representation of the average peak heights (in RFU) by locus for 150 profiles generated using the standard extraction method and profiled using PowerPlex® 18D. Error bars represent the standard deviation.

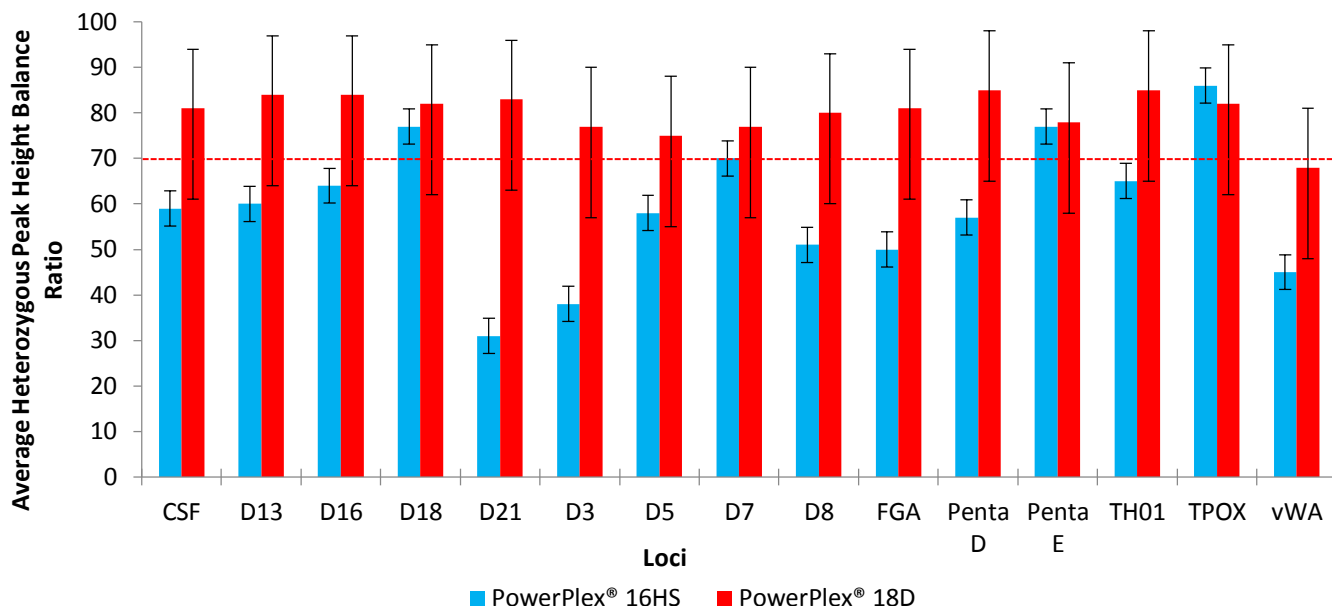


Figure 4.3: Bar graph representation of the average heterozygous peak height balance ratio by locus for 50 profiles generated for the *Mexican* population using both PowerPlex® 16HS and PowerPlex® 18D. The red line indicates the 0.70 Hb threshold for the heterozygous peak balances. Error bars represent the standard deviation.

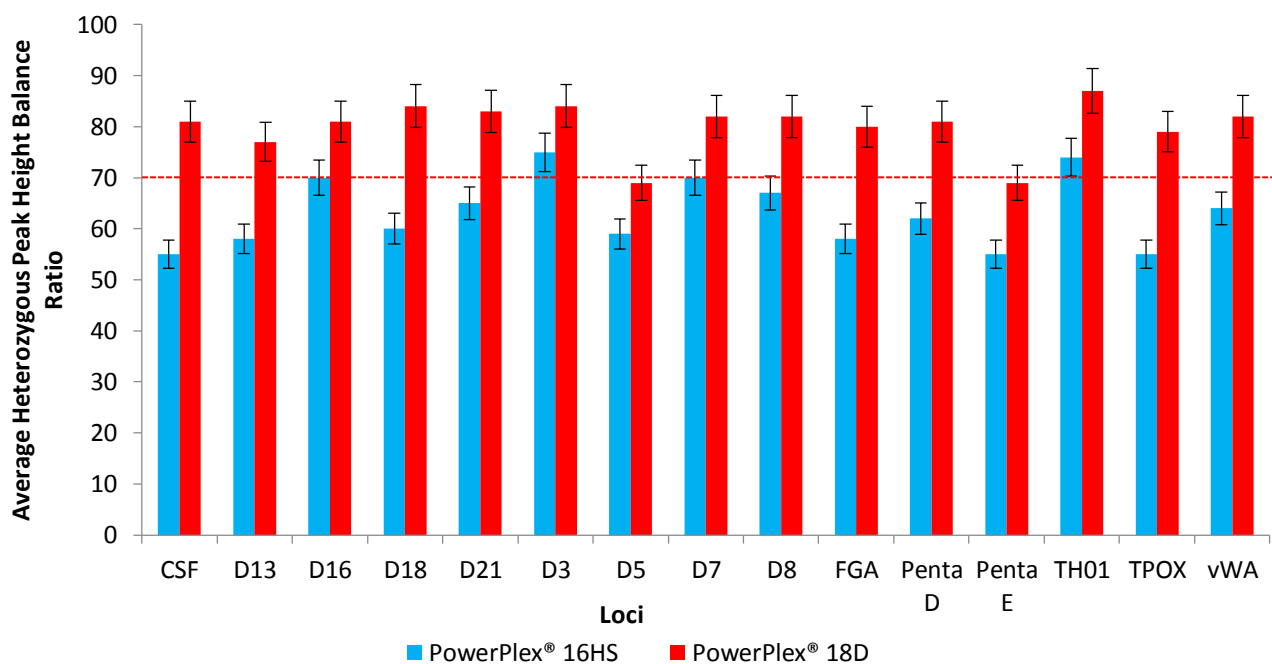


Figure 4.4: Bar graph representation of the average heterozygous peak height balance ratio by locus for 50 profiles generated for the *Caucasian* population using both PowerPlex® 16HS and PowerPlex® 18D. The red line indicates the 0.70 Hb threshold for the heterozygous peak balances. Error bars represent the standard deviation.

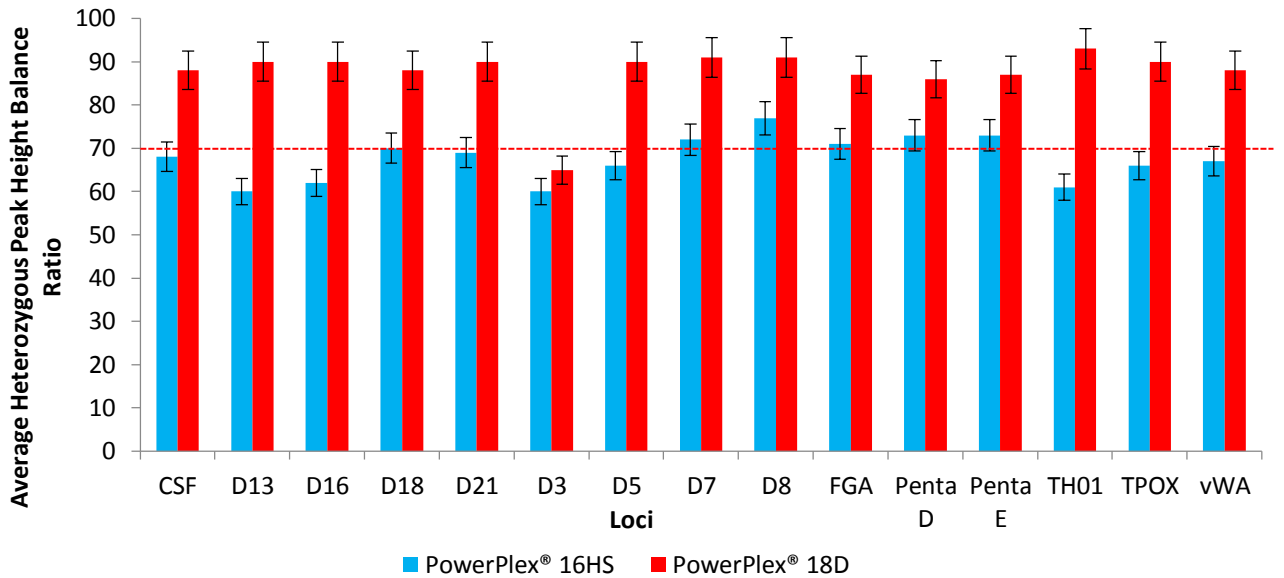


Figure 4.5: Bar graph representation of the average heterozygous peak height balance ratio by locus for 50 profiles generated for the African American population using both PowerPlex® 16HS and PowerPlex® 18D. The red line indicates the 0.70 Hb threshold for the heterozygous peak balances. Error bars represent the standard deviation.

The peak maximum and minimum for PowerPlex® 16HS were 1574 RFU and 50 RFU respectively. The peak maximum and minimum for PowerPlex® 18D were 5974 RFU and 50 RFU respectively.

Peak balance (Hb) was observed more in PowerPlex® 18D with more heterozygous loci appearing above the 0.70 threshold. Figures 4.3-4.5 represent a comparison of each of the populations which had samples displaying heterozygous alleles within their profiles.

4.3.3 Variant Alleles

During the analysis of the samples several microvariants and/or off ladder alleles were observed. All microvariants and/or off ladder alleles were correctly called in both kits. A list of these alleles, their structure and size are listed in Table 4.2.

Table 4.2: Microvariant (MV) and off ladder (OL) alleles produced in both PowerPlex® 16HS and PowerPlex® 18D kits.

<i>Sample</i>	<i>Locus</i>	<i>Allele</i>	<i>Repeat Structure</i>	<i>Size</i>	<i>Reference</i>
25M	D7	10.3 (MV)	<i>Not Published</i>	234bp	(Allor et al., 2005)
46W	D16	7 (OL)	[GATA] ₇	272bp	STRBase (Butler, 2015)
41B	D18	15.2 (MV)	[AGAA] ₁₅ AG	320 bp	(Barber and Parkins, 1996)
11M	D18	16.1 (MV)	[AGAA] ₃ A[AGAA] ₁₃	323 bp	(Allor et al., 2005)

4.3.4 CSF1PO

Previous publications indicate that allele 9 in CSF1PO may be observed to drop out. For the data collected, no samples were observed to have a homozygous allele 9. Six samples out of the 150 produced were observed to have a heterozygous CSF1PO containing an allele 9. All six samples were called correctly. In 4 of the 6 samples, PowerPlex® 18D provided peak balances closer to 1.0 which is reflected in Table 4.3. All samples produced alleles above the ≥ 0.70 Hb threshold.

Table 4.3: CSF1PO peak balance ratios for profiles containing allele 9 for PowerPlex® 16HS and PowerPlex® 18D.

Sample	Allele Call	PP16HS	PP18D
		<i>Peak Height Percentage</i>	<i>Peak Height Percentage</i>
9M	9,10	0.94	0.92
13B	9,12	0.85	0.92
15M	9,10	0.70	0.84
17B	9,11	0.96	0.95
23B	9,12	0.98	0.95
33B	9,12	0.73	0.92

4.3.5 Allele Frequencies

While the samples collected were not sufficient for a population study, the allele frequencies were calculated and compared to the published allele frequency tables provided by Promega Corporation. Allele frequency data for 16 STRs included in PowerPlex 16HS System (CSF1PO, D3S1358, D5S818, D7S820, D8S1179, D13S317, D16S539, D18S51, D21S11, FGA, Penta D, Penta E, TH01, TPO and VWA) and 18 STRs included in PowerPlex 18d which contains all the loci listed above in addition to D19S433 and D2S1338 in a sample of 150 unrelated individuals was reported. The allele frequency, observed heterozygosity (H_{ob}), expected heterozygosity (H_{ex}), power of discrimination (PD) and probability of exclusion (PE) were also calculated using Powerstats version 1.2 (Promega Corporation) for all 150 samples (Appendix 9). Data tables were also created to compare the allele frequencies calculated and the standard deviations for each calculated (Appendix 9). Details of each of the loci contained in the kits can be found in Appendix 8.

4.4 Discussion

PowerPlex[®] 18D produced well-balanced profiles across all loci tested. More profiles with heterozygosity peak height balances at or over 0.70 were observed with 18D (91%) than when compared to 16HS (63%). The ability to produce higher quality profiles when using the direct amplification kit has been attributed to an improved Master Mix which helps to overcome inhibition and allows for some level of tolerance in primer mismatching. While the exact components of the new reagents are not published one could guess that higher salt concentrations and possibly different DNA polymerases aid in reducing inhibition and allow for the tolerance of primer binding site mismatches (Zhang et al., 2010; Bellstedt et al., 2010). PowerPlex[®] 16HS failed to produce full profiles for 28 of the samples and 12 profiles were not observed at all. Of the full and partial profiles which were produced all alleles matched when comparing both kits.

Microvariants are common variations encountered when reviewing DNA profiles generated with STR markers. Alleles that contain an incomplete repeat unit compared to the more commonly observed alleles are referred to as microvariants. When reviewing the data generated for this chapter, three microvariants alleles were noted as reflected in Table 4.2. These alleles were seen in both profiles generated by both kits, PowerPlex[®] 16HS and PowerPlex[®] 18D.

Off-ladder alleles may also be noted when reviewing data. Off-ladder alleles manifest themselves in two ways; 1) peaks that appear smaller or larger than the allelic ladder and/or 2) peaks that lie between the designated allelic ladder peaks. One off-ladder allele, 7 in D16, was also seen and falls between designated alleles in the allelic ladder. As this allele was repeated with a different kit with the same result, it is accepted as a true microvariant allele which falls between alleles 5 and 8 in the allelic ladder. When reviewing the National Institute for Standards and Technology STRBase, the allele has been documented 3 other times; two in casework scenarios and one in a paternity case involving a mother and child (Butler, 2015). This was noted in both profiles generated by both, PowerPlex[®] 16HS and PowerPlex[®] 18D and is reflected in Table 4.2.

4.4.1 CSF1PO

Publications produced by NIST (The U.S. National Institute for Standards and Technology) and subsequently presented at the ISFG Conference (International Society of Forensic Genetics) show that CSF1PO exhibits drop-out in regards to allele 9 when analysing with PowerPlex[®] 16 (Vallone et al., 2011). This comes from the C→T single nucleotide polymorphism (SNP) at the end of the CSF1PO reverse primer. In some cases when using PowerPlex[®] 16HS[®], the allele is exhibited with a low signal resulting in a peak height imbalance within a heterozygous profile. PowerPlex[®] 18D has not shown any drop-out of the allele supporting the notion that the Master Mix has been enhanced. The allele 9 drop-out/low signal (signal below the 0.70 Hb threshold) was not observed in any of the samples analysed for this experiment as described in Section 4.3.4. In future chapters of this thesis, an evaluation of the data will include an assessment of allele 9 as the known profile for sample A in the chemical enhancement of blood chapter (Chapter 6) and sample B in the enhancement of epithelial cells chapter (Chapter 5), have a heterozygous 9, 12 allele call for CSF1PO.

CHAPTER 5.

EVALUATION OF EPITHELIAL CELL SAMPLES PROCESSED WITH FINGERPRINT POWDERS

The following section describes the evaluation and comparison of Promega® PowerPlex® 16HS and Promega® PowerPlex® 18D human identifications systems on the mock latent fingerprint samples which have been processed with standard black powder, magnetic flake, and standard white powder.

5.1 Overview

A common physical method for processing latent fingerprints is the application of a fine powder to enhance or visualize the latent print (Bridges, 1942). This is generally accomplished by utilizing a fibre-glass or camel hair brush for powder application to the latent fingerprint. While the powder binds to the ridges which are deposited onto the substrate, biological material is also transferred to the surface providing a second viable source of DNA evidence which can be individualizing. However, limitations apply when a fingerprint is smudged or does not contain enough identifying characteristics and the print cannot be analyzed. In such cases, DNA evidence becomes the primary focus in identification and individualization of the print.

While the deposit of the print varies greatly from individual to individual as outlined in Chapter 1, it is relevant to review the effects of fingerprint enhancements on subsequent DNA profiling. This is especially crucial when evaluating a direct amplification method which does not require standard DNA extraction in order to provide a high quality, pure DNA sample free from potential contaminants and PCR inhibitors such as proteins, other cellular debris and the powder residue deposited on the print. Through careful experimental design, which eliminates the variability of deposit by touching, a comparison can be conducted between two DNA profiling methods, one which employs extracted DNA and the other lysed cells which are directly amplified on samples which have been processed with various fingerprint powders.

Three common powders were selected for this study: black powder, magnetic flake, and white powder. Black powder is manufactured from a variety of carbon-based powders (such as lampblack, graphite, and charcoal) which readily adheres to the deposit (Bleay et.al, 2012; Miller, 2013). Black powder is applied with a fibre-glass brush (Figure 5.1A). Magnetic flake is composed of a black or other pigmented powder (black was used for the samples in this study) and a magnetic component such as iron particles (Miller, 2013). A magnetic brush (Figure 5.1B) consisting of a magnet inside plastic sheath or a non-ferrous metal wand attracts the magnetic flake creating a bulb of powder at the end of the sheath/wand. This is utilized like a brush and gently moved across the deposit to develop the area. White powder is composed of titanium dioxide or other white powder which adheres to the deposit left on a surface (Bleay et.al, 2012). White powder is also applied with a fibre-glass brush. A review of the different compositions of fingerprint powders can be seen in Chapter 1, Table 1.3.



Figure 5.1: (A) Example of a fibre-glass brush used for powder processing (Evident, 2015). (B) Example of a magnetic wand with a ‘bulb’ of powder at the end of the wand (Arrowhead Forensics, 2015). This ‘bulb’ acts as the brush when processing a surface.

The specific objectives of this chapter are to:

1. Amplify and analyse samples which have been processed with three commonly used fingerprinting powders- black powder, magnetic flake, and white powder and used to generate DNA profiles with PowerPlex[®] 16HS and PowerPlex[®] 18D and
2. Assess the ability to generate complete DNA profile with PowerPlex[®] 16HS and PowerPlex[®] 18D under various sample dilutions which have been exposed to the commonly used fingerprinting powders. This is done by evaluating the electropherograms in terms of number of loci amplified and peak height imbalances;

3. Evaluate the profiles for artefacts such as dye blobs, stutters, pull-up, and split peaks which may be present in the generated profiles.

5.2 Experimental Design

Two buccal swabs were collected from two unrelated individuals (individuals A and B) using sterile OmniSwabs (Whatman®). Epithelial cells were then isolated using the process described in Section 2.4.3. The cells were then deposited onto the laminate substrates, allowed to dry and then developed using the three selected powders: black powder, magnetic flake, and white powder following the procedure outlined in Section 2.4.3.2. Black and white laminate were used in order to maximize visual contrast of the powders once the samples were processed. Standard black powder and magnetic flake were processed using a fibre-glass brush (black powder) and a magnetic wand (magnetic flake) on white laminate while white powder was processed using a fibre-glass brush on black laminate. Once processed with the individual powders, photographs were taken to document the developed deposit. Using cotton swabs, samples from each of the laminates were then taken and subsequently processed in accordance with section 2.5.

In addition to the samples processed with powder, a series of samples which were not exposed to powder processing were analysed using the same methods described in section 2.5. This data was used for comparison and is labelled as ‘no powder’ on subsequent data charts.

5.3 Results

Results were generated utilizing three separate dilutions; x1, x2, and x10 as was determined in the sensitivity study to give a full profile above the 50 RFU threshold (Section 3.3.2). Each sample was photographed post processing to document sample size consistency across samples, dilutions and powder types (Figure 5.2). The samples were photographed post-processing only due to the epithelial cell solution being transparent once dry. Each sample deposit was approximately 10-15mm. It was important for the sample sizes to be consistent in order for the powder deposit to be roughly the same.

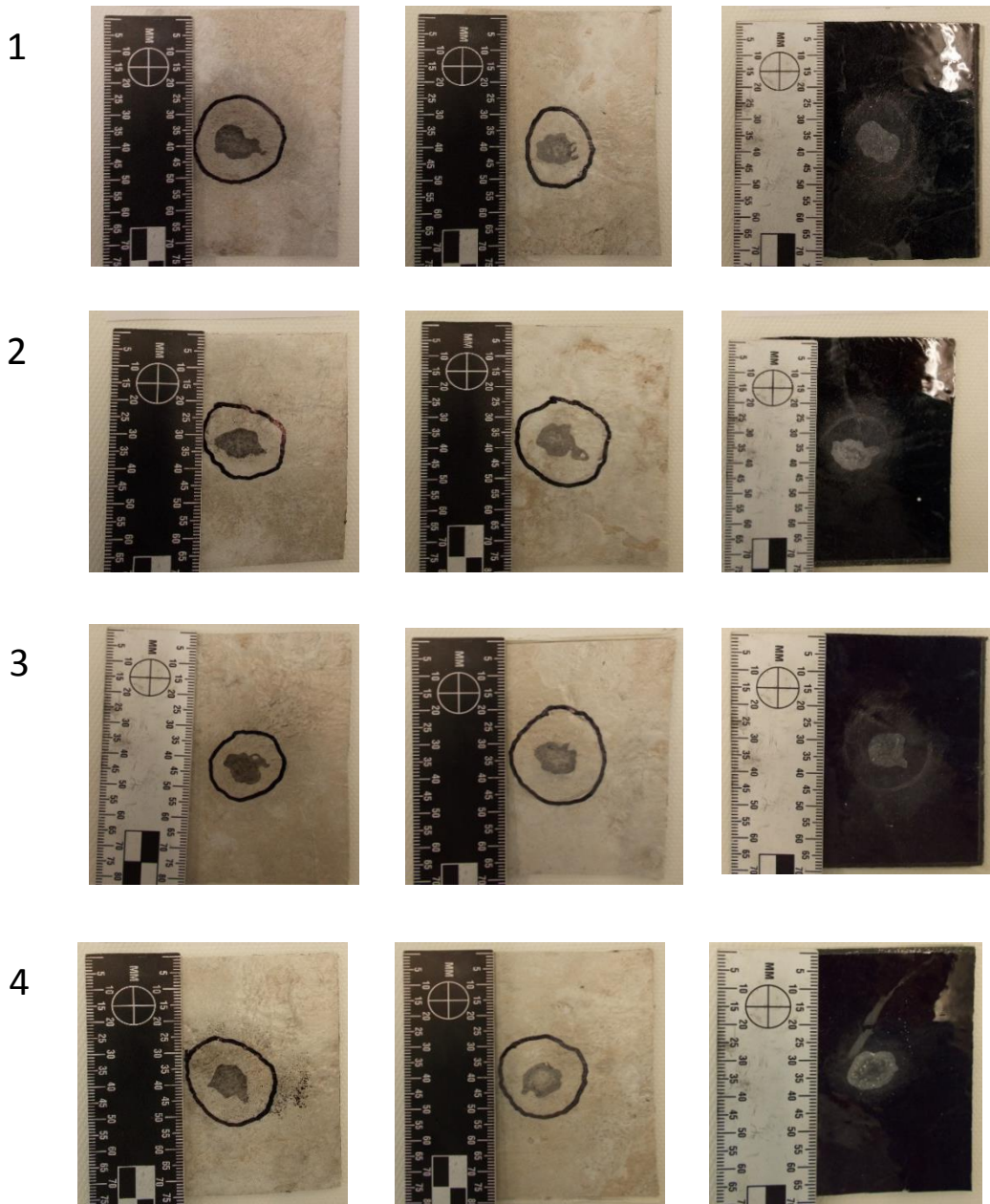


Figure 5.2: Photographs of white and black laminate which exhibit developed epithelial deposits with standard black powder, magnetic flake and white powder (left to right, respectively) for samples A and B with a x2 dilution. Row 1 depicts sample A which was analysed with PowerPlex[®] 16HS. Row 2 depicts sample A which was analysed with PowerPlex[®] 18D. Row 3 depicts sample B which was analysed with PowerPlex[®] 16HS. Row 4 depicts sample B which was analysed with PowerPlex[®] 18D.

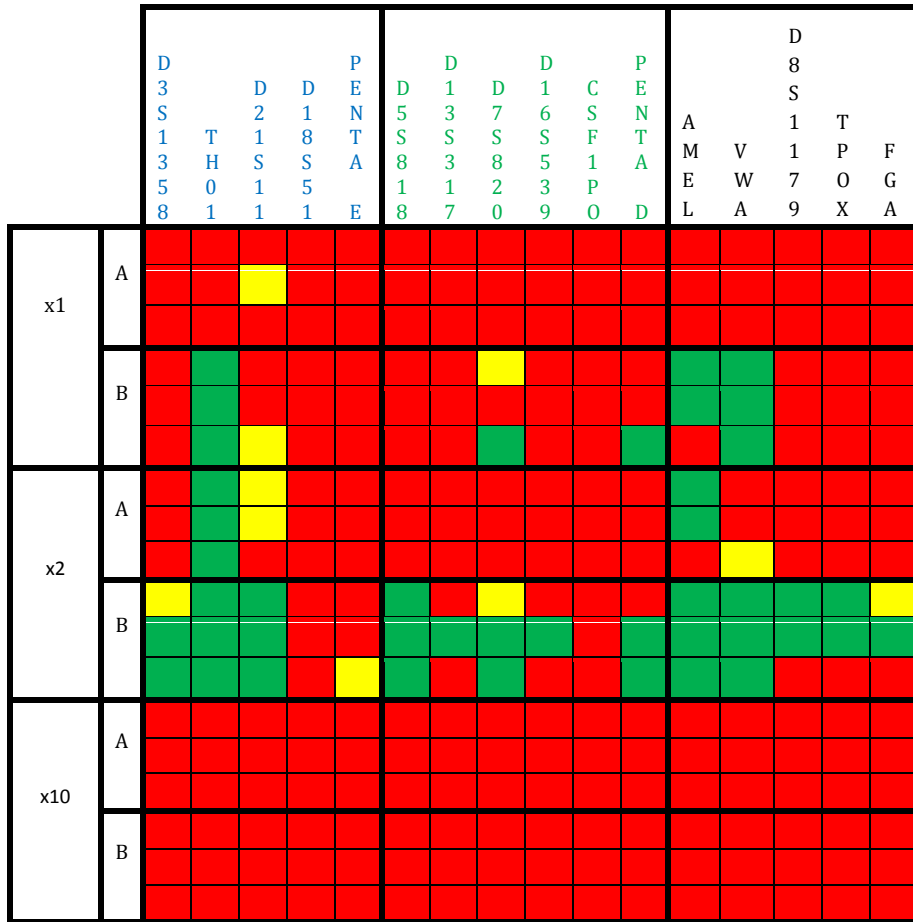
5.3.1 Assessment of Profile Quality

The effect on amplification effectiveness and autosomal STR kit sensitivity was evaluated using peak heights and locus/allele drop-out. Each sample was evaluated and placed into a chart based on their exhibition of alleles above the threshold of 50 RFU. Figures 5.3-5.5 are organized by powder and subsequently by the autosomal STR kit used to generate the profiles. PowerPlex® 18D was more successful at generating profiles above the analytical values for samples which were enhanced using powders, in the dilutions which were previously determined during the sensitivity study, than PowerPlex® 16HS. The PowerPlex® 18D samples were explicitly better when processed with standard black powder or white powder than with magnetic flake(Figure 5.8). While the magnetic flake was the least successful when evaluating both STR kits, the PowerPlex® 18D kit did produce a full profile and/or partial profiles for all dilutions which exceeded 12 loci for 4 of the 6 samples. An evaluation of the individual powders and their comparisons to the untreated samples follow in section 5.3.2, ‘Comparison of Individual Factors’.

DNA profiles were also assessed based on profile properties such as minimum peak heights, maximum peak heights, average peak heights, total PCR product and the PCR product concentration. Standard deviations were also calculated for the triplicates and included in the chart. For Tables 5.1 and 5.2, three replicates of each sample, A and B, were assessed. Sample A presents 12 heterozygous loci and 3 homozygous loci when analysed with PowerPlex® 16HS and 14 heterozygous loci and 3 homozygous loci when analysed with PowerPlex® 18D. Sample B presents 8 heterozygous loci and 7 homozygous loci when analysed with PowerPlex® 16HS and 9 heterozygous loci and 8 homozygous loci when analysed with PowerPlex® 18D.

Profiles were successfully generated in both PowerPlex® 16HS and 18D; however, the quality of the profile was much better when processed with PowerPlex® 18D. When evaluating two of the same samples processed with the same powder at the same dilution with different kits, the visual variability in peak heights is noted.

Loci in Promega Powerplex 16HS



Loci in Promega Powerplex 18D

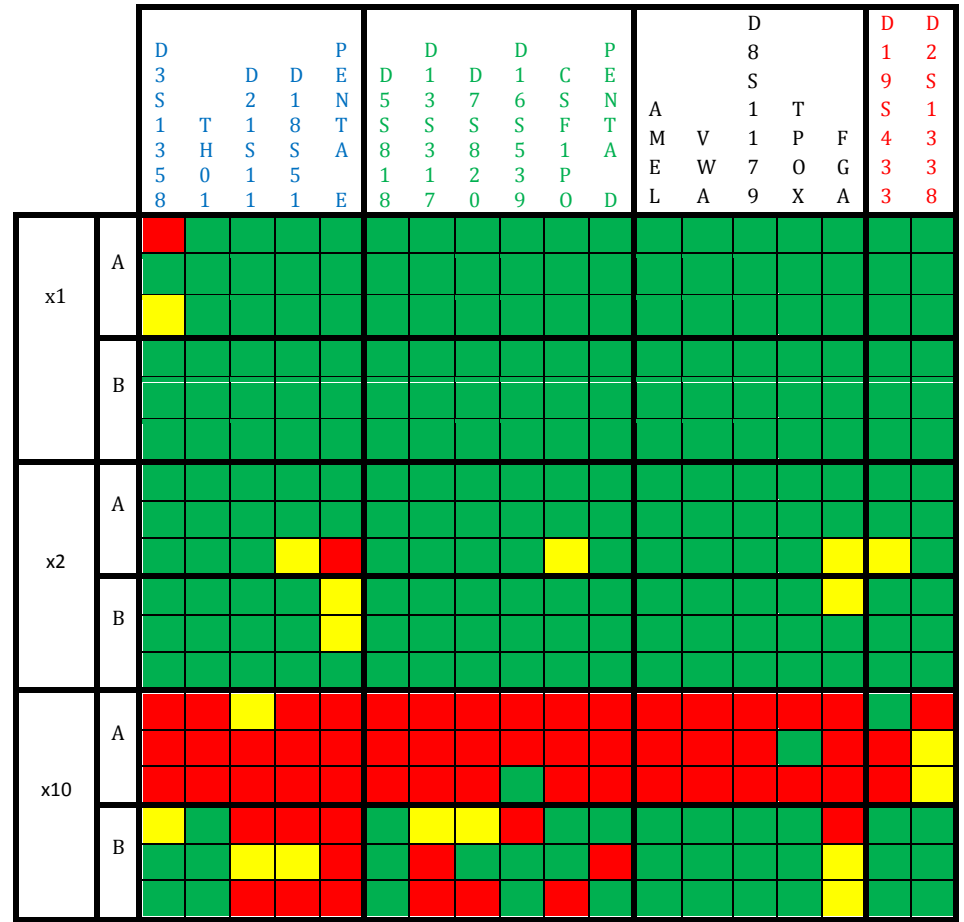


Figure 5.4: A diagrammatic representation of the quality of the profiles obtained from the PowerPlex® 16HS (left) and PowerPlex® 18D (right) kits. Different dilutions (x1, x2, x10) of the two DNA samples (A and B) were processed in triplicate using magnetic flake powder and amplified with PowerPlex® 16HS and PowerPlex® 18D. Green squares indicate that the full correct alleles were observed for those loci. Yellow squares represent one allele drop out. Red squares represent loci where both expected alleles are missing.

Table 5.1: Results for profiles generated with PowerPlex® 16HS showing the minimum, maximum and average peak heights, the profile type, total PCR product and PCR concentration for the various dilutions of samples A and B, amplified using half (12.5µl) reactions, and processed with the 3 powders (black, magnetic, and white). The values are averages of three replicates.

Powder Type	Sample	Dilution	Profile Properties				Total PCR Product (in RFU)	PCR product concentration (in RFU/µl)
			Max PH	Min PH	Average PH	Profile Type		
Black	A	x1	94 (s.d. 17.35)	63 (s.d. 1)	74.89	PP2	611 (s.d. 176.69)	55.55 (s.d. 1.35)
		x2	116 (s.d. 15.72)	52 (s.d. 0.58)	77.13	PP2	1157 (s.d. 33.08)	105.18 (s.d. 3.00)
		x10	--	--	--	NP	--	--
	B	x1	736 (s.d. 194.10)	50 (s.d. 1.16)	144.07	PP9	2017 (s.d. 804.62)	267.45 (s.d. 73.15)
		x2	2157 (s.d. 463.77)	56 (s.d. 2.65)	471.75	PP15	32079 (s.d. 1188.26)	2916.17 (s.d. 107.97)
		x10	--	--	--	NP	--	--
Magnetic	A	x1	--	--	--	NP	--	--
		x2	104 (s.d. 15.53)	56 (s.d. 8.33)	75.88	PP2	607 (s.d. 43.02)	55.18 (s.d. 3.90)
		x10	--	--	--	NP	--	--
	B	x1	198 (s.d. 27.54)	52 (s.d. 23.09)	109.92	PP3	1492 (s.d. 117.00)	129.91 (s.d. 10.64)
		x2	1121 (s.d. 451.45)	53 (s.d. 34.64)	208.83	PP9	8562 (s.d. 2605.27)	778.36 (s.d. 236.84)
		x10	--	--	--	NP	--	--
White	A	x1	405 (s.d. 133.10)	53 (s.d. 0.58)	118.32	PP7	5206 (s.d. 753.27)	473.27 (s.d. 68.48)
		x2	2157 (s.d. 463.77)	56 (s.d. 2.66)	471.75	PP14	32079 (s.d. 1188.26)	2916.27 (s.d. 108.02)
		x10	--	--	--	NP	--	--
	B	x1	1320 (s.d. 280.10)	53 (s.d. 8.15)	314.75	PP14	19200 (s.d. 2222.15)	1745.46 (s.d. 202.02)
		x2	705 (s.d. 243.52)	53 (s.d. 2.52)	175.19	PP9	6482 (s.d. 1843.16)	589.27 (s.d. 167.56)
		x10	--	--	--	NP	--	--

Note: PH = Peak height; FP=Full Profile; PP# = Partial Profile and the number of loci genotyped; NP = No profile; s.d = standard deviation of the replicates.

Table 5.2: Results for profiles generated with PowerPlex® 18D showing the minimum, maximum and average peak heights, the profile type, total PCR product and PCR concentration for the various dilutions of samples A and B, amplified using half (12.5µl) reactions, and processed with the 3 powders (black, magnetic, and white). The values are averages of three replicates.

Powder Type	Sample	Dilution	Profile Properties				Total PCR Product (in RFU)	PCR product concentration (in RFU/µl)
			Max PH	Min PH	Average PH	Profile Type		
Black	A	x1	1540 (s.d.682.63)	50 (s.d. 20.60)	354.49	FP	29423 (s.d. 7258.21)	2674.82 (s.d. 659.8381)
		x2	6952 (s.d. 727.5)	51 (s.d. 15.37)	195.9	FP	18611 (s.d. 727.5)	1692 (s.d. 66.13)
		x10	188 (s.d. 45.54)	51 (s.d. 2)	85.14	PP6	2469 (s.d. 449.22)	224.45 (40.84)
	B	x1	3261 (s.d. 475.98)	264 (s.d. 119.78)	1029.80	FP	83414 (s.d. 270.49)	7582.91 (s.d. 24.69)
		x2	946 (s.d. 112.71)	92 (s.d. 45.94)	325.06	FP	26330 (s.d. 856.66)	2393.64 (s.d. 77.88)
		x10	711 (s.d. 166.01)	54 (s.d. 11.24)	215.70	FP	16609 (s.d. 1242.39)	1509.91 (s.d. 112.94)
Magnetic	A	x1	739 (s.d. 226.60)	50 (s.d. 7.23)	175.13	PP17	13310 (s.d. 3323.02)	1210 (s.d. 302.09)
		x2	568 (s.d. 142.85)	50 (s.d. 8.39)	142.36	FP	12670 (s.d. 1652.25)	1151.82 (s.d. 150.20)
		x10	--	--	--	NP	--	--
	B	x1	3427 (s.d. 508.64)	323 (s.d. 44.55)	1135.99	FP	92015 (s.d. 3636.28)	8365 (s.d. 330.57)
		x2	704 (s.d. 220.95)	52 (s.d. 11.36)	182.27	PP17	14217 (s.d. 2753.87)	1292.45 (s.d. 250.35)
		x10	254 (s.d. 42.78)	50 (s.d. 2.89)	108.16	PP12	481.82 (s.d. 371. 67)	481.82 (s.d. 33.78)
White	A	x1	370 (s.d. 22.12)	50 (s.d. 1.52)	123.90	PP16	10655 (s.d. 556.45)	322.87 (s.d. 50.58)
		x2	6369 (s.d. 3247.44)	56 (s.d. 286.35)	1381.80	FP	129889 (s.d. 34636.57)	11808.09 (s.d. 3148.78)
		x10	173 (s.d. 25.54)	51 (s.d. 4.93)	88.30	PP3	2384 (s.d. 204.16)	216.72 (s.d. 18.56)
	B	x1	3400 (s.d. 622.87)	218 (s.d. 240.83)	1026.43	FP	83141 (s.d. 7324.73)	7558.27 (s.d. 665.89)
		x2	1592 (s.d. 99.16)	170 (s.d. 38.37)	580.67	FP	47034 (s.d. 1677.18)	7180.63 (s.d. 1636.54)
		x10	687 (s.d. 193.99)	52 (s.d. 13.58)	164.94	FP	12865 (s.d. 1522.71)	1169.55 (s.d. 138.43)

Note: PH = Peak height; FP=Full Profile; PP# = Partial Profile and the number of loci genotyped; NP = No profile; s.d = standard deviation of the replicates.

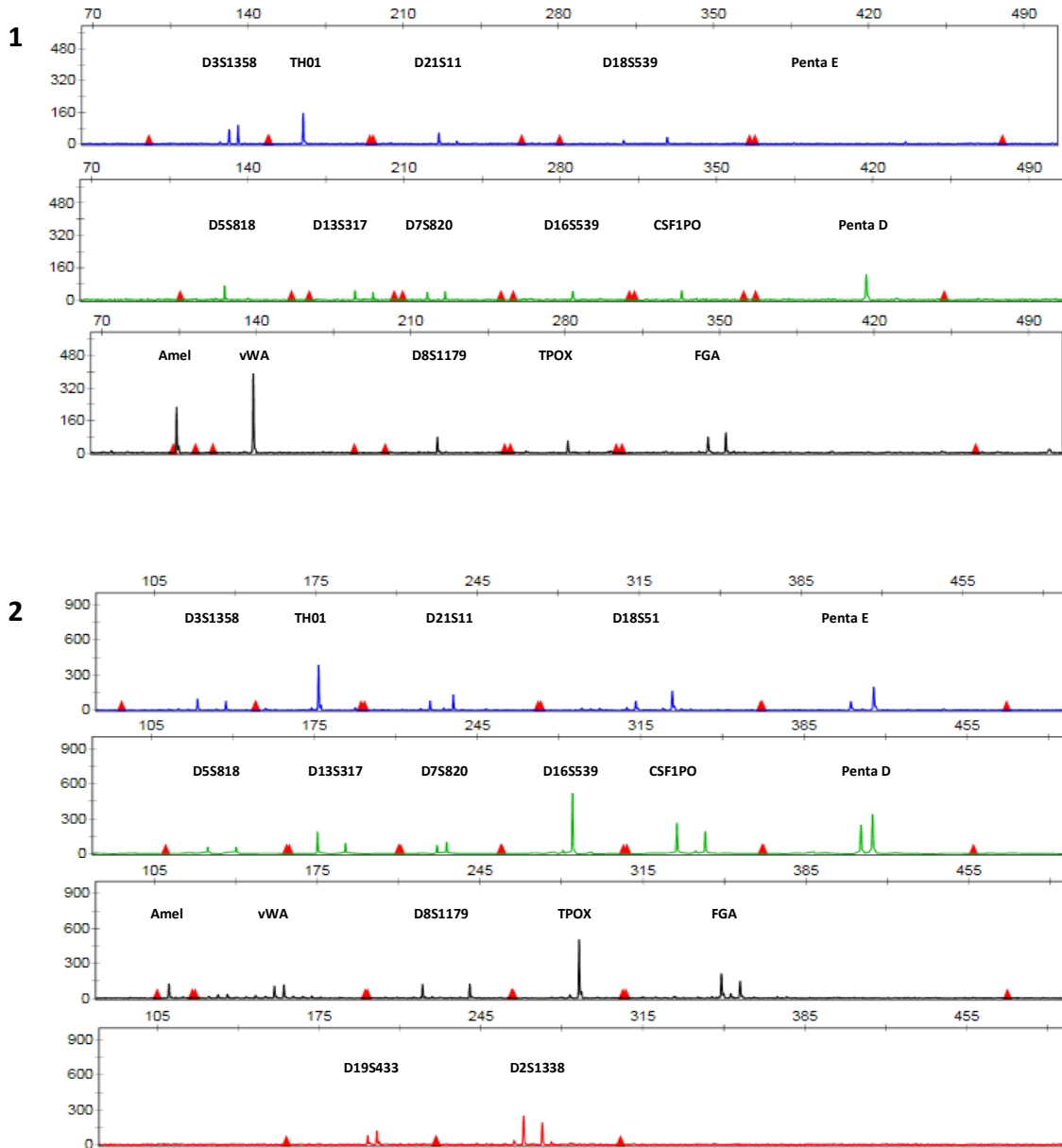


Figure 5.6: (1) Electropherogram of sample B processed with black powder, x1 dilution and analysed with PowerPlex[®] 16HS on a scale of 560 RFU. (2) Electropherogram of sample B processed with black powder, x1 dilution and analysed with PowerPlex[®] 18D on a scale of 1050 RFU. The x-axis represents relative fluorescent units (RFU) and the y-axis fragment size in base pairs.

Magnetic flake powder was the least successful of the powders tested. Most samples processed with PowerPlex[®] 16HS were unsuccessful in producing a profile; however, samples processed with PowerPlex[®] 18D were successful in completing either a full or partial profile at least three times across all three dilutions. Figure 5.6 displays profiles

generated using PowerPlex® 16HS and PowerPlex® 18D (sample B, x2 dilution). PowerPlex® 18D was successful in producing a full profile.

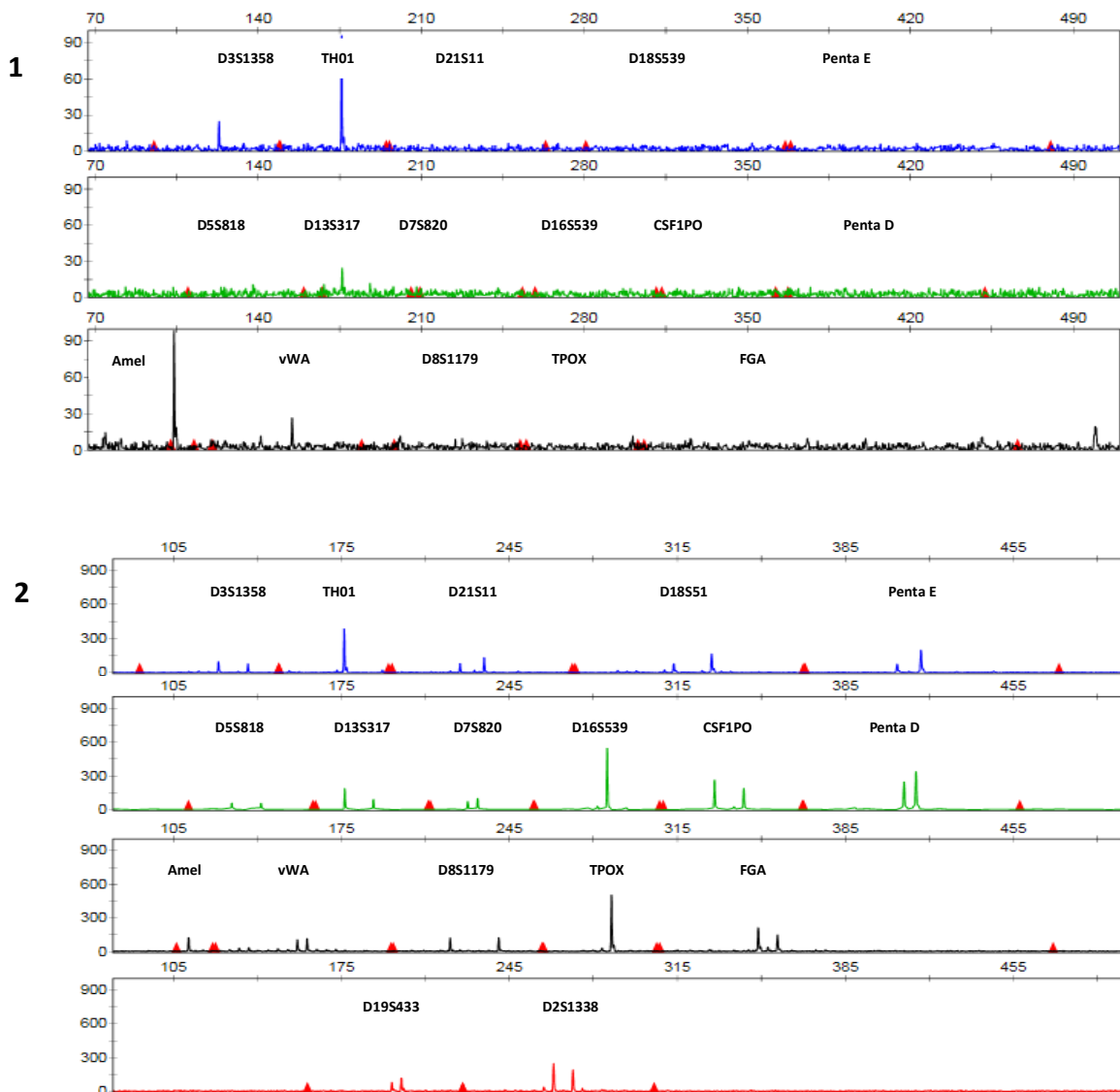


Figure 5.7: (1) Electropherogram of sample B processed with magnetic flake powder, x2 dilutions and analysed with PowerPlex® 16HS on a scale of 100 RFU. (2) Electropherogram of sample B processed with magnetic flake powder, x2 dilution and analysed with PowerPlex® 18D on a scale of 900 RFU. The x-axis represents relative fluorescent units (RFU) and the y-axis fragment size in base pairs.

5.3.2 Comparison of Individual Factors

All profiles were evaluated to determine the overall completeness of the profile as well as to assess the quality of the peaks within each profile. The average RFU value of the total PCR product of all samples generated with each of the human identification kits above the 50 RFU thresholds was plotted using each of the powders against the dilutions present in the experiment. For all samples analysed with PowerPlex® 18D, the data for the loci D2S1338 and D19S433 was removed from the totals in order to normalize the data when comparing it to PowerPlex® 16HS, which does not contain these loci. Samples which were not exposed to any powder enhancement and included only the epithelial cell deposit were labelled as 'no powder'. The results are displayed in Figures 5.8 and 5.9.

When reviewing dilutions versus powders, PowerPlex® 16HS has the largest RFU values exhibited in the x2 dilutions across all powders with the x1 dilution and x10 dilutions following respectively. The mean in this case is not significantly different between the dilutions in regards to powder used to process the samples [$F(2,12)= 1.22$, $p= 0.330$]. This was not seen when looking at the 'no powder' samples with the x2 dilution samples falling between the x1 and x10 dilutions. The 'no powder' samples followed an expected trend given that the amount of DNA was being reduced as the dilutions increased.

PowerPlex® 18D does show larger values than PowerPlex® 16HS in regards to average total PCR product (Figure 5.9). PowerPlex® 18D 'no powder' samples produced average PCR products which were much lower than any of the other dilution samples processed with powder. When analysing the white powder, the x2 dilution exceeds the x1 and x10 when compared to the two other powders. The white powder also shows the strongest overall RFU values for the x2 and x10 dilutions when processed with PowerPlex® 18D. However, the difference between the dilutions in regard to powder does not appear to be significantly different [$F(2,12)= 1.54$, $p=0.231$].

When disregarding powder type (Figure 5.10) and focusing on the kit versus the dilutions only, the trend of the samples is as expected. PowerPlex® 18D does show stronger RFU values than PowerPlex® 16HS and are statistically significant [$F(1, 30)= 10.65$, $p=0.003$].

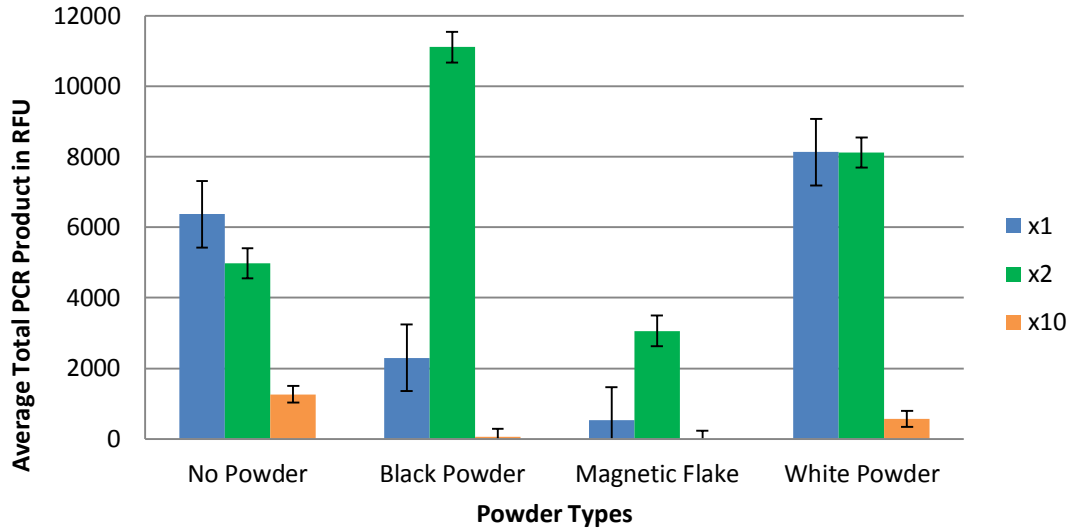


Figure 5.8: Variation in the average total PCR product (RFU) between the powders and dilutions processed with PowerPlex® 16HS. Error bars represent the standard deviation. No samples with a x10 dilution produced a profile for any of the powders.

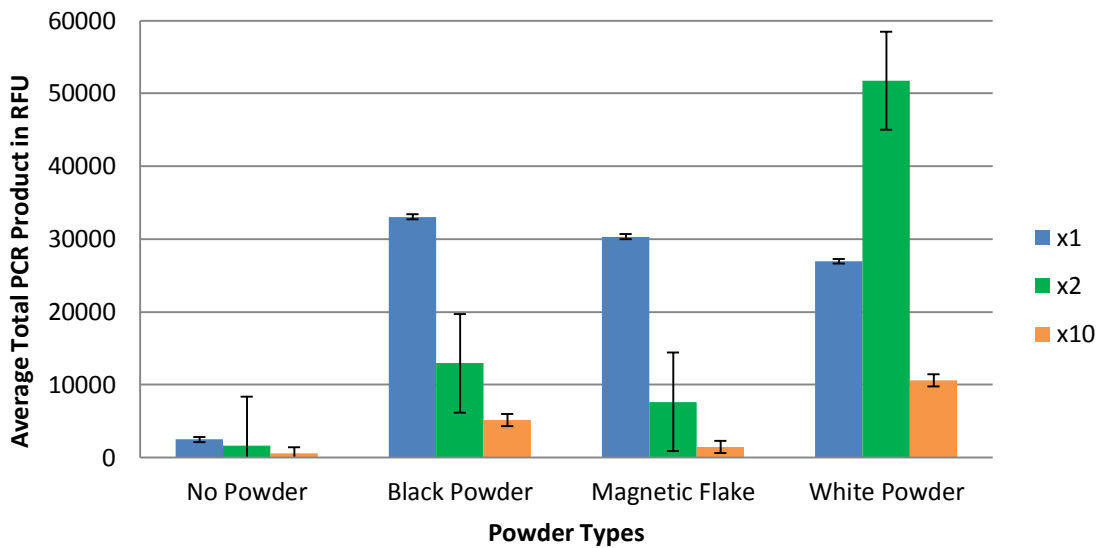


Figure 5.9: Variation in the average total PCR product (RFU) between the powders and dilutions processed with PowerPlex® 18D. Error bars represent the standard deviation.

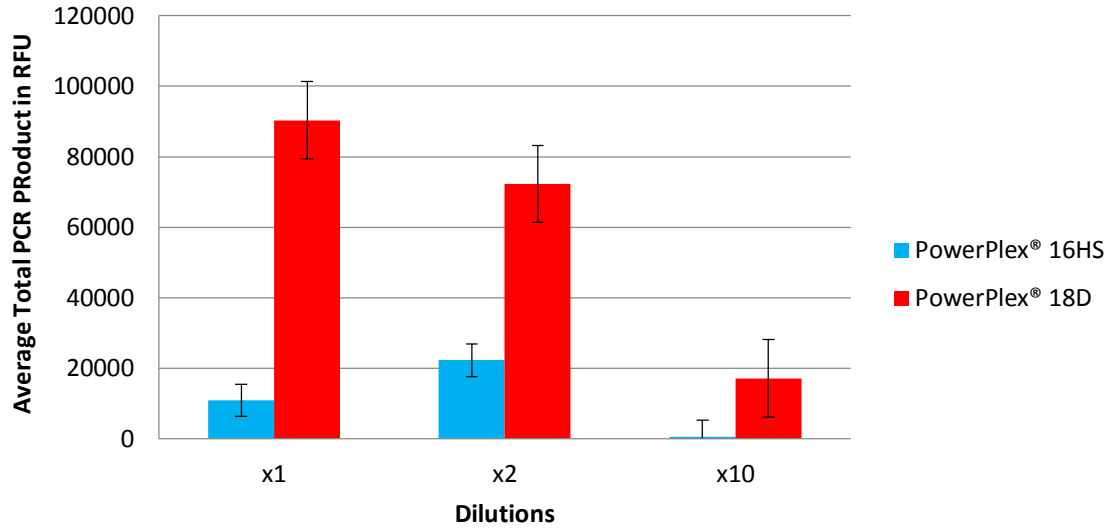


Figure 5.10: Variation in the average total PCR product (RFU) between the dilutions and kits utilized to process the powder samples. Error bars represent the standard deviation.

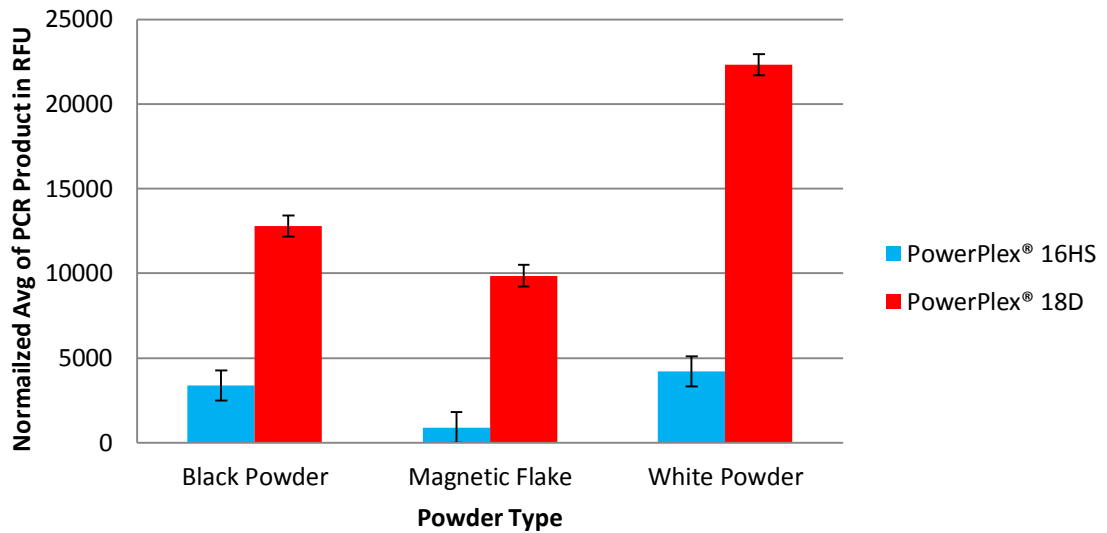


Figure 5.11: Variation of the average total PCR product (RFU) between the powders and kits utilized to process the powder samples. Error bar represent the standard deviation.

Another consideration when assessing the quality of the profiles generated is the evaluation of heterozygous peak balance (Hb) which is the ratio of the two peaks present at a heterozygous locus. This is determined mathematically by dividing the allele with the lower peak height value by the allele with the greater peak height value. Results range from 0 to 1 with 1 representing alleles of equal height. An Hb value which is below 0.70 indicates peak imbalance. Figures 5.12 through 5.17 exhibit heterozygous loci which are present in both sample A and B and are colour coded based on the different dilutions. A red dotted line indicates the 0.70 Hb threshold for the results.

For PowerPlex[®] 18D samples for all powder types and all dilutions, 237 of 432 of the samples appear over the Hb 0.70 threshold (Figure 5.13, 5.15, and 5.17). PowerPlex[®] 16HS was not as successful and only produced 46 of 432 samples above the Hb 0.70 threshold (Figure 5.12, 5.14, and 5.16).

Peak height ratios for samples at the x1 dilution revealed that only 19 of the 144 samples when analysed with PowerPlex[®] 16HS were above the 0.7 Hb threshold while x1 dilution samples analysed with PowerPlex[®] 18D produced 98 of 144 samples above the threshold. The majority (84 of the 144) of the samples processed with PowerPlex[®] 18D at the x2 dilution were above the 0.7 Hb limit. PowerPlex[®] 16HS only produced samples above the threshold for 26 of the 144 samples at a x2 dilution. PowerPlex[®] 16HS samples processed with x10 dilutions failed to produce any data for the samples in regards to heterozygous peak balance. PowerPlex[®] 18D, however, was able to successfully amplify and produce samples which were above the 0.70 (Hb) threshold for 34 of the 144 samples across all powder types. While this is only 24% of the samples, it was still deemed a success in comparison to the PowerPlex[®] 16HS samples.

Standard black powder and white powder produced 83 of 144 samples and 96 of 144, respectively when processed with PowerPlex[®] 18D (Figure 5.13 and 5.17). Peak height ratios for samples exposed to black powder using PowerPlex[®] 16HS were less successful displaying 14 out of 144 samples (Figure 5.12). The white powder deposits were slightly more successful 25 of 144 samples (figure 5.16).

PowerPlex® 16HS was deemed unsuccessful when samples were processed with magnetic flake; few heterozygous loci (6 of the 144 samples) were above threshold when looking at all dilutions (Figure 5.14). Of the heterozygous loci which exhibited both alleles when samples were processed with magnetic flake and analysed with PowerPlex® 18D, 40 % (59 of 144) of the samples were above the 0.70 (Hb) leading to the conclusion that while the overall profile RFU totals were lower than the other two powders and did not include as many full profiles, the heterozygous peak balance for samples processed with magnetic flake did meet analysis standards for acceptance. Of the samples analysed with PowerPlex® 18D and exposed to magnetic flake, all x1 and x2 dilution samples produced full or partial profiles which only lacked, D3 in sample A for x1 and Penta E in samples B for x2 dilution.

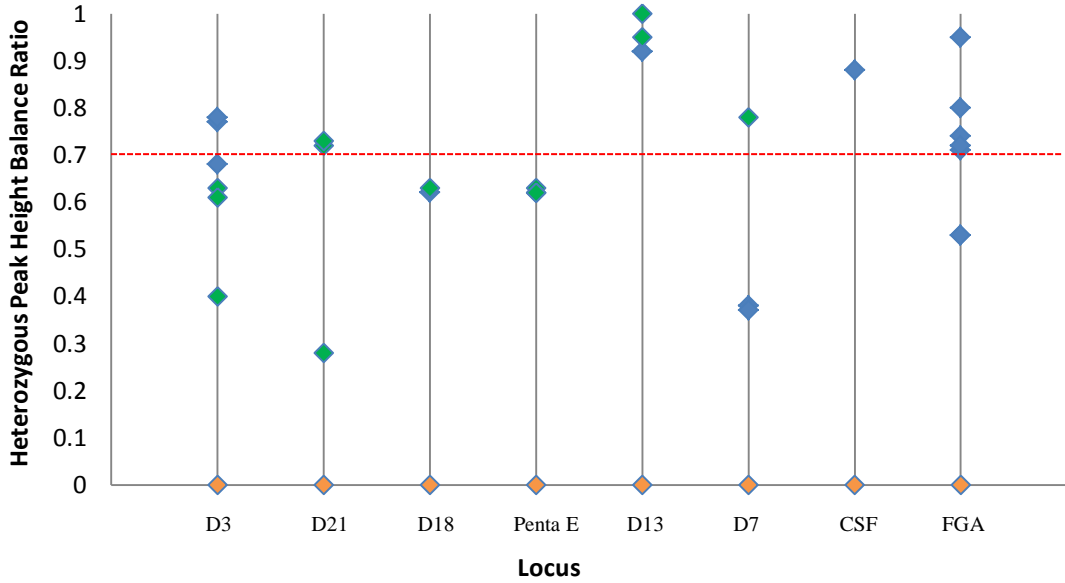


Figure 5.12: Peak height ratios of the various heterozygous loci present in both samples A and B processed with *black powder* and analysed with PowerPlex[®] 16HS. The red line indicates the 0.70 Hb threshold for the heterozygous peak balances. Blue diamond symbols represent x1 dilutions, green diamonds represent x2 dilutions, and orange diamonds represent x10 dilution samples.

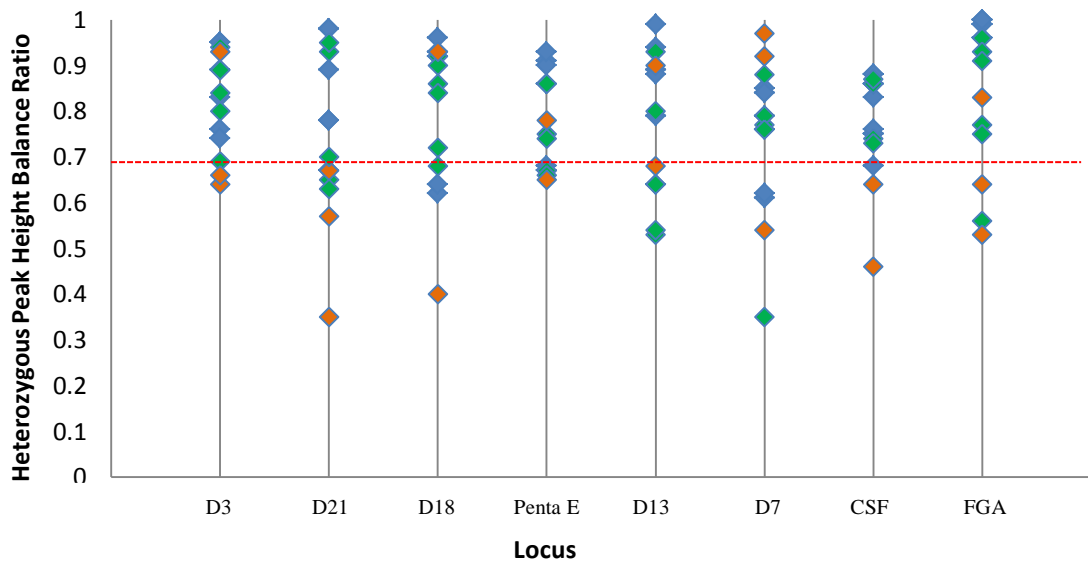


Figure 5.13: Peak height ratios of the various heterozygous loci present in both samples A and B processed with *black powder* and analysed with PowerPlex[®] 18D. The red line indicates the 0.70 Hb threshold for the heterozygous peak balances. Blue diamond represent x1 dilutions, green diamonds represent x2 dilutions and the orange diamonds x10 dilution samples.

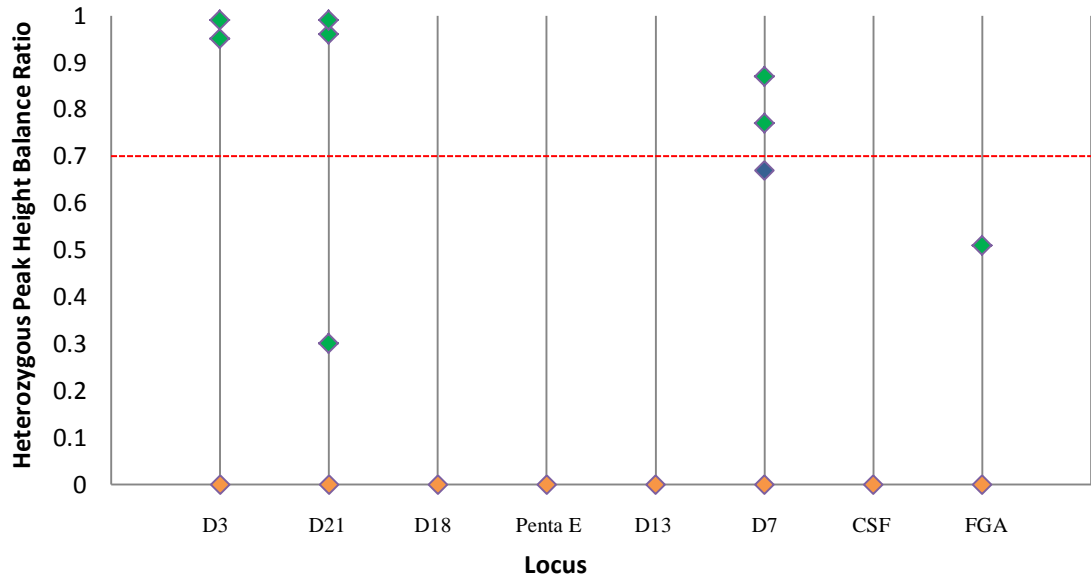


Figure 5.14: Peak height ratios of the various heterozygous loci present in both samples A and B processed with *magnetic flake* and analysed with PowerPlex[®] 16HS. The red line indicates the 0.70 Hb threshold for the heterozygous peak balances. Blue diamond symbols represent x1 dilutions, green diamonds represent x2 dilutions, and orange diamonds represent x10 dilution samples.

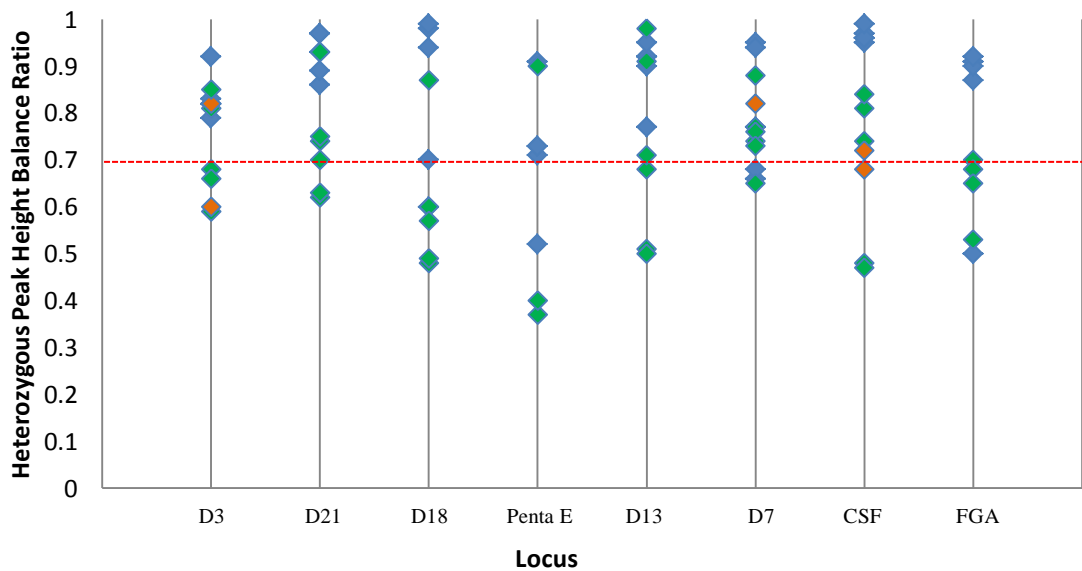


Figure 5.15: Peak height ratios of the various heterozygous loci present in both samples A and B processed with *magnetic flake* and analysed with PowerPlex[®] 18D. The red line indicates the 0.70 Hb threshold for the heterozygous peak balances. Blue diamond represent x1 dilutions, green diamonds represent x2 dilutions and the orange diamonds x10 dilution samples.

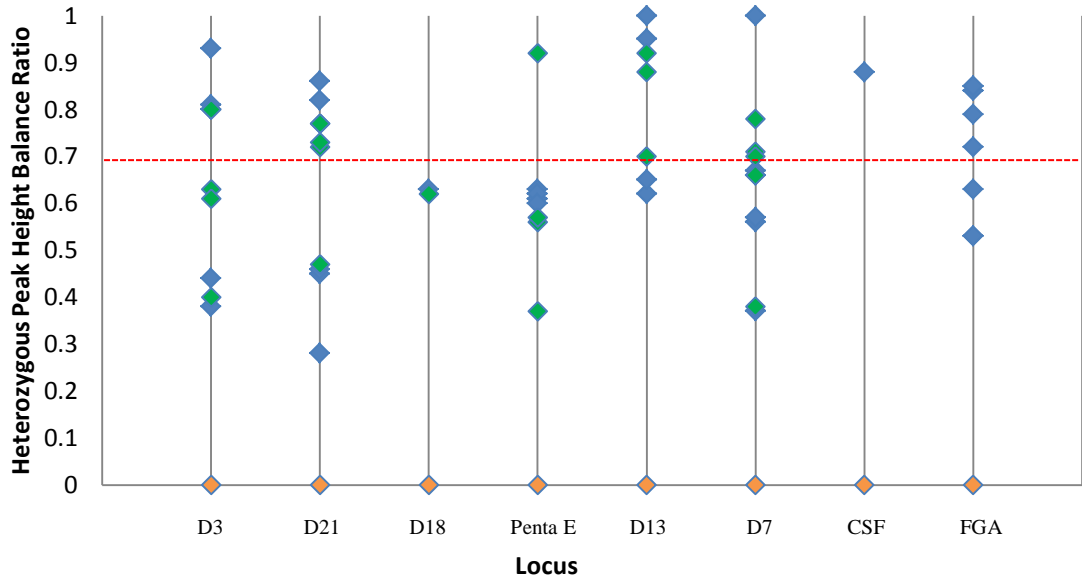


Figure 5.16: Peak height ratios of the various heterozygous loci present in both samples A and B processed with *white powder* and analysed with PowerPlex[®] 16HS. The red line indicates the 0.70 Hb threshold for the heterozygous peak balances. Blue diamond symbols represent x1 dilution, green diamonds represent x2 dilutions, and orange diamonds represent x10 dilution samples.

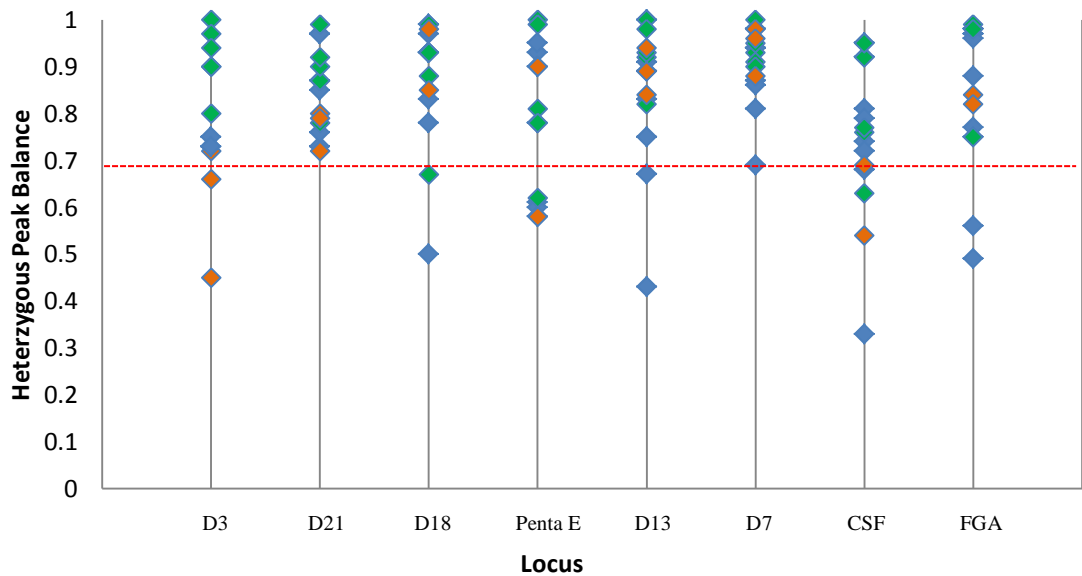


Figure 5.17: Peak height ratios of the various heterozygous loci present in both samples A and B processed with *white powder* and analysed with PowerPlex[®] 18D. The red line indicates the 0.70 Hb threshold for the heterozygous peak balances. Blue diamond represent x1 dilutions, green diamonds represent x2 dilutions and the orange diamonds x10 dilution samples.

5.3.2.1 Evaluation of CSF1PO

A heterozygous allele call of CSF1PO was present in sample B samples for the powder samples. CSF1PO was more successful in displaying both alleles when processed with PowerPlex® 18D. Both alleles were displayed in 2 of 27 samples analysed with PowerPlex® 16HS when compared to PowerPlex® 18D where both alleles were present in 26 of the 27 samples processed (Figures 5.2-5.4). The two samples which displayed the heterozygous allele call for PowerPlex® 16HS both showed peak height balance ratio above the 0.70 Hb threshold (Figure 5.12, 5.16). 14 of 27 analysed with PowerPlex® 18D were over 0.70 Hb threshold (Figure 5.13, 5.15, and 5.17).

5.4 Discussion

Powder dusting techniques are the simplest, most effective and most commonly used procedures when developing latent prints on nonporous surfaces (Sodhi and Kaur, 2001). While this process has been around for decades, the research to determine if it is possible to obtain a viable full or partial DNA profile from substrates that have been processed with these powders is limited (VanOorschot and Jones, 1997; VanHoofstat et al., 1999; Norlin et al., 2013). Different studies have shown that skin contact to a surface does transfer enough biological material to obtain a full or partial profile and that the amount of DNA transferred is dependent on the individual who is touching the surface (VanOorschot and Jones, 1997; Alessandrini et al., 2003; Lowe et al., 2002).

Results in a recent study by Tozzo (2014) indicate that it is possible to obtain a profile from samples which have been processed with various powders under laboratory conditions including magnetic powder. In the study, magnetic powder did yield the lowest number of successfully typed samples. The kit used in the study was not direct PCR. The results of this project agreed with this study in regards to results reflected in the extraction based kit (PowerPlex® 16HS), however, found using a direct amplification kit (PowerPlex® 18D) was more successful when attempting to produce profiles from samples exposed to magnetic flake. The extraction based samples (PowerPlex® 16HS) did not produce a full or partial profile for any of the samples except for sample B, x2 dilution. The direct amplification kit (PowerPlex® 18D) produced full or partial profiles at all dilutions.

To date, the few publications that discuss direct amplification generally use samples which have been transferred to blood or buccal FTA[®] cards (Park et al., 2008; Patel et al.; 2014). This is the recommended method for samples that have not been extracted and it should be noted that the samples processed in this work were not placed on FTA[®] paper prior to processing. In order for direct amplification to possibly be used in a field setting it was important for the samples in this work to be processed as if they were enhanced at a crime scene, collected and brought back to a laboratory for analysis.

Sensitivity is a key factor in the acceptance of direct amplification. When using direct amplification it is not necessary to undertake the extraction process. Using an extraction method can reduce the amount of raw sample which was actually recovered from the substrate at the scene. In this study, a range of dilutions (x1, x2, and x10) were evaluated. The samples which were extracted and prepared at a x10 dilution failed to produce a profile whereas samples processed with PowerPlex[®] 18D gave partial profiles when exposed to the powders. Since the deposit was of known quantity, the ability of an individual person to deposit cells on the surface was not a factor and the results appear to show that the low starting template could be a factor in the results (Raymond et al., 2004; Hanson and Ballantyne, 2005). Future work could be conducted by altering the amplification parameters and retesting the samples with a higher number of amplification cycles.

The white powder samples were the most successful for both kits when evaluating total PCR product concentration. In regards to heterozygous peak balance (Hb) however, white powder samples analysed with PowerPlex[®] 16HS were less successful when reviewing all dilutions. The samples processed with PowerPlex[®] 18D were better and the majority of all dilutions appear above the 0.70 Hb limit. Black powder samples displayed similar results when evaluating the total PCR product concentration for both kits and were only slightly less successful when evaluating the heterozygous peak balance. Previous publications have indicated that both white powder and black powder do not inhibit the STR profiling process ((Raymond et al., 2004; Roux et al., 1999; Stein et al., 1996; vanOorschot et al., 2003; vanOorschot et al., 2005). The data generated for this study agrees with the earlier findings.

This study has shown that it is possible to obtain a DNA profile using direct amplification from a surface which has been treated with various latent print

enhancement powders and that the results of the direct amplification samples, when compared to the extracted samples, have a significantly stronger profile [$F(1, 30)= 10.65$, $p=0.003$].

Overall, PowerPlex[®] 16HS appears to be the less productive of the two kits when reviewing the data for samples which have been enhanced with powder. One possible explanation for the lower total PCR product is the loss of biological sample during the extraction process which is eliminated when using a direct amplification system (Kemp et al., 2014; Qiagen, 2011). Another possible explanation for the lack of profiles in PowerPlex[®] 16HS samples or low yields when processing with PowerPlex[®] 18D, could have been the starting amount of template DNA which ranged from 0.009 ng/ μ l (x10 dilution) to 0.041 ng/ μ l (x1 dilution) (Chapter 3, Table 3.1).

Despite, the positive results which were obtained in regards to the direct amplification system, PowerPlex[®] 18D, it should be noted these were obtained under laboratory conditions. Casework materials are often exposed to foreign contaminants and personnel working the case. Shedder status is also a factor which must be carefully considered when employing these techniques (Zoppis et al., 2004; Alessandrini et al., 2003; Lowe et al., 2002). The samples in the experiment were also not exposed to cyanoacrylate ester fuming, also referred to as superglue fuming. Applying this technique to the fingerprints prior to powder processing may help in stabilize the print and minimizing the loss of additional epithelial cells which can come with direct powder processing (Bhoelai et al., 2011; Bille et al., 2009). In addition, PowerPlex[®] 16HS has also been marketed as a kit which could be used in a 'direct' amplification capacity. A further study on the difference between extracted and direct samples utilizing the same kit may prove beneficial in determining the loss of biological sample during the extraction process. Future work must be undertaken to explore these areas and evaluate their individual effects on the samples. While more work needs to be conducted, the PowerPlex[®] 18D, direct amplification kit does appear to be a possible alternative to traditional typing methods.

Chapter 6.

EVALUATION OF BLOOD SAMPLES ENHANCED WITH CHEMICAL PROCESSES

The following section describes the evaluation and comparison of Promega® PowerPlex® 16HS and Promega® PowerPlex® 18D human identifications systems on the mock blood marks which have been processed with leucocrystal violet (LCV), amido black and ninhydrin on a variety of substrates.

6.1 Overview

Improvements in DNA analysis by increasing speed and accuracy for the development of profiles has become an invaluable tool for the forensic community over the past several years. Many techniques and advancements strive to increase the rate at which a DNA profile can be produced while also being cost effective. As many agencies battle budget constraints the ability to increase efficiency and productivity are on the rise. There is also increased emphasis in producing mobile or portable devices capable of producing rapid real-time results (Gray et al., 2014) which would eliminate time consuming practices and limit consumables and equipment in the laboratories. These advancements have the potential to revolutionize the field; however, much research needs to be conducted on the effects of enhancement chemicals which are used to better visualize and document evidence in the field. Direct amplification has been successful in generating profiles from a variety of different types of crime scene samples such as a single hair follicle, tape lifts, swabs and FTA based samples, however, not much research has been conducted on the chemical enhancement techniques in relation to blood (Gray et al., 2014). Latent blood transfers can occur under a variety of scenarios during the commission of a crime and may not always contain ridge detail for fingerprint analysis; however, they could yield clues as to the identity of the perpetrator via DNA profile. In order for direct amplification to be a viable option for crime laboratories these samples need to be rigorously tested.

Glass, gypsum, raw wood, lead, plastic, glass, laminate, and tile were used as substrates for the work. The substrates were selected based on published works which contained samples processed on these substrates and/or were noted limitation in other works as substrates which should be considered in future research (Gino and Omedei, 2011; Praska and Langenberg, 2013; Swaran and Welch, 2012; Bhoelai et al., 2011; Frégeau et al., 2000; Alessandri et al., 2003; Daly et al., 2012; Zoppis et al., 2014).

Leucocrystal violet (LCV) is a haem reactive chemical responding to the haemoglobin found within red blood cells (Praska and Langenburg, 2013). The components of the chemical contain hydrogen peroxide which aids in binding to the haemoglobin and the crystal violet stain colours the stain a bright purple (Bodziak et al., 1996). LCV can be used on porous and nonporous surfaces which may be encountered at scenes of crime. LCV has been shown to not inhibit profiles generated with extraction based PCR products (Spear et al., 2002; Bleay et al., 2012). Amido black is a protein reactive chemical. Amido black binds to the cationic groups of proteins found in blood and is the most specific of the dye stain proteins (Bossler, 2011). Amido black stain is dark blue to black in colour and can be used on nonporous surfaces. It has also been shown not to inhibit profiles generated with extraction-based PCR products (Spear et al., 2002; Bleay et al., 2012). Ninhydrin is a chemical which reacts to amino acids within the stain. It stains a dark purple colour. Ninhydrin is used on porous surfaces and has shown no inhibition when generating DNA profiles (Bleay et al., 2012; Bever et al.; Stein et al., 1996).

Leucocrystal violet, amido black and ninhydrin were used for this study. Chemicals chosen were selected based on accessibility, usage in laboratories and ultimately with which molecules they react. It was the goal of the work to target chemicals which responded to each component found within the blood, i.e. haem-reactive, protein-reactive and amino acid-reactive. Substrates identified as those commonly encountered at crime scenes were processed. The substrates include glass, gypsum, raw wood, lead, plastic, glass, laminate, and tile. Specific objectives for this chapter are to:

1. Amplify and analyse samples which have been processed with the three chemicals selected for analysis- leucocrystal violet, amido black, and ninhydrin, and used to generate DNA profiles with PowerPlex[®] 16HS and PowerPlex[®] 18D;
2. Consider any visual abnormalities which may have occurred while processing the substrates with their respective chemicals;

3. Assess the ability to generate complete and good quality profiles for each dilution across multiple substrates for each chemical and kit, PowerPlex[®] 16HS and PowerPlex[®] 18D under various sample dilutions;

4. Evaluate the profiles for artefacts such as dye blobs, stutters, pull-up, and split peaks which may be present in the generated profiles.

6.2 Experimental Design

All substrates were prepared using 20µl bloody marks which were applied to white laminate (12in x 12in carrara marble), tile (Value White Wall Tile 150mm x 150mm), glass (Microscope slide), metal (lead), plastic (acetate sheets), gypsum board and raw wood (Section 2.3). These substrates were selected based on their usage as substrates in other publications regarding DNA analysis. Metal (lead), gypsum board and raw wood have also been noted as samples which have produced little to no profile when using standard DNA analysis techniques (Spear et al., 2002). Each substrate was then labelled and photographed. After photographing the substrates were then processed using leucocrystal violet, amido black, and ninhydrin as depicted in Table 2.3. Each of the substrates was again photographed post chemical exposure to note the colour change which indicates that a biological substance is present. A Swabstick (Dynarex[®]) was used to swab the area which produced a colour change on the substrate using the dual swab technique (Sweet et al., 1997). The colour change indicates the chemical reacted with the biological material. The samples were then processed in accordance to the whole blood procedure outlined in section 2.5. All samples were conducted in triplicate.

An additional set of samples were run with the three dilutions on the substrates listed above with no chemical processing. These samples were analysed to see if the substrate played a possible role in profile inhibition and were also used to compare the overall peak heights and PCR product concentrations between the ‘no chemical’ samples in comparison to those processed with the chemicals. These samples were also processed in accordance to the whole blood procedure outlined in section 2.5. All samples were conducted in triplicate.

All PowerPlex[®] 18D data used in comparative figures with PowerPlex[®] 16HS have been normalized by removing the data for D2S1338 and D19S433. D2S1338 and D19S433 are not present in PowerPlex[®] 16HS.

6.3 Results and Discussion

6.3.1 Leucocrystal Violet (LCV)

Overall results for samples processed with LCV indicated that the extracted samples produced with PowerPlex® 16HS gave lower peak heights and PCR product concentrations compared to samples which were subjected to direct amplification with PowerPlex® 18D.

The kits were also compared to samples on substrates which were not exposed to LCV (no chemical processing). In this case, the samples which were not exposed to LCV showed much higher peak heights and PCR product concentrations when evaluating both kits. The difference was statistically significant yielding a p -value < 0.05 [$F(1, 82) = 4.48$, p -value = 0.038]. Figure 6.1 displays the average PCR product concentration for all samples and dilutions processed with both PowerPlex® 16HS and 18D compared to all samples and dilutions analysed with PowerPlex® 16HS and 18D which contained no LCV on the substrates.

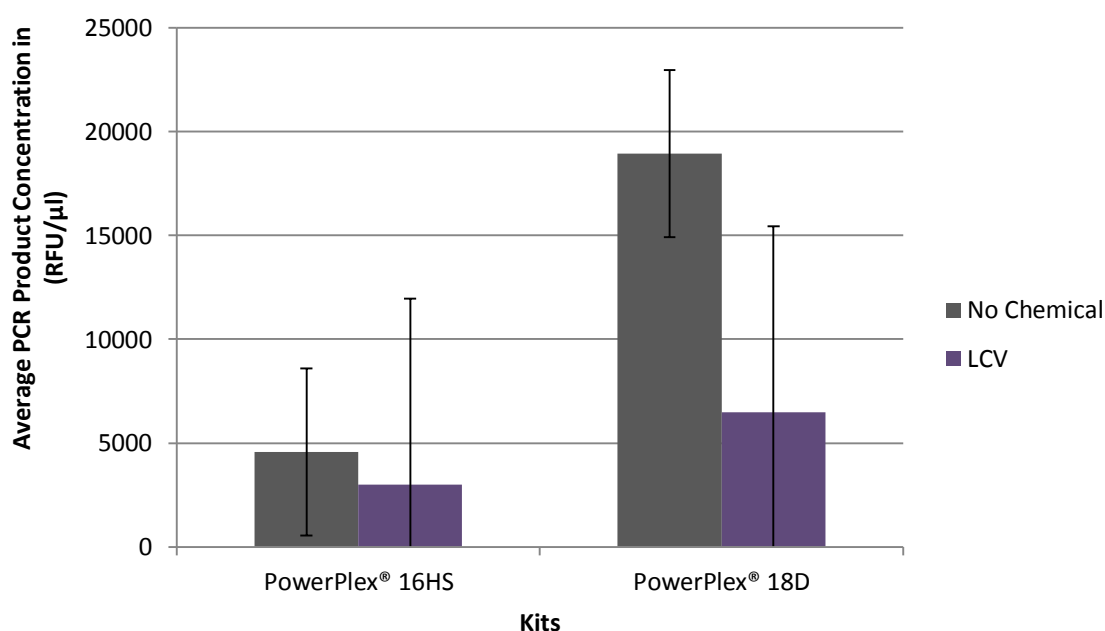


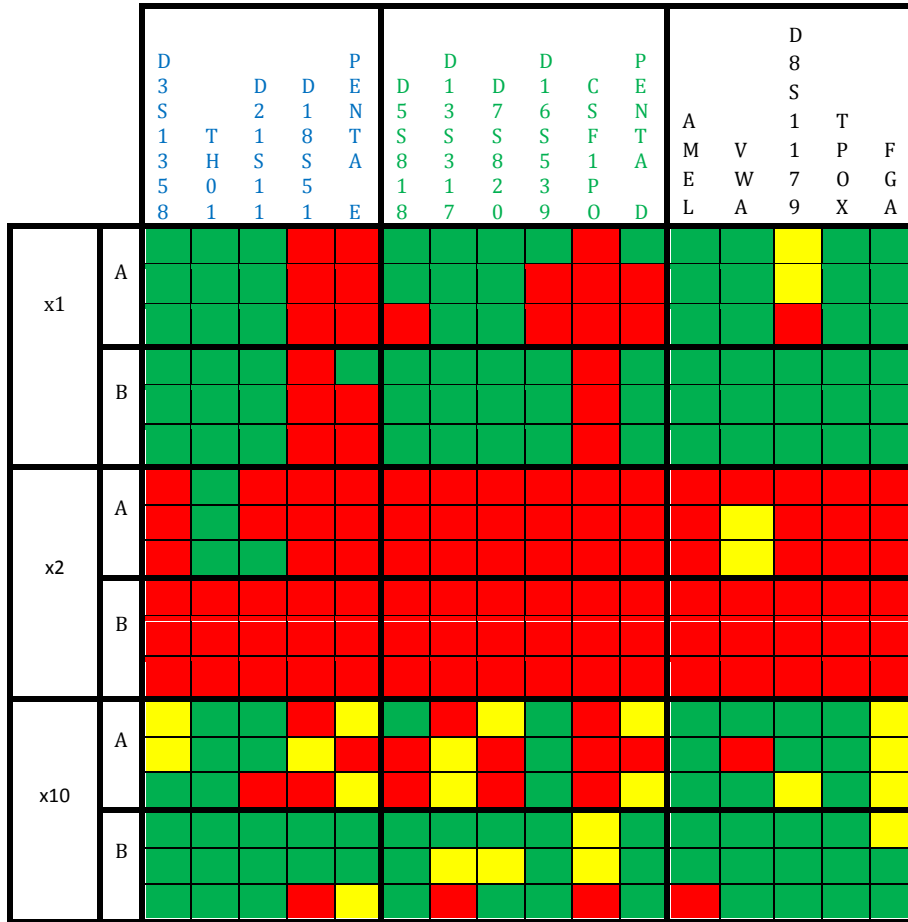
Figure 6.1: Graph displaying the average PCR product concentration (RFU/μl) for each kit, PowerPlex® 16HS and PowerPlex® 18D, for all samples processed using LCV (purple bars) and for all samples processed with no chemical enhancement (grey bars). The error bars represent the standard deviations for each of the kits.

The successfulness of direct PCR amplification and autosomal STR kit sensitivity were evaluated using peak heights and locus/allele drop-out. Each sample was evaluated and placed into a chart based on their exhibition of alleles above the predetermined threshold of 50 RFU. Sample A presents 12 heterozygous loci and 3 homozygous loci when analysed with PowerPlex[®] 16HS and 14 heterozygous loci and 3 homozygous loci when analysed with PowerPlex[®] 18D. Sample B presents 8 heterozygous loci and 7 homozygous loci when analysed with PowerPlex[®] 16HS and 9 heterozygous loci and 8 homozygous loci when analysed with PowerPlex[®] 18D.

Figures 6.2 -6.8 are organized by substrate processed with LCV and subsequently by the autosomal STR kit used to generate the profiles. These figures were used to examine the variation in the amplification between the different dilution volumes, chemicals, substrates and autosomal STR kits. They were also used to assess each locus to determine if all alleles were present. If all alleles were present the locus was determined to be complete. Profiles were noted as either full profiles (FP) where all alleles at all locations were observed, partial profiles (PP) where the number after indicates the number of loci which presented the alleles and no profile (NP) where the chromosomal location did not display the proper allele call at any location in the whole profile. This information is reflected under 'Profile Type' in Tables 6.1-6.2.

Direct PCR gave full profiles in almost all (31 of 39) the substrates which were processed with LCV across all three dilutions (Table 6.2). Direct amplification exhibited a gradual decrease as the amount of starting biological material decreased. Plastic was the only substrate which yielded a higher RFU value for all dilutions when analysed with PowerPlex[®] 16HS. While the RFU values were higher with PowerPlex[®] 16HS, a full profile was obtained with PowerPlex[®] 18D in all dilutions where PowerPlex[®] 16HS only produced partial profiles at the x10 dilution. These results are consistent with results obtained from Swaran and Welch (2012); however, it should be noted that in Swaran and Welch (2012) the substrates were only placed on a variety of substrates with no chemical exposure. Lead also failed to give full profiles for most of the dilutions processed and was even less successful when using the extracted method, PowerPlex[®] 16HS. Tile yielded the highest RFU values and produced full profiles in both kits when reviewing samples created with the x1 and x2 dilutions.

Loci in Promega® Powerplex® 16HS



Loci in Promega® Powerplex® 18D

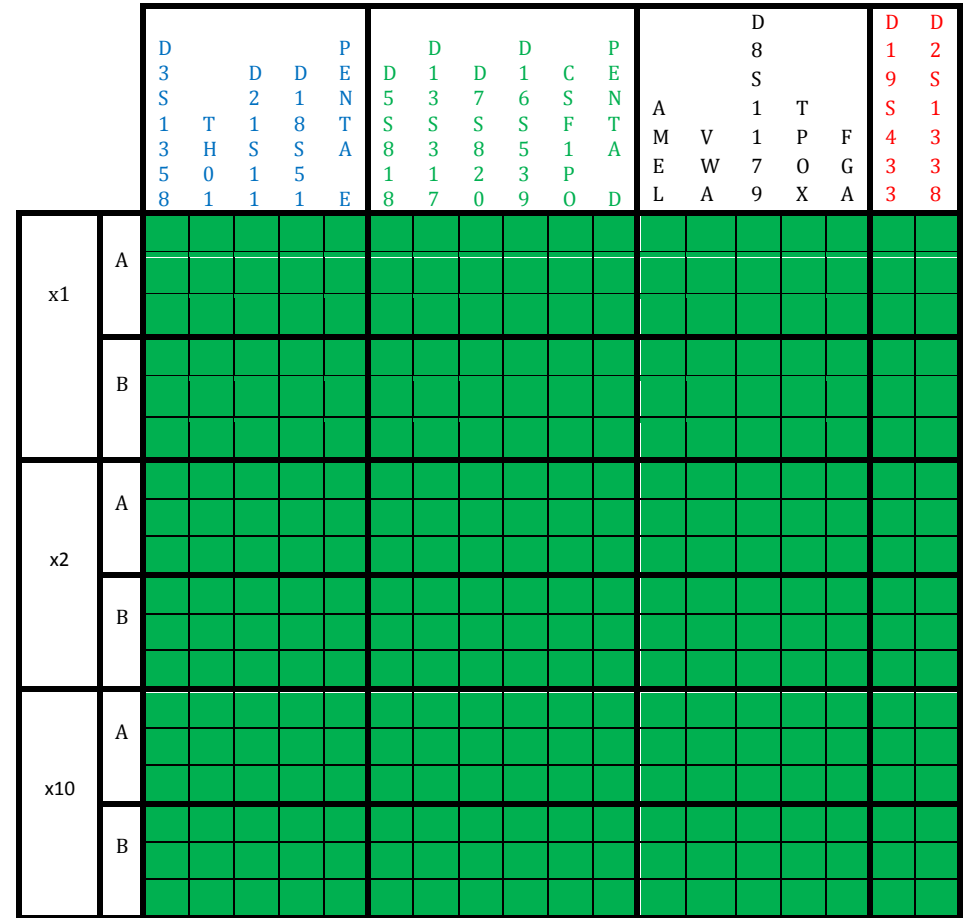


Figure 6.7: A diagrammatic representation of the quality of the profiles obtained from the PowerPlex® 16HS (left) and PowerPlex® 18D (right) kits. Different dilutions (x1, x2, and x10) of the two samples (A and B) were processed in triplicate using *LCV on Gypsum* and amplified with PowerPlex® 16HS and PowerPlex® 18D. Green squares indicate that the full correct alleles were observed for that locus. Yellow squares represent one allele drop out. Red squares specify loci where both expected alleles are missing.

Loci in Promega® PowerPlex® 16HS

Loci in Promega® PowerPlex® 18D

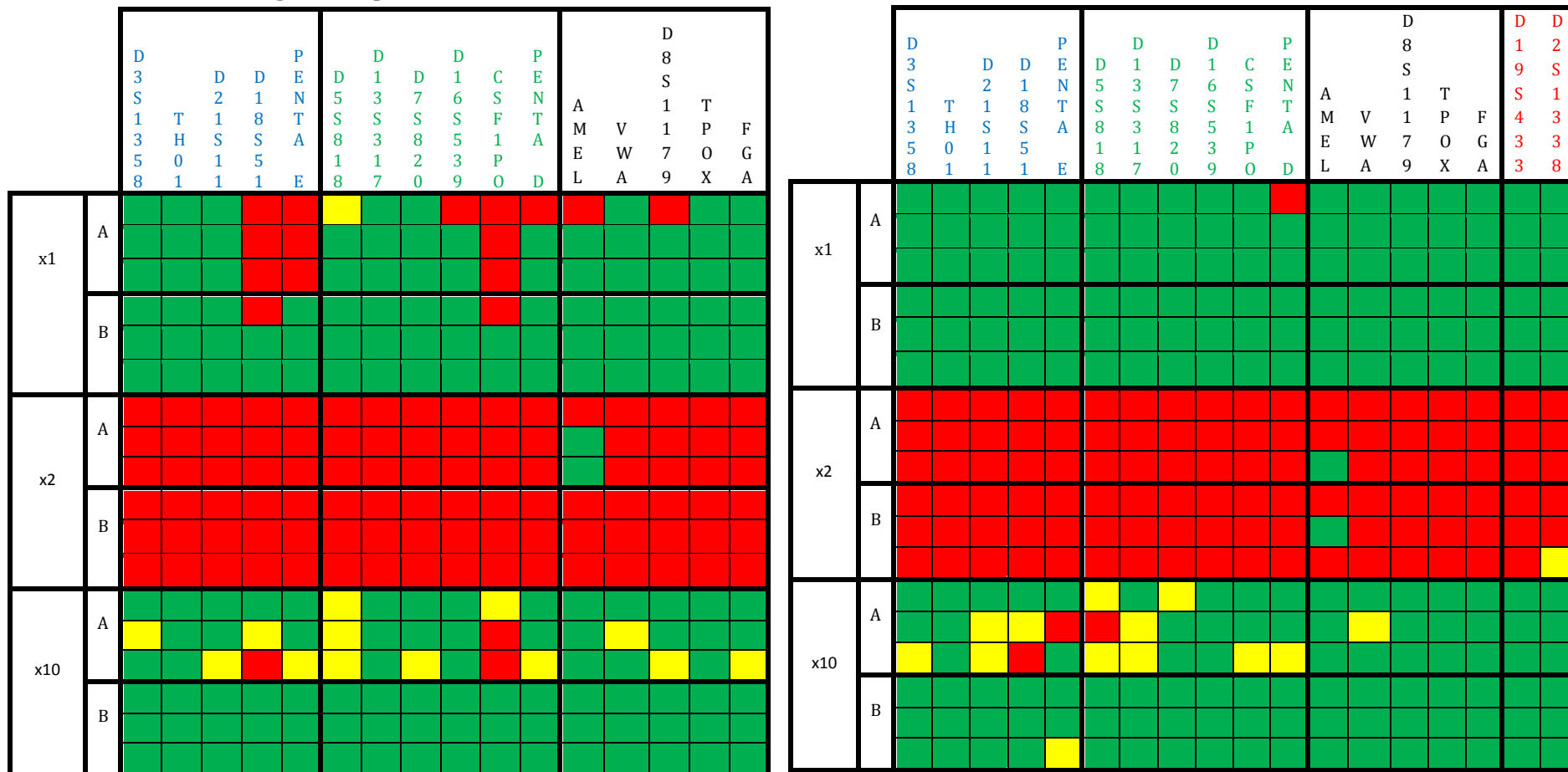


Table 6.1: Results for LCV profiles using PowerPlex® 16HS showing the minimum, maximum and average peak heights, the profile type, total PCR product and PCR concentration for the various dilutions of samples A and B, amplified using half (12.5µl) reactions, and processed on various substrates. The values are averages of three replicates.

Substrate Sample	Dilution	Profile Properties				Total PCR Product (in RFU)	PCR product concentration (in RFU/µl)	
		Max PH	Min PH	Average PH	Profile Type			
Glass A	x1	694 (s.d. 152)	54 (s.d. 1.15)	220.05	PP13	12983 (s.d. 1622.87)	1038.6 (s.d. 129.8)	
	x2	--	--	--	--	--	--	
	x10	1262 (s.d. 290.24)	50 (s.d. 10.81)	223.08	PP13	14500 (s.d. 1834.49)	1160 (s.d. 146.7)	
	B	x1	9208 (s.d. 1085.15)	56 (s.d. 38.02)	2207.27	FP	150094 (s.d. 10374.02)	12007.5 (s.d.829.9)
		x2	--	--	--	--	--	--
		x10	6195 (s.d. 512.11)	293 (s.d. 29.14)	1561.64	FP	112438 (s.d. 2356.71)	8995.0 (s.d. 188.5)
Gypsum A	x1	666 (s.d. 198.68)	51 (s.d. 5.29)	178.65	PP10	9647 (s.d. 3215.67)	771.8 (s.d. 93.4)	
	x2	149 (s.d. 53.43)	50 (s.d. 11.68)	69.85	PP1	489 (s.d. 91.16)	39.1 (s.d.7.3)	
	x10	826 (s.d. 221.50)	50 (s.d. 3.79)	169.07	PP7	7101 (s.d. 539.26)	568.1 (s.d.43.1)	
	B	x1	4666 (s.d. 1441.76)	106 (s.d. 44.43)	760.79	PP13	42604 (s.d. 5840.47)	3408.3 (s.d. 467.2)
		x2	--	--	--	--	--	--
		x10	1076 (s.d. 68.43)	55 (s.d. 5.50)	309.55	PP14	18573 (s.d. 1734.60)	1485.8 (s.d. 138.8)
Laminate A	x1	4817 (s.d. 1187.35)	51 (s.d. 46.87)	1005.97	PP14	75448 (s.d. 8745.46)	6035.8 (s.d. 699.6)	
	x2	68 (s.d. 35.91)	68 (s.d. 35.91)	61	NP	122 (s.d. 35.91)	9.8 (s.d. 2.9)	
	x10	3977 (s.d. 1054.33)	50 (s.d. 24.66)	551.20	FP	45750 (s.d. 2815.17)	3660 (s.d. 225.2)	
	B	x1	1440 (s.d. 477.19)	50 (s.d. 4.58)	369.04	PP13	20297 (s.d. 2921.17)	1623.08 (s.d.233.7)
		x2	--	--	--	--	--	--
		x10	1095 (s.d. 229.65)	51 (s.d. 34.70)	301.39	PP14	19289 (s.d. 2506.31)	1543.12 (s.d. 200.5)
Lead A	x1	1192 (s.d. 223.50)	53 (s.d. 11.72)	297.03	PP13	19604 (s.d. 1654.93)	1568.3 (s.d. 132.4)	
	x2	2499 (s.d. 822.05)	54 (s.d. 12.74)	448.65	PP1	32303 (s.d. 3914.68)	2584.2 (s.d. 313.2)	
	x10	1221 (s.d. 380.40)	52 (s.d. 1.53)	244.16	PP11	17091 (s.d. 2299.44)	1367.3 (s.d. 183.9)	
	B	x1	1341 (s.d. 185.63)	56 (s.d. 31.56)	373.53	PP13	20544 (s.d. 1512.09)	1643.5 (s.d. 120.9)
		x2	--	--	--	NP	--	--
		x10	1370 (s.d. 481.88)	52 (s.d. 6.03)	252.57	PP14	15154 (s.d. 1276.31)	1212.32 (s.d. 102.1)
Plastic A	x1	16166 (s.d. 4422.25)	591 (s.d. 269.69)	4267.52	FP	358472 (s.d. 50015.92)	28677.8 (s.d. 4001.2)	
	x2	1414 (s.d. 87.61)	83 (s.d. 27.14)	451.51	FP	37927 (s.d. 834.52)	3034.2 (s.d. 66.8)	
	x10	1749 (s.d. 489.25)	60 (s.d. 24.85)	338.75	PP14	26761 (s.d. 1826.98)	2140.9 (s.d. 146.2)	
	B	x1	8374 (s.d. 1209.49)	97 (s.d. 239.45)	3203.60	FP	230659 (s.d. 12675.04)	18452.7 (s.d. 1014)
		x2	13975 (s.d. 2595.32)	553 (s.d. 121.70)	3684.93	FP	265315 (s.d. 11204.71)	21225.2 (s.d. 896.4)
		x10	520 (s.d. 113.90)	50 (s.d. 4.16)	187.49	PP13	9937 (s.d. 1260.82)	794.9 (s.d. 100.9)
Raw Wood A	x1	21696 (s.d. 1374.60)	1319 (s.d. 234.51)	6703.66	FP	563107 (s.d. 18312.81)	45048.6 (s.d. 1465)	
	x2	3114 (s.d. 949.90)	77 (s.d. 3.61)	625.95	FP	51328 (s.d. 8044.37)	4106.2 (s.d. 643.5)	
	x10	1452 (s.d.78.01)	52 (s.d. 8.08)	342.29	PP15	27041 (s.d. 1502.75)	2163.3 (s.d. 120.2)	
	B	x1	19871 (s.d. 4541.80)	863 (s.d. 100.18)	5362.72	FP	386116 (s.d. 31887.91)	30889.13 (s.d. 2551.0)
		x2	1472 (s.d. 481.57)	52 (s.d. 29.57)	295.30	PP13	16832 (s.d. 2838.23)	1346.6 (s.d. 227.1)
		x10	1795 (s.d. 377.59)	71 (s.d. 7)	401.72	PP14	26915 (s.d. 1823.00)	2153.2 (s.d. 145.8)
Tile A	x1	24963 (s.d. 2918.66)	1701 (s.d. 305.93)	8119.94	FP	682075 (s.d. 8976.29)	54566 (s.d. 718.1)	
	x2	667 (s.d. 81.57)	51 (s.d. 10.69)	181.76	FP	13632 (s.d. 468.12)	1090.6 (s.d. 37.4)	
	x10	1700 (s.d. 200.85)	62 (s.d. 8.89)	466.96	PP15	38291 (s.d. 3468.11)	3063.3 (s.d. 277.4)	
	B	x1	20189 (s.d. 2262.67)	1812 (s.d. 115.70)	7870.76	FP	566695 (s.d. 15063.92)	45335.6 (s.d. 1205.1)
		x2	8309 (s.d. 1235.50)	484 (s.d. 114.96)	2904.36	FP	209114 (s.d. 9084.61)	167929.1 (s.d. 726.8)
		x10	2203 (s.d. 781.86)	50 (s.d. 19.08)	471.28	PP15	32518 (s.d. 3699.13)	2601.4 (s.d. 295.9)

Table 6.2: Results for LCV profiles using PowerPlex® 18D showing the minimum, maximum and average peak heights, the profile type, total PCR product and PCR concentration for the various dilutions of samples A and B, amplified using half (12.5µl) reactions, and processed on various substrates. The values are averages of three replicates.

Substrate Sample	Dilution	Profile Properties				Total PCR Product (in RFU)	PCR product concentration (in RFU/µl)	
		Max PH	Min PH	Average PH	Profile Type			
Glass A	x1	19558 (s.d. 3704.26)	334 (s.d. 2368.95)	7657.30	FP	735101 (s.d. 36771.26)	58808.1 (s.d.2941.7)	
	x2	3718 (s.d. 471.05)	438 (s.d. 163.79)	1205.60	NP	115738 (s.d. 9183.91)	9259.0 (s.d.734.7)	
	x10	218 (s.d. 14.93)	51 (s.d. 2.08)	96.19	PP14	7503 (s.d. 367.04)	600.2 (s.d. 29.4)	
	x1	3310 (s.d. 502.43)	108 (s.d. 83.69)	784.36	FP	68239 (s.d. 1451.52)	5459.1 (s.d. 116.1)	
	B	x2	156 (s.d. 24.68)	50 (s.d. 4.04)	81.4	NP	3256 (s.d. 212.86)	260.5 (s.d. 17.0)
		x10	639 (s.d. 154.63)	64 (s.d. 2)	182.99	FP	14639 (s.d. 646.36)	1171.1 (s.d. 51.7)
Gypsum A	x1	14923 (s.d. 2787.38)	239 (s.d. 694.87)	4861.54	FP	466708 (s.d. 32773.74)	37336.6 (s.d. 2621.9)	
	x2	4343 (s.d. 23.46)	51 (s.d. 385.52)	1857.12	FP	180141 (s.d. 6943.96)	14411.3 (s.d. 555.5)	
	x10	919 (s.d. 118.59)	124 (s.d. 11.02)	349.48	FP	33550 (s.d. 2028.29)	2684 (s.d. 162.3)	
	x1	14967 (s.d. 805.98)	193 (s.d. 707.67)	5845.51	FP	473486 (s.d. 16101.98)	37878.9 (s.d. 1288.2)	
	B	x2	5846 (s.d. 483.17)	966 (s.d. 45.76)	2516.99	FP	203876 (s.d. 5877.48)	16310.1 (s.d. 470.2)
		x10	971 (s.d. 87.69)	121 (s.d. 6.24)	374.10	FP	30302 (s.d. 520.76)	2424.2 (s.d. 41.7)
Laminate A	x1	22050 (s.d. 1743.80)	535 (s.d. 2425.11)	8673.31	FP	832638 (s.d. 18691.51)	66611.0 (s.d. 1495.3)	
	x2	1609 (s.d. 328.07)	238 (s.d. 60.26)	451.92	FP	43384 (s.d. 4118.29)	3470.7 (s.d. 329.5)	
	x10	665 (s.d. 71.60)	67 (s.d. 35.02)	211.39	FP	20293 (s.d. 1176.53)	1623.4 (s.d. 94.1)	
	x1	6164 (s.d. 1368.25)	340 (s.d. 164.43)	1824.60	FP	147793 (s.d. 8750.86)	11823.4 (s.d. 700.1)	
	B	x2	112 (s.d. 64.66) ¹	52 (s.d. 30.02)	70.14	NP	491 (s.d. 283.48)	39.3 (s.d. 22.7)
		x10	193 (s.d. 20.66)	51 (s.d. 8.89)	95.87	PP11	3643 (s.d. 194.64)	291.4 (s.d. 15.6)
Lead A	x1	2533 (s.d. 127.69)	108 (s.d. 74.54)	757.48	FP	71961 (s.d. 7083.82)	5758.9 (s.d. 566.7)	
	x2	242 (s.d. 95.13)	50 (s.d. 0.58)	74.31	PP1	966 (s.d. 149.36)	77.3 (s.d. 11.9)	
	x10	323 (s.d. 38.44)	50 (s.d. 0.58)	119.54	FP	10998 (s.d. 387.79)	879.8 (s.d. 31.0)	
	x1	2471 (s.d. 406.25)	101 (s.d. 15.87)	544.51	PP4	40294 (s.d. 699.85)	3223.5 (s.d. 55.9)	
	B	x2	183 (s.d. 96.39)	50 (s.d. 96.39)	163.5	PP1	327 (s.d. 96.39)	26.2 (s.d. 7.7)
		x10	107 (s.d. 10.97)	51 (s.d. 3.79)	74.73	PP6	1644 (s.d. 231.92)	131.5 (s.d. 18.6)
Plastic A	x1	5299 (s.d. 1614.24)	316 (s.d. 368.57)	1480.22	FP	142101 (s.d. 21347.76)	11368.0 (s.d. 1707.8)	
	x2	6288 (s.d. 886.31)	834 (s.d. 203.44)	2245.49	FP	215567 (s.d. 2881.03)	17245.4 (s.d. 230.5)	
	x10	312 (s.d. 46.82)	50 (s.d. 1.15)	120.65	PP16	10979 (s.d. 310.70)	878.3 (s.d. 24.8)	
	x1	7505 (s.d. 1457.58)	762 (s.d. 314)	2555.95	FP	207032 (s.d. 12223.42)	16562.6 (s.d. 977.9)	
	B	x2	6812 (s.d. 900.60)	800 (s.d. 264.83)	2663.26	FP	215724 (s.d. 3834.25)	17257.9 (s.d. 306.7)
		x10	590 (s.d. 170.16)	58 (s.d. 6.35)	184.80	PP17	13675 (s.d. 1399.30)	1094 (s.d. 111.9)
Raw Wood A	x1	16848 (s.d. 4654.91)	2145 (s.d. 766.87)	5652.81	FP	542670 (s.d. 55405.93)	43413.6 (s.d. 4432.5)	
	x2	4616 (s.d. 165.06)	557 (s.d. 116.65)	1953.74	FP	187559 (s.d. 6297.10)	15004.7 (s.d. 503.8)	
	x10	1024 (s.d. 86.60)	111 (s.d. 44.23)	390.16	FP	37455 (s.d. 1569.59)	2996.4 (s.d. 125.6)	
	x1	10648 (s.d. 2677.06)	1003 (s.d. 520.17)	3576.59	FP	289704 (s.d. 36083)	23176.3 (s.d. 2886.6)	
	B	x2	7401 (s.d. 1560.54)	544 (s.d. 228.58)	2555.67	FP	207009 (s.d. 15777.90)	16560.7 (s.d. 1262.2)
		x10	592 (s.d. 119.65)	71 (s.d. 6.51)	215.13	FP	16995 (s.d. 2122.40)	1359.6 (s.d. 169.8)
Tile A	x1	9190 (s.d. 1797.22)	1313 (s.d. 491.99)	3526.33	FP	338528 (s.d. 33517.45)	27082.2 (s.d. 2681.4)	
	x2	22680 (s.d. 6013.82)	51 (s.d. 2141.12)	6074.65	FP	589241 (s.d. 63291.16)	47139.3 (s.d. 5063.3)	
	x10	886 (s.d. 144.44)	119 (s.d. 11.02)	308.06	FP	29574 (s.d. 1386.85)	2365.9 (s.d. 110.9)	
	x1	1841 (s.d. 389.23)	117 (s.d. 64.30)	688.46	FP	55765 (s.d. 2643.46)	4461.2 (s.d. 211.5)	
	B	x2	29197 (s.d. 2843.63)	4895 (s.d. 103.23)	13136.31	FP	1064041 (s.d. 32860.98)	85123.3 (s.d. 2628.9)
		x10	660 (s.d. 28.36)	67 (s.d. 26.46)	271.42	FP	21985 (s.d. 444.71)	1758.8 (s.d. 35.6)

¹ The alleles obtained in this profile were one of two in a heterozygous locus (yellow box) or a homozygous peak in a locus (green box); however, in both cases, were not reproducible thus not added to the 'profile type' determination.

Dilutions were a significance factor when evaluating the samples [$F(2,74)= 13.11$, $p= 0.001$) without regard to the kit used. This was to be expected since decreasing dilutions of DNA were used in the study. Figure 6.9 displays each dilution in regard to average PCR product concentration and compares ‘no chemical’ samples to samples processed with LCV.

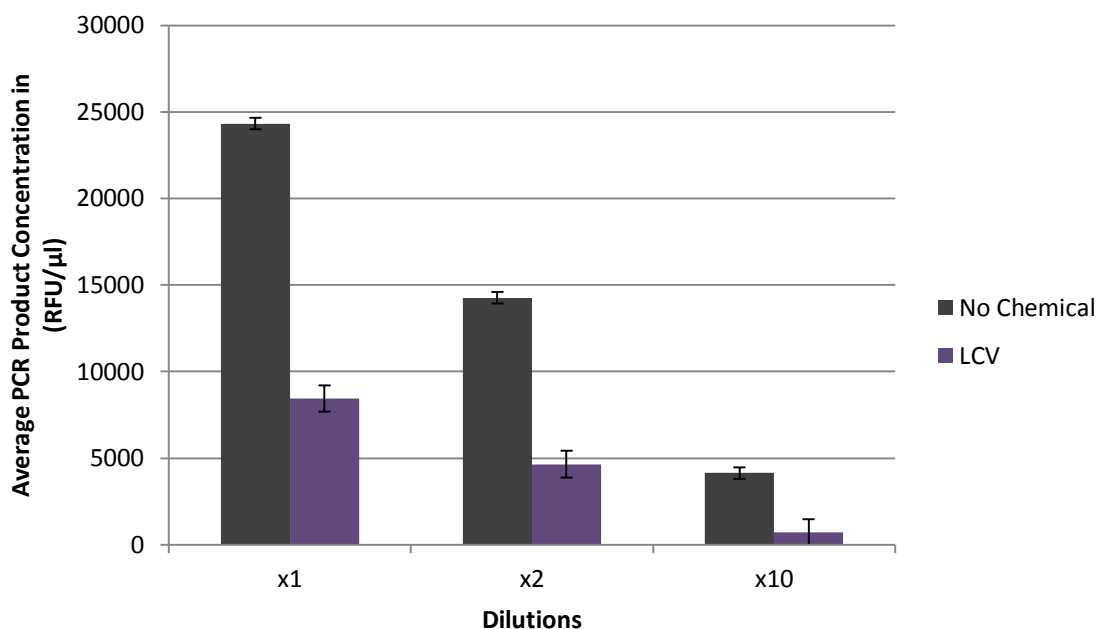
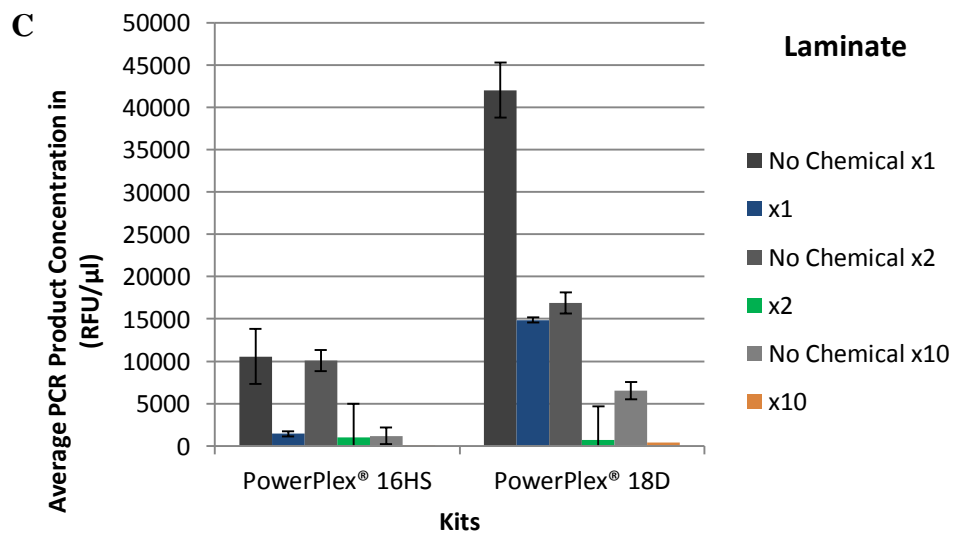
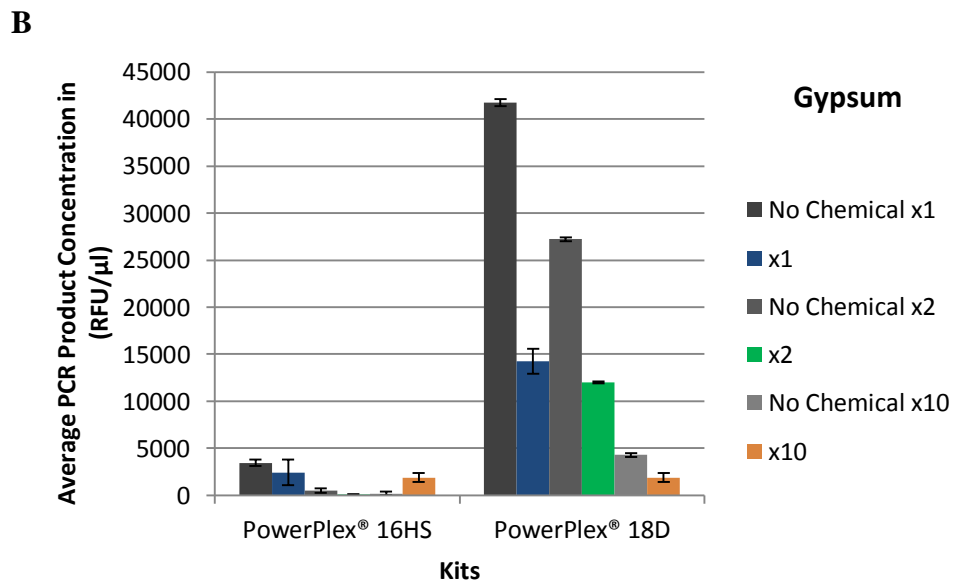
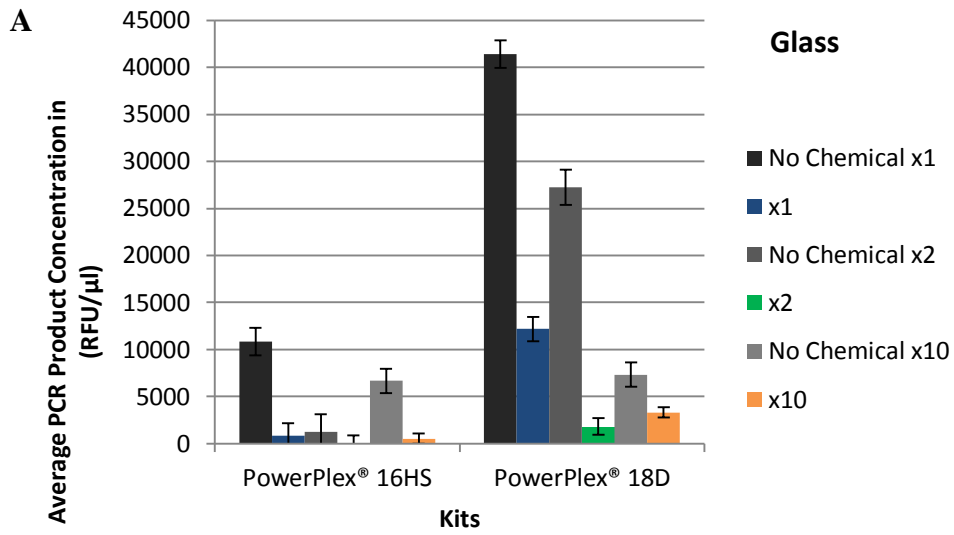
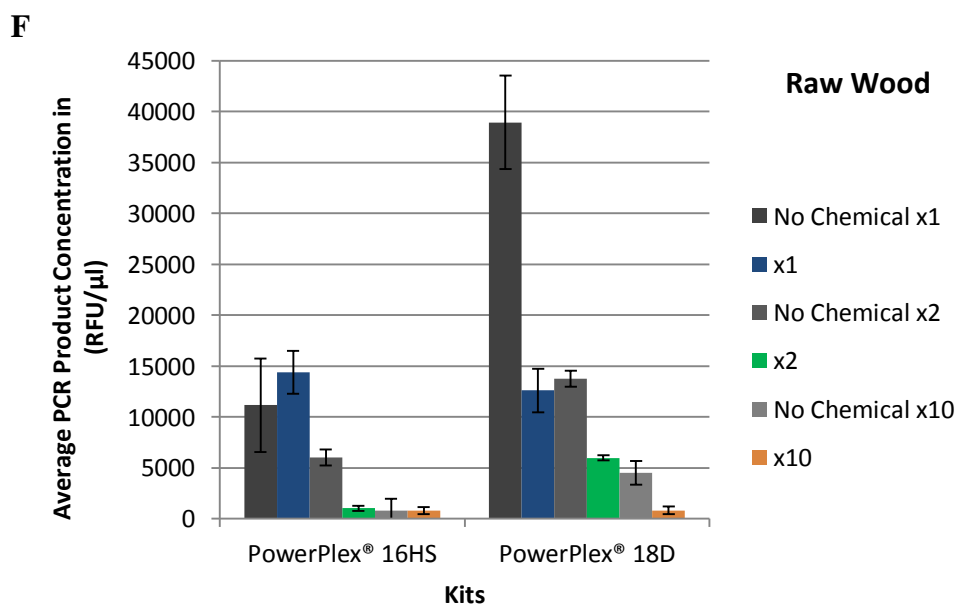
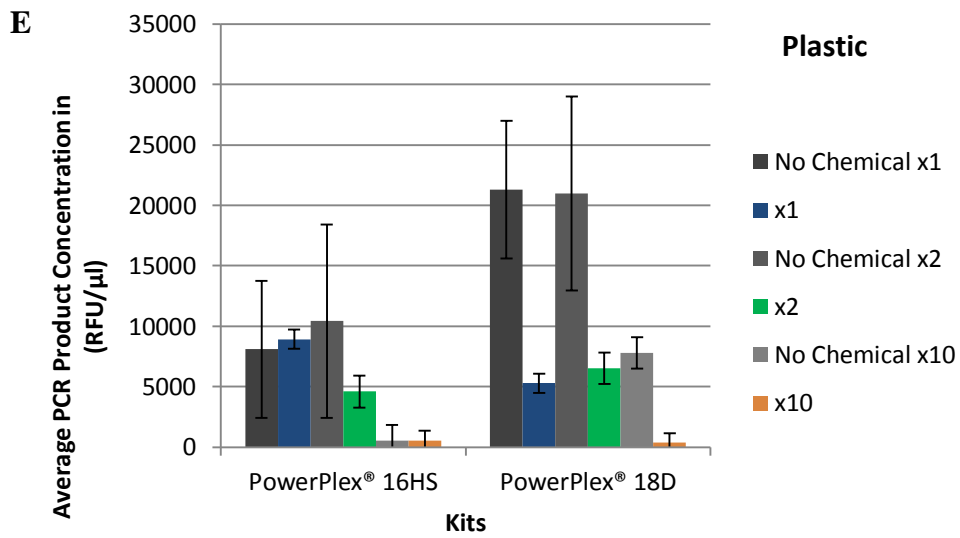
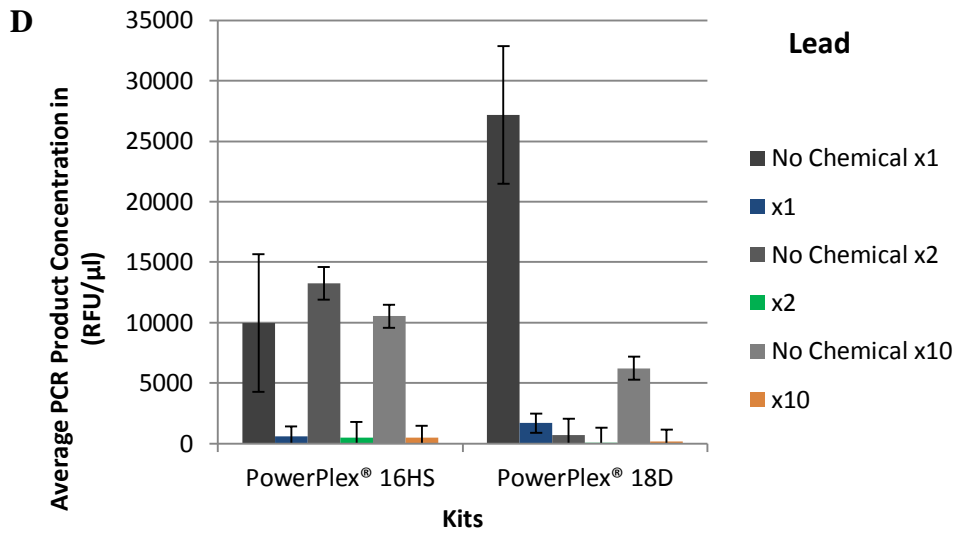


Figure 6.9: Average PCR product concentration (RFU/μl) for each kit, PowerPlex® 16HS and PowerPlex® 18D, for all samples processed using LCV (purple bars) and for all samples processed with no chemical enhancement (grey bars). The error bars represent the standard deviations for each of the dilutions.

The substrates proved to play a noteworthy role in the average PCR product concentration values with a significant variance noted [$F(6, 32)= 2.96$, $p\text{-value } 0.012$]. Tile yielded the strongest profiles and lead the weakest across all dilutions. Gypsum also provided full profiles with high peak height values across all dilutions but the total PCR product concentrations were lower than those of tile. This is also consistent with results obtained from Swaran and Welch (2012). Figures 6.10 (A-G) show a comparison of both kits for each substrate by average PCR product concentration. Both the ‘no chemical’ samples and LCV processed samples can be seen broken down by dilution.

An evaluation of the samples used in the study, A and B, showed no significant difference [$F(1, 82)= 0.48$, $p\text{-value}= 0.491$].





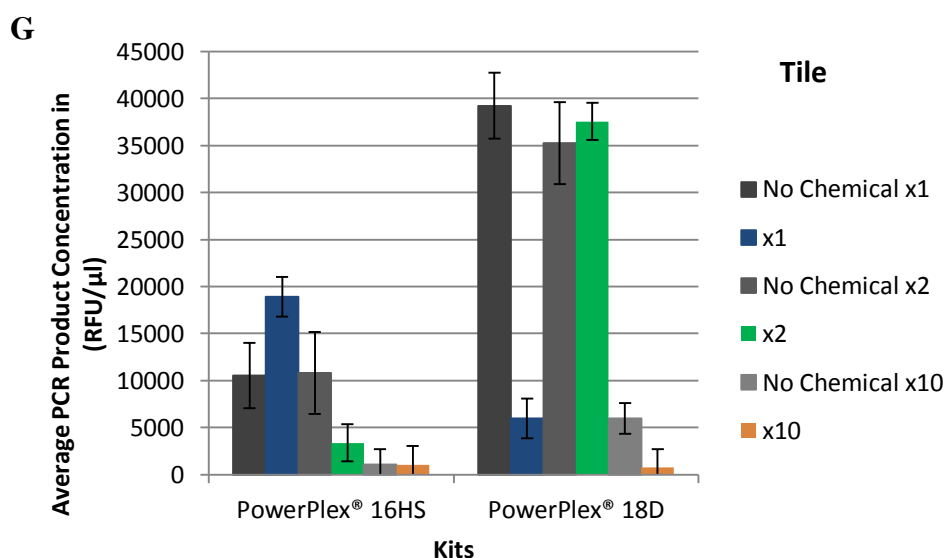


Figure 6.10 (A-G): The average PCR product concentration in (RFU/ μ l) by dilution for samples processed with no chemicals and samples processed with LCV on A) glass, B) gypsum, C) laminate, D) lead, E) plastic, F) raw wood, and G) tile. The error bars represent the standard deviations for each of the dilutions and processed/unprocessed sample averages.

6.3.1.1 Heterozygous Peak Height Balance

Heterozygous peak balance was also assessed for each heterozygous locus present in both sample A and B. Heterozygous peak balance (Hb) is the ratio of the two peaks present at a heterozygous locus. This is determined mathematically by dividing the allele with the lower peak height value by the allele with the greater peak height value (Frégeau et al. 2004). Results range from 0 to 1 with 1 representing alleles of equal height. An Hb value which is below 0.70 indicates peak height imbalance. Symbols which are present at the baseline (0) indicate that only 1 of the 2 alleles present in the heterozygous locus was above threshold. Figures 6.11 through 6.18 exhibit heterozygous loci which are present in both sample A and B and their dilutions by substrate processed. A red dotted line indicates the 0.7 Hb threshold for the results.

Profiles which displayed peak imbalance ($Hb < 0.70$) were observed in both extracted and direct PCR samples. Overall peak imbalance within the PowerPlex® 18D processed samples was lower than those processed with PowerPlex® 16HS for all observed loci. Samples which were exposed to the x10 dilution fell below the 0.7 limit more often; this was to be expected given the decreased amount of DNA template available. The majority appear to be from sample B which quantitatively was weaker than sample A

(*Data Quantitation*) and samples which were prepared with the x10 dilution. Tile contained the fewest loci with peak imbalances for all samples, dilutions and loci evaluated. Loci Penta E, D18, CSF, and FGA displayed the most peak imbalances for both kits.

6.3.1.1.1 Evaluation of CSF1PO

The heterozygous allele of CSF1PO was present in sample A. CSF1PO was more successful in displaying both alleles when processed with PowerPlex® 18D. Both alleles were displayed in 25 of 63 samples analysed with PowerPlex® 16HS as compared to PowerPlex® 18D where both alleles were present in 50 of the 63 samples processed (Figures 6.2-6.8). Of the samples producing both alleles, 15 of the 25 samples processed with PowerPlex® 16HS displayed peak height balance ratios of 0.70 Hb or higher. This is a lower percentage than the 42 of 50 which were over 0.70 when analysed with PowerPlex® 18D.

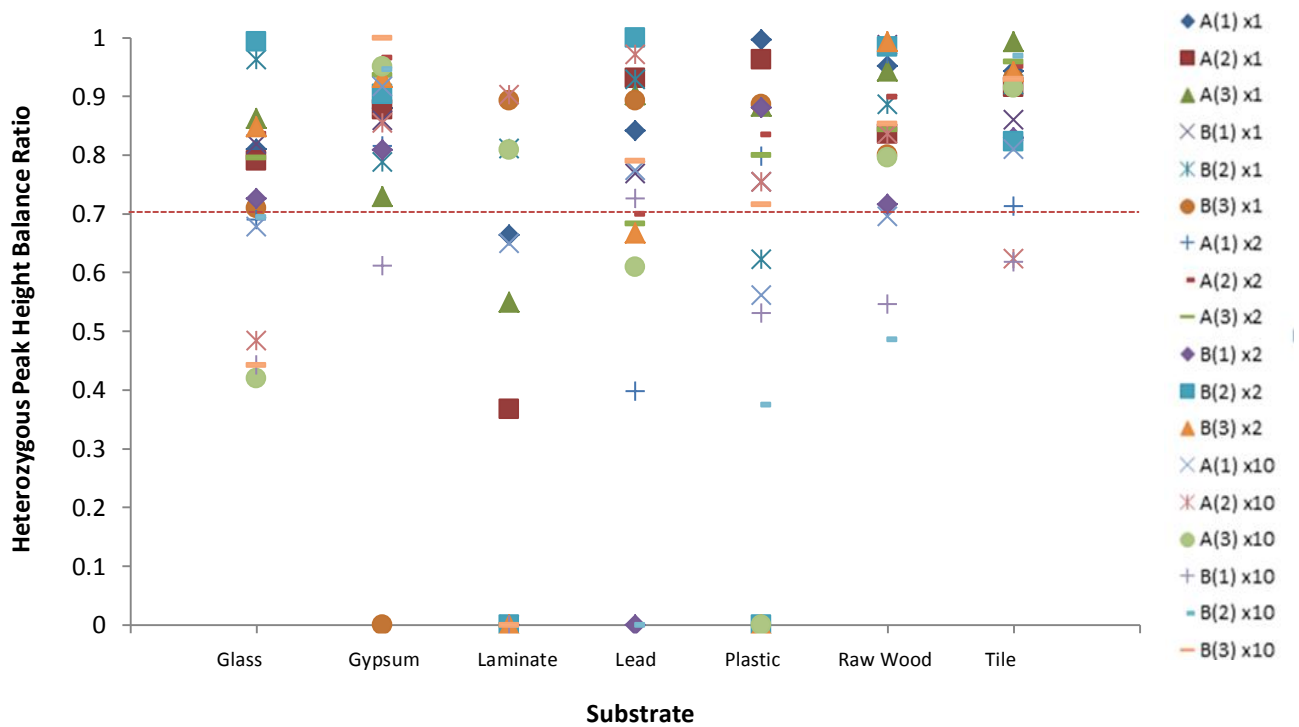
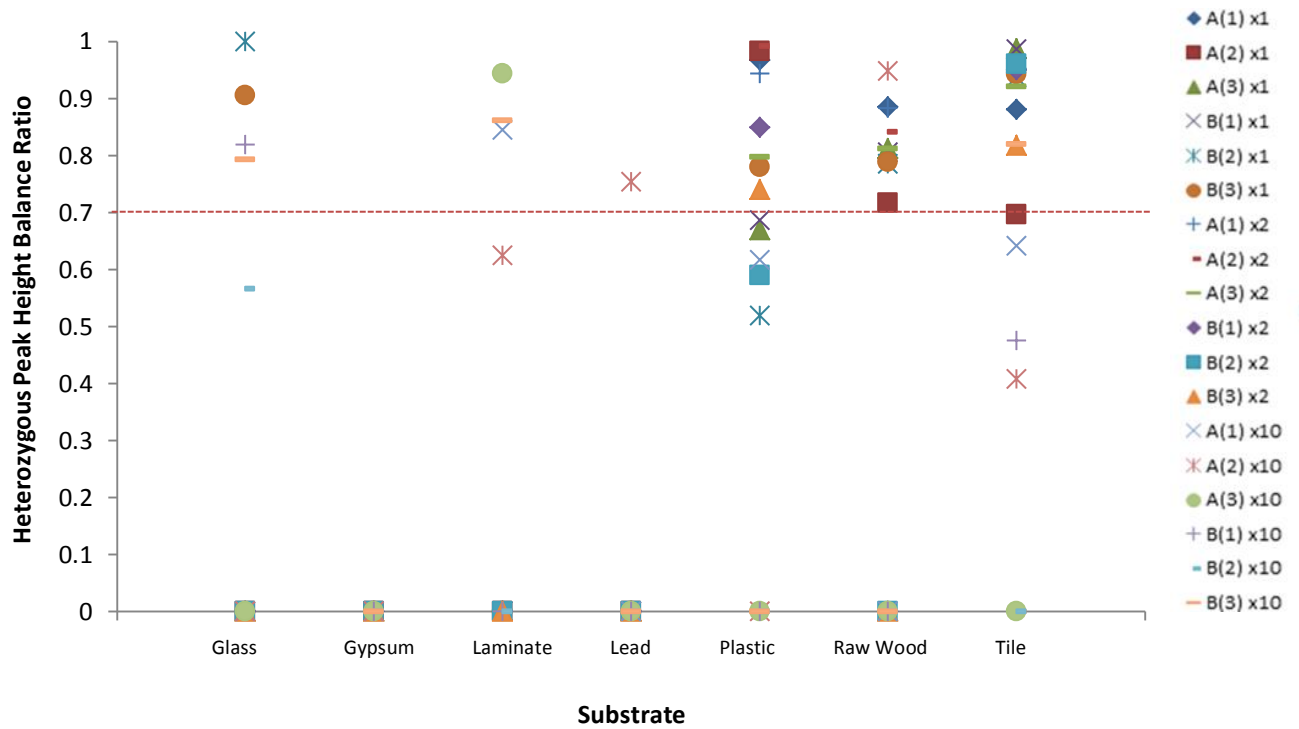


Figure 6.11: (Top) Peak height ratios for *CSFIPO* produced for various substrates when analysed with PowerPlex[®] 16HS. (Bottom) Peak height ratios for *CSFIPO* produced for various substrates when analysed with PowerPlex[®] 18D. All three replicates of each sample (A and B) for each dilution are represented.

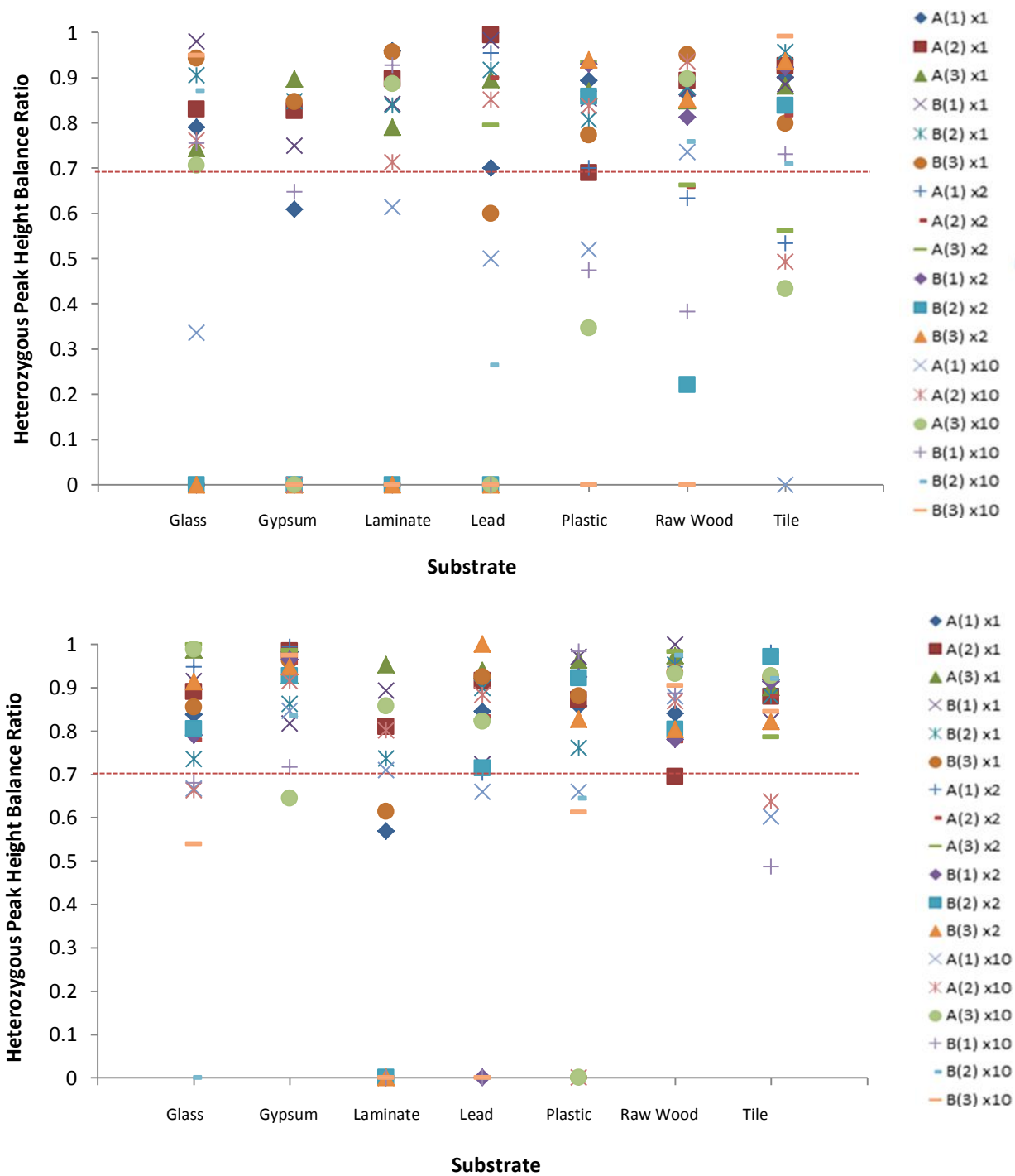


Figure 6.12: (Top) Peak height ratios for *DI3S317* produced for various substrates when analysed with PowerPlex® 16HS. (Bottom) Peak height ratios for *DI3S317* produced for various substrates when analysed with PowerPlex® 18D. All three replicates of each sample (A and B) for each dilution are represented.

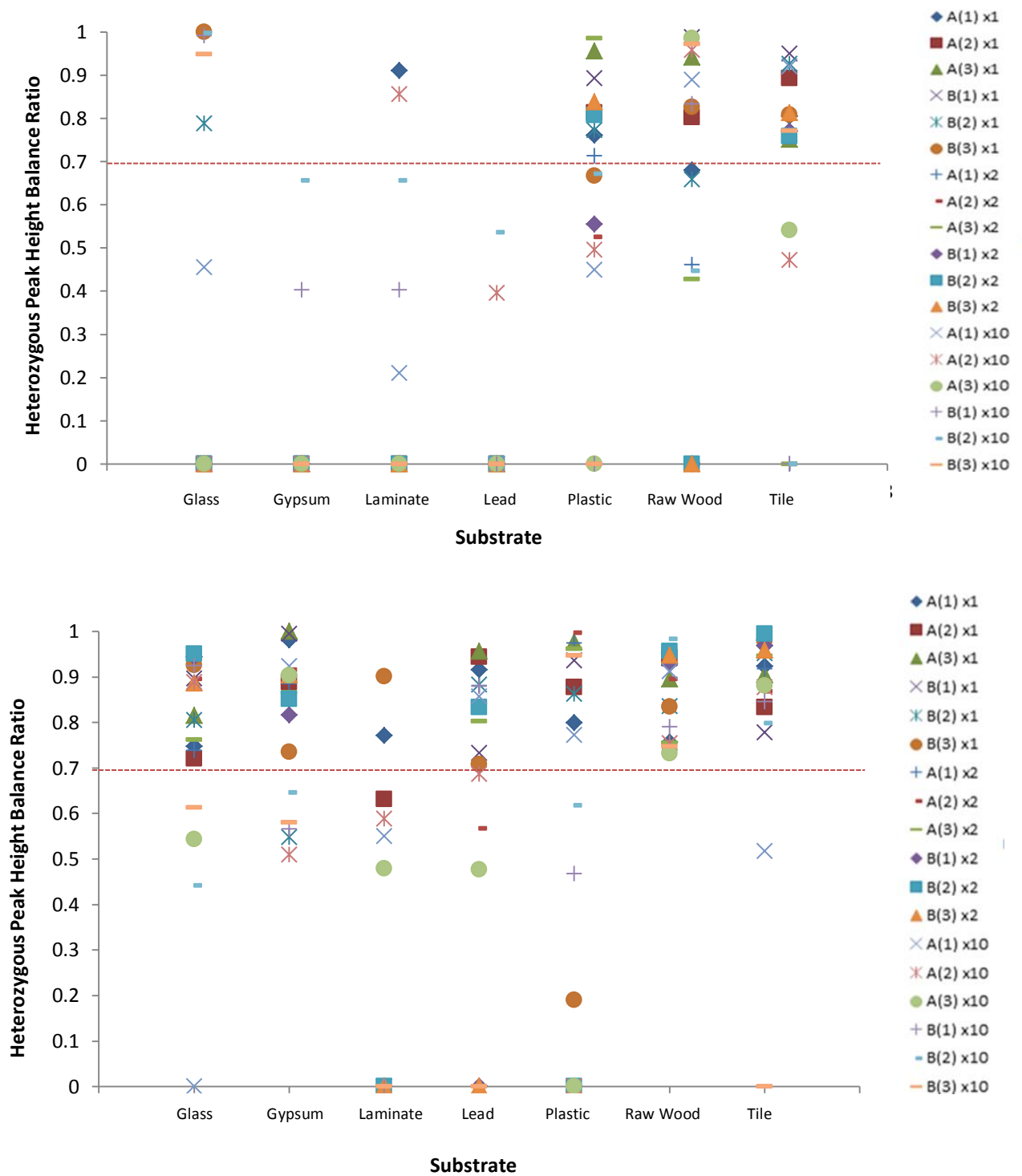


Figure 6.13: (Top) Peak height ratios for *DI8S51* produced for various substrates when analysed with PowerPlex[®] 16HS. (Bottom) Peak height ratios for *DI8S51* produced for various substrates when analysed with PowerPlex[®] 18D. All three replicates of each sample (A and B) for each dilution are represented.

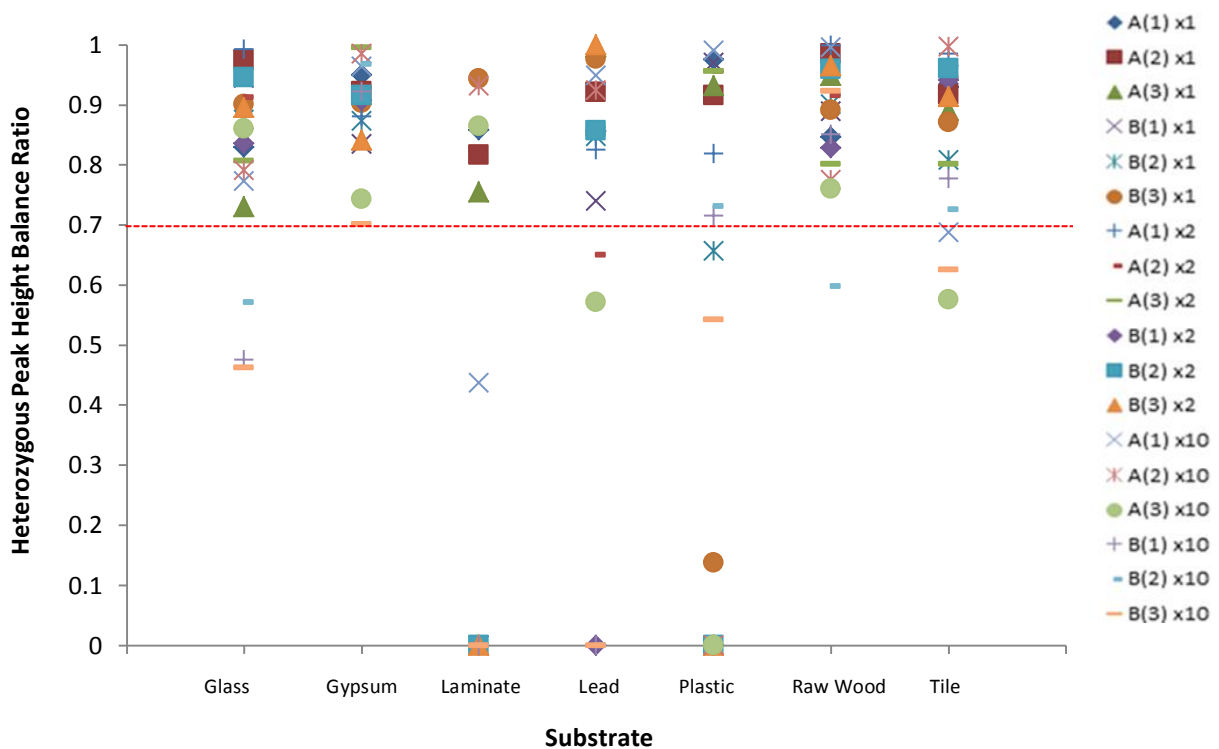
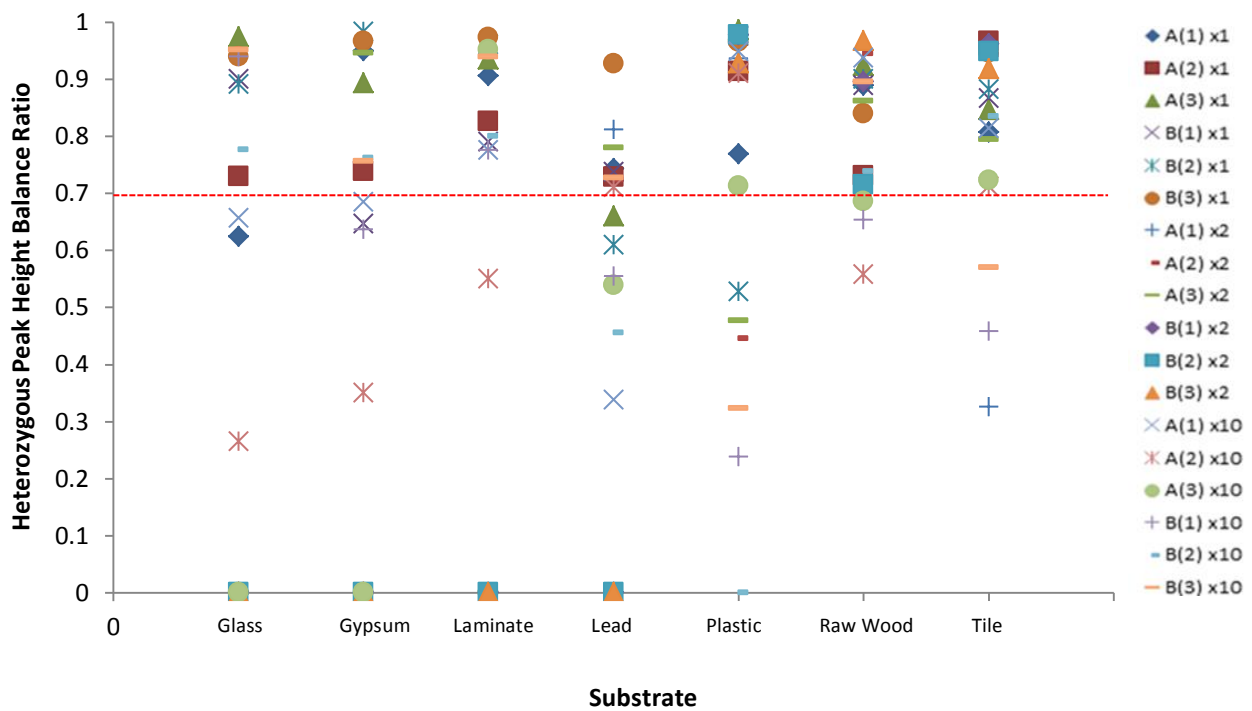


Figure 6.14: (Top) Peak height ratios for *D2IS11* produced for various substrates when analysed with PowerPlex[®] 16HS. (Bottom) Peak height ratios for *D2IS11* produced for various substrates when analysed with PowerPlex[®] 18D. All three replicates of each sample (A and B) for each dilution are represented.

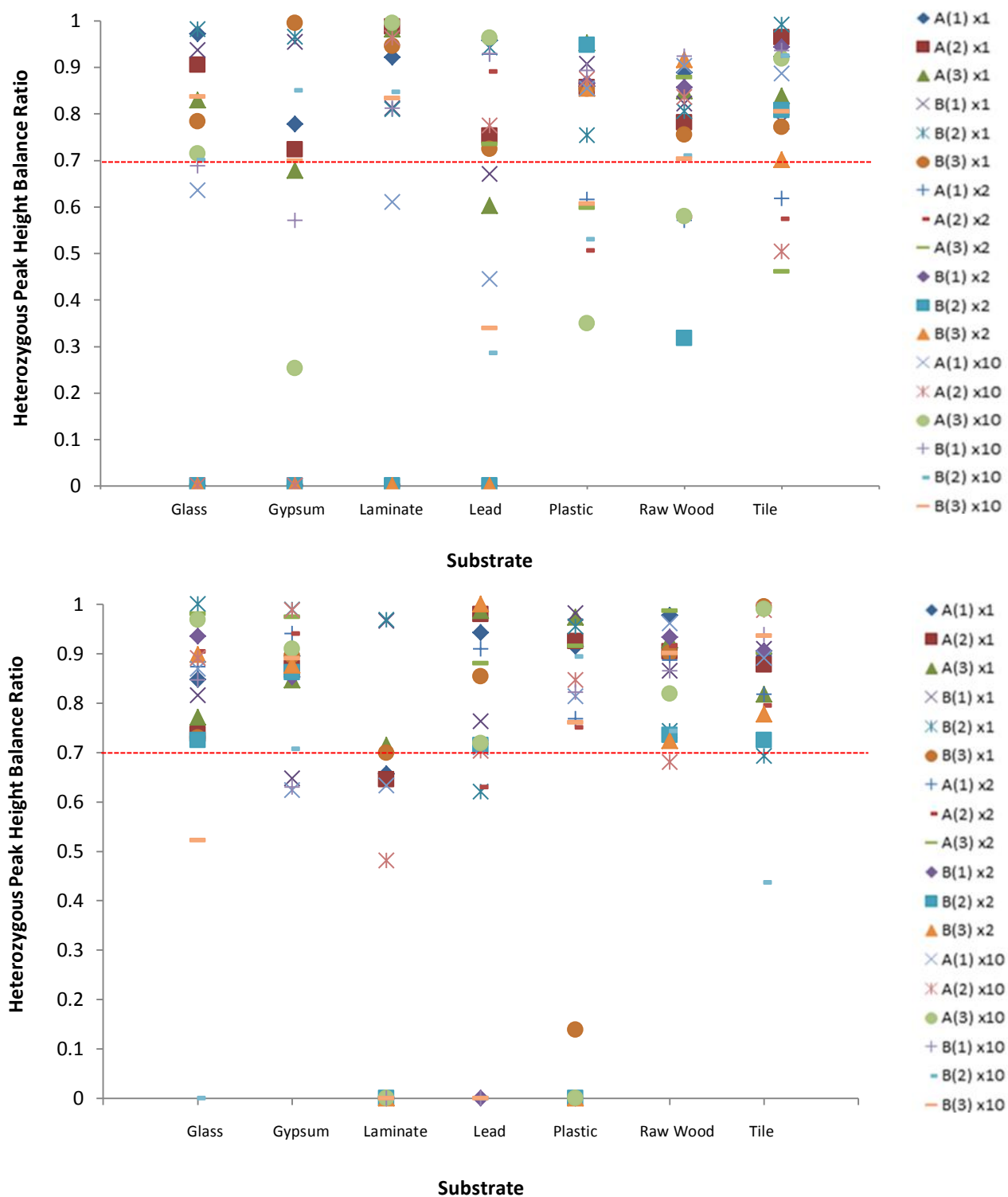


Figure 6.15: (Top) Peak height ratios for *D3S1358* produced for various substrates when analysed with PowerPlex® 16HS. (Bottom) Peak height ratios for *D3S1358* produced for various substrates when analysed with PowerPlex® 18D. All three replicates of each sample (A and B) for each dilution are represented.

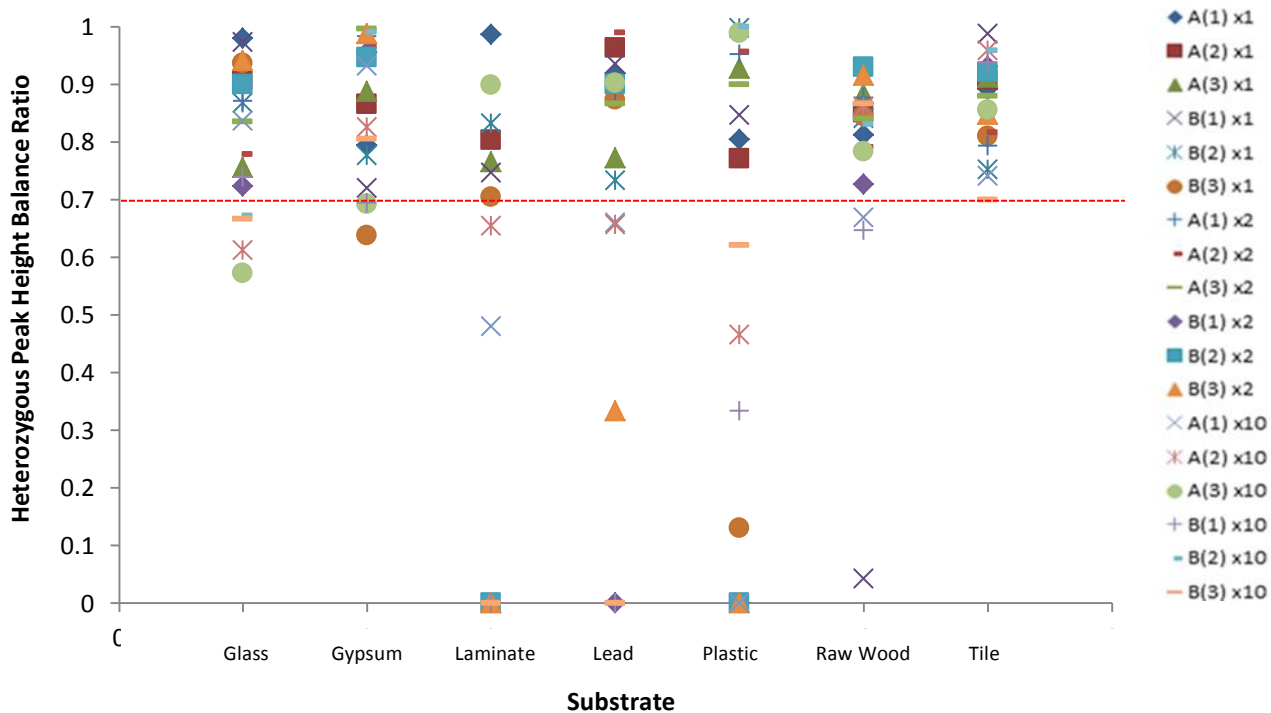
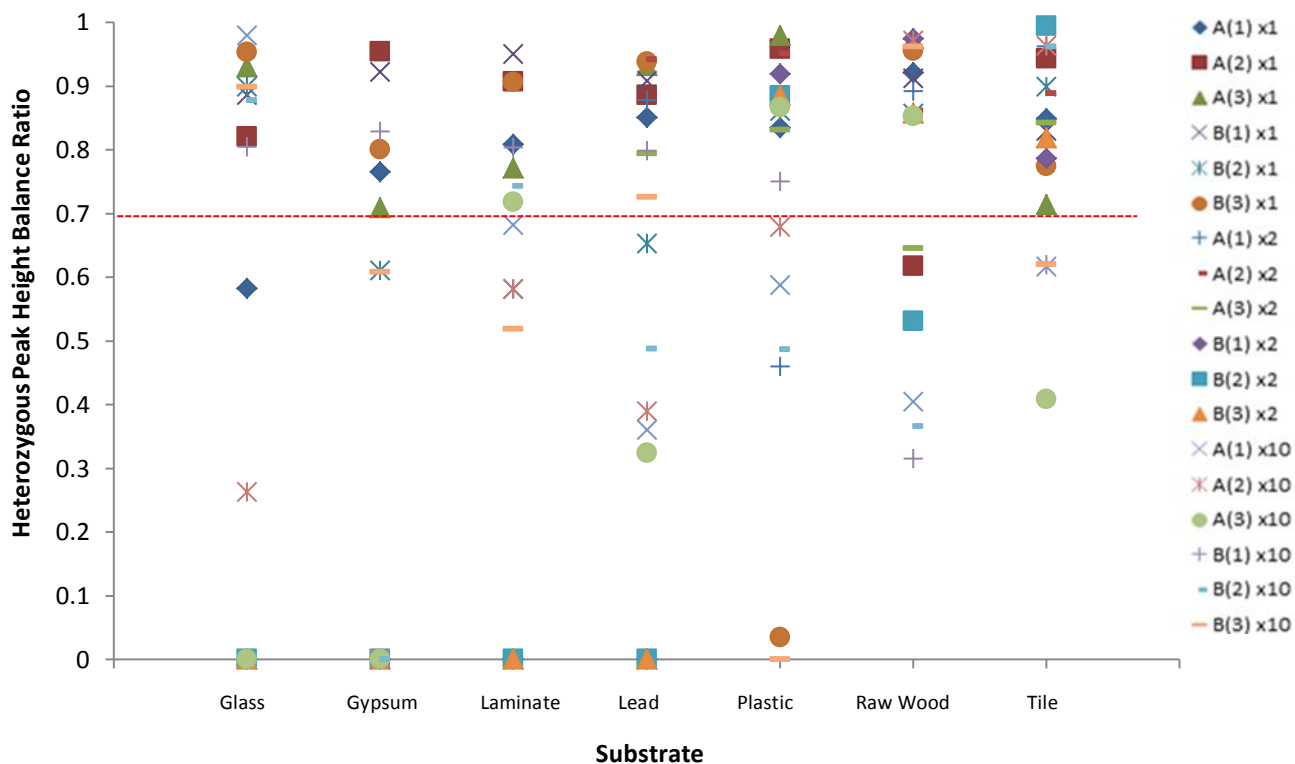


Figure 6.16: (Top) Peak height ratios for *D7S820* produced for various substrates when analysed with PowerPlex[®] 16HS. (Bottom) Peak height ratios for *D7S820* produced for various substrates when analysed with PowerPlex[®] 18D. All three replicates of each sample (A and B) for each dilution are represented.

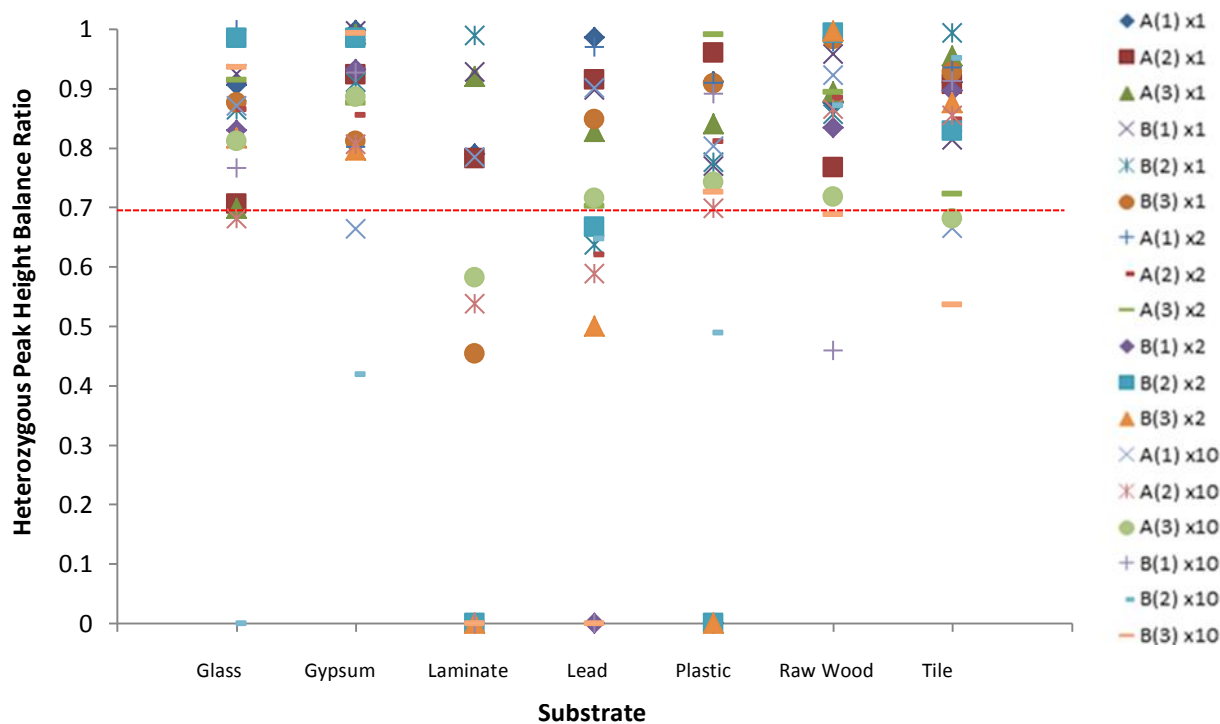
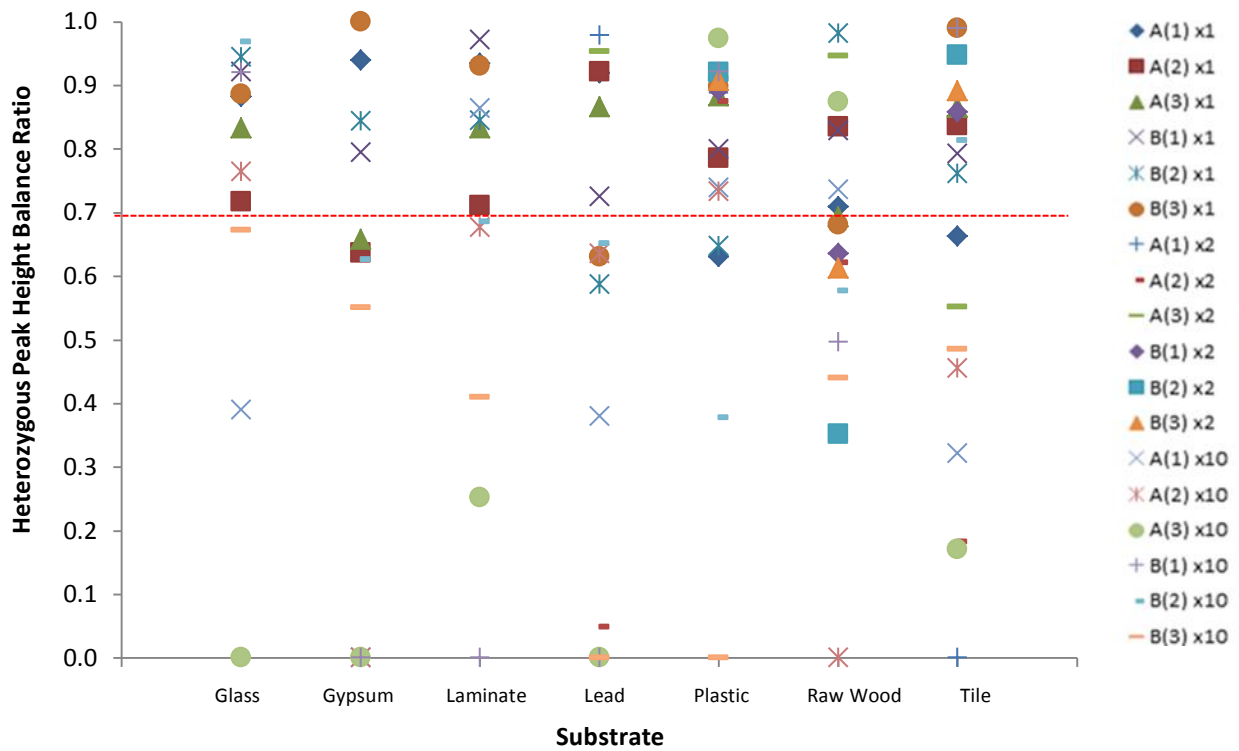


Figure 6.17: (Top) Peak height ratios for FGA produced for various substrates when analysed with PowerPlex[®] 16HS. (Bottom) Peak height ratios for FGA produced for various substrates when analysed with PowerPlex[®] 18D. All three replicates of each sample (A and B) for each dilution are represented.

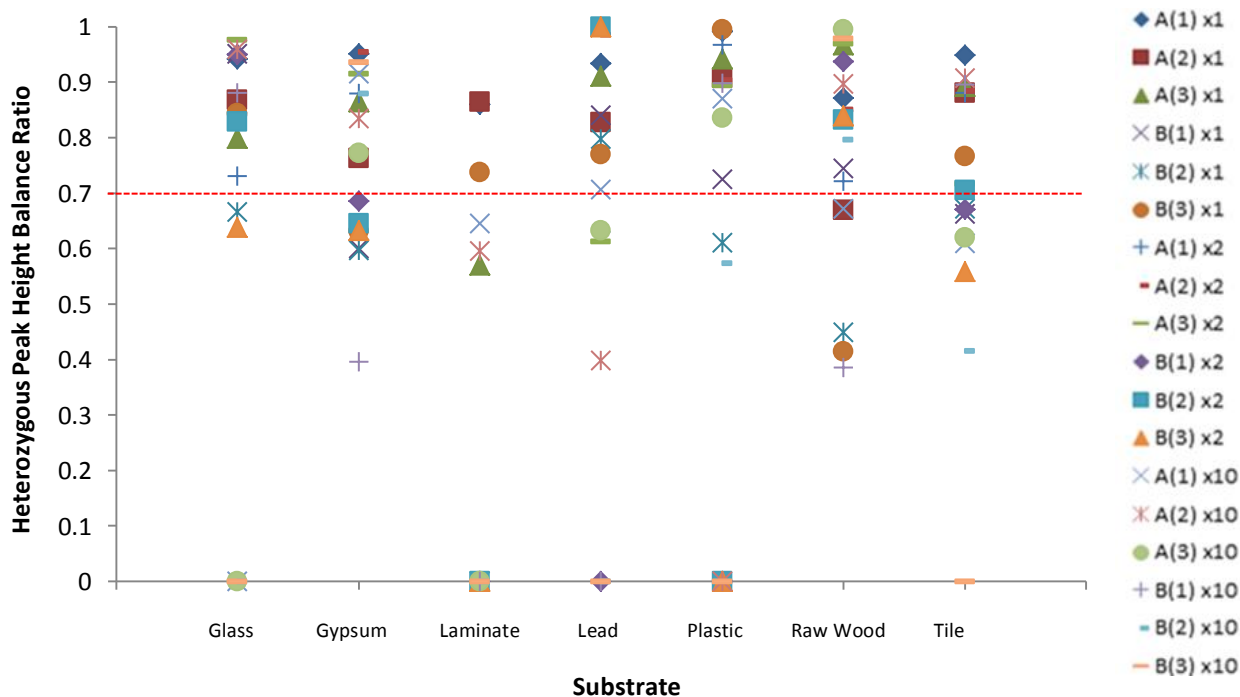
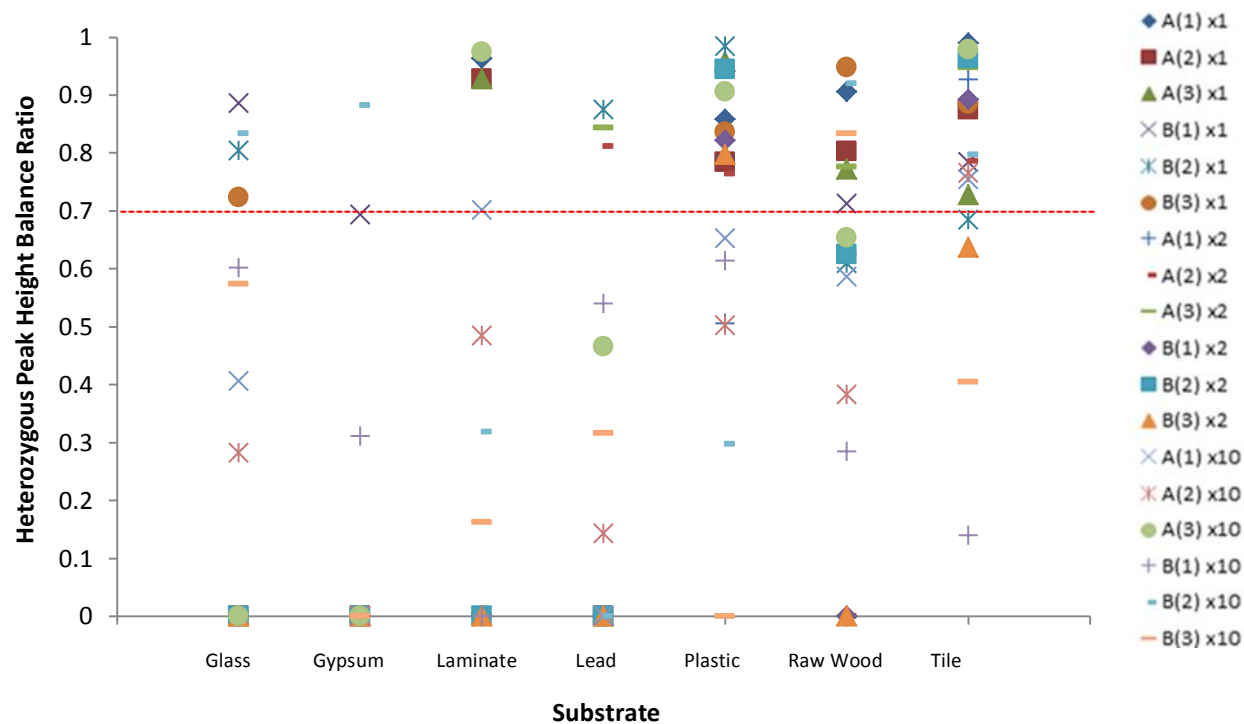


Figure 6.18: (Top) Peak height ratios for Penta E produced for various substrates when analysed with PowerPlex[®] 16HS. (Bottom) Peak height ratios for Penta E produced for various substrates when analysed with PowerPlex[®] 18D. All three replicates of each sample (A and B) for each dilution are represented.

In general, the profiles generated from direct amplification gave higher peak height values and were less prone to peak imbalances than those processed after DNA extraction. An example of this is Glass, x1 dilution. Figure 6.19, shows sample A which was processed with LCV on glass at the x1 dilution. Powerplex® 18D exhibits stronger overall peak heights (over 2,000RFU for all loci) and less peak imbalance than PowerPlex® 16HS.

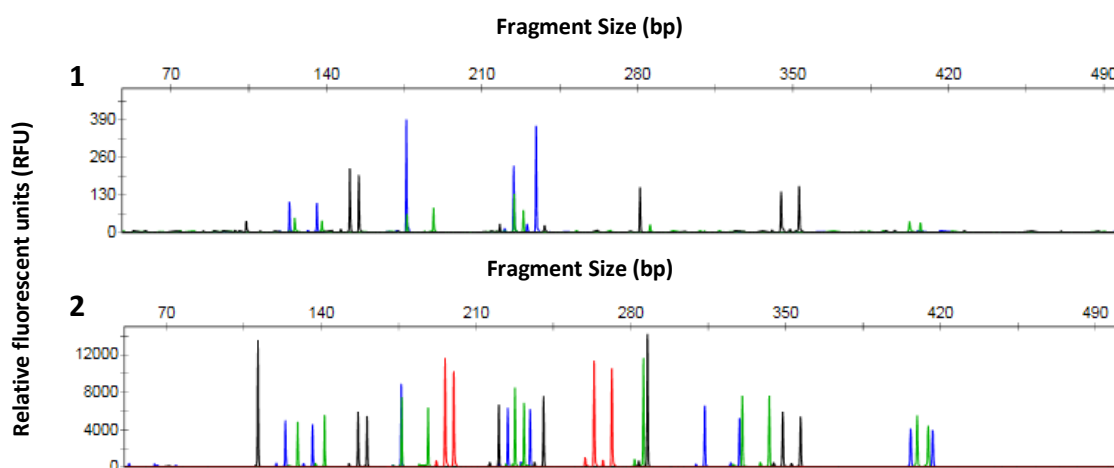


Figure 6.19: Combined dye electropherogram displaying (1) sample A (Glass, x1) processed with PowerPlex® 16HS displayed at 500 RFU. Combined dye electropherogram displaying (2) sample A (Glass, x1) processed with PowerPlex® 18D displayed at 15000 RFU.

Lead was the weakest substrate, yielding the lowest total PCR product and peak heights. While processing the surface prior to swabbing a noticeable reaction occurred after exposing the lead to the LCV solution. It is hypothesized that the LCV caused an oxidation effect possibly affecting the blood on the surface and negatively impacting the profile. Figure 6.20 shows sample A, x1 dilution substrate after processing with the LCV solution. The photograph on the right was the sample swabbed and analysed with PowerPlex® 18D and the left with PowerPlex® 16HS. Electropherograms displaying the profiles generated from the samples in Figure 6.20 can be seen in Figure 6.21.

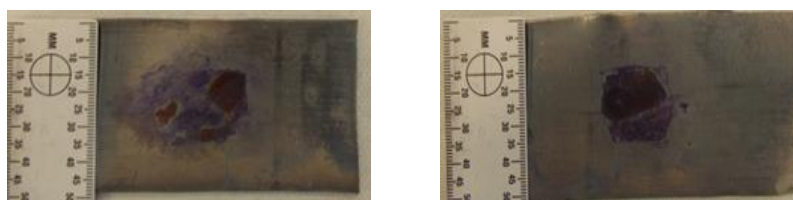
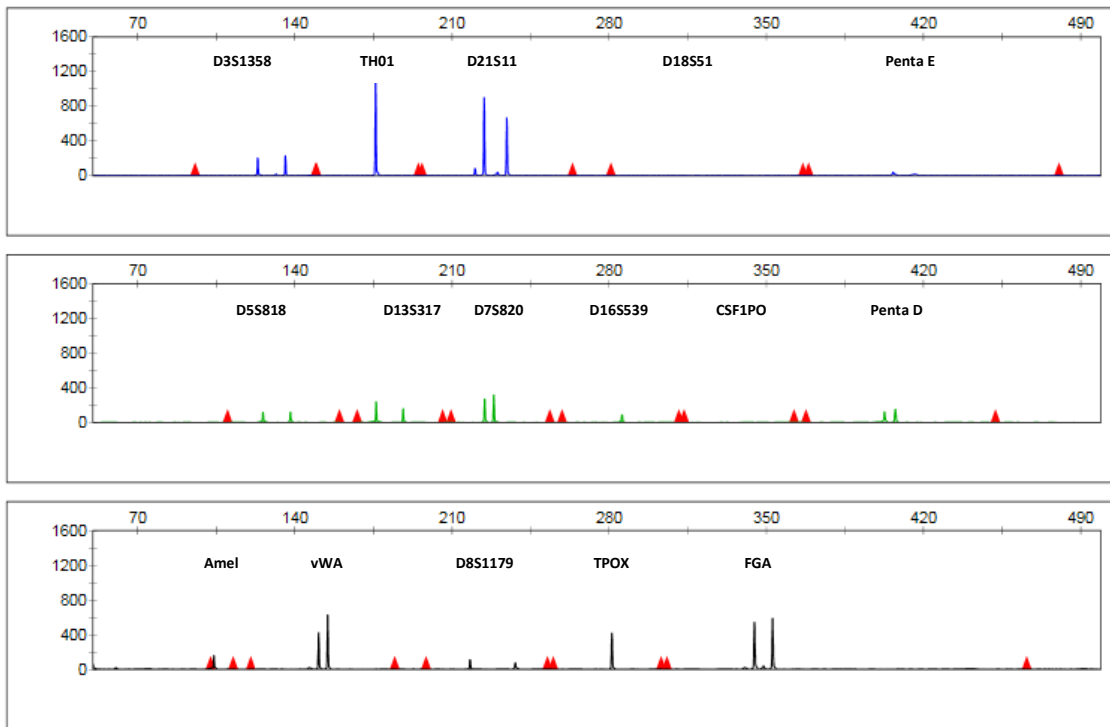


Figure 6.20: Sample A, x1 dilution (left) and processed with PowerPlex® 16HS. Sample A, x1 dilution (right) processed with PowerPlex® 18D.

1



2

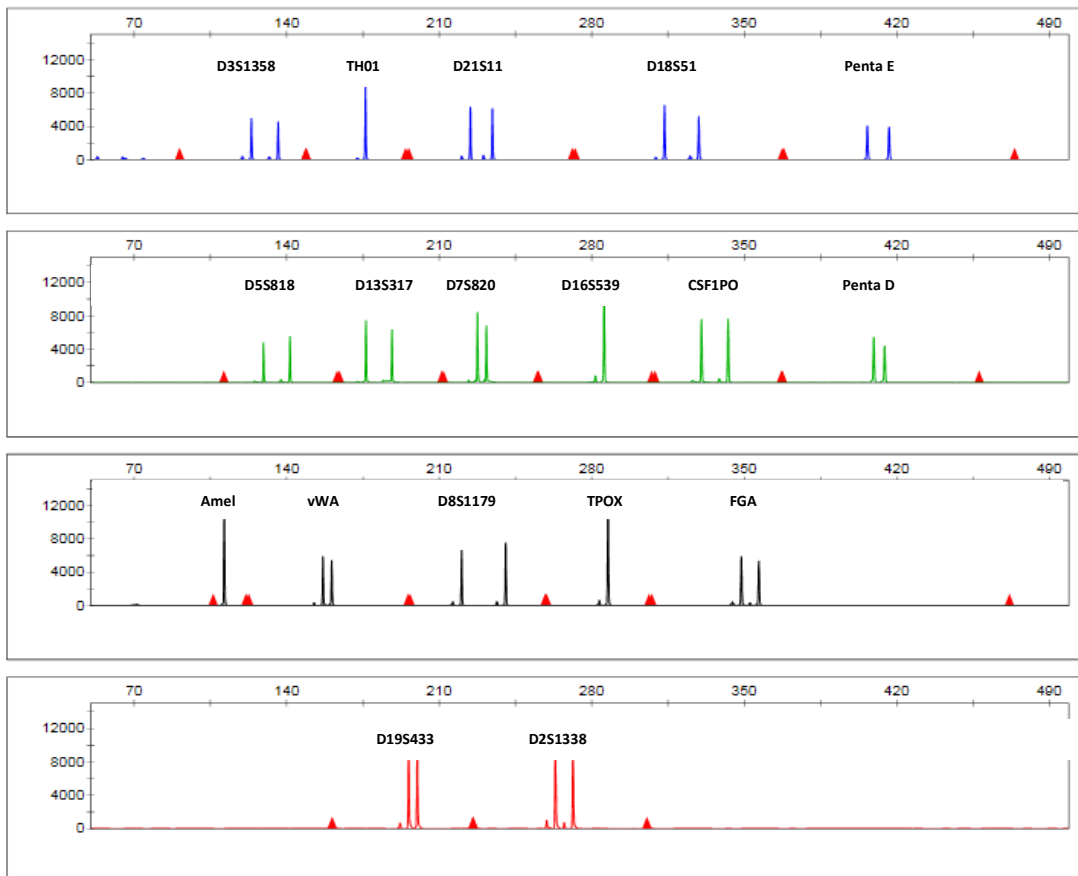


Figure 6.21: Electropherograms demonstrating profiles produced with PowerPlex[®] 16HS and 18D. (1) Sample A, x1 dilution and processed with PowerPlex[®] 16HS on lead. (2) Sample A, x1 dilution and processed with PowerPlex[®] 18D on lead. The x-axis represents relative fluorescent units (RFU) and the y-axis fragment size in base pairs.

6.3.1.2 Stutter and other Artefacts

Stutter peaks are commonly seen in electropherograms when analysing data. Stutter is identified as a small peak which is generally one repeat unit less/more than the true allele. The levels of stutters were all lower (10.1% for a combined average of both kits) than the limit recommended by the manufacturer, which is usually 15%.

The profiles generated from the amplification of x2 and x10 dilutions, in general, were of good quality, with no drop-ins or split peaks. The only exception was the profiles generated from x1 solution of DNA. An abundance of biological material within the smaller loci gave peaks which were split. Split peaks, also referred to as +A/-A peaks, are due to non-template addition generally of adenosine which occurs at the 3'-end of the PCR product. Amplifying higher quantities of DNA than the recommended amount can result in the incomplete 3' A nucleotide addition.

6.3.2 Amido Black

Overall results for amido black samples indicated that the extracted samples produced with PowerPlex® 16HS gave lower peak heights (RFU) compared to samples which were subjected to direct amplification with PowerPlex® 18D.

The kits were also compared to samples on substrates which were not exposed to amido black (no chemical processing). In this case, the samples which were not exposed to amido black showed higher peak heights and PCR product concentrations when evaluating both kits. The difference was statistically significant yielding a p-value<0.05 [F(1, 58)= 4.75, p-value= 0.014]. Figure 6.22 displays the average PCR product concentration for all samples and dilutions processed with both PowerPlex® 16HS and 18D compared to all samples and dilutions analysed with PowerPlex® 16HS and 18D which contained no chemicals on the substrates.

The successfulness of direct PCR amplification and autosomal STR kit sensitivity were evaluated for amido black in the same manner as described in Section 6.3.1. Figures 6.23-6.27 are organized by substrate processed with amido black and subsequently by the autosomal STR kit used to generate the profiles. These figures were used to examine the variation in the amplification between the different dilution volumes, chemicals, substrates and autosomal STR kits.

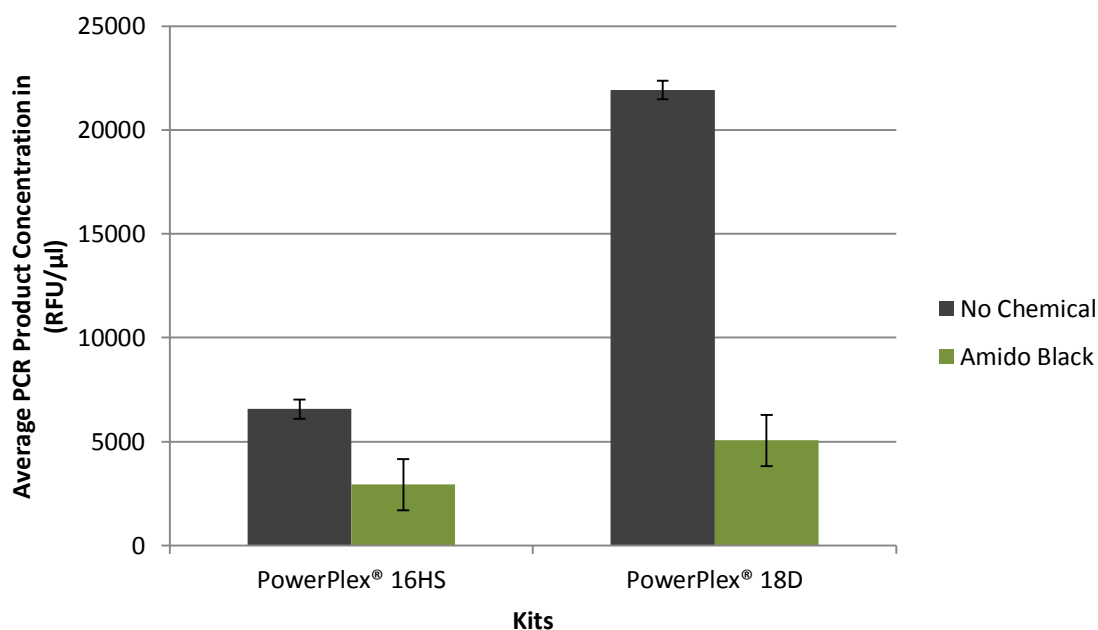
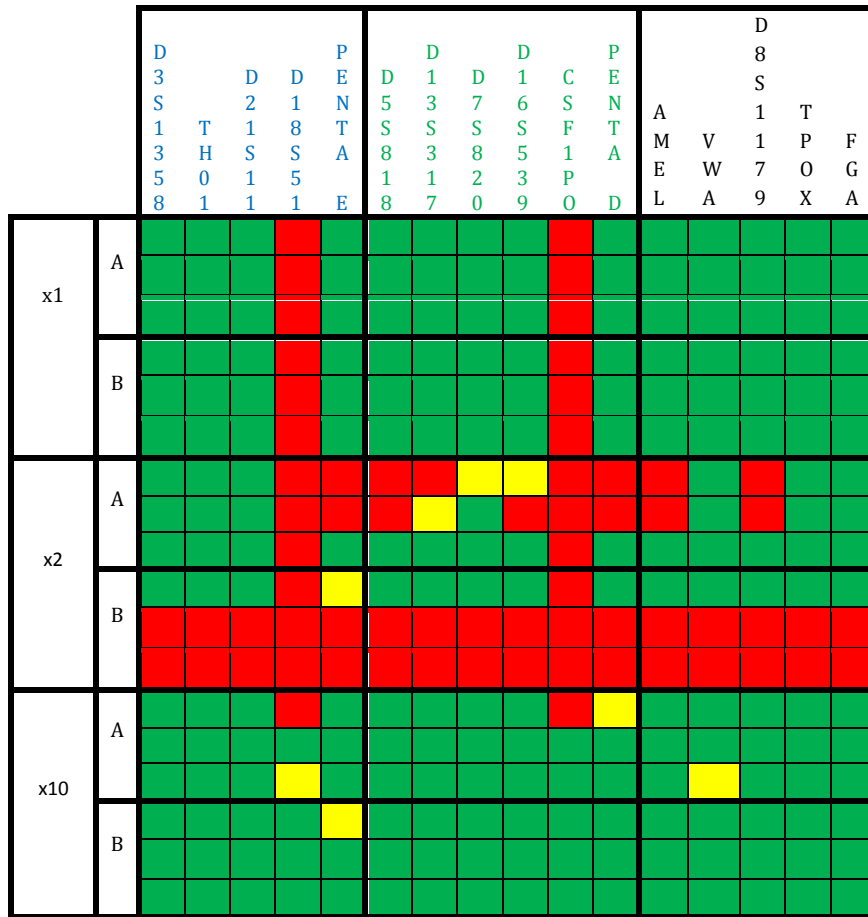


Figure 6.22: The average PCR product concentration (RFU/μl) for each kit, PowerPlex® 16HS and PowerPlex® 18D, for all samples processed using amido black and for all samples processed with no chemical enhancement. The error bars represent the standard deviations for each of the kits.

Profiles generated using amido black were also used to assess how complete a profile was and to determine the maximum and minimum peak heights for each allele present. The PCR product concentrations and total RFUs were used for this assessment. Profiles were also noted as either full profiles (FP) where all alleles at all locations were observed, partial profiles (PP) where the number after indicates the number of loci which presented the alleles for that specific location and no profile (NP) where the chromosomal location did not display the proper allele call at any location in the whole profile. This information is reflected under 'Profile Type' in Tables 6.2-6.3.

Loci in Promega® Poweplex® 16HS



Loci in Promega® Poweplex® 18D

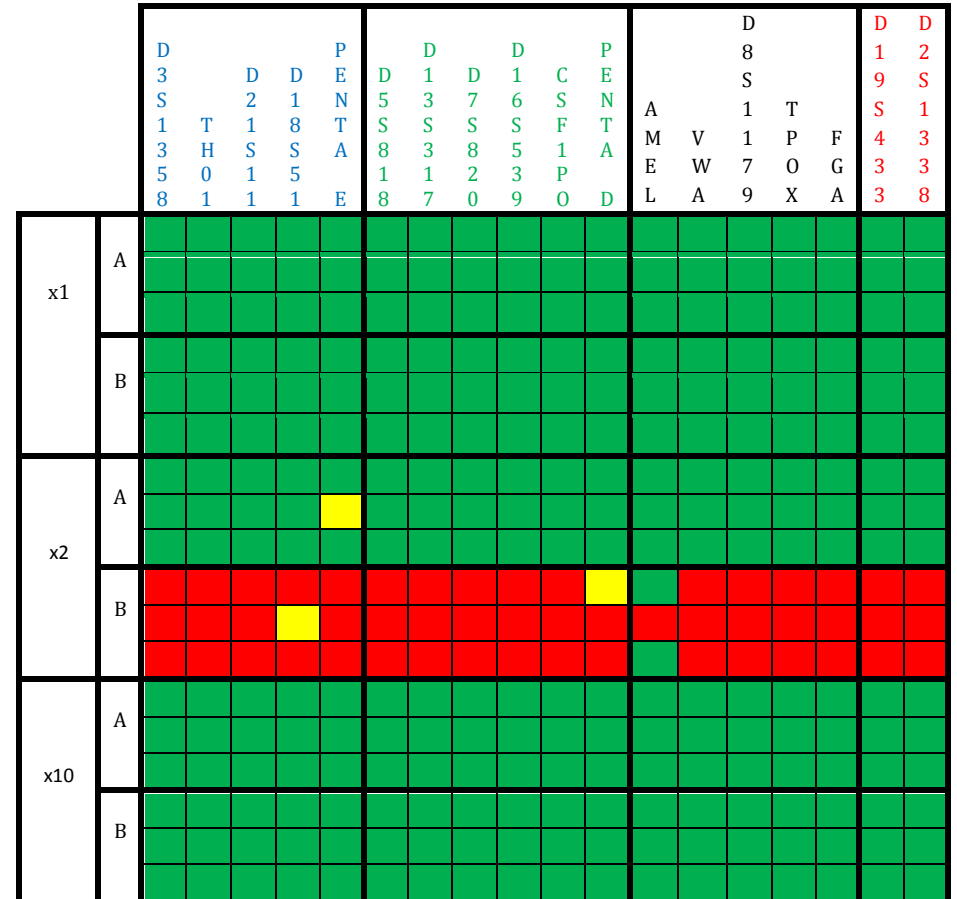


Figure 6.27: A diagrammatic representation of the quality of the profiles obtained from the PowerPlex® 16HS (left) and PowerPlex® 18D (right) kits. Different dilutions (x1, x2, and x10) of the two samples (A and B) were processed in triplicate using *Amido Black on Glass* and amplified with PowerPlex® 16HS and PowerPlex® 18D. Green squares indicate that the full correct alleles were observed for that locus. Yellow squares represent one allele drop out. Red squares represent loci where both expected alleles are missing.

Table 6.3: Results for Amido Black profiles using PowerPlex® 16HS showing the minimum, maximum and average peak heights, the profile type, total PCR product and PCR concentration for the various dilutions of samples A and B, amplified using half (12.5µl) reactions, and processed on various substrates. The values are averages of three replicates.

Substrate	Sample	Dilution	Profile Properties				Total PCR Product (in RFU)	PCR product concentration (in RFU/µl)
			Max PH	Min PH	Average PH	Profile Type		
Glass	A	x1	1661 (s.d. 104.52)	64 (s.d. 17.16)	534.88	PP14	38511 (s.d. 851.72)	3080.9 (s.d. 68.1)
		x2	1324 (s.d. 613.05)	53 (s.d. 8.39)	288.92	PP7	13868 (s.d. 5481.04)	1109.4 (s.d. 438.5)
		x10	1868 (s.d. 471.71)	64 (s.d. 9.54)	360.63	PP15	28490 (s.d. 711.33)	2279.2 (s.d. 56.9)
	B	x1	2664 (s.d. 282.00)	50 (s.d. 18.72)	659.933	PP14	39596 (s.d. 1258.04)	3167.7 (s.d. 100.6)
		x2	2497 (s.d. 516.66)	50 (s.d. 3.46)	502.93	NP ²	29673 (s.d. 2020.39)	2373.8 (s.d. 161.6)
		x10	2150 (s.d. 614.70)	56 (s.d. 59.02)	531.99	FP	37771 (s.d. 4464.37)	3021.7 (s.d. 357.1)
Laminate	A	x1	3679 (s.d. 511.85)	119 (s.d. 23.01)	1032.69	PP14	74354 (s.d. 4635.73)	5948.3 (s.d. 370.8)
		x2	5465 (s.d. 3099.28)	50 (s.d. 9.71)	1221.15	PP2	41519 (s.d. 23502.60)	3321.5 (s.d. 1880.2)
		x10	4352 (s.d. 820.98)	186 (s.d. 49.33)	928.25	FP	77973 (s.d. 2624.52)	6237.8 (s.d. 209.9)
	B	x1	1611 (s.d. 143.12)	53 (s.d. 22.54)	464.89	PP13	26499 (s.d. 385.95)	2119.9 (s.d. 30.9)
		x2	605 (s.d. 145.11)	50 (s.d. 8.14)	152.33	PP9	6093 (s.d. 606.33)	487.4 (s.d. 48.5)
		x10	1656 (s.d. 410.97)	51 (s.d. 21.22)	316.84	FP	21862 (s.d. 1789.00)	1748.9 (s.d. 143.1)
Lead	A	x1	423 (s.d. 31.76)	52 (s.d. 4.04)	150.32	PP10	7967 (s.d. 472.89)	637.3 (s.d. 37.8)
		x2	--	--	--	NP	--	--
		x10	331 (s.d. 9.24)	51 (s.d. 2)	123.15	PP9	6527 (s.d. 235.84)	522.1 (s.d. 18.8)
	B	x1	1378 (s.d. 166.01)	55 (s.d. 12.29)	386.29	PP13	21632 (s.d. 610.76)	1730.5 (s.d. 48.8)
		x2	--	--	--	NP	--	--
		x10	1759 (s.d. 573.20)	51 (s.d. 5.51)	384.75	PP15	25778 (s.d. 4362.07)	2062.2 (s.d. 348.9)
Plastic	A	x1	22975 (s.d. 2946.32)	1767 (s.d. 353.84)	7182.79	FP	603354 (s.d. 21139.86)	48268.3 (s.d. 1691.2)
		x2	1891 (s.d. 187.80)	63 (s.d. 27.07)	494.84	FP	41072 (s.d. 2757.07)	3285.7 (s.d. 220.6)
		x10	1275 (s.d. 274.38)	60 (s.d. 12.66)	294.68	FP	23869 (s.d. 2021.36)	1909.5 (s.d. 161.7)
	B	x1	15946 (s.d. 2262.56)	1184 (s.d. 244.25)	6179.51	FP	444925 (s.d. 17965.93)	35594 (s.d. 1437.2)
		x2	3437 (s.d. 322.97)	167 (s.d. 118.03)	1191.36	PP12	85778 (s.d. 3206.34)	6862.2 (s.d. 256.5)
		x10	1747 (s.d. 351.42)	55 (s.d. 39.72)	465.88	PP15	31680 (s.d. 2138.60)	2534.4 (s.d. 171.1)
Tile	A	x1	17262 (s.d. 1930.67)	1529 (s.d. 326.17)	5963.45	FP	500930 (s.d. 27876.16)	40074.4 (s.d. 2230.0)
		x2	1065 (s.d. 228.41)	64 (s.d. 6.81)	320.75	PP15	25660 (s.d. 1734.48)	2052.8 (s.d. 138.7)
		x10	1096 (s.d. 243.69)	53 (s.d. 9.29)	253.84	PP14	19292 (s.d. 683.18)	1543.3 (s.d. 54.6)
	B	x1	23519 (s.d. 1553.36)	1599 (s.d. 84.04)	8005.08	FP	5763.66 (s.d. 9115.91)	46109.2 (s.d. 729.3)
		x2	680 (s.d. 29.96)	56 (s.d. 17.93)	251.02	FP	14559 (s.d. 1197.22)	1164.7 (s.d. 95.7)
		x10	2234 (s.d. 483.63)	53 (s.d. 14.19)	462.36	FP	33290 (s.d. 582.70)	2663.2 (s.d. 46.6)

² The alleles obtained in this profile were one of two in a heterozygous locus (yellow box) or a homozygous peak in a locus (green box); however, in both cases, were not reproducible thus not added to the 'profile type' determination.

Table 6.4: Results for Amido Black profiles using PowerPlex® 18D showing the minimum, maximum and average peak heights, the profile type, total PCR product and PCR concentration for the various dilutions of samples A and B, amplified using half (12.5µl) reactions, and processed on various substrates. The values are averages of three replicates.

Substrate Sample	Dilution	Profile Properties				Total PCR Product (in RFU)	PCR product concentration (in RFU/µl)	
		Max PH	Min PH	Average PH	Profile Type			
<i>Glass</i> A	x1	20028 (s.d. 1267.01)	3727 (s.d. 442.85)	7544.29	FP	724252 (s.d. 27750)	57940.1 (s.d. 2220)	
	x2	5703 (s.d. 541.00)	818 (s.d. 80.53)	1965.53	FP	188691 (s.d. 6738.15)	15095.2 (s.d. 539.0)	
	x10	821 (s.d. 46.92)	86 (s.d. 15.01)	258.04	FP	24772 (s.d. 418.72)	1981.7 (s.d. 33.4)	
	B	x1	23301 (s.d. 1321.30)	104 (s.d. 2246.17)	9857.20	FP	798433 (s.d. 16326.32)	63874.6 (s.d. 1306.1)
		x2	573 (s.d. 117.41)	59 (s.d. 6.51)	194.23	NP	15733 (s.d. 1170.83)	1258.6 (s.d. 93.6)
		x10	1370 (s.d. 200.25)	229 (s.d. 34.30)	563.98	FP	45682 (s.d. 1829.21)	3654.5 (s.d. 146.3)
<i>Laminate</i> A	x1	23654 (s.d. 3908.26)	236 (s.d. 2365.27)	8226.35	FP	789730 (s.d. 33207.55)	63178.4 (s.d. 2656.6)	
	x2	743 (s.d. 60.92)	67 (s.d. 10.69)	250.04	FP	24004 (s.d. 303.98)	1920.3 (s.d. 24.3)	
	x10	899 (s.d. 257.93)	70 (s.d. 56.57)	248.78	FP	23883 (s.d. 2292.53)	1910.6 (s.d. 183.4)	
	B	x1	21667 (s.d. 2202.45)	2519 (s.d. 667.16)	8501.51	FP	688622 (s.d. 26281.34)	55089.7 (s.d. 2102.5)
		x2	320 (s.d. 55.37)	51 (s.d. 0)	108.31	PP12	6607 (s.d. 271.02)	528.5 (s.d. 21.6)
		x10	859 (s.d. 111.84)	126 (s.d. 5.51)	312.53	FP	25315 (s.d. 1063.65)	2025.2 (s.d. 85.0)
<i>Lead</i> A	x1	1411 (s.d. 585.84)	364 (s.d. 585.84)	735.67	PP1	2207 (s.d. 585.84)	176.5 (s.d. 46.8)	
	x2	--	--	--	NP	--	--	
	x10	--	--	--	NP	--	--	
	B	x1	1674 (s.d. 165.29)	102 (s.d. 38.63)	539.50	PP4	6474 (s.d. 347.64)	517.9 (s.d. 27.8)
		x2	--	--	--	--	--	--
		x10	77 (s.d. 12.53)	52 (s.d. 8.08)	62.60	PP2	313 (s.d. 47.01)	25.0 (s.d. 3.7)
<i>Plastic</i> A	x1	17007 (s.d. 318.40)	3925 (s.d. 268.97)	6763.46	FP	649292 (s.d. 9118.68)	51943.3 (s.d. 729.4)	
	x2	3566 (s.d. 1007.41)	280 (s.d. 253.99)	1132.20	FP	108691 (s.d. 13728.29)	8695.2 (s.d. 1098.2)	
	x10	412 (s.d. 52.85)	50 (s.d. 4.58)	130.52	PP17	12138 (s.d. 344.91)	971.0 (s.d. 27.5)	
	B	x1	6750 (s.d. 1863.11)	424 (s.d. 673.19)	2044.53	FP	165607 (s.d. 32166.49)	13248.5 (s.d. 2573.3)
		x2	4549 (s.d. 398.95)	743 (s.d. 87.18)	2019.31	FP	163564 (s.d. 1497.65)	13085.12 (s.d. 119.8)
		x10	341 (s.d. 70.50)	51 (s.d. 0.58)	104.15	PP12	6457 (s.d. 396.40)	516.5 (s.d. 31.7)
<i>Tile</i> A	x1	11594 (s.d. 1982.86)	61 (s.d. 1280.21)	3701.92	FP	355384 (s.d. 31587.03)	28430.7 (s.d. 2526.9)	
	x2	4204 (s.d. 479.28)	542 (s.d. 47.63)	1487.53	FP	142803 (s.d. 2911.79)	11424.2 (s.d. 232.9)	
	x10	510 (s.d. 81.59)	56 (s.d. 1716)	173.01	FP	16609 (s.d. 641.36)	1328.7 (s.d. 51.3)	
	B	x1	380 (s.d. 77.03)	50 (s.d. 3.06)	117.78	FP	8127 (s.d. 676.35)	650.1 (s.d. 54.1)
		x2	397 (s.d. 122.40)	50 (s.d. 0.58)	125.61	PP12	7411 (s.d. 763.20)	592.8 (s.d. 61.0)
		x10	135 (s.d. 20.11)	51 (s.d. 0.58)	75.56	PP15	1889 (s.d. 68.99)	151.1 (s.d. 5.5)

Dilutions were a significant factor when evaluating the samples, $p < 0.05$ [$F(2,23) = 8.03$, $p\text{-value} = 0.002$]. Again, this was again to be expected as decreasing dilution samples were used for amido black as well. Figure 6.28 displays each dilution in regard to average PCR product concentration and compares ‘no chemical’ samples to samples processed with amido black.

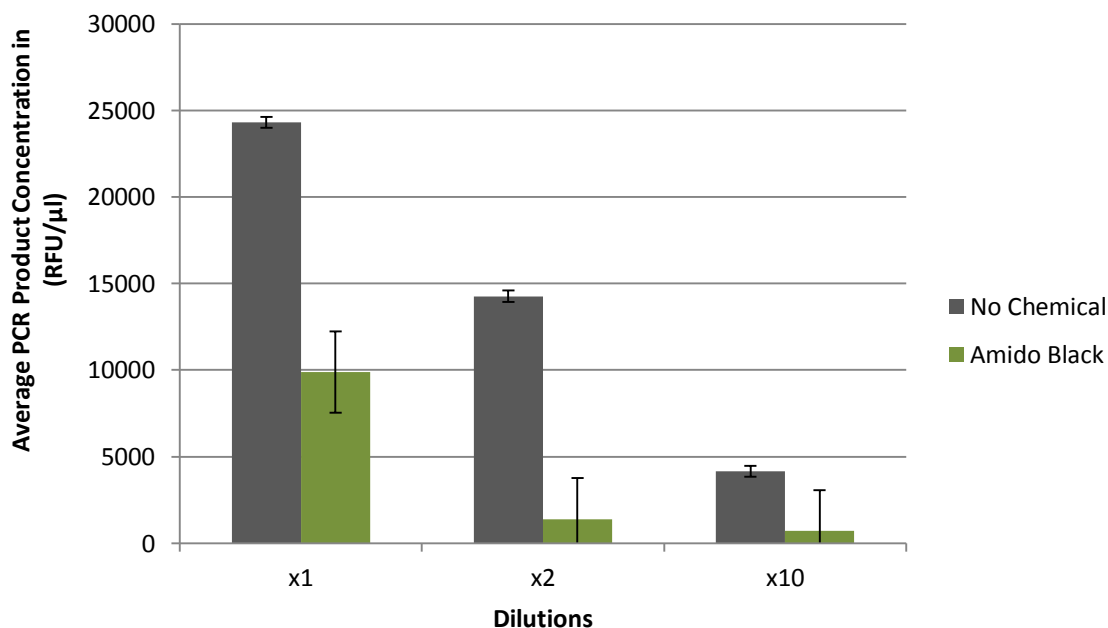
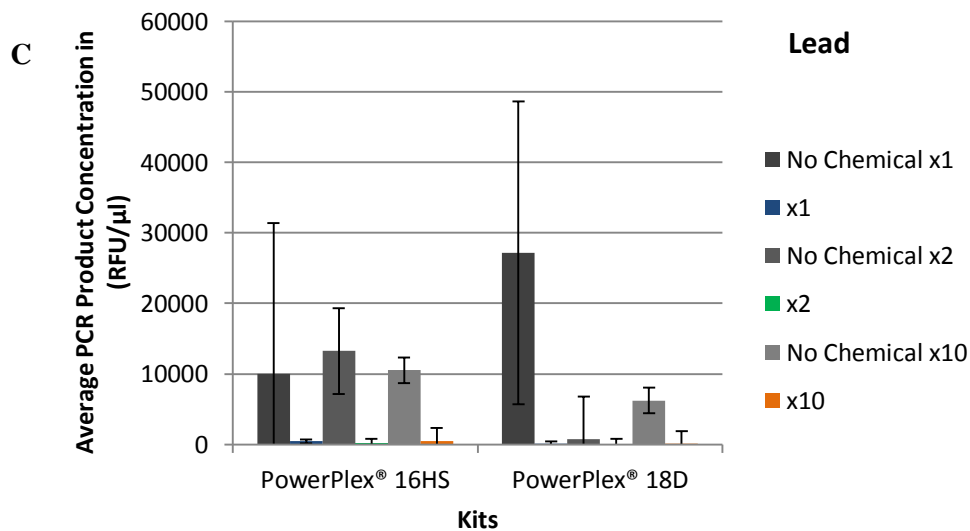
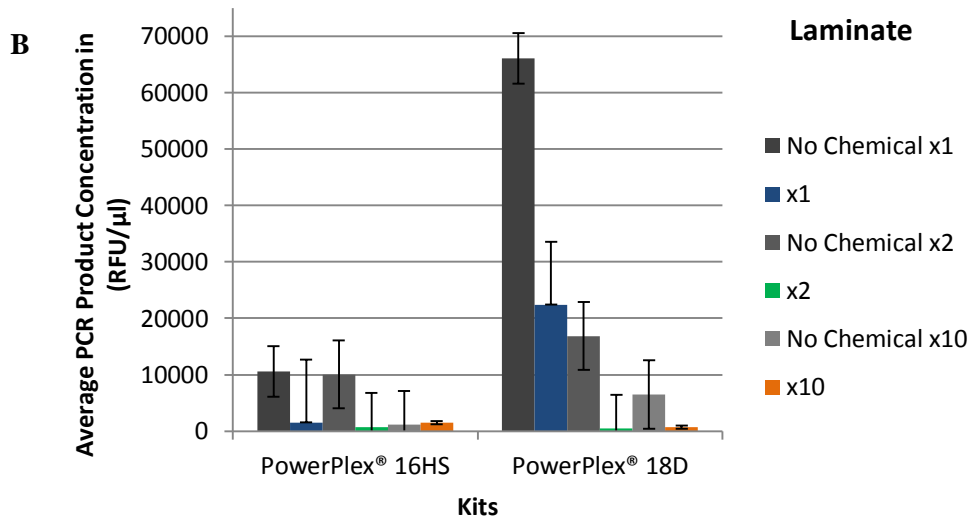
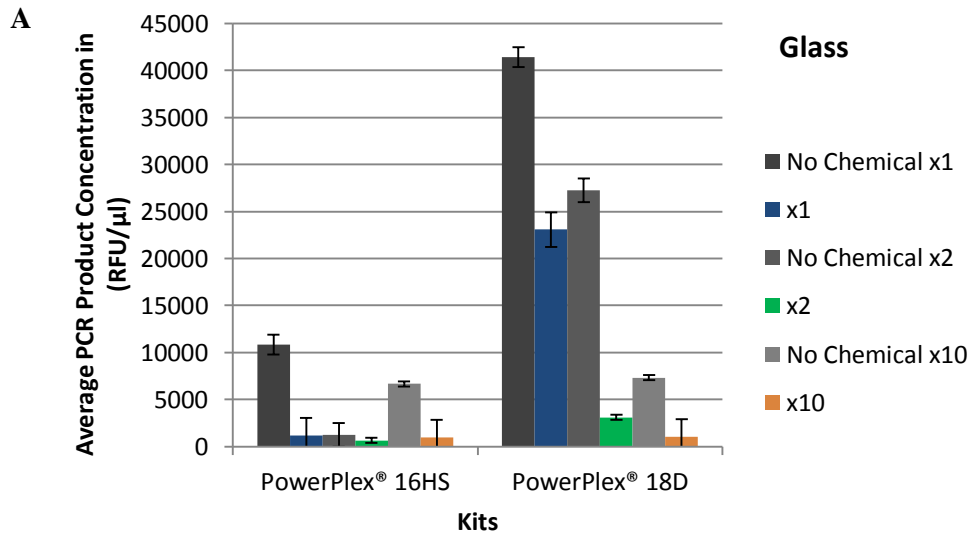


Figure 6.28: The average PCR product concentration (RFU/μl) for each kit, PowerPlex® 16HS and PowerPlex® 18D, for all samples processed using amido black (green bars) and for all samples processed with no chemical enhancement (grey bars). The error bars represent the standard deviations for each of the dilutions.

The substrates had a significant effect on the average PCR product concentration with a significant variance noted [$F(4, 23) = 3.11$, $p\text{-value} = 0.035$]. Overall, plastic was observed yielded the strongest PCR product concentration when observing the PowerPlex® 16HS was used and glass the strongest PowerPlex® 18D data was used. Lead was the weakest across all dilutions and both kits. Figure 6.29 (A-E) reflects a comparison of both kits for each substrate by average PCR product concentration. Both the ‘no chemical’ samples and amido black processed samples can be seen broken down by dilution.



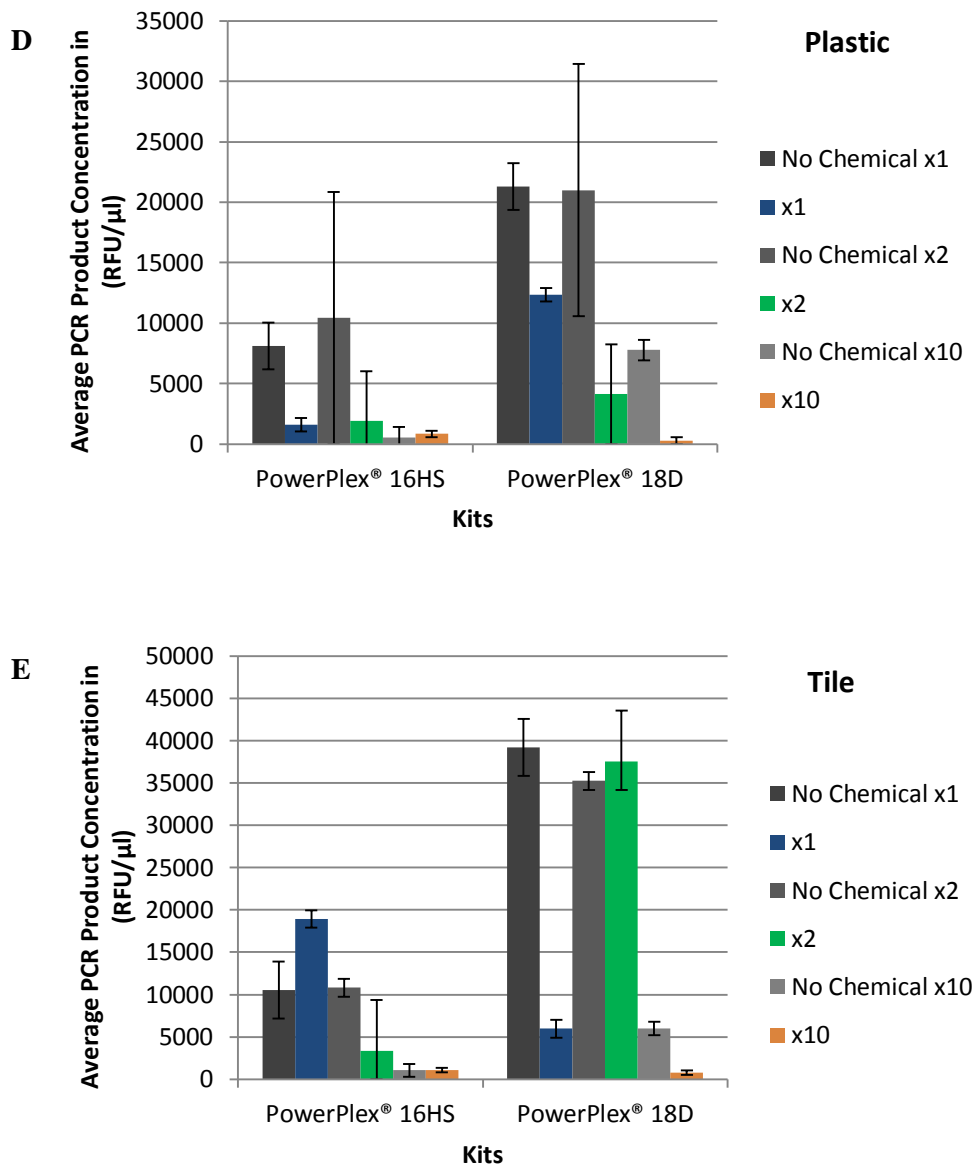


Figure 6.29 (A-E): The average PCR product concentration in (RFU/ μ l) by dilution for samples processed with no chemicals and samples processed with amido black on A) Glass, B) Laminate, C) Lead, D) Plastic, and E) Tile. The error bars represent the standard deviations for each of the dilutions and processed/unprocessed sample averages.

6.3.2.1 Heterozygous Peak Height Balance

Heterozygous peak balance was also assessed for each heterozygous locus present in both sample A and B. Heterozygous peak balance (Hb) exhibits the ratio of the two peaks present at a heterozygous locus. Again, this was determined mathematically by utilizing methods described by Leclair, et al. (2004). Results range from 0 to 1 with 1 representing alleles of equal height. An Hb value which is below 0.70 indicates peak height imbalance. Symbols (sample representation) which are present at the baseline (0)

indicate that allele drop-out was present in the heterozygous locus and only 1 allele was above threshold. Figures 6.26 through 6.33 exhibit heterozygous loci which are present in both sample A and B and their dilutions by substrate processed. A red dotted line indicates the 0.70 Hb threshold for the results.

Profiles which displayed peak imbalance were observed in both extracted and direct PCR samples. Overall peak imbalance within the PowerPlex® 18D processed samples was lower than those processed with PowerPlex® 16HS for all observed loci. x10 dilution samples fell below the 0.70 limit more often which was to be expected with the decreased amount of DNA template available. All loci seen at '0' (the baseline) indicate allele drop-out was present in the heterozygous locus present in the profile. An example of this is seen in all the substrates in Figure 6.30 (Top). The majority of the samples which appear at '0' appear to be from sample B which quantitatively was weaker than sample A (*Output Data*) and samples which were prepared with the x10 dilution. Glass contained the least amount of peak imbalances for all samples, dilutions and loci evaluated. Loci Penta E, D21S11, D13S1358, and FGA displayed the most peak imbalances for both kits.

6.3.2.1.1 Evaluation of CSF1PO

A heterozygous allele call of CSF1PO was present in sample A during the course of this project. Both CSF1PO alleles were observed more consistently when samples were processed with PowerPlex® 18D. Both alleles were displayed in 21 of 45 samples analysed with PowerPlex® 16HS as compared to PowerPlex® 18D where both alleles were present in 29 of the 45 samples processed (Figures 6.23-6.27). Of the samples producing both alleles, 8 of the 21 samples processed with PowerPlex® 16HS displayed peak height balance ratios of 0.70 Hb or higher (Figure 6.30). This is a lower percentage than the 24 of 29 which were over 0.70 Hb when analysed with PowerPlex® 18D (Figure 6.30).

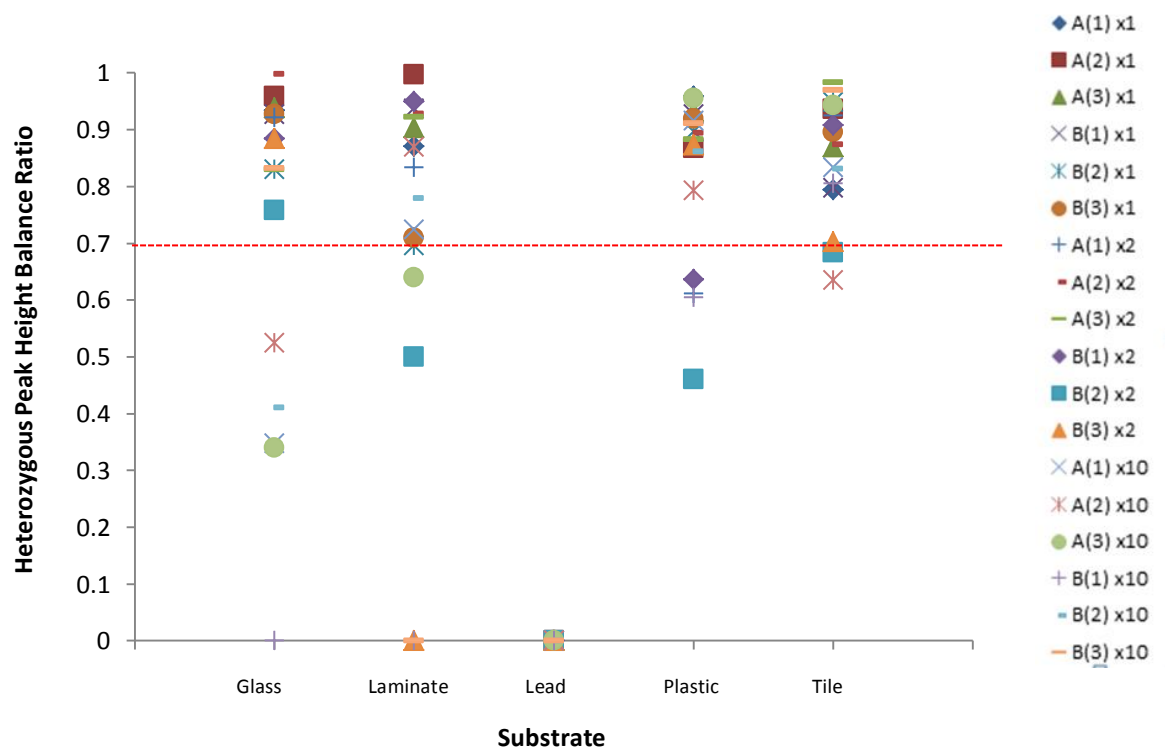
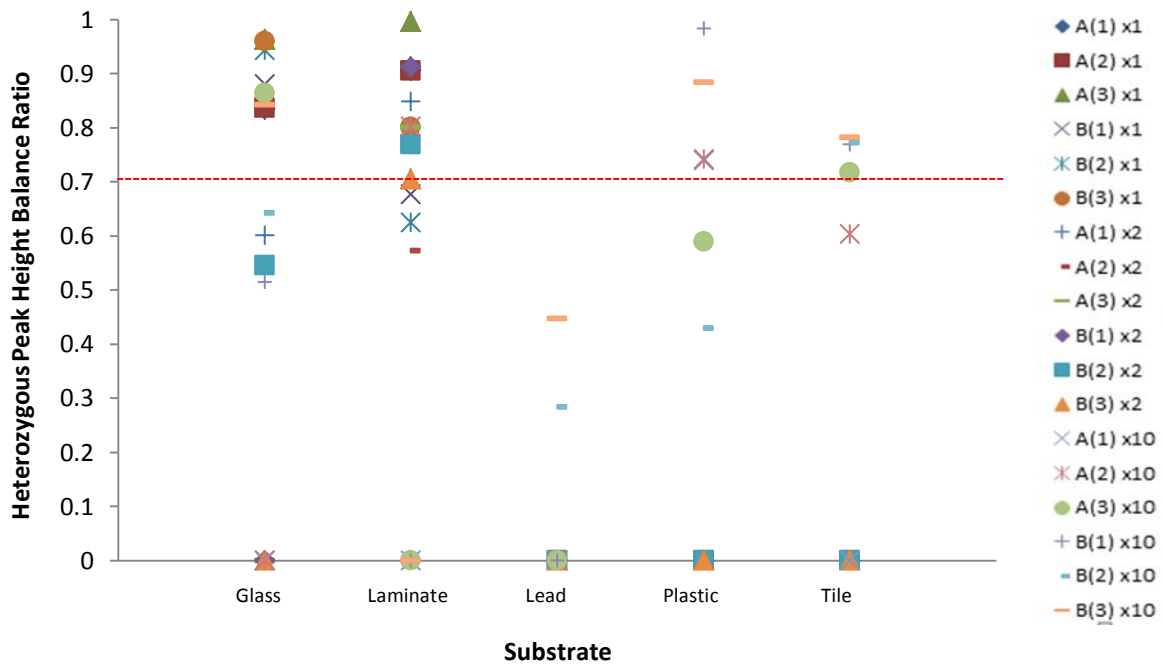


Figure 6.30: (Top) Peak height ratios for CSFIPO produced for various substrates processed with amido black and analysed with PowerPlex[®] 16HS. (Bottom) Peak height ratios for CSFIPO produced for various substrates processed with amido black and analysed with PowerPlex[®] 18D. All three replicates of each sample (A and B) for each dilution are represented.

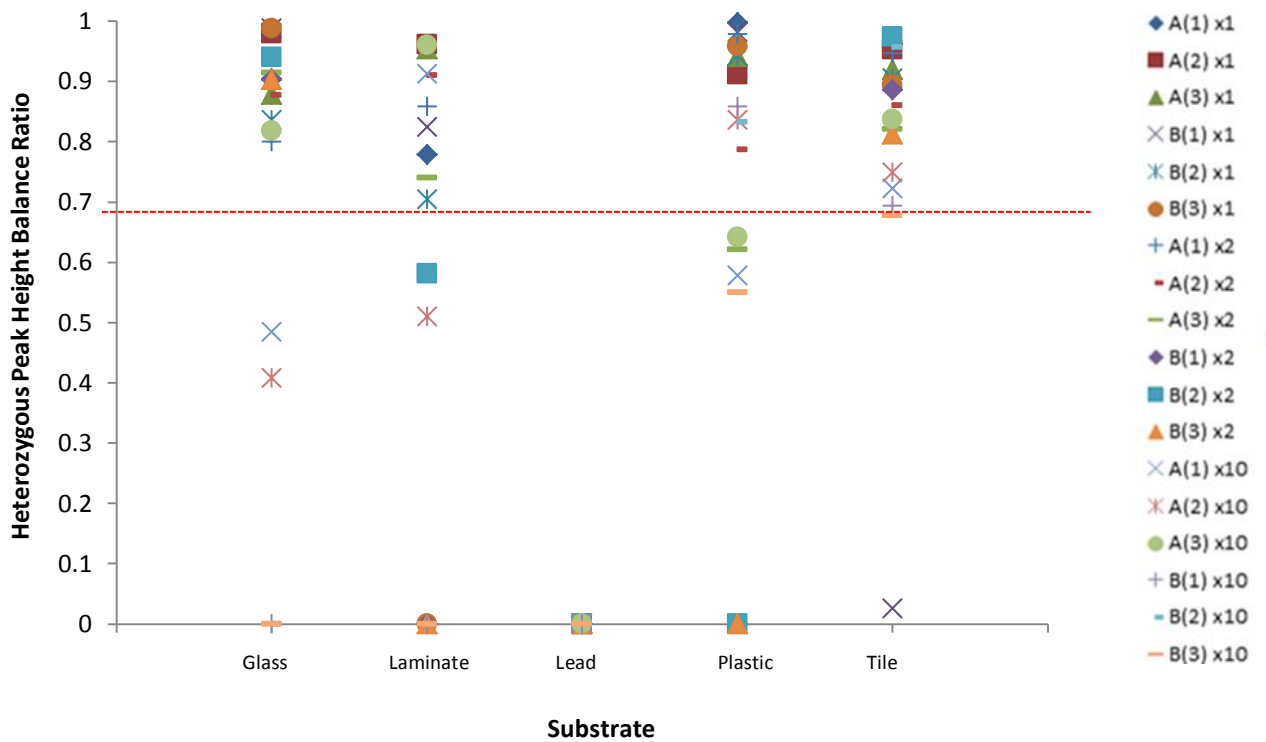
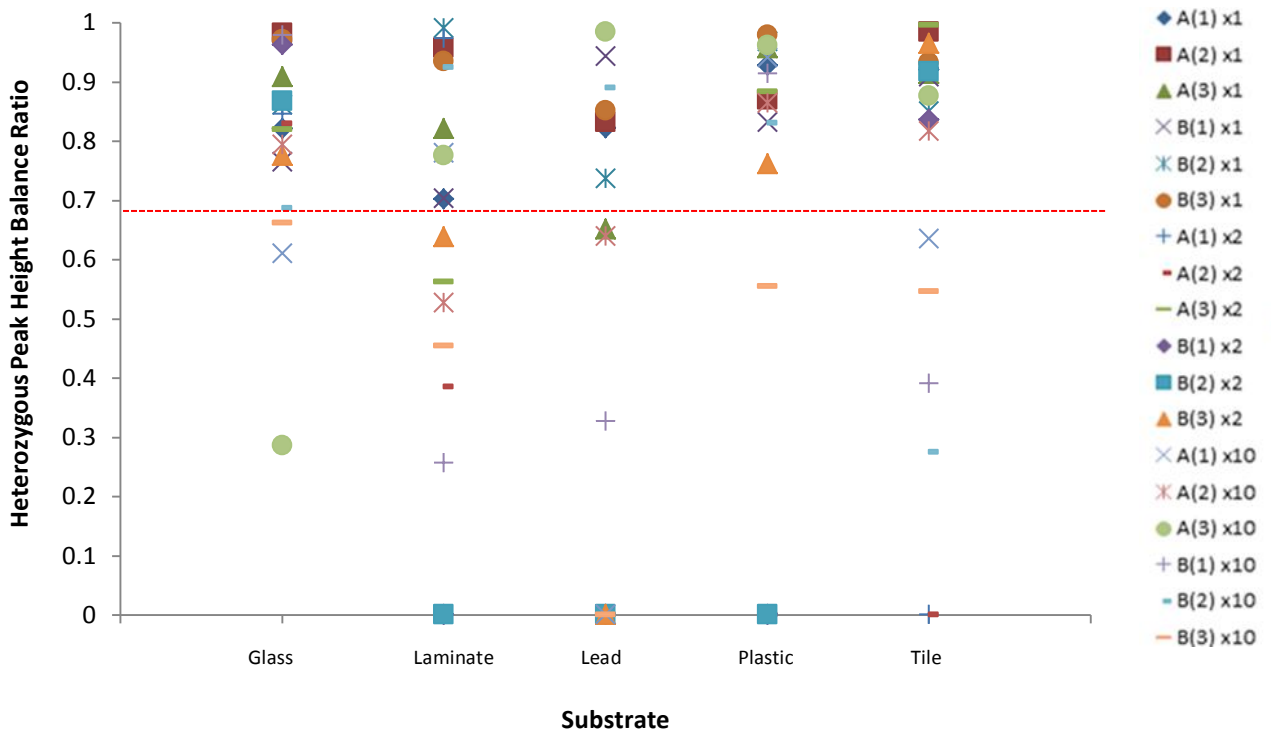


Figure 6.31: (Top) Peak height ratios for *DI3S317* produced for various substrates processed with amido black and analysed with PowerPlex[®] 16HS. (Bottom) Peak height ratios for *DI3S317* produced for various substrates processed with amido black and analysed with PowerPlex[®] 18D. All three replicates of each sample (A and B) for each dilution are represented.

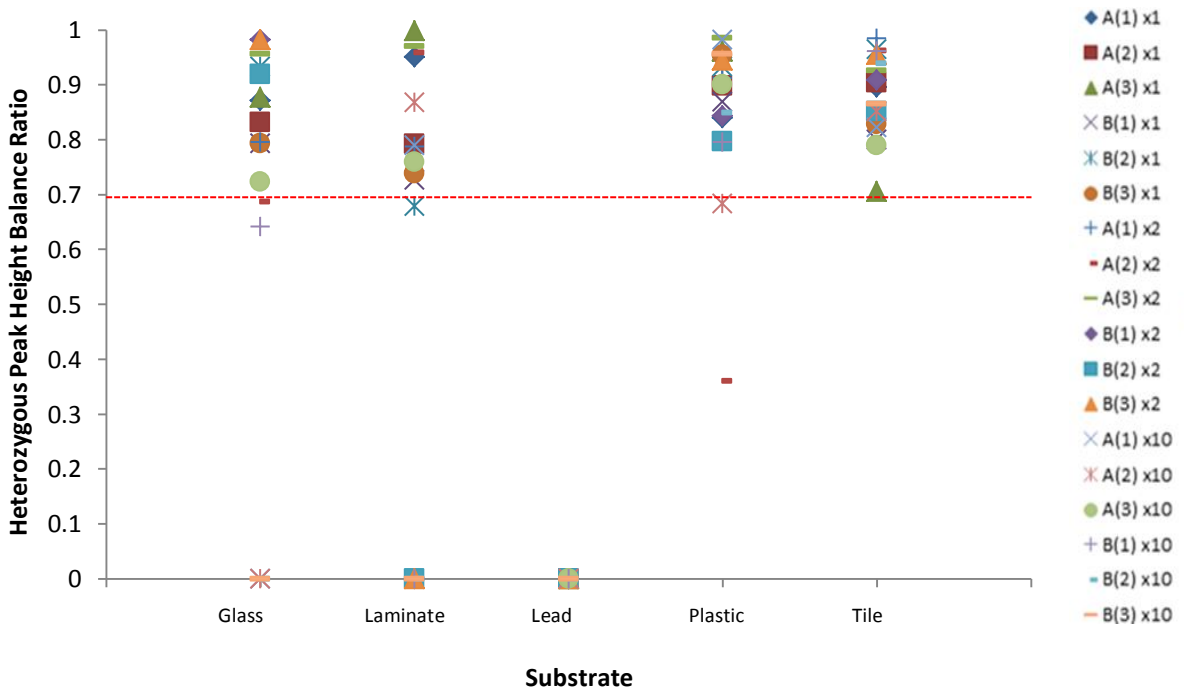
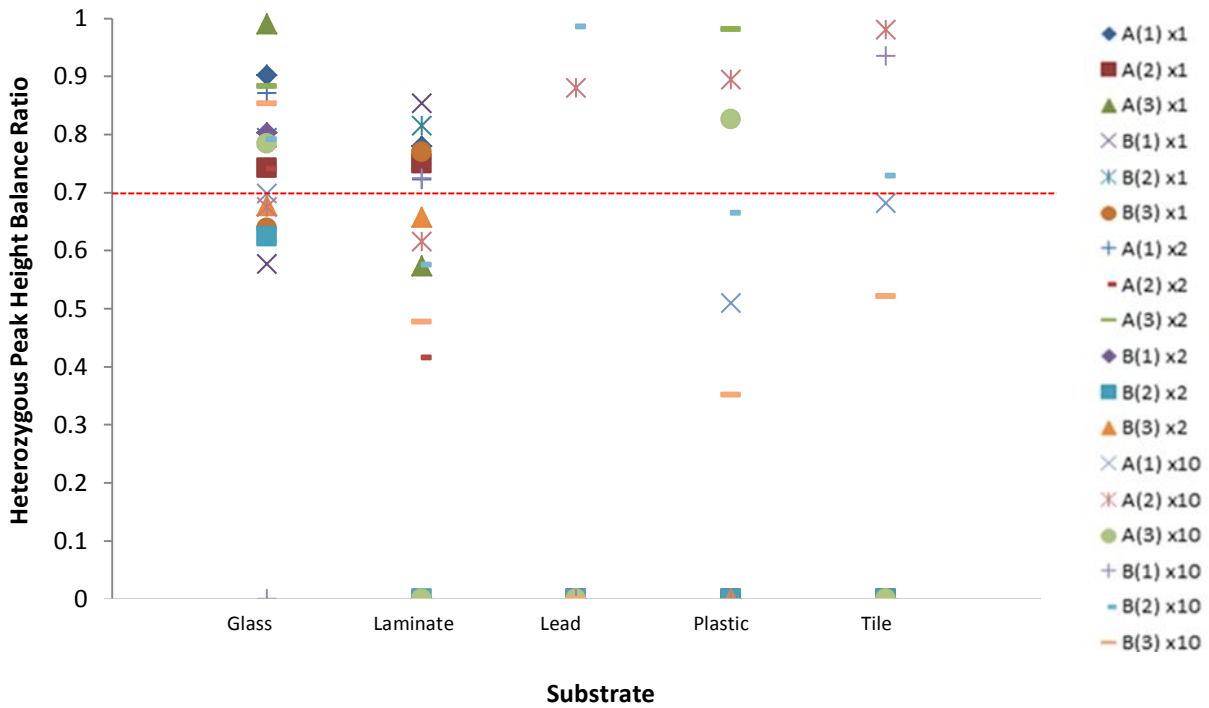


Figure 6.32: (Top) Peak height ratios for *DI8S51* produced for various substrates processed with amido black and analysed with PowerPlex[®] 16HS. (Bottom) Peak height ratios for *DI8S51* produced for various substrates processed with amido black and analysed with PowerPlex[®] 18D. All three replicates of each sample (A and B) for each dilution are represented.

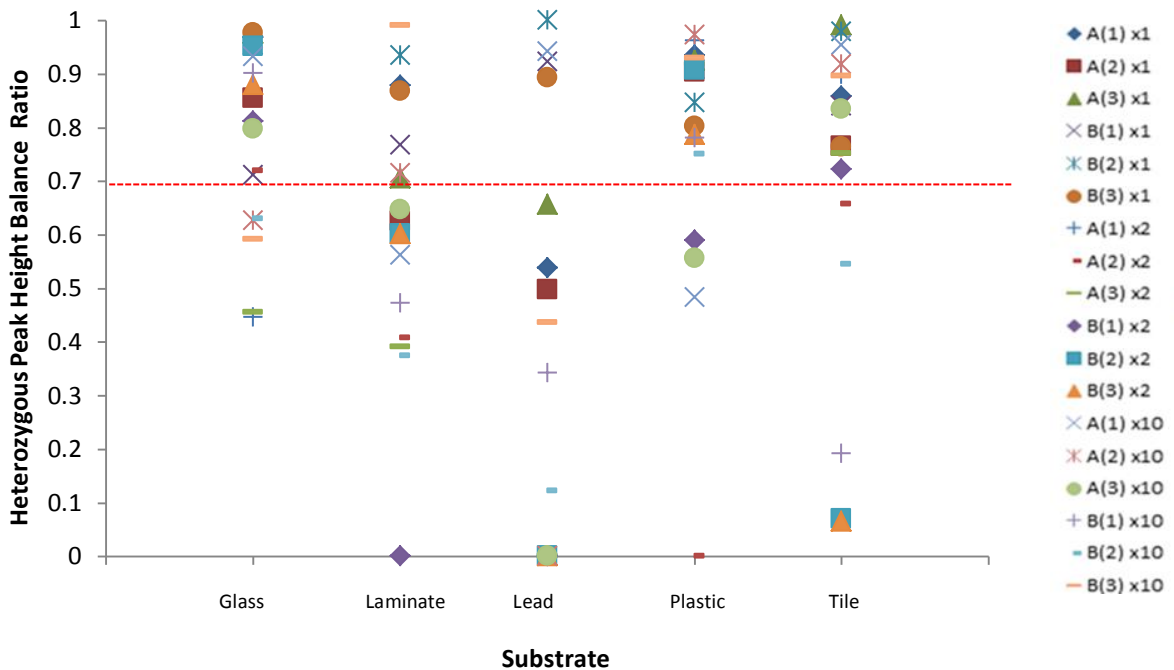
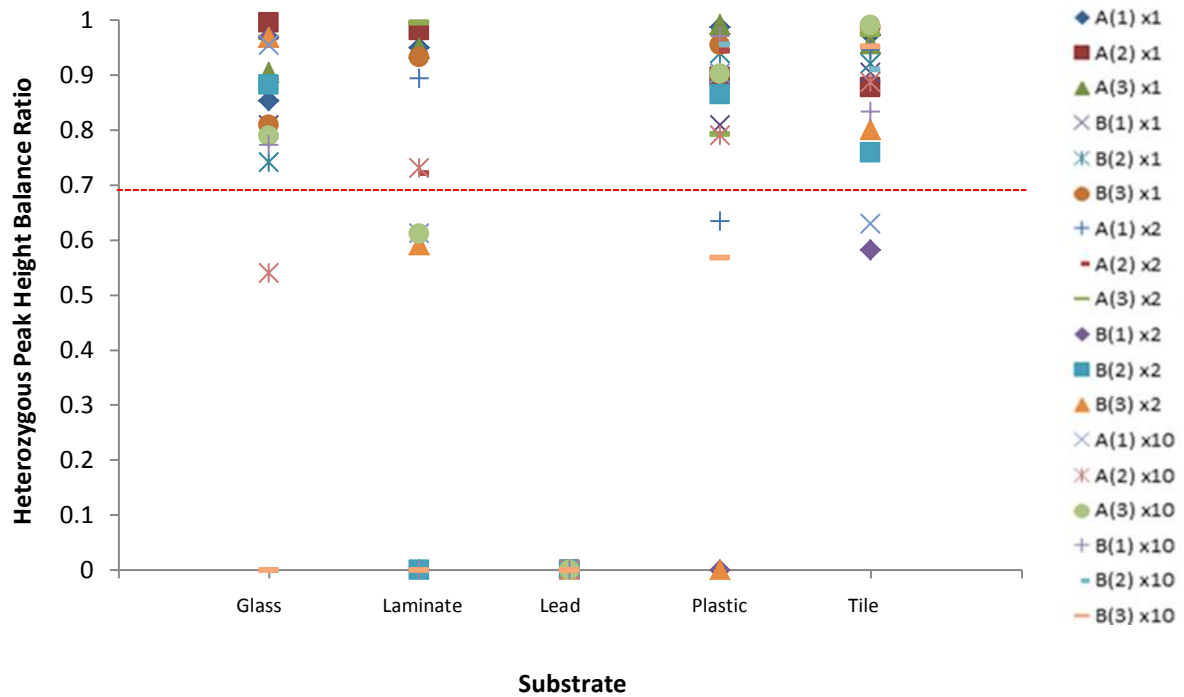


Figure 6.33: (Top) Peak height ratios for *D21S11* produced for various substrates processed with amido black and analysed with PowerPlex[®] 16HS. (Bottom) Peak height ratios for *D21S11* produced for various substrates processed with amido black and analysed with PowerPlex[®] 18D. All three replicates of each sample (A and B) for each dilution are represented.

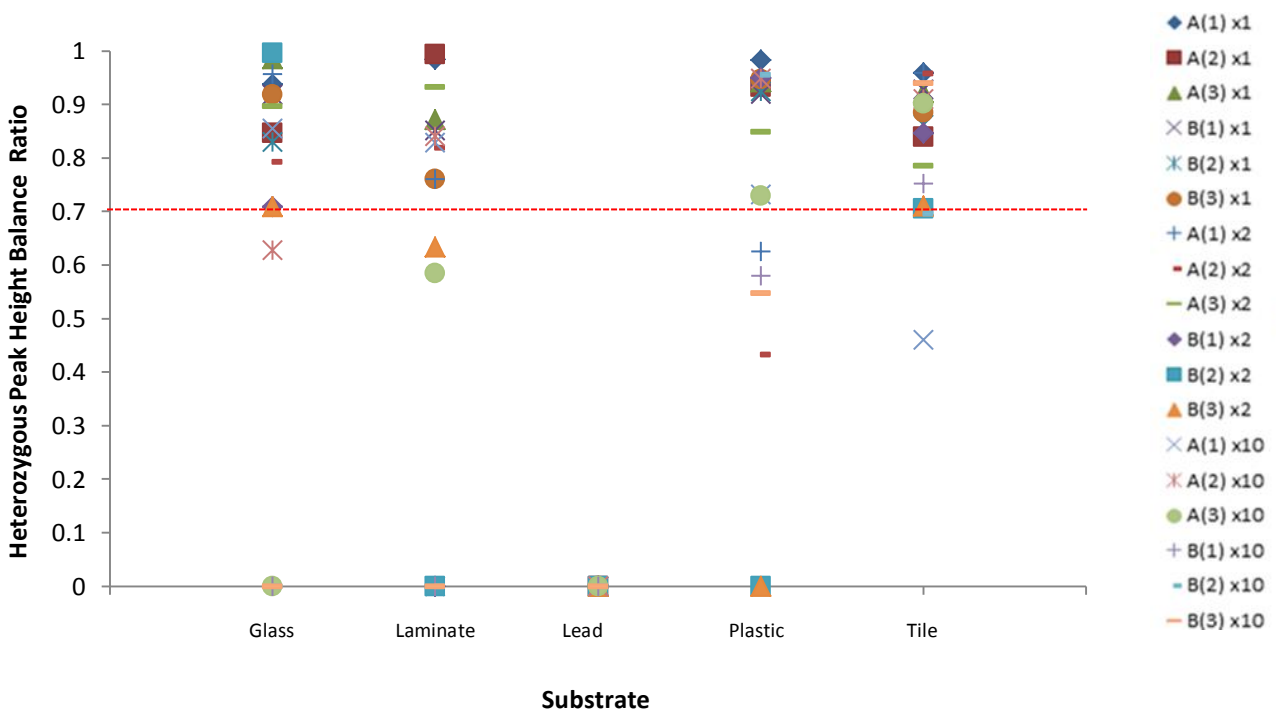
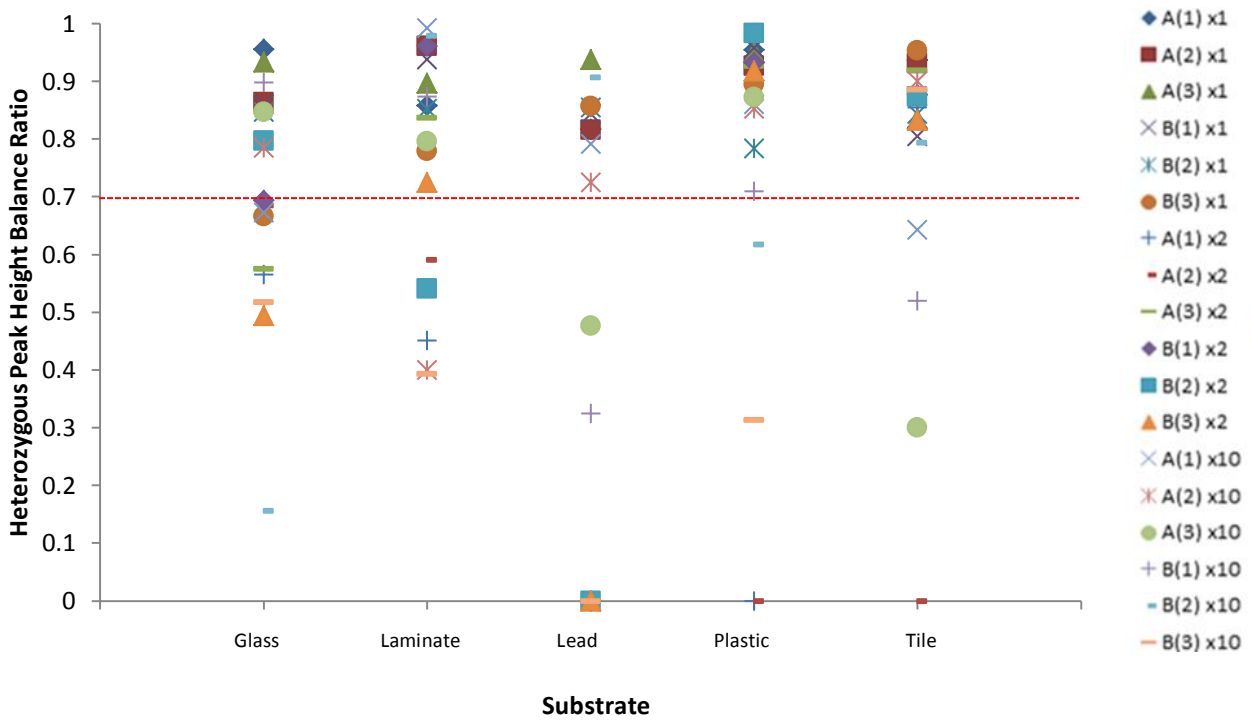


Figure 6.34: (Top) Peak height ratios for *D3S1358* produced for various substrates processed with amido black and analysed with PowerPlex[®] 16HS. (Bottom) Peak height ratios for *D3S1358* produced for various substrates processed with amido black and analysed with PowerPlex[®] 18D. All three replicates of each sample (A and B) for each dilution are represented.

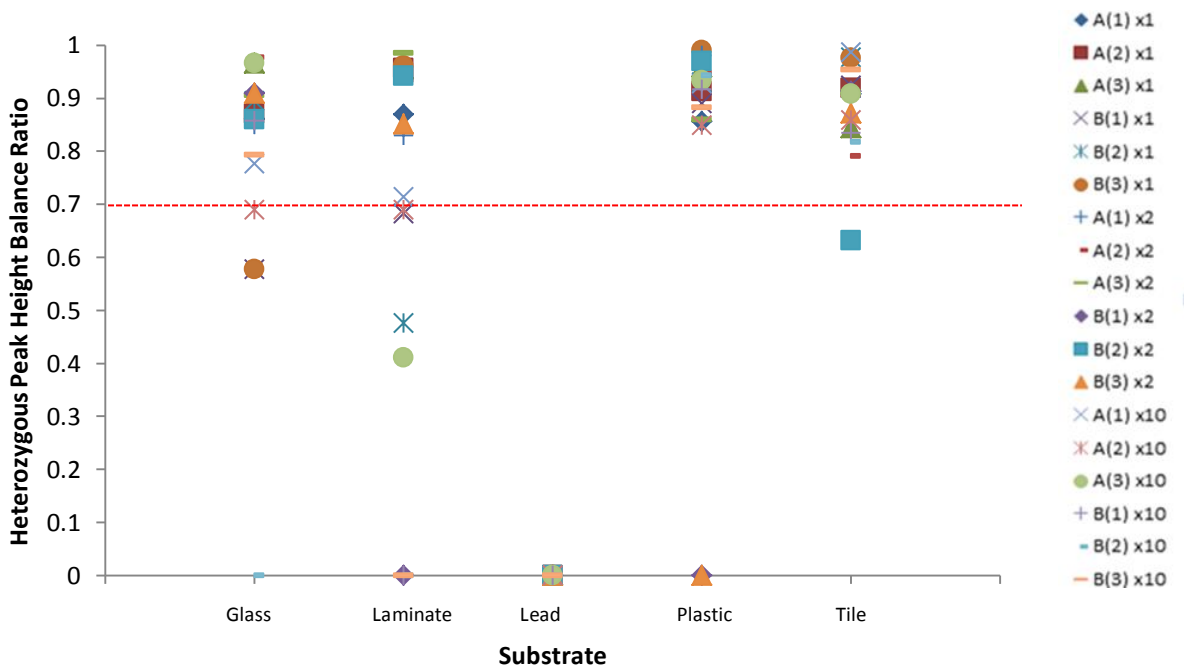
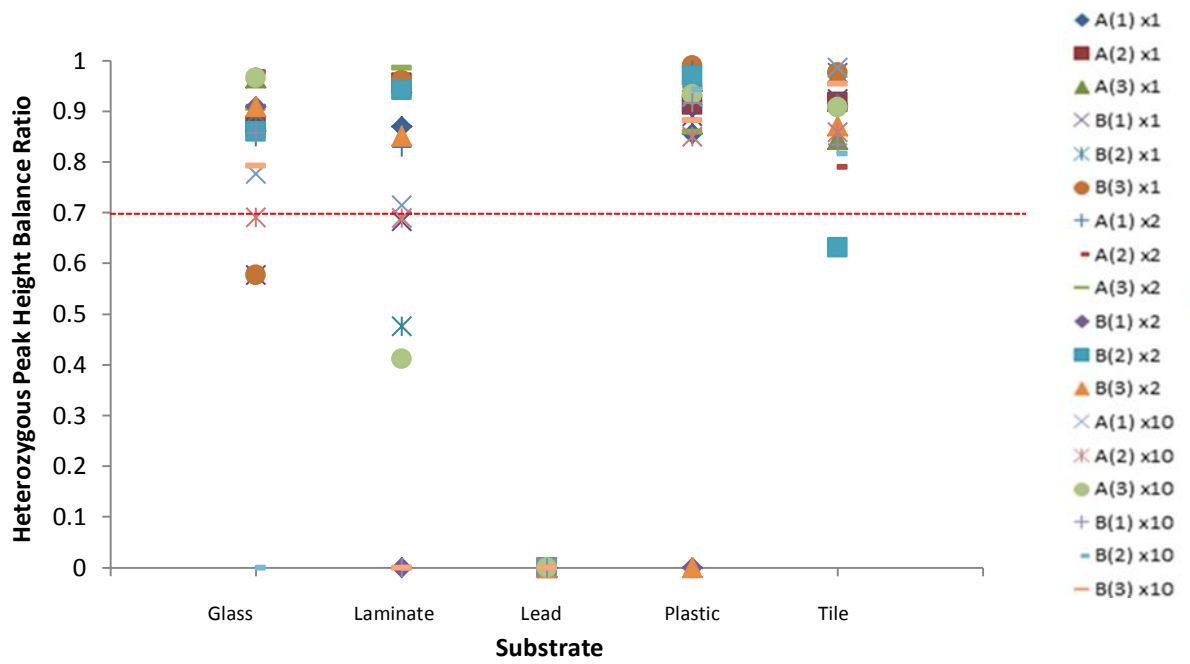


Figure 6.35: (Top) Peak height ratios for *D7S820* produced for various substrates processed with amido black and analysed with PowerPlex[®] 16HS. (Bottom) Peak height ratios for *D7S820* produced for various substrates processed with amido black and analysed with PowerPlex[®] 18D. All three replicates of each sample (A and B) for each dilution are represented.

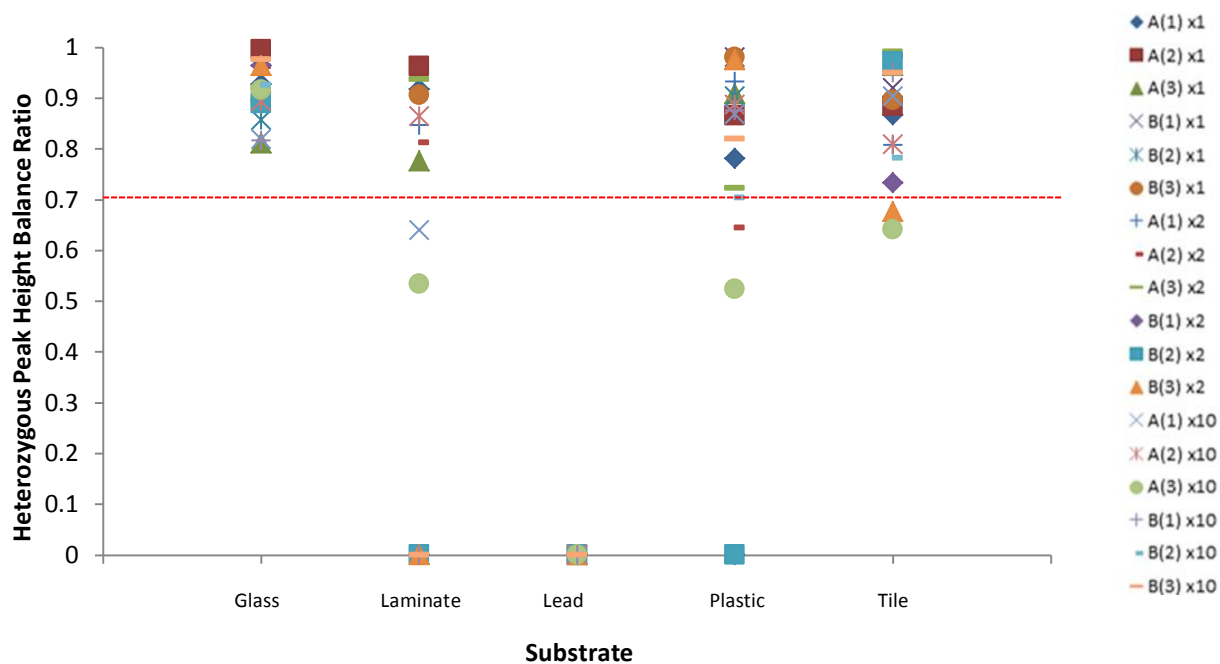
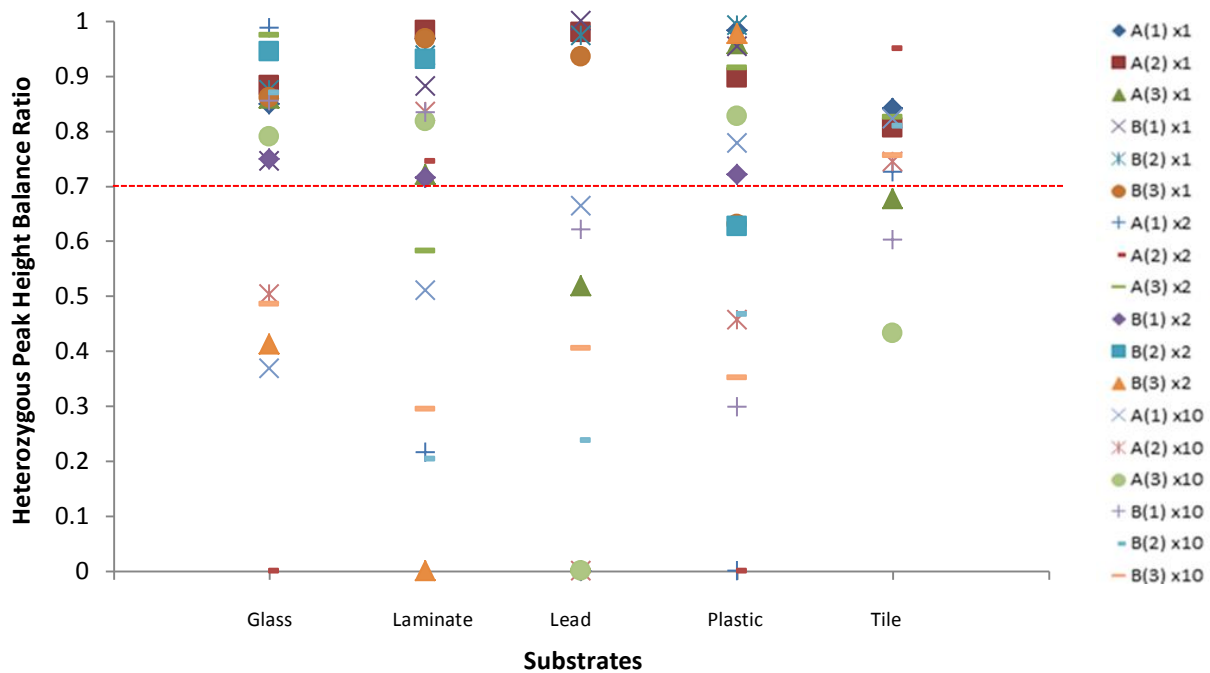


Figure 6.36: (Top) Peak height ratios for FGA produced for various substrates processed with amido black and analysed with PowerPlex[®] 16HS. (Bottom) Peak height ratios for FGA produced for various substrates processed with amido black and analysed with PowerPlex[®] 18D. All three replicates of each sample (A and B) for each dilution are represented.

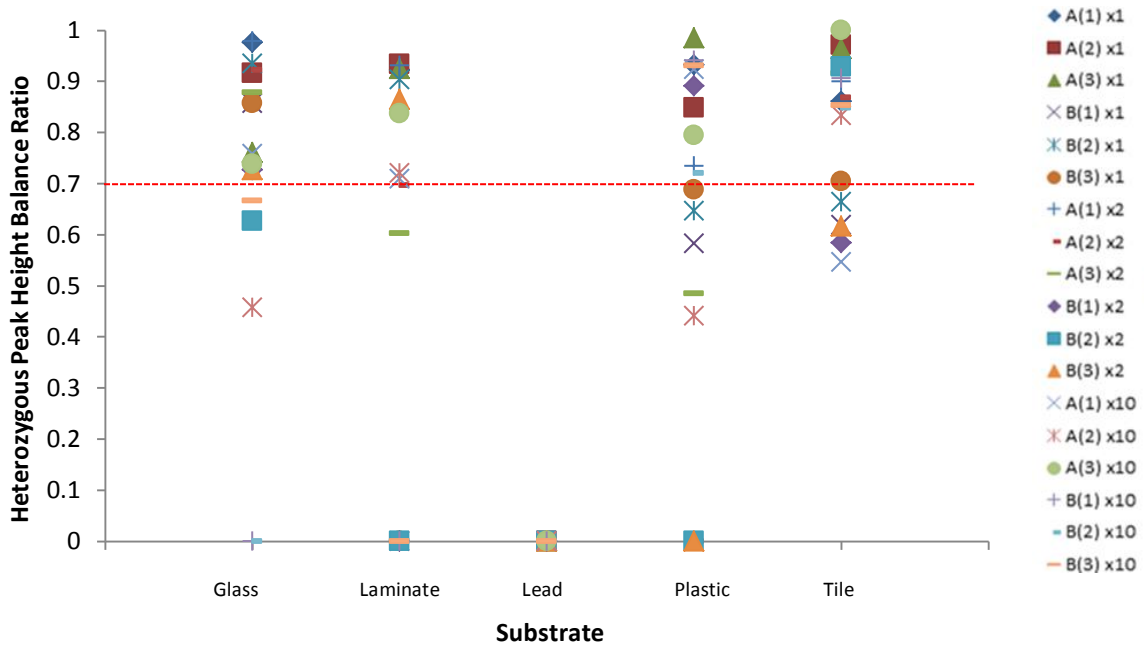
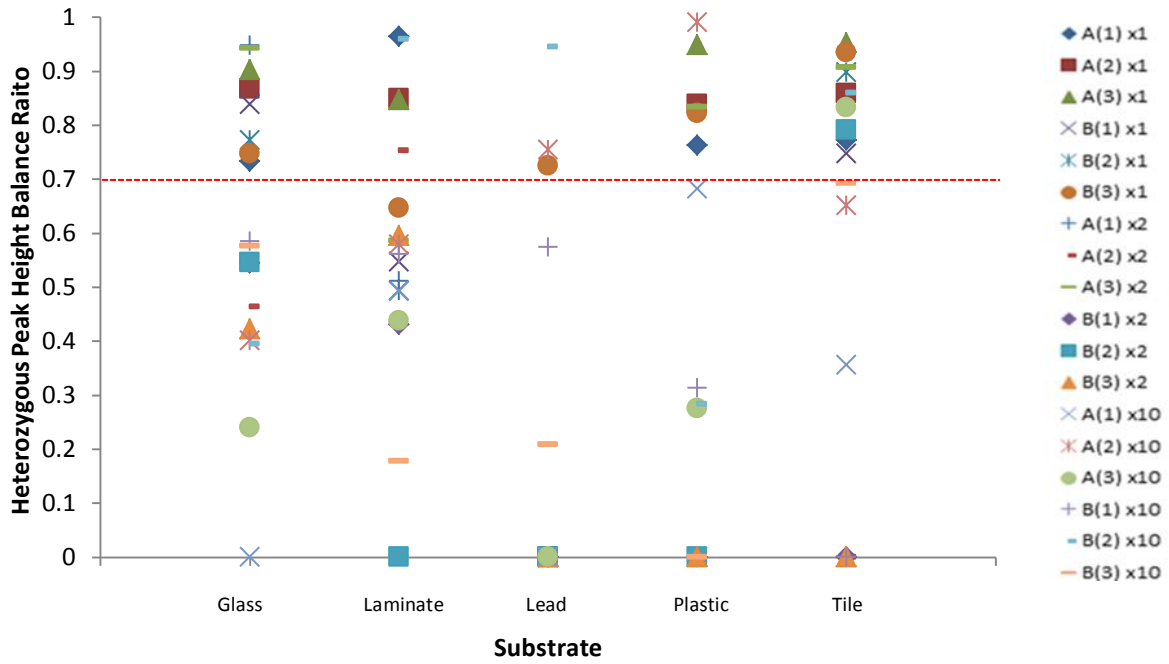


Figure 6.37: (Top) Peak height ratios for *Penta E* produced for various substrates processed with amido black and analysed with PowerPlex[®] 16HS. (Bottom) Peak height ratios for *Penta E* produced for various substrates processed with amido black and analysed with PowerPlex[®] 18D. All three replicates of each sample (A and B) for each dilution are represented.

The overall profiles generated using substrates processed with amido black paralleled those used with LCV. The profiles generated from direct PCR gave higher peak heights and were less prone to peak imbalances than those processed with extracted samples. Figure 6.38 shows sample B which was processed with amido black on laminate at the x1 dilution. Powerplex® 18D exhibits strong overall peak heights and less peak imbalance (2) than the sample processed with PowerPlex® 16HS (1).

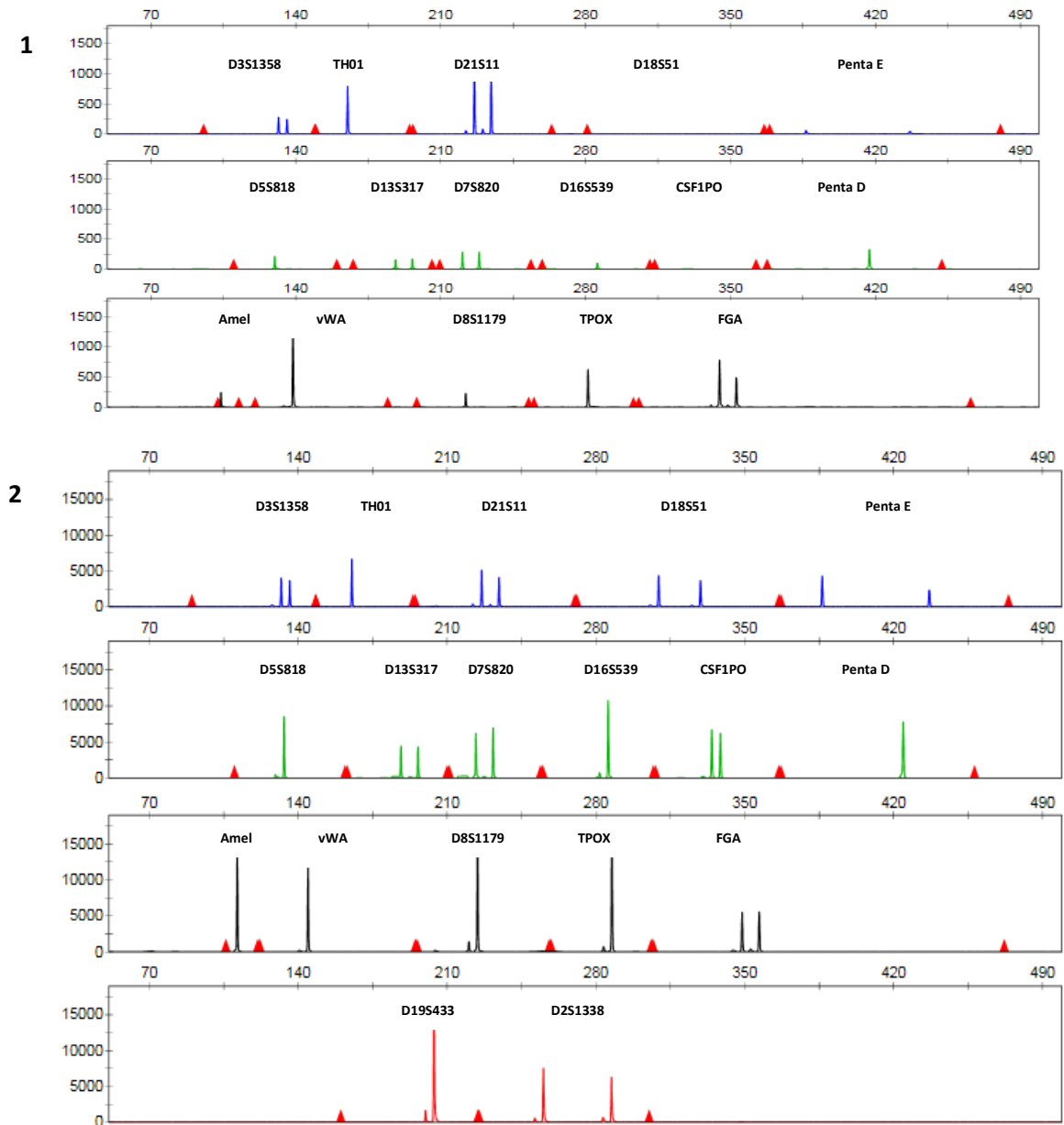


Figure 6.38: Electropherograms of (1) Sample B (x1, Laminate) processed with PowerPlex® 16HS and displayed at 2000RFU. (2) Sample B (x1, Laminate) processed with PowerPlex® 18D and displayed at 20000RFU. The y-axis shows the relative fluorescent units (RFU) and x-axis numbers indicate the fragment size in base pairs.

Lead was the weakest substrate processed yielding the lowest peak heights and total PCR product. While processing the surface a noticeable reaction occurred after exposing the lead to the amido black solution. It is hypothesized that in the same manner as LCV, the acidic component of the solution caused an oxidation effect possibly affecting the blood on the surface and negatively impacting the profile. Amido black does differ in its appearance of the reaction in that the lead almost appears to have a ‘marble’. The best examples of this were captured via photograph on samples A, x1 dilution processed with PowerPlex® 16HS and A, x2 dilutions processed with PowerPlex® 18D (Figure 6.39).

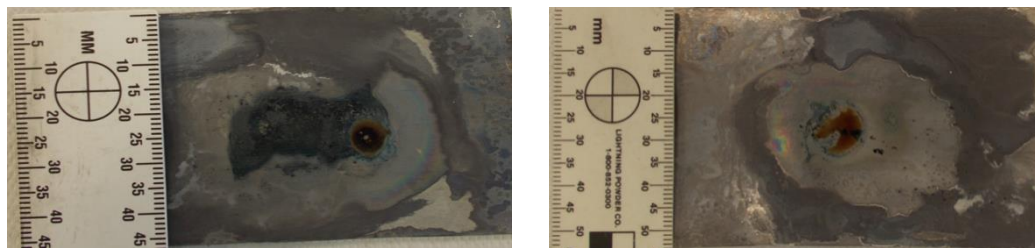


Figure 6.39: (Left) Sample A prepared with x1 dilution on lead and processed with amido black. This sample was processed with PowerPlex® 16HS. (Right) Sample A prepared with x2 dilution on lead and processed with amido black. This sample was processed with PowerPlex® 18D.

6.3.2.2 Stutter and other Artefacts

Stutter peaks are commonly seen in electropherograms when analysing data. Stutter is identified as a small peak which is generally one repeat unit less/more than the true allele. The levels of stutters were all lower (8.2% for a combined average of both kits) than the limit recommended by the manufacturer, which is usually 15%.

The profiles generated from the amplification of x2 and x10 dilutions, in general, were of good quality, with no drop-ins or split peaks. The only exception was the profiles generated from x1 solution of DNA. An abundance of biological material within the smaller loci gave peaks which were split. Split peaks, also referred to as +A/-A peaks, are due to non-template addition generally of adenosine which occurs at the 3'-end of the PCR product. Amplifying higher quantities of DNA than the recommended amount can result in the incomplete 3' A nucleotide addition.

6.3.3 Ninhydrin

In contrast to the previous two chemicals, ninhydrin samples showed that the extracted samples produced with PowerPlex® 16HS gave higher peak heights (RFU) and PCR product concentrations (RFU/ μ l) compared to samples which were subjected to direct amplification with PowerPlex® 18D. However, more full profiles were developed and less peak height imbalances were exhibited with PowerPlex® 18D.

The kits were also compared to samples on substrates which were not exposed to ninhydrin (no chemical processing). In this case, the samples which were not exposed to ninhydrin showed higher peak heights and PCR product concentrations when evaluating PowerPlex® 18D but this was not the case with samples processed with ninhydrin and analysed with PowerPlex® 16HS. In this instance, the extracted samples obtained a higher average PCR product concentration after exposure to the chemical. While the numerical values are visibly noticeable the difference was not statistically significant yielding a p -value > 0.05 [$F(1, 18) = 2.28$, p -value = 0.149]. Figure 6.40 shows the average PCR product concentration for all samples and dilutions processed with both PowerPlex® 16HS and 18D compared to all samples and dilutions analysed with PowerPlex® 16HS and 18D which contained no ninhydrin on the substrates.

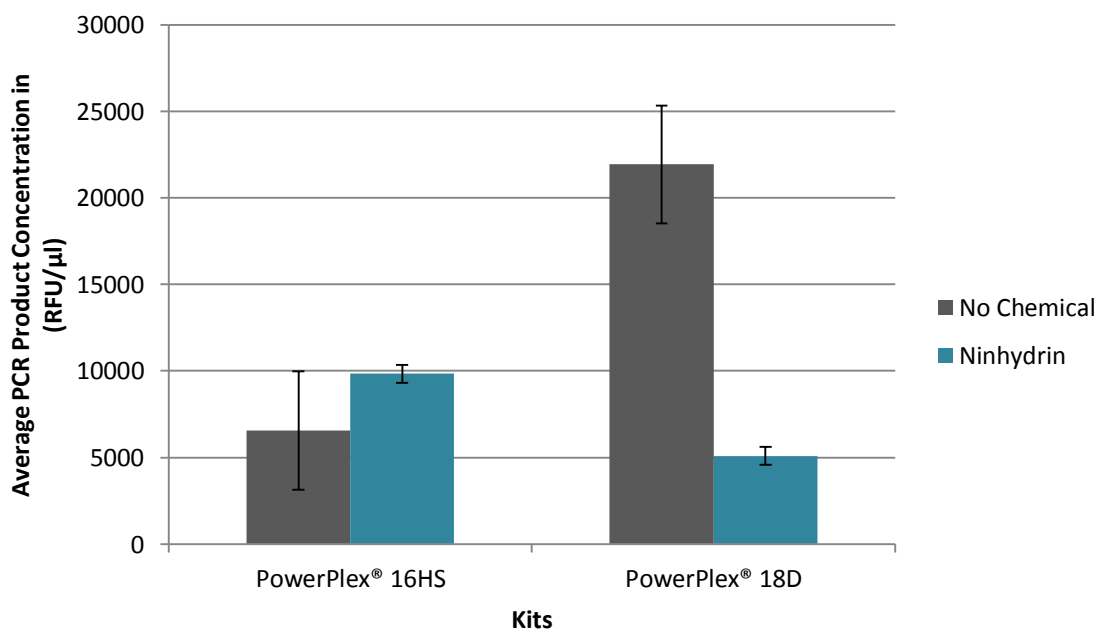


Figure 6.40: Graph displaying the average PCR product concentration (RFU/ μ l) for each kit, PowerPlex® 16HS and PowerPlex® 18D, for all samples processed using ninhydrin and for all samples processed with no chemical enhancement. The error bars represent the standard deviations for each of the kits.

Figures 6.41 and 6.42 are organized by substrate processed with Ninhydrin and subsequently by the autosomal STR kit used to generate the profiles. The boxes are reflective of information as previously described in Section 6.3.1. These figures were used to examine the variation in the amplification between the different dilution volumes, chemicals, substrates and autosomal STR kits.

Profiles generated using ninhydrin were also used to assess how complete a profile was and to determine the maximum and minimum peak heights for each allele present. The PCR product concentrations and total RFUs were also calculated. Profiles were noted as either full profiles (FP) where all alleles at all locations were observed, partial profiles (PP) where the number after indicates the number of loci which presented the alleles for that specific location and no profile (NP) where the chromosomal location did not display the proper allele call at any location in the whole profile. This information is reflected under 'Profile Type' in Tables 6.5 and 6.6.

Dilutions were a factor of significance when evaluating the samples, p -value <0.05 [$F(2, 18)= 11.22$, p -value $=0.001$). This was again to be expected since, just with the other two chemicals, a decreasing dilution was used.

Samples processed with ninhydrin using direct PCR (PowerPlex[®] 18D) gave full profiles in all x1 and x2 dilutions for both substrates.

The substrates [$F(1, 18)= 0.14$, p -value $=0.708$] and samples [$F(1, 18)= 1.06$, p -value $=0.318$] when processed with ninhydrin did not yield a significant difference as their values were both well above 0.05 (p -value >0.05).

Table 6.5: Results for Ninhydrin profiles using PowerPlex® 16HS showing the minimum, maximum and average peak heights, the profile type, total PCR product and PCR concentration for the various dilutions of samples A and B, amplified using half (12.5µl) reactions, and processed on various substrates. The values are averages of three replicates.

Substrate Sample	Dilution	Profile Properties				Total PCR Product (in RFU)	PCR product concentration (in RFU/µl)	
		Max PH	Min PH	Average PH	Profile Type			
Gypsum A	x1	27105 (s.d. 5156.78)	1403 (s.d. 239.50)	5954.86	FP	500208 (s.d. 28149.02)	40016.6 (s.d. 2251.9)	
	x2	679 (s.d. 115.76)	53 (s.d. 7.23)	200.84	PP9	11247 (s.d. 705.92)	899.7 (s.d. 56.4)	
	x10	2305 (s.d. 779.98)	55 (s.d. 7.81)	298.41	PP15	23873 (s.d. 1556.10)	1909.8 (s.d. 124.4)	
	B	x1	18773 (s.d. 1551.65)	1056 (s.d. 525.83)	5709.28	FP	411068 (s.d. 29556.51)	32885.4 (s.d. 2364.5)
		x2	393 (s.d. 77.11)	52 (s.d. 18.48)	150.33	PP7	4961 (s.d. 436.56)	396.8 (s.d. 34.9)
		x10	1607 (s.d. 312.63)	51 (s.d. 8.96)	358.42	PP14	24014 (s.d. 1040.37)	1921.1 (s.d. 83.2)
Raw Wood A	x1	12604 (s.d. 1918.51)	82 (s.d. 473.22)	3650.91	FP	306676 (s.d. 14012.81)	24534.0 (s.d. 1121.0)	
	x2	2481 (s.d. 223.60)	106 (s.d. 36.91)	668.61	FP	56163 (s.d. 2444.56)	4493.0 (s.d. 195.5)	
	x10	1069 (s.d. 202.15)	53 (s.d. 5.77)	218.64	PP14	16398 (s.d. 1198.67)	1311.8 (s.d. 95.8)	
	B	x1	21860 (s.d. 1207.16)	1254 (s.d. 174.02)	6884.57	FP	495689 (s.d. 13298.51)	39655.1 (s.d. 1063.8)
		x2	9745 (s.d. 1504.36)	792 (s.d. 96.74)	3229.83	FP	232548 (s.d. 14289.08)	18603.8 (s.d. 1143.1)
		x10	2035 (s.d. 155.09)	54 (s.d. 24.97)	512.79	PP15	34870 (s.d. 2521.26)	278.9 (s.d. 201.7)

Table 6.6: Results for Ninhydrin profiles using PowerPlex® 18D showing the minimum, maximum and average peak heights, the profile type, total PCR product and PCR concentration for the various dilutions of samples A and B, amplified using half (12.5µl) reactions, and processed on various substrates. The values are averages of three replicates.

Substrate Sample	Dilution	Profile Properties				Total PCR Product (in RFU)	PCR product concentration (in RFU/µl)	
		Max PH	Min PH	Average PH	Profile Type			
Gypsum A	x1	14192 (s.d. 989.85)	2489 (s.d. 273.23)	5186.57	FP	497911 (s.d. 14269.19)	39832.8 (s.d. 1141.5)	
	x2	1982 (s.d. 158.00)	50 (s.d. 126.06)	735.23	FP	71317 (s.d. 2117.90)	5705.3 (s.d. 169.4)	
	x10	370 (s.d. 69.95)	66 (s.d. 3.51)	136.27	PP17	12673 (s.d. 459.41)	1013.8 (s.d. 36.7)	
	B	x1	6951 (s.d. 434.84)	586 (s.d. 133.99)	2574.69	FP	208550 (s.d. 2855.03)	16684 (s.d. 228.4)
		x2	18277 (s.d. 5011.88)	240 (s.d. 1056.96)	4945.63	FP	395650 (s.d. 57820.21)	31652 (s.d. 4625.6)
		x10	410 (s.d. 96.03)	51 (s.d. 6.50)	135.19	PP17	10680 (s.d. 334.34)	854.4 (s.d. 26.7)
Raw Wood A	x1	6809 (s.d. 382.57)	1119 (s.d. 208.16)	2659.32	FP	255295 (s.d. 1485.66)	20423.6 (s.d. 118.8)	
	x2	1654 (s.d. 244.08)	81 (s.d. 104.07)	634.60	FP	60922 (s.d. 2166.67)	4873.7 (s.d. 173.3)	
	x10	166 (s.d. 24.01)	50 (s.d. 2.65)	83.09	PP7	4819 (s.d. 305.91)	385.5 (s.d. 24.4)	
	B	x1	14108 (s.d. 2652.13)	67 (s.d. 1412.12)	5257.47	FP	425855 (s.d. 18240.38)	34068.4 (s.d. 1459.2)
		x2	1762 (s.d. 145.75)	195 (s.d. 62.51)	737.78	FP	59760 (s.d. 387.28)	4780.8 (s.d. 30.9)
		x10	367 (s.d. 41.86)	55 (s.d. 5.57)	157.85	FP	12628 (s.d. 291.25)	1010.2 (s.d. 23.2)

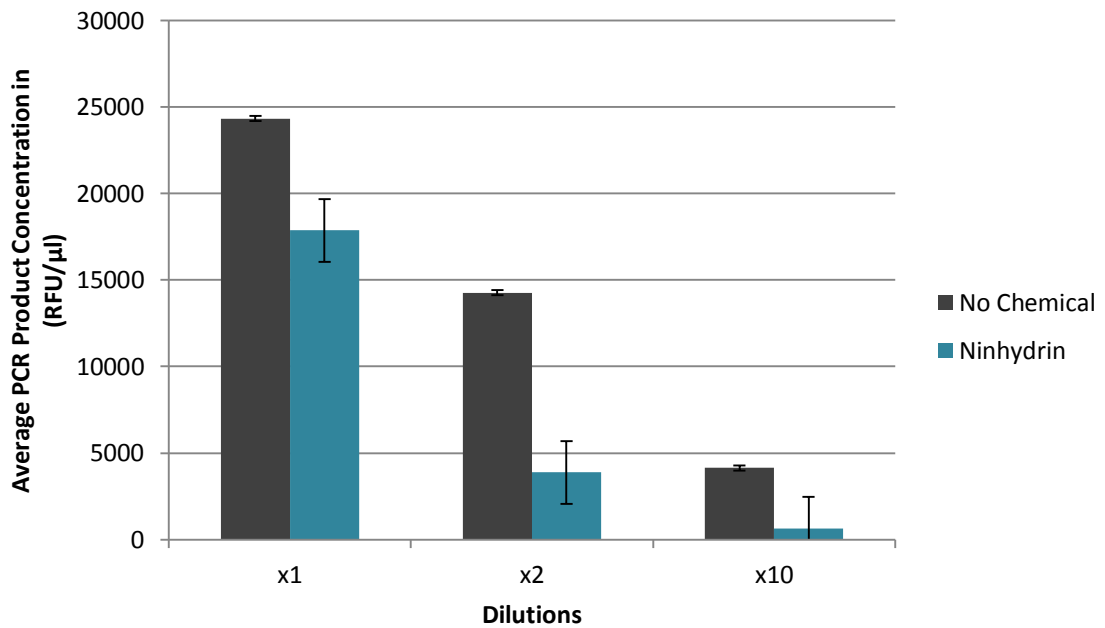


Figure 6.43: The average PCR product concentration (RFU/μl) for each kit, PowerPlex® 16HS and PowerPlex® 18D, for all samples processed using ninhydrin and for all samples processed with no chemical enhancement. The error bars represent the standard deviation for each dilution.

6.3.3.1 Heterozygous Peak Height Balance

Heterozygous peak balance was also assessed for each heterozygous locus present in both sample A and B. Heterozygous peak balance (Hb) was generated the same as in the previous two sections. Figures 6.44 through 6.51 exhibit heterozygous loci which are present in both sample A and B and their dilutions by substrate processed. A red dotted line indicates the 0.70 Hb threshold for the results.

Profiles which displayed peak imbalance were observed in both extracted and direct PCR samples. Overall peak imbalance within the PowerPlex® 18D processed samples was lower than those processed with PowerPlex® 16HS for all observed loci. Samples which were exposed to the x10 dilution fell below the 0.7 limit more often which was to be expected with the decreased amount of DNA template available. All loci exhibited on the baseline when evaluating laminate and gypsum indicate allele drop-out was present in the heterozygous locus. Glass contained the least amount of peak imbalances for all samples, dilutions and loci evaluated. Penta E has the most imbalanced heterozygous loci.

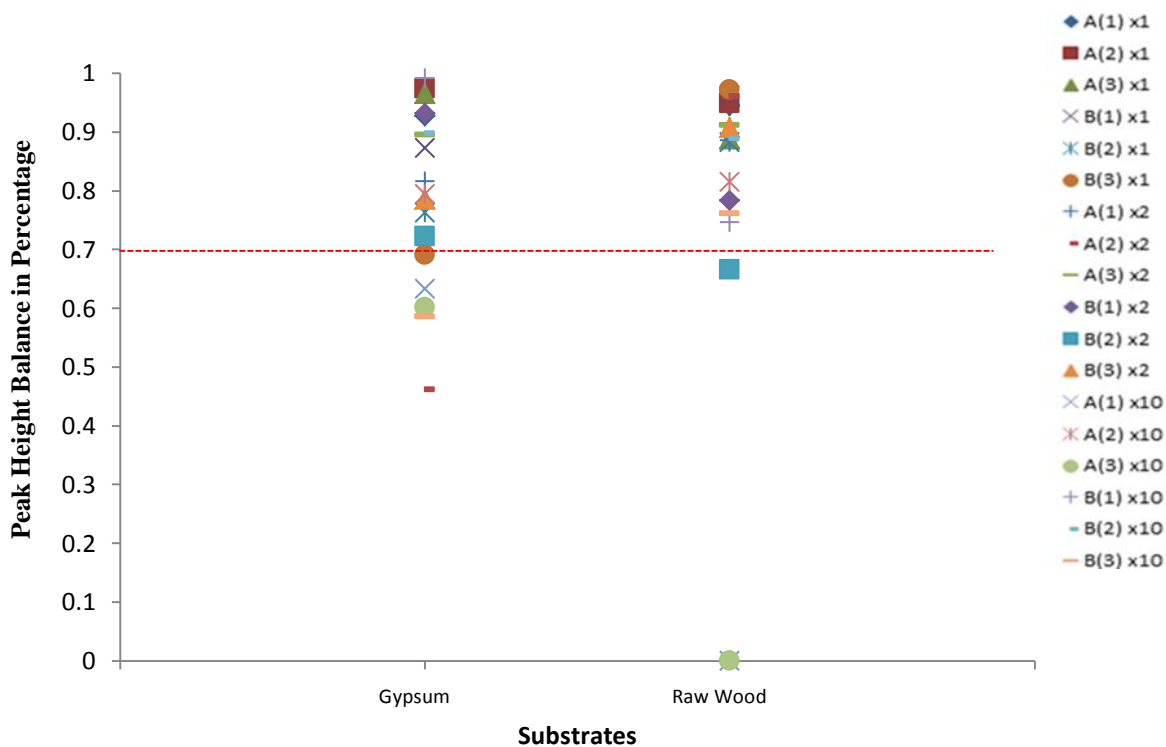
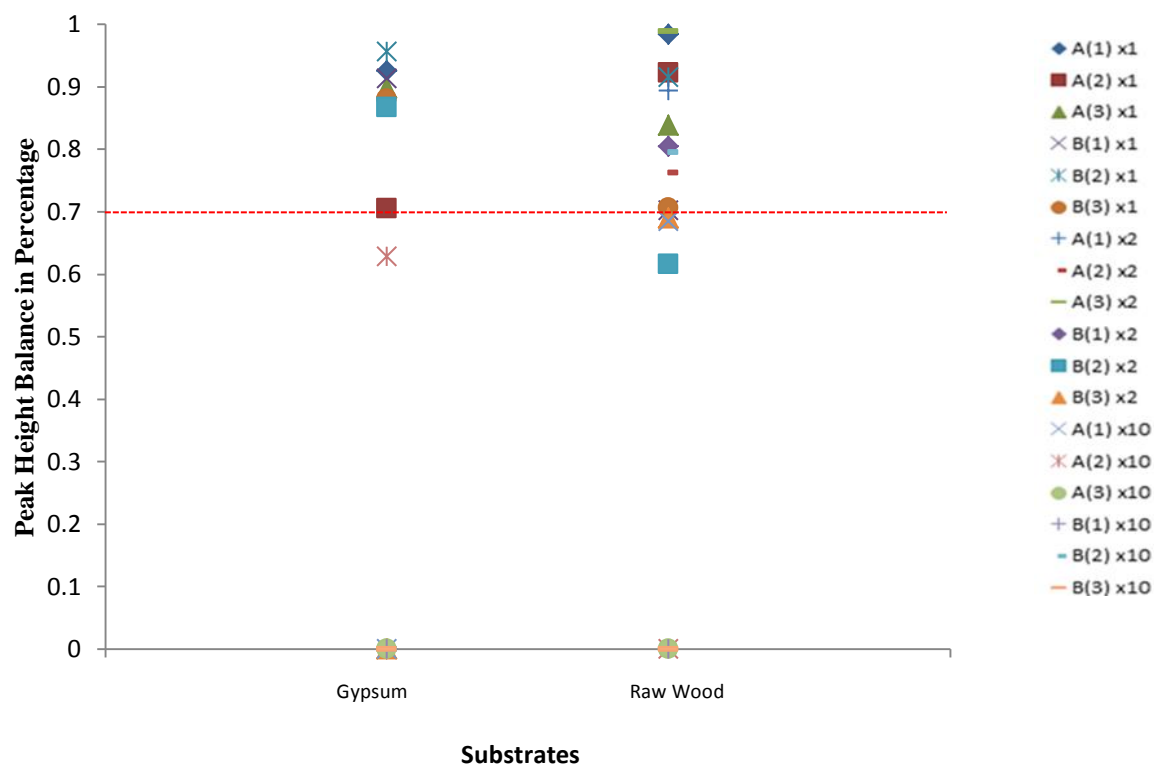


Figure 6.44: (Top) Peak height ratios for CSFIPO produced for various substrates processed with ninhydrin and analysed with PowerPlex[®] 16HS. (Bottom) Peak height ratios for CSFIPO produced for various substrates processed with ninhydrin and analysed with PowerPlex[®] 18D. All three replicates of each sample (A and B) for each dilution are represented.

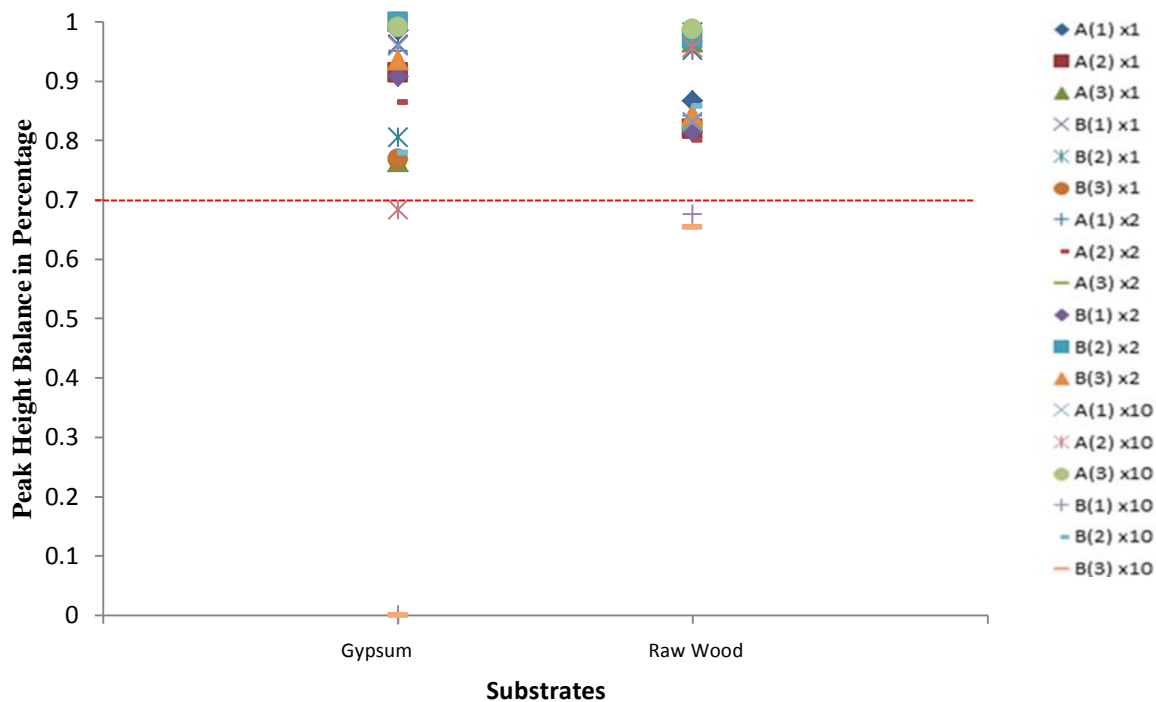
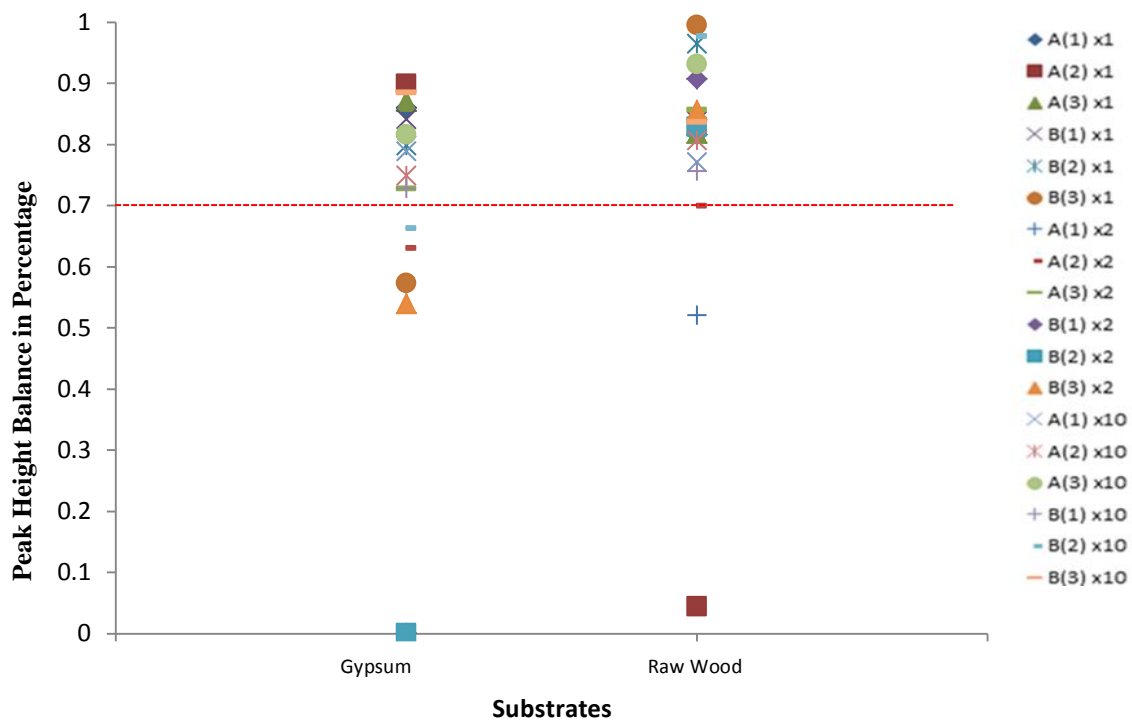


Figure 6.45: (Top) Peak height ratios for *DI3S317* produced for various substrates processed with ninhydrin and analysed with PowerPlex[®] 16HS. (Bottom) Peak height ratios for *DI3S317* produced for various substrates processed with ninhydrin and analysed with PowerPlex[®] 18D. All three replicates of each sample (A and B) for each dilution are represented.

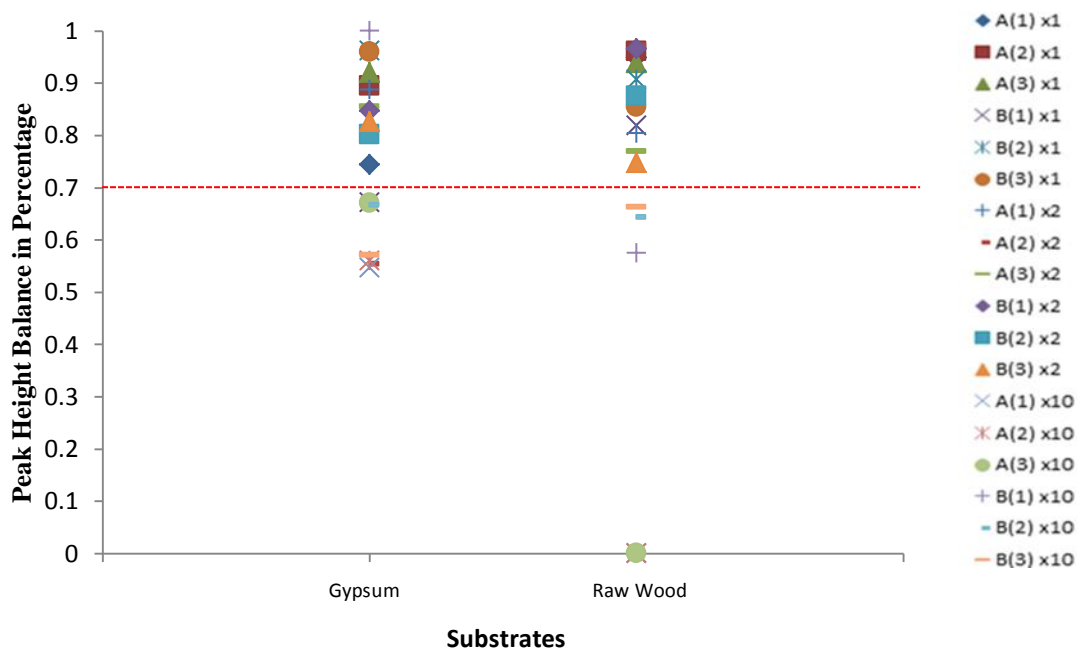
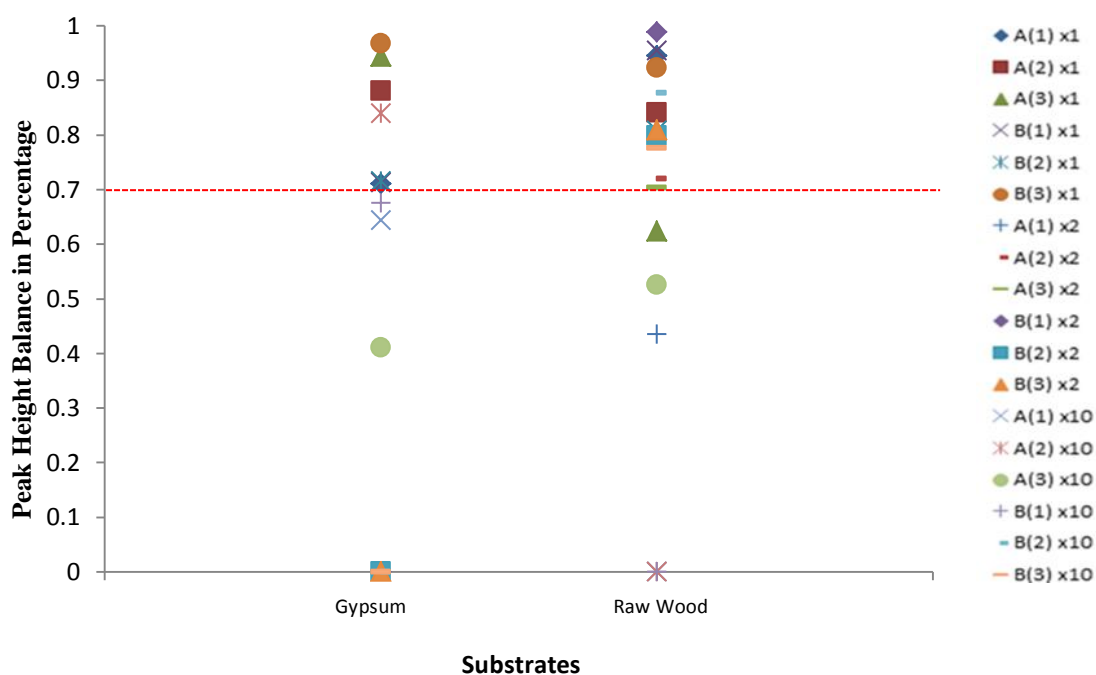


Figure 6.46: (Top) Peak height ratios for *D18S51* produced for various substrates processed with Ninhydrin and analysed with PowerPlex[®] 16HS. (Bottom) Peak height ratios for *D18S51* produced for various substrates processed with Ninhydrin and analysed with PowerPlex[®] 18D. All three replicates of each sample (A and B) for each dilution are represented.

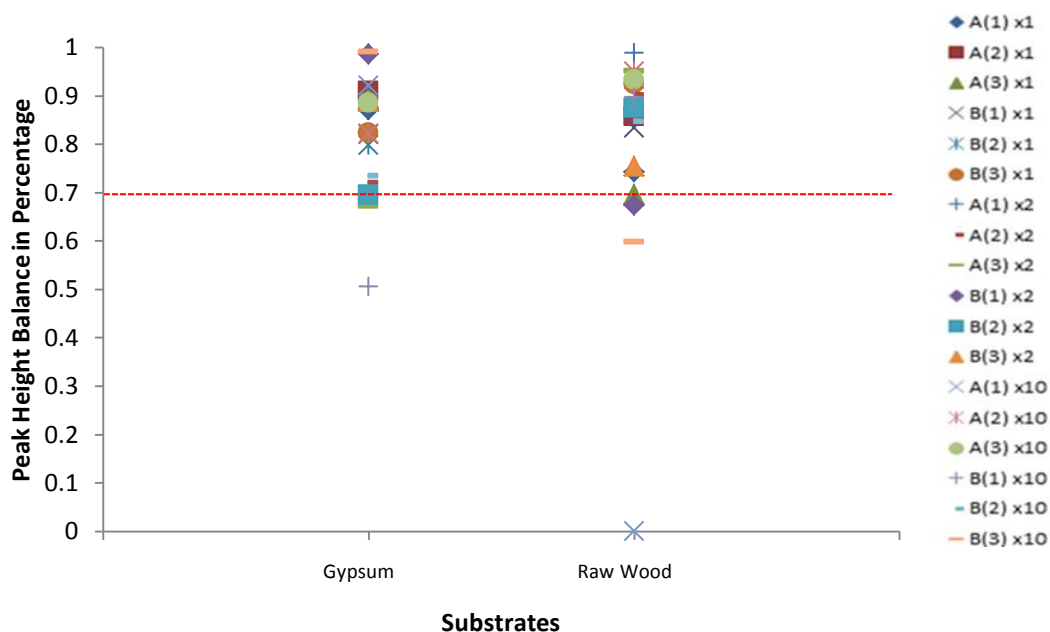
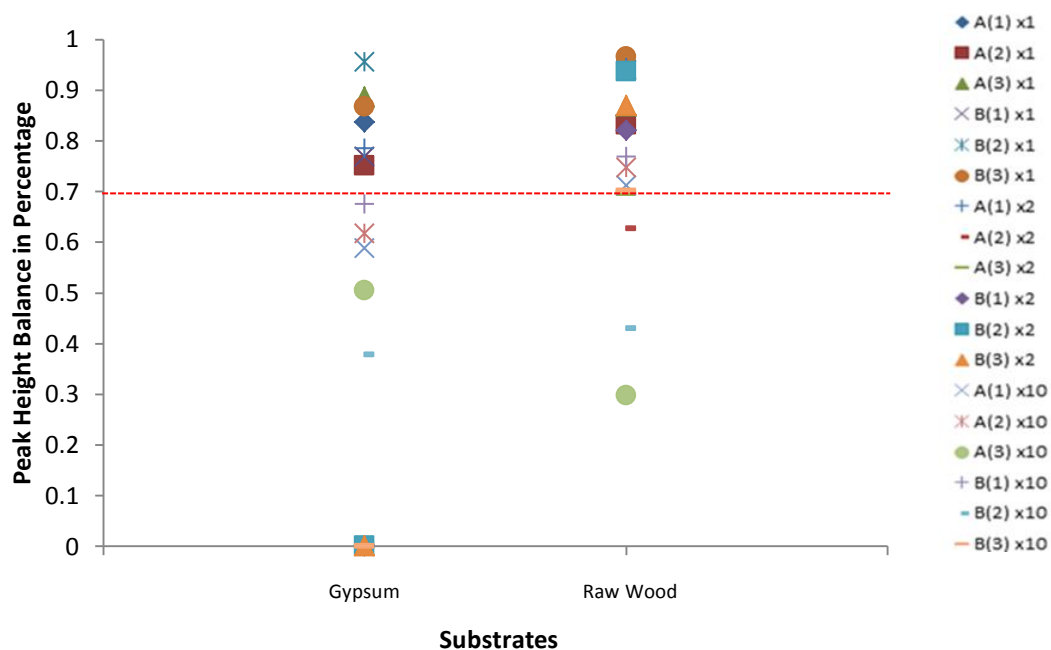


Figure 6.47: (Top) Peak height ratios for *D21S11* produced for various substrates processed with Ninhydrin and analysed with PowerPlex[®] 16HS. (Bottom) Peak height ratios for *D21S11* produced for various substrates processed with Ninhydrin and analysed with PowerPlex[®] 18D. All three replicates of each sample (A and B) for each dilution are represented.

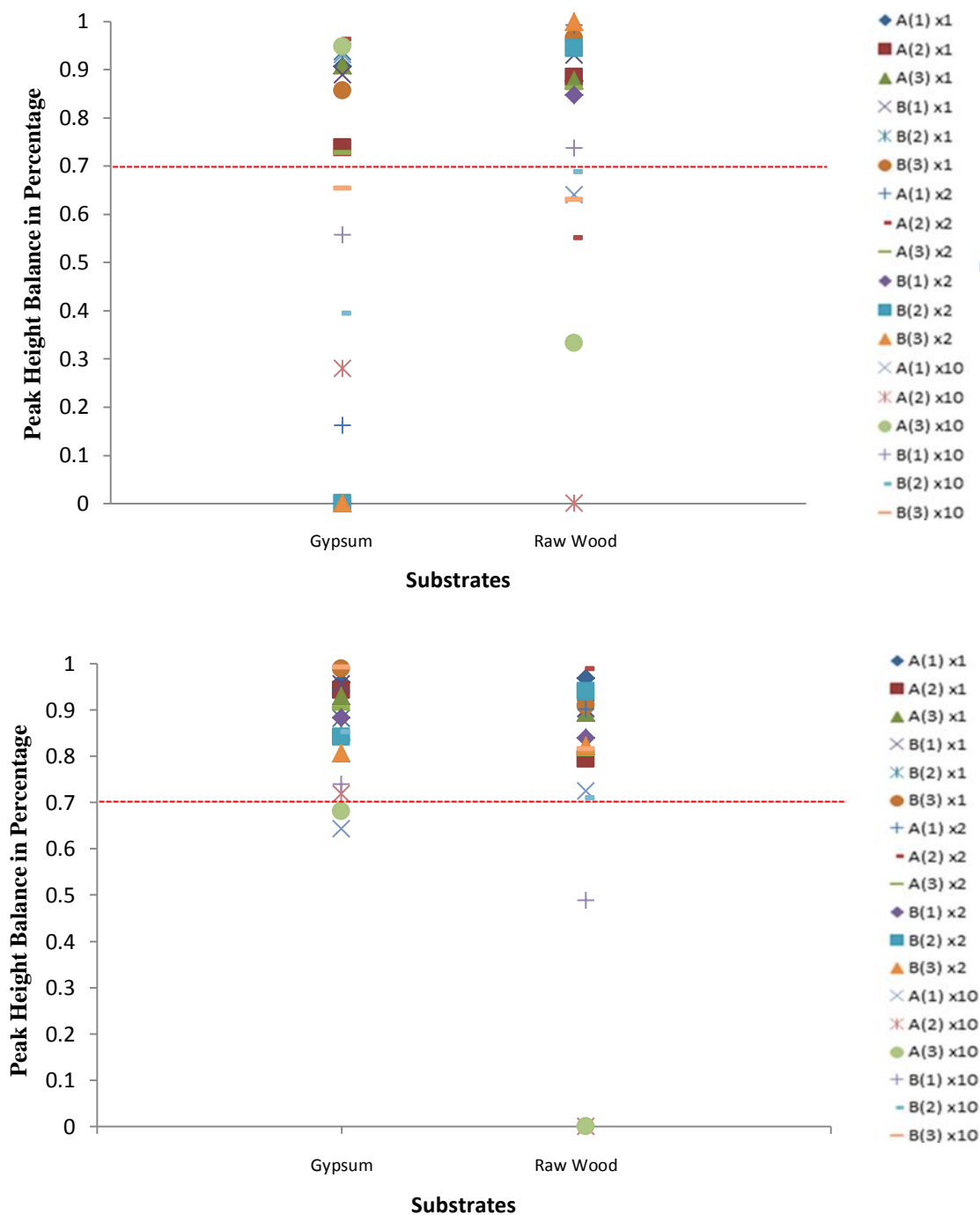


Figure 6.48: (Top) Peak height ratios for *D3SI358* produced for various substrates processed with Ninhydrin and analysed with PowerPlex® 16HS. (Bottom) Peak height ratios for *D3SI358* produced for various substrates processed with Ninhydrin and analysed with PowerPlex® 18D. All three replicates of each sample (A and B) for each dilution are represented.

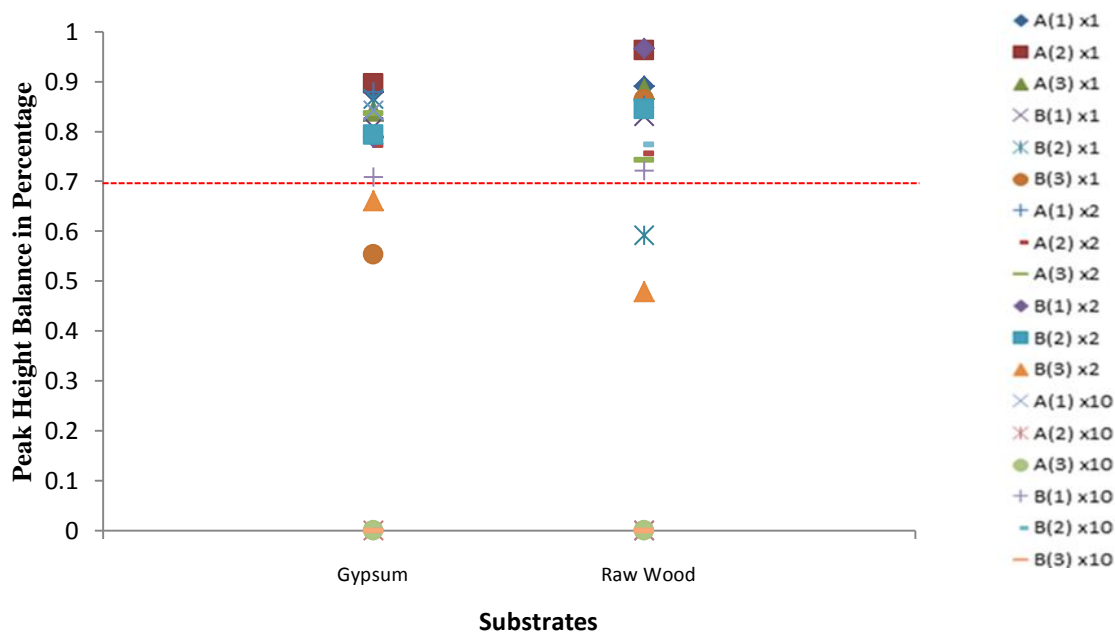
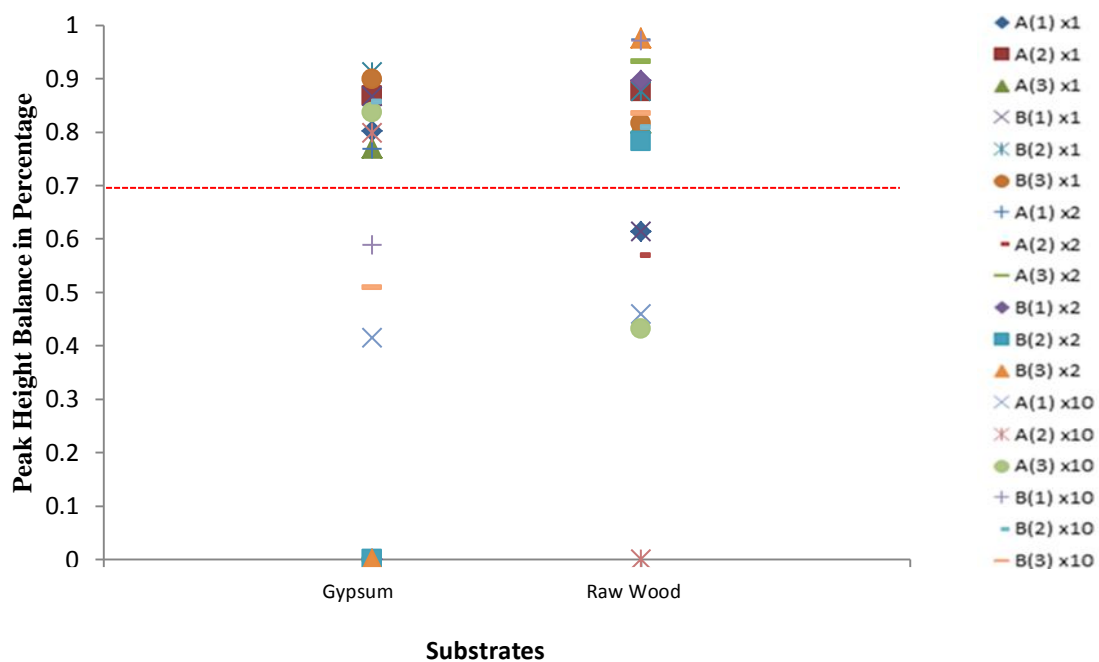


Figure 6.49: (Top) Peak height ratios for *FGA* produced for various substrates processed with Ninhydrin and analysed with PowerPlex[®] 16HS. (Bottom) Peak height ratios for *FGA* produced for various substrates processed with Ninhydrin and analysed with PowerPlex[®] 18D. All three replicates of each sample (A and B) for each dilution are represented.

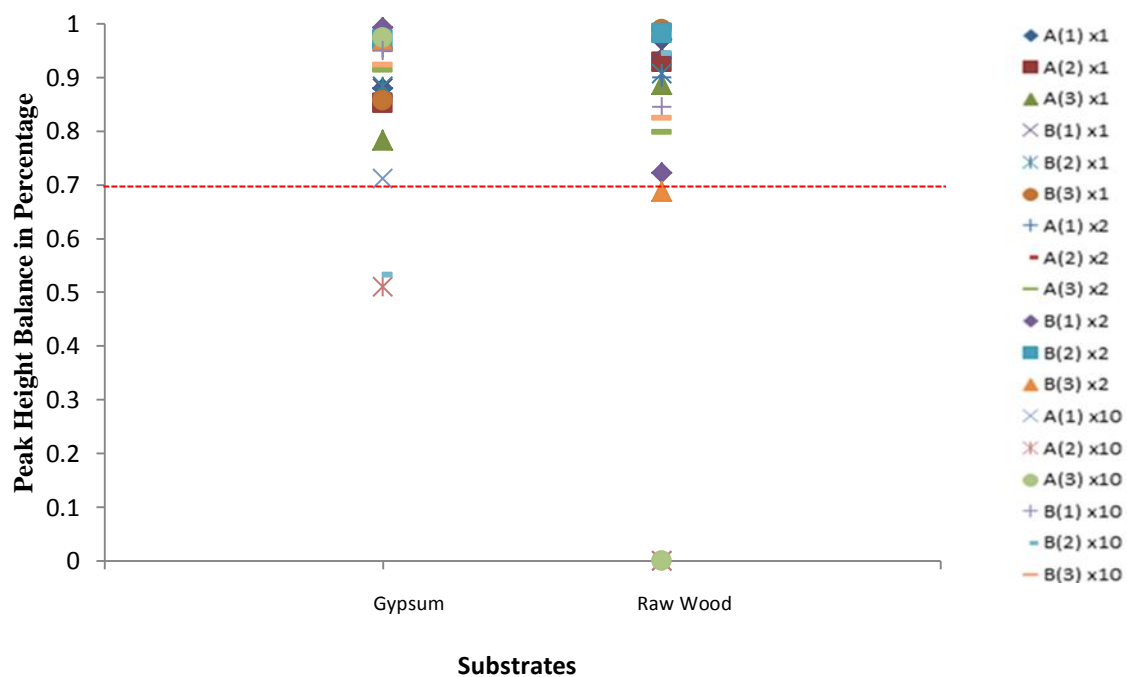
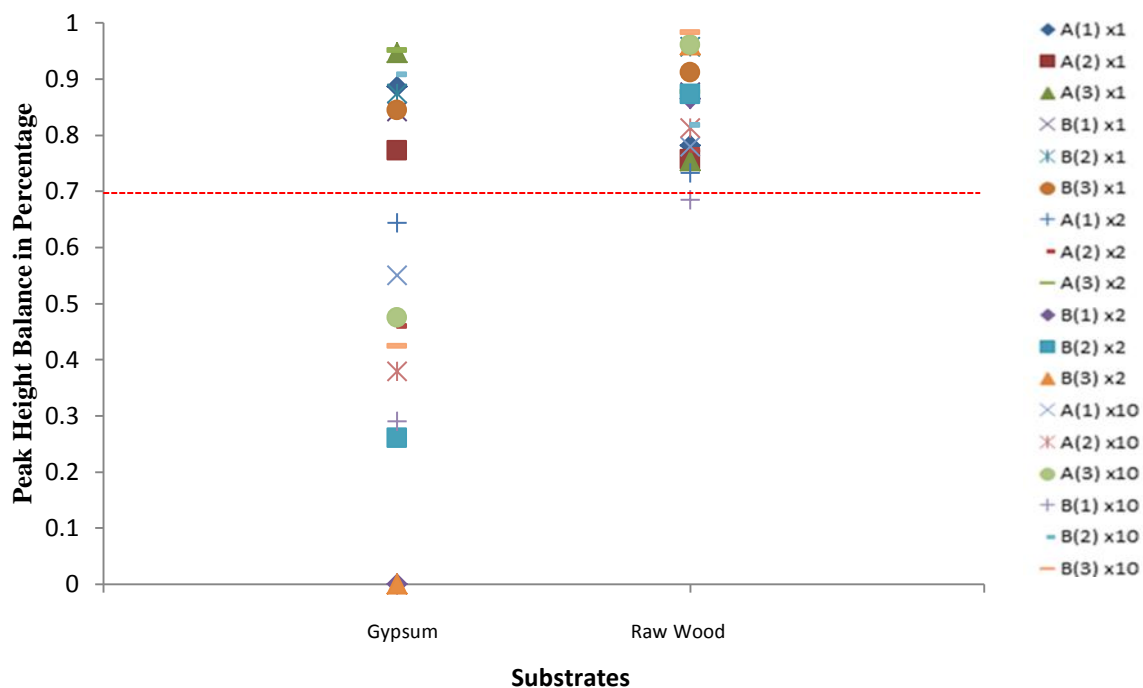


Figure 6.50: (Top) Peak height ratios for *D7S820* produced for various substrates processed with Ninhydrin and analysed with PowerPlex[®] 16HS. (Bottom) Peak height ratios for *D7S820* produced for various substrates processed with Ninhydrin and analysed with PowerPlex[®] 18D. All three replicates of each sample (A and B) for each dilution are represented.

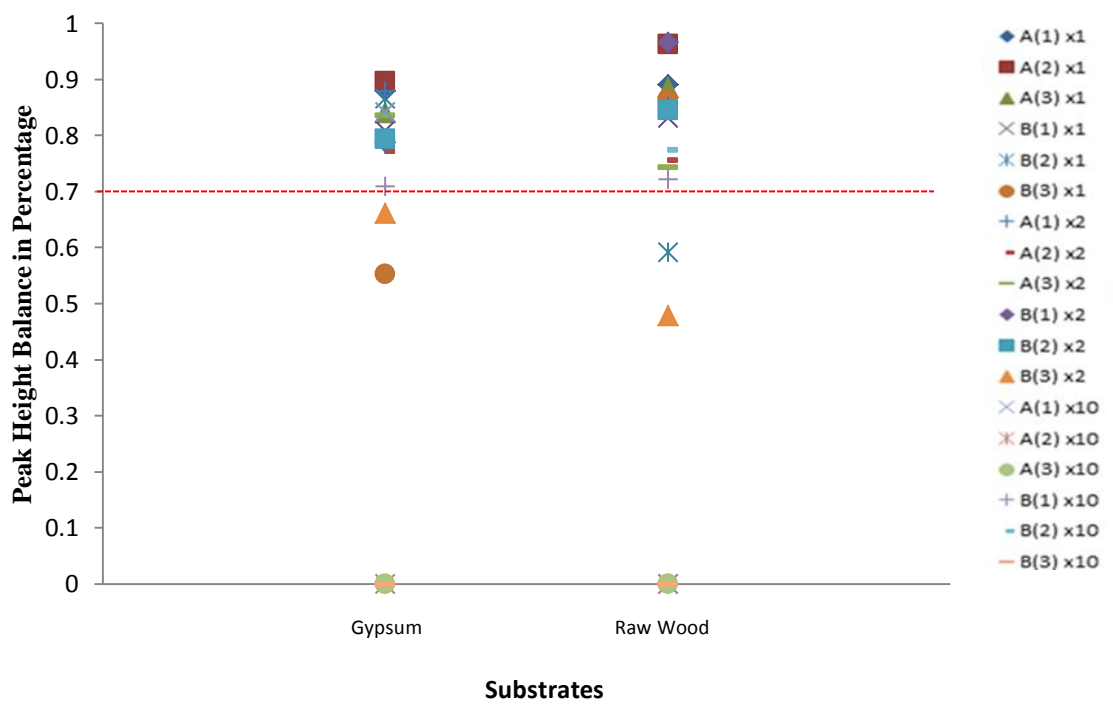
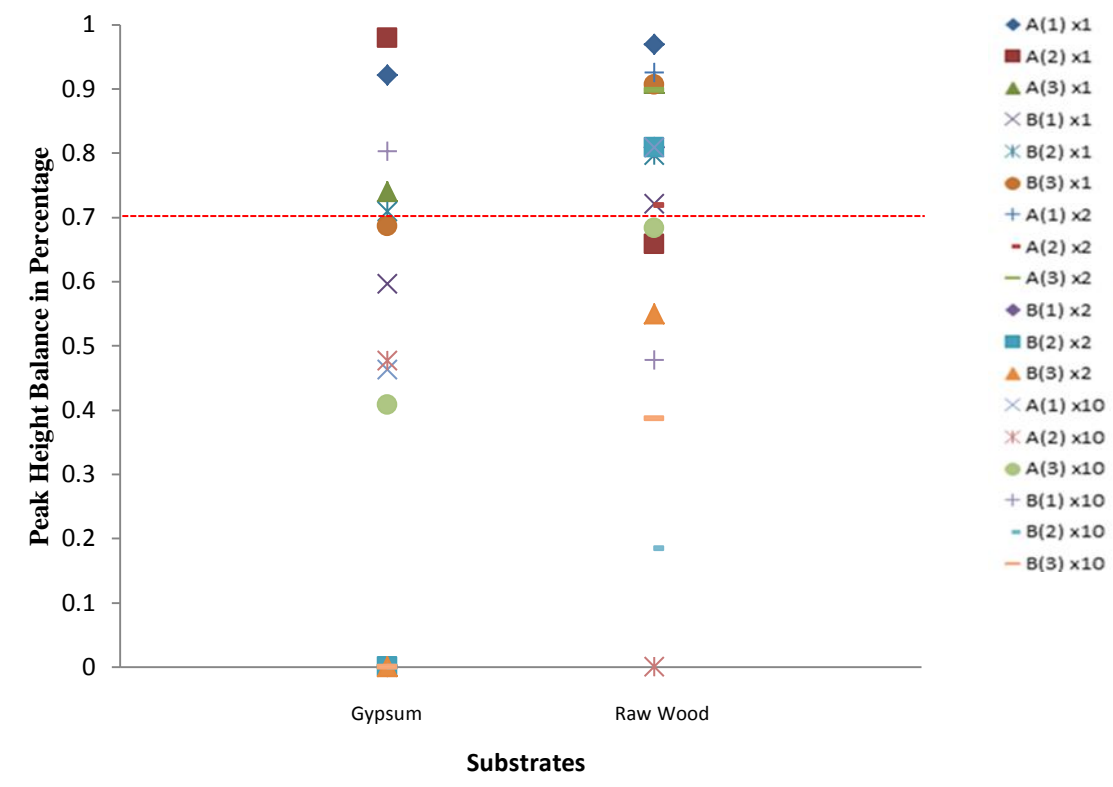


Figure 6.51: (Top) Peak height ratios for *Penta E* produced for various substrates processed with Ninhydrin and analysed with PowerPlex[®] 16HS. (Bottom) Peak height ratios for *Penta E* produced for various substrates processed with Ninhydrin and analysed with PowerPlex[®] 18D. All three replicates of each sample (A and B) for each dilution are represented.

PowerPlex[®] 16HS exhibited higher total PCR product values (500,208 RFU for x1 Gypsum, sample A) with PowerPlex[®] 18D giving a slightly lesser number (497,911 RFU) for the same sample; the overall peak quality of the in regards to peak balance (Hb >.70) was superior when analysed with PowerPlex[®]18D (Table 6.5 and 6.6).

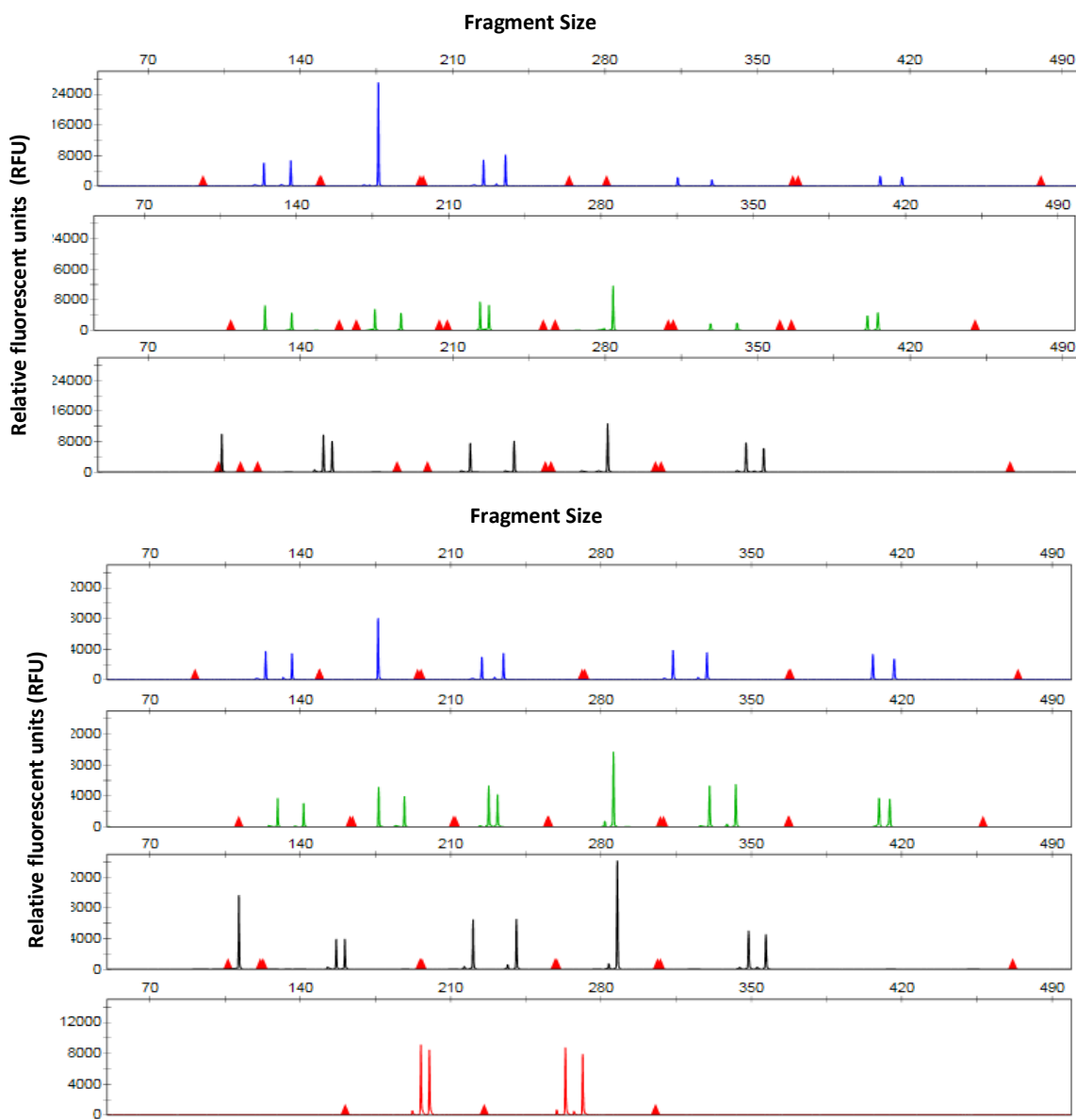


Figure 6.52: Electropherograms demonstrating the two profiles generated from sample A (x1, Gypsum). (Top) The profile generated with PowerPlex[®] 16HS. (Bottom) The profile generated with PowerPlex[®] 18D.

6.3.3.1.1 Evaluation of CSF1PO

A heterozygous allele call of CSF1PO was present in sample A. CSF1PO was more successful in displaying both alleles when processed with PowerPlex® 18D. Both alleles were displayed in 21 of 45 samples analysed with PowerPlex® 16HS when compared to PowerPlex® 18D where both alleles were present in 29 of the 45 samples processed (Figures 6.23-6.27). Of the samples producing both alleles, 8 of the 21 samples processed with PowerPlex® 16HS displayed peak height balance ratios of 0.70 Hb or higher (Figure 6.30). This is a lower percentage than the 24 of 29 which were over 0.70 Hb when analysed with PowerPlex® 18D (Figure 6.30).

6.3.3.2 Stutter and other Artefacts

The profiles generated from the amplification of x1, x2 and x10 dilutions were of good quality, with no drop-ins or split peaks. The levels of stutters were all lower (11.1% for a combined average of both kits) than the limit recommended by the manufacturer, which are usually 15%.

6.3.4 Collective Evaluation of All Chemicals

Sections 6.3.1-6.3.3 has evaluated each chemical independently but it is also important to analyse both kits with all chemicals, dilutions, and substrates as factors.

6.3.4.1 Chemicals

Prior to the study, amido black was thought to give the lowest peak height values due to the methodology employed to use this stain. Amido black is the only chemical in this experiment with a rinse step which was thought to possibly cause additional loss of the DNA sample. Careful consideration was taken when gently rinsing the substrates, however, the data does indicate that the overall sample totals were lower than the other two chemicals.

Ninhydrin was observed to give the highest total PCR product. This was to be expected as the blood soaked into the substrate and when swabbing a lot of the blood would adhere to the swab. Ninhydrin did not have a rinse step and appeared to retain the most in regards to blood on surface. Numerical values only slightly differed and there was no statistical difference between any of the chemicals [$F(2, 165) = 1.57$, $p\text{-value} = 0.210$].

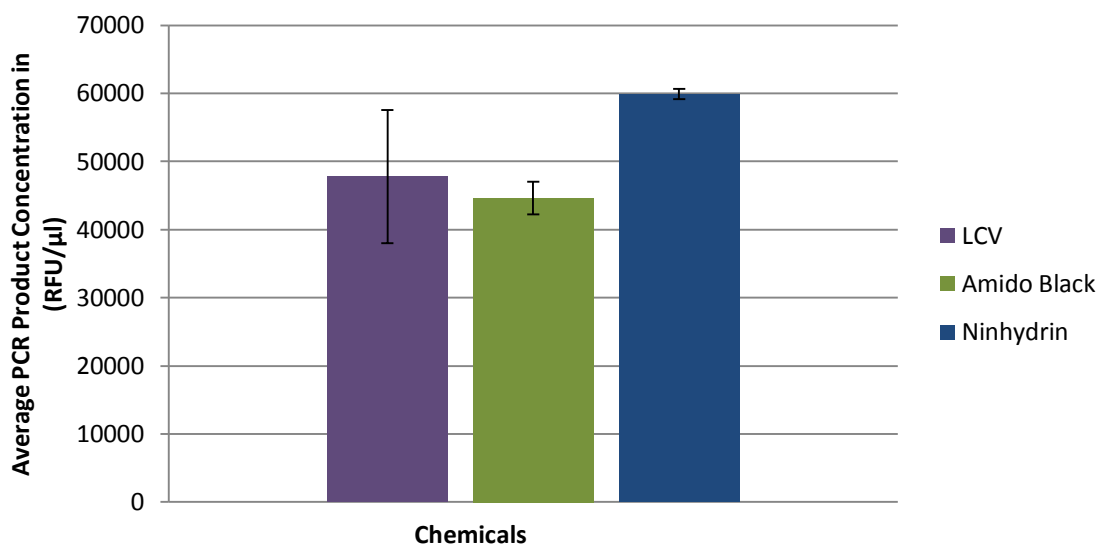


Figure 6.53: Average of the total PCR products for each of the chemicals used as enhancements for the substrates in this project. Error bars represent the standard deviations for each of the chemicals.

6.3.4.2 Dilutions

Across all chemicals, the dilution factor was in most cases statistically significant. The same conclusion can be drawn for dilutions when compared across kits, all chemicals and all substrates where statistically significant [$F(2, 1256) = 40.85$, $p\text{-value} = 0.001$]. Dilutions are an important factor when determining sensitivity. Based on the samples produced in this study there definitely needed to be balance between the amount of sample on the substrate and the amount of chemical used in order for the reaction to produce a quality profile. x2 dilutions were the most successful of the dilutions used for this work.

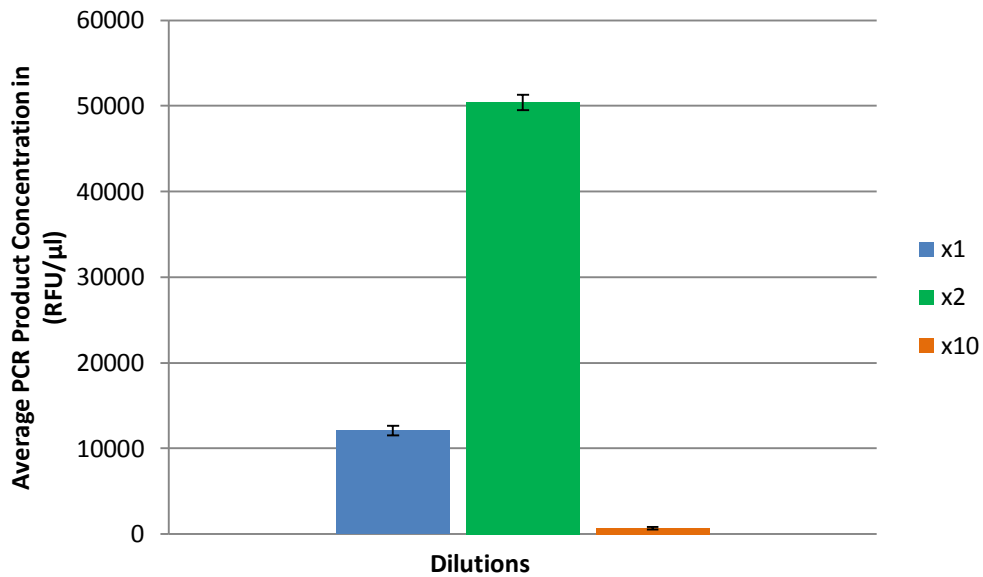


Figure 6.54: Average of the total PCR products for all of the chemicals used as enhancements for the substrates without regard to kit or specific chemical. Error bars represent the standard deviations for each of the dilutions.

6.3.4.3 Substrates

Tile was the substrate which produced the highest total PCR concentration. This was an expected result as tile is a smooth nonporous surface. Lead produced the lowest numerical values of all substrates and was statistically different when compared to tile, gypsum, glass, plastic, and raw wood [$F(7, 156) = 2.69$, $p\text{-value} = 0.012$]. The two porous substrates, raw wood and gypsum, displayed higher total PCR concentrations than expected. Since the surface was porous, it was hypothesized the blood would soak into the medium and would be difficult to remove via swabbing from the surface; however, this did not appear to be the issue based on the concentrations in Figure 6.55.

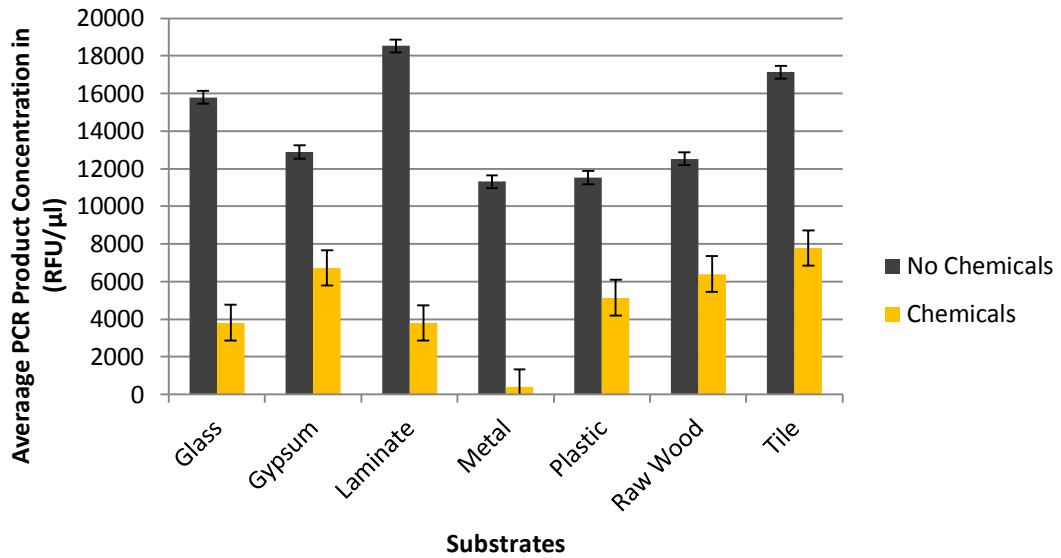


Figure 6.55: The total PCR concentrations for all substrates: glass, gypsum, laminate, lead, plastic, raw wood, and tile without regard to kit or chemical. Error bars represent the standard deviation.

6.3.4.4 Human Identification Kits

PowerPlex® 16HS and PowerPlex® 18D were compared across all substrates, chemicals, samples and dilutions. A comparison between the two kits failed to show a statistically significant difference [$F(1, 166) = 2.07, p\text{-value} = 0.152$]. This could be attributed to the small sample set and upon running more samples; the p-value should decrease.

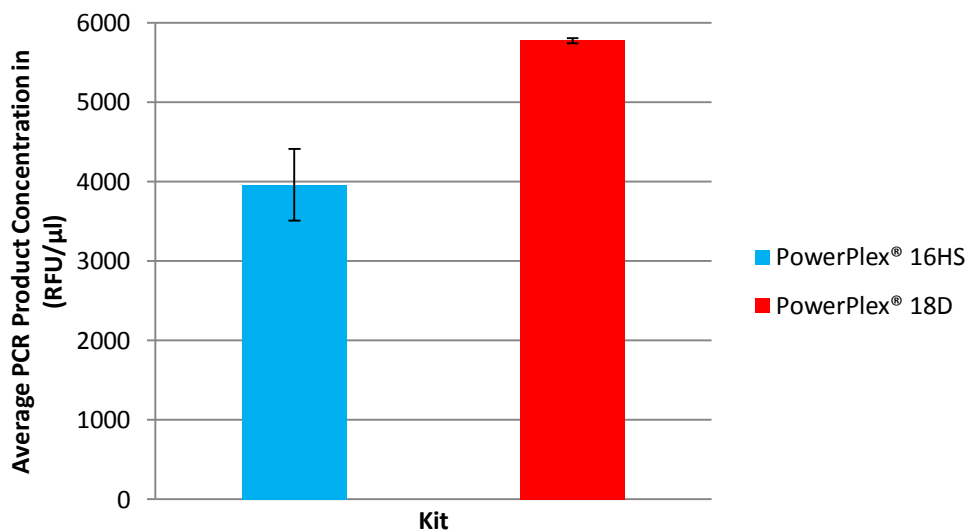


Figure 6.56: Total PCR concentrations for both kits, PowerPlex® 16HS and PowerPlex® 18D. Error bars represent the standard deviations for the total PCR concentration.

6.4 Discussion

PowerPlex[®] 18D performed better than PowerPlex[®] 16HS when analysing samples which have been exposed to chemical enhancement techniques. The ability to compensate for haem inhibition could be attributed to the enhanced PCR master mix and the possible utilization of a new or mutant polymerase (*Taq or other*) as one of the components of the PowerPlex[®] 18D kit.

The proposal of an alternate form of polymerase is not novel and has been studied from a biochemical perspective for many years (Eckert and Kunkel, 1991; Tindall and Kunkel, 1988). In recent years, novel mutants of Taq polymerase have been proposed to compensate for various inhibitors which can be found in whole blood and other biological samples (Zhang et al., 2010). OmniTaq (Taq-22), a double mutant of Taq polymerase, is an enzyme which is resistant to the inhibitory effects of blood, soil, crude soil extracts, and some food media (Zhang et al., 2010). Omni KlenTaq LA (Klen-taq-10) is a triple mutant of the KlenTaq polymerase which makes the enzyme resistant to the same inhibitory effects as OmniTaq with the inclusion of fluorescent dyes (Kermekchiev et al., 2009). Clontech Laboratories, part of Takara Biotech Company, has also released 'Terra[™] PCR direct polymerase' which is a novel enzyme developed for direct amplification from tissue samples and crude extracts (Lin et al., 2013). The utility of these novel alterations to polymerase are especially notable in regards to whole blood samples which have often been a source of contention for the DNA analyst because of the inhibition displayed due to haemoglobin which can copurify with DNA (Akane et al., 1994). This ultimately leads to the inactivation of the DNA polymerase, nonbinding primers, and/or degradation of the target DNA rendering these samples non-viable for development of a partial or full profile (Al-Soud and Radstrom, 2001).

It should also be noted the optimization of the polymerase alone cannot avoid sample inhibition. PCR enhancers may also aid in the robustness of the newly configured kits. Dimethyl sulfoxide, tetramethylxene, betaine, and homoectoine have all been documented as chemicals which can have positive effects on PCR (Bachman et al., 1990; Schnoor et al., 2004; Zhang et al., 2010). Also, an increase in magnesium chloride and bovine serum albumin (BSA) concentration have been suggested as other alternatives for the increase in strong profiles generated from the new kits (vanOorschot et al., 2010).

It should also be noted in the validation of PowerPlex[®] 18D it has been optimized for direct PCR while PowerPlex[®] 16HS was developed for extracted samples (Ensenberger et al., 2010; Oostdik et al., 2013). A validation which also confirms, that while optimized for direct amplification, whole blood samples were validated on FTA cards. This study did not use FTA cards for any whole blood samples. Regardless of the individual components, PowerPlex[®] 18D was successful in developing full or partial profiles for samples for the majority of samples which have been exposed to chemical processing better than PowerPlex[®] 16HS.

6.4.1 Substrates

The deposit of the biological material is important to the development of the profiles but the substrates on which they are deposited are also of equal concern. Different substrates have shown to have different effects on the generation of a DNA profile due to the physical properties of the surface which can affect the retention of the biological material deposited (Allen et al., 2008; Linacre et al., 2010; Templeton et al., 2015). Several surfaces were found to have very little data regarding the ability to obtain a DNA profile from their surface; this included gypsum board (drywall) and raw wood (Praska and Langenberg, 2013). The results of this study concluded both surfaces were viable options for retrieving biological materials for subsequent DNA analysis.

Plastics, particularly those composed of polypropylene, are known to cause denaturation of DNA (Belotserkovskii and Johnson, 1997). The plastic used in the course of this study was polypropylene based and decreased peak heights and reduced concentrations were to be expected. These were only observed in the samples processed with LCV, however, not noted in any other chemical. Therefore, it is theorized that the LCV was inhibiting the samples causing the samples to reflect decreased peak heights and reduced concentrations.

The lead which was used in this study contained an oxide film which when exposed to sulfosalicylic acid (a strong oxidizing agent) contained in the LCV solution mix, caused a redox reaction which adversely affected the biological material (LabChem, 2012). This reaction was observed again with amido black presumably due to the acidic compound found within its solution. Lead was the least successful substrate and was not successful when utilized with PowerPlex[®] 16HS as only partial profiles ranging from 1 locus to 13 loci were able to be generated.

6.4.2 Chemicals

Many experiments have been conducted on various paper products and the ability to develop a viable DNA profile post exposure to the chemical (Sewell et al., 2008; Thomas and Farrugia, 2013; Stein et al., 1996; Jelly et al., 2009; Bosser et al., 2011; Roux et al., 1999; Frégeau et al., 2000; Moore et al., 2008). To date, ninhydrin has shown little to no inhibition when trying to obtain a DNA profile from a surface which has been exposed to the enhancement techniques (Bhoelai et al., 2011; Schultz et al., 2004). These data were reinforced with the results obtained within this chapter as the majority of the dilutions tested for ninhydrin yielded full profiles. Its versatility to process latent fingerprints as well as being utilized as a blood enhancement technique has allowed laboratories to invest in a single chemical which has multiple purposes. Ninhydrin has a limitation in crime-scene- based work in that it can only be utilized on porous surfaces. Several published articles mention paper as the substrate for development of DNA profiles with little to no mention of other porous surfaces such as raw wood or gypsum board. Therefore, during the course of this work, those two substrates were the primary focal point. The data generated from those surfaces further displayed ninhydrin was a good option when selecting a chemical for enhancement on porous surfaces as the chemical did not appear to inhibit the samples and gave the highest average total PCR products when compared to all other chemicals processed in this study.

Leucocrystal violet (LCV) is most commonly known for its ability to enhance shoe prints in blood which is how it was first reported from J. F. Fischer of the Federal Bureau of Investigations in the early 1990's (Bodziak, 1995; Theeuwen et al., 1998; Cullen et al., 2010). It was chosen for this project for its haem- reactive qualities and while there is very little available documentation on the effects of LCV on DNA profiling, there is a need to explore all chemicals which could be used for blood enhancement (Spear et al., 2002; Fox et al., 2014). LCV was moderately successful in obtaining DNA profiles during this study; exceeding those which were chemically enhanced with Amido Black. This could be due to the highly acidic nature of the LCV formulation which does not require a de-staining step when processing the samples; therefore, high concentrations of hydrogen peroxide, sodium acetate and sulfosalicylic acid solution remain on the surface and are collected with the sample when swabbing (Fox et al., 2014). More work is needed to explore the reactive nature of the chemical with other substrates as well as a possible improvement of the formulation of the chemical which would allow for greater success when DNA profiling is conducted.

Some research has been conducted on amido black, a diazo dye that stains proteins within blood samples (Fox et al., 2014; Gino and Omedei, 2011; Sears and Prizeman, 2000). Amido black can be found in two formulations, a water-based formula and a methanol-based formula. The water-based formulation is good for general use at crime scenes and was used in this work in order to simulate what field technicians would most likely be using (Sears and Prizeman, 2000). Amido black was the least successful of the chemicals tested which is consistent with one would anticipate as the protocol to use the chemical requires a de-staining step after the chemical exposure which would ultimately lead to sample loss. Lead was the least successful substrate when examining the data and may be due to the substrate reacting with the acidic composition of the amido black. A review of the untreated data further supports this in that the untreated samples were more successful when generating profiles from samples that were placed on lead and not exposed to amido black (Figure 6.29(E)). Further research should be conducted on the methanol-based formulation of amido black in order to determine if it exceeds the results of the water-based formula. It would also be beneficial to see a direct comparison of the two formulations with comparable samples.

The chemical processing methods evaluated in this experiment influenced the quality and robustness of the DNA profiles generated. The process by which retrieval of the DNA occurred and the amplification process played a major role in determining how successful the DNA profile was generated. The substrate on which the biological material is deposited is statistically significant in determining the quality of the profile across all chemicals reviewed. The properties, both physical and chemical, of the substrate to be processed and the iteration of the chemical used to develop the stain on the DNA plays a critical role in determining the quality and quantity of the DNA recovered. While PowerPlex[®] 18D was more successful in developing full and partial profiles, ultimately, more work needs to be conducted regarding the effects of chemical and substrate on the subsequent recovery of DNA.

CHAPTER 7.

GENERAL DISCUSSION

The studies carried out during this project showed that the ability to develop a DNA profile from samples which have been exposed to powder and chemical processing techniques can be produced with direct PCR. The project also concluded that in most cases the use of PowerPlex[®] 18D, PCR direct kit, was more successful in generating full profiles of a robust nature than its counterpart PowerPlex[®] 16HS, an extraction-based kit.

7.1 Overview of the study and main outcomes

The main aim of this project was to compare the effects an extraction-based human identification system, PowerPlex[®] 16HS, to a PCR direct kit, PowerPlex[®] 18D on forensic based samples. In order to be cost effective, it was necessary to determine if lowering the reaction volume to 12.5 µl would be sufficient in producing the profiles from the two different kits. The limit of detection for each kit with the two sample types, epithelial cells and whole blood, were also conducted in order to maximise the reagents allotted for this work. In regards to the forensic-based samples, a set of epithelial-cell-based samples were exposed to latent fingerprint powders (black, white and magnetic flake) on a nonporous substrate (laminite) at varying dilutions (x1, x2 and x10). A second set of forensic-based samples comprised of whole blood were exposed to chemical enhancement liquids on a variety of substrates (glass, gypsum, metal, raw wood, plastic, tile, and laminite) at varying dilutions (x1, x2 and x10).

The application of direct PCR to samples which have been exposed to techniques used for visualization was a concern when developing this project. While publications reflect that profiles can be generated using extraction based processing methodologies, direct PCR does not remove inhibitors rather it relies on a more enhanced and robust reaction mix to compensate for the remaining inhibitors in the sample. Samples processed in this project were not subjected to FTA[®] paper and were swabbed as evidentiary samples

collected in the field. Taking a systematic approach, each sample was carefully prepared and analysed, assessing their profile qualities and evaluating their limitations.

Chapter 3 evaluated lowering the volume of the PCR by half, 12.5 μ l. While published research indicates this would not affect the overall quality, a short study was conducted to confirm their results (Ensenberger et al., 2010; Oostdik et al., 2013). During this study, it was found that reducing the volume of the reaction to 12.5 μ l yielded an increase the sensitivity and amplification efficiency of the assay towards low amount of DNA. The stochastic effects usually related to reduce volume reactions were observed when using amounts lower than 0.5 ng/ μ l were evaluated. The results observed exceed those in the recommended publications for the standard PowerPlex[®] 16 (Hoffman and Fenger, 2010). The half reactions were slightly more successful with PowerPlex[®] 16HS then were reflected in the PowerPlex[®] 16 as input DNA at 0.13 ng produced a full profile. This could be due in part to the enhanced buffer system included in PowerPlex[®] 16HS which is not part of the original PowerPlex[®] 16 kit (Ensenberger et al., 2010; Hoffman and Fenger, 2010). The heterozygous peak balance (Hb) for samples generated with PowerPlex[®] 16HS proved to be almost equal when looking at full (45% below threshold) versus half reactions (50%) across all dilutions and heterozygous loci. This was slightly lower than values presented in the validation studies; however, decreasing amounts of DNA were not evaluated in this study (Ensenberger et al., 2010). Overall, the 12.5 μ l reaction was not seen to negatively impact the profiles generated.

For PowerPlex 18D, full profiles were obtained for DNA input at 2.0 ng and 1 ng with a 12.5 μ l reaction. Reaction volumes of 25 μ l produced full profiles only in samples with 2.0 ng of DNA. Partial profiles were generated at all other input DNA volumes, except for 0.06 ng where no profile was generated. PCR product concentrations (RFU/ μ l) were higher when evaluating 12.5 μ l reactions than with 25 μ l. While PowerPlex[®] 18D was not as successful as PowerPlex[®] 16HS in producing full profiles, the peak heights values were higher and more loci were present in the 12.5 μ l reactions than with the 25 μ l. This is possibly due to the direct amplification materials which are typically cruder than purified samples and often include inhibitors from the raw DNA sample (Oostdik et al., 2013). It has been noted that adding the same amount of direct amplification material recommended for a full reaction into a reduced reaction volume can negatively impact performance; however, the developmental validation of PowerPlex[®] 18D showed reaction volumes \geq 12.5 μ l produced reliable full profiles

(Oostdik et al., 2013). For the purposes of this project, a half volume (12.5 µl) reaction was used for all samples.

Chapter 3 also determined the limit of detection for the epithelial-cell-based samples and the whole blood samples. The x10 dilutions for both types of samples appeared to be the limit when evaluating both PowerPlex[®] 16HS and PowerPlex[®] 18D. For the epithelial-cell samples this could be due to the low amount of DNA template present in the samples and for the PowerPlex[®] 16HS samples the additional loss of sample during the extraction process. For the whole blood samples the low sample profiles could be due to the amount of inhibitors such as haem which are still present in the sample. Instead of an extraction step, PowerPlex[®] 18D relies on the ability of the reaction mix to compensate for the level of inhibition which is still in the sample throughout the profiling process. Based on these results the samples in this project were processed at the x1, x2 and x10 dilution.

Confirming concordance was also an area which was reviewed. As discussed in Chapter 4, the primary focus was to determine that the two kits produced concordant results when amplifying the same sample. The two kits used were both from Promega[®] and contained the same primers. The results obtained did demonstrate the ability of the two kits to produce profiles with concordant results. It was also noted that micro variants which were observed in a small number of the samples were also identified in both kit. For all alleles which were produced, all were the same. It should be noted; however, that PowerPlex[®] 16HS failed to produce full profiles for several of the samples. This could be attributed to donor deposit and variability between individuals.

Epithelial cell samples exposed to powder processing techniques were the first of the forensic-based samples to be analysed. In chapter 5, black powder and white powder achieve the highest total PCR and total PCR concentrations while magnetic powder was the weakest of those processed. Earlier publications have indicated that both white powder and black powder do not inhibit the STR profiling process and the data generated in this study agreed with these findings (Raymond et al., 2004; Roux et al., 1999; Stein et al., 1996; vanOorschot et al., 2003; vanOorschot et al., 2005). Magnetic powder has been problematic for DNA analysts and while it has been shown to develop profiles they are much weaker than their standard powder counterparts (Tozzo, 2014). However, in this study PowerPlex[®] 18D was more successful when attempting to

produce profiles from samples exposed to magnetic flake than with PowerPlex[®] 16HS. This is an important finding in this study given the low amount of starting template with epithelial-cell-based samples and the crude nature of the sample being placed into the thermal cycler.

Chapter 6 outlines the whole blood samples which were the second set of samples to be processed and analysed. These samples were exposed to three different chemicals (leucocrystal violet, amido black and ninhydrin) on multiple substrates (glass, gypsum, metal, raw wood, plastic, tile, and laminate). As haem is a known inhibitor, it was hypothesized that these samples would only work in a minimal capacity (Akane et al., 1994; Al-Soud and Radstrom 2001). However, the majority of the samples worked across a variable of substrates and dilutions. Direct PCR produced more full profiles than the extraction-based PCR and in the majority of samples provided higher RFU values. One consideration for this result is utilization of an alternative polymerase (improved taq or other polymerase) and enhanced PCR buffers which overcome the inhibition in the samples (Zhang et al., 2010).

Overall the work clearly shows the potential of implementing direct PCR into forensic casework samples. The majority of casework samples obtained from crime laboratories contain blood or latent material; however, it will be important to continue to evaluate other types of biological evidence such as semen, urine, saliva and evaluate if comparable results are obtained.

7.4 Application of Direct Amplification for Forensic Casework

The possibility of implementing direct amplification into forensic casework can have a major positive impact on backlog reduction and lower operating costs for laboratories. Direct amplification uses samples which skip the extraction step and use faster cycling times than standard DNA methods. Overall these factors will help reduce the amount of time it takes to generate a profile for analysis.

Financial implications are also at the forefront of the discussions regarding direct amplification. With the elimination of robotics made for automated extraction, consumables and general maintenance contracts, monies could be saved thus improving the efficiency of the lab.

A reduction in the laboratory work conducted by analysts would also be reduced. This would allow for more time to analyse data and generate reports for submitting agencies. With reports generated in a faster manner, law enforcement could be more proactive in prosecuting crimes in a timely manner.

7.3 Crime Scene Personnel

Crime scene technicians are at the forefront of evidence collection. Continuing education and training of proper processing techniques via surface encountered could help to increase the chance of obtaining a profile for use in developing a DNA profile. To date, there are no general quick reference resources for technicians. A failure to collect the stain encountered at a crime scene with the proper chemical could be detrimental to a case.

7.4 Future work

This study was intended to be an evaluation of a direct amplification system on epithelial cells and blood samples using common enhancement techniques which are used on crime-scene-based samples. Further studies should be carried out to explore other chemicals, surfaces and types of biological material which may also need to be processed using direct amplification should this method be implemented into casework laboratories.

The chemicals selected for this work were chosen based on their reactivity to various components within blood. There are an abundance of other chemicals which are currently on the market and used for forensic samples. These chemicals use a variety of techniques to expose the substrates to the chemical some by staining and washing or staining alone. Each of these techniques could affect the yield of DNA obtained and best practices should be evaluated along with their ability to produce a DNA profile with direct amplification.

Fluorescence has also become a useful tool when looking for valuable biological evidence and latent prints which may be deposited on surfaces and difficult to visualize in ambient light. The use of an alternative light source to locate such evidence has become common practice when processing a crime scene. The use of fluorescent dyes and powders has also become a popular form of enhancement. Dyes such as Basic Yellow and 1,8-diaza-9-fluorenone (DFO) are frequently used to process items of

evidence (Schwarz and Klenke, 2007). Deriving a DNA profile from samples with a fluorescent component could be problematic as it may interfere with capillary electrophoresis. A new mutant Omni KlenTaq LA is marketed as an enzyme which is resistant to the inhibitory effects of fluorescent dyes. It would be beneficial to evaluate samples with this new form of taq polymerase to monitor the effects, if any; fluorescent powders and dyes may have on a profile.

Substrates in this work were limited due to amount of available resources. More work should be conducted to explore the effects of direct amplification on more common porous substrates. This is especially important in regards to the different types of paper which can be located within crime scenes. For example, thermal paper can be extremely problematic when determining what process to use for visualization of fingerprints and subsequent DNA analysis. Most thermal paper is composed of a solid-state mixture dye such as Yamamoto Blue (or other leuco dye) and needs an acid in order to change have a colour change reaction (Yamamoto et al., 2008). This type of paper can have an adverse reaction when exposed to Ninhydrin causing the paper to turn black thus destroying any type of fingerprint analysis and possible jeopardizing the chance of developing a DNA profile (Jasuja and Singh, 2009; Schwarz and Klenke, 2007).

Sequential processing is a technique often utilized to maximize the material left behind on a surface. Sequential processing involves using multiple viewing techniques and chemicals to optimize the chance of obtaining individualizing information from a piece of evidence (Bleay et al., 2012) Using multiple chemicals on a surface prior to swabbing for DNA analysis may complicate the ability to obtain a profile, even if the chemicals tested independently show no inhibition.

7.2 Conclusion

The PowerPlex[®] 18D system should be seriously considered for implementation into laboratory protocols. With reduced processing times, cost efficiency and providing results that supersede extraction-based methods, there is no reason not to consider the process.

PowerPlex[®] 18D has the ability to provide full and/or partial profiles of a good quality using reduced volume reactions for epithelial-cell-based samples which are exposed to latent fingerprint powders as well as single source blood samples which have been chemically enhanced on different substrates using leucocrystal violet, amido black and ninhydrin.

REFERENCES

FTA/FTA Elute Sample Collection Cards and Kits: Product Information 2011-last update [Homepage of General Electric], [Online]. Available:

http://www.gelifesciences.com/webapp/wcs/stores/servlet/catalog/en/GELifeSciences-us/products/AlternativeProductStructure_17096 [May 15, 2015].

ABI LIFE TECHNOLOGIES, 2011. *AmpFlSTR NGM PCR Amplification Kit: User's Manual*. USA: Life Technologies.

AKANE, A., 1998. Sex determination by PCR analysis of the X-Y amelogenin gene. *Methods in Molecular Biology*, **98**(7/29/2015), pp. 245-249.

AKANE, A., MATSUBARA, K., TAKAHASHI, S. and KIMURA, K., 1994. Identification of the heme compound copurified with deoxyribonucleic acid (DNA) from bloodstains, a major inhibitory of polymerase chain reaction (PCR) amplification. *Journal of Forensic Sciences*, **39**(2), pp. 362-372.

ALESSANDRINI, F., CECATI, M., PESARESI, M., TURCHI, C., CARLE, F. and TAGLIABRACCI, A., 2003. Fingerprints as evidence for a genetic profile: morphological study on fingerprints and analysis of exogenous and individual factors affecting DNA typing. *Journal of Forensic Sciences*, **48**(3), pp. 586-592.

ALLEN, R., POGEMILLER, J., JOSLIN, J., GULICK, M. and PRITCHARD, J., 2008. Identification through typing of DNA recovered from touch transfer evidence: parameters affecting yield of recovered human DNA. *Journal of Forensic Identification*, **58**(1), pp. 33-41.

ALLOR, C., EINUM, D.D. and SCARPETTA, M., 2005. Identification and characterization of variant alleles at CODIS STR loci. *Journal of Forensic Sciences*, **50**(5), pp. 1128-1133.

AL-SOUD, W.A. and RADSTROM, P., 2001. Purification and characterization of PCR-inhibitory components in blood cells. *Journal of Clinical Microbiology*, **39**(2), pp. 485-493.

ANDERSON, S., BANKIER, A.T., BARRELL, B.G., DE BRUIJN, M.H.L., COULSON, A.R., DROUIN, J., EPERON, I.C., NIERLICH, D.P., ROE, B.A., SANGER, F., SCHREIER, P.H., SMITH, A.J.H., STADEN, R. and YOUNG, I.G., 1981. Sequence and organization of the human mitochondrial genome. *Nature*, **290**(5806), pp. 457-465.

ARROWHEAD FORENSICS, 2015. *Zenith Magnetic Applicator*. Arrowhead Forensics Website: Company. [Online]. Available:

<http://www.crime-scene.com/store/brushes.shtml>[November 28, 2015].

AVWIORO, G., 2011. Histochemical uses of haematoxylin—a review. *Journal of Physics: Conference Series*, **1**, pp. 24-34.

BACHMANN, B., LUKE, W. and HUNSMANN, G., 1990. Improvement of PCR amplified DNA sequencing with the aid of detergents. *Nucleic Acids Research*, **18**(5), pp. 1309.

BAILES, S.M., DEVERS, J.J., KIRBY, J.D. and RHOADS, D.D., 2007. An inexpensive, simple protocol for DNA isolation from blood for high-throughput genotyping by polymerase chain reaction or restriction endonuclease digestion. *Poultry Science*, **86**(1), pp. 102-106.

BANDELT, H.J., KLOSS-BRANDSTATTER, A., RICHARDS, M.B., YAO, Y.G. and LOGAN, I., 2014. The case for the continuing use of the revised Cambridge Reference Sequence (rCRS) and the standardization of notation in human mitochondrial DNA studies. *Journal of Human Genetics*, **59**(2), pp. 66-77.

BARBARO, A., CORMACI, P. and AGOSTINO, A., 2011. Validation of AmpF ℓ STR NGM SELECT™ PCR amplification kit on forensic samples. *Forensic Science International: Genetics Supplement Series*, **3**(1), pp. e67-e68.

BARBARO, A., CORMACI, P. and VOTANO, S., 2011. Direct PCR by the AmpF ℓ STR NGM™ kit for database purpose. *Forensic Science International: Genetics Supplement Series*, **3**(1), pp. e103-e104.

- BARBER, M.D. and PARKIN, B.H., 1996. Sequence analysis and allelic designation of the two short tandem repeat loci D18S51 and D8S1179. *International Journal of Legal Medicine*, **109**(2), pp. 62-65.
- BARBUJANI, G., MAGAGNI, A., MINCH, E. and CAVALLI-SFORZA, L.L., 1997. An apportionment of human DNA diversity. *Proceedings of the National Academy of Sciences of the United States of America*, **94**(9), pp. 4516-4519.
- BARNI, F., LEWIS, S.W., BERTI, A., MISKELLY, G.M. and LAGO, G., 2007. Forensic application of the luminol reaction as a presumptive test for latent blood detection. *Talanta*, **72**(3), pp. 896-913.
- BEALE, S.C., 1998. Capillary Electrophoresis. *Analytical Chemistry*, **70**(12), pp. 279-300.
- BELLSTEDT, D.U., PIRIE, M.D., VISSER, J.C., DE VILLIERS, M.J. and GEHRKE, B., 2010. A rapid and inexpensive method for the direct PCR amplification of DNA from plants. *American Journal of Botany*, **97**(7), pp. e65-8.
- BELOTSEKOVSKII, B.P. and JOHNSTON, B.H., 1997. Denaturation and association of DNA sequences by certain polypropylene surfaces. *Analytical Biochemistry*, **251**(2), pp. 251-262.
- BERGERON, J., 2003. Development of bloody prints on dark surfaces with titanium dioxide and methanol. *Journal of Forensic Identification*, **53**(2), pp. 149-159.
- BEVEL, T. and GARDNER, R., 2008. *Bloodstain Pattern Analysis with an Introduction to Crime Scene Reconstruction*. 1 edn. Boca Raton, Florida: CRC Press.
- BEVER, B., GROSS, N. and CURRENCE, S., *DNA typing from chemically processed fingerprints*. Springfield, VA: Bode Technology Group.
- BHOELAI, B., DEJONG, B., DEPUIT, M. and SIJEN, T., 2011. Effect of common fingerprint detection techniques on subsequent STR profiling. *Forensic Science International: Genetics Supplement Series*, **3**, pp. e429-e430.

- BILLE, T.W., CROMARTIE, C. and FARR, M., 2009. Effects of cyanoacrylate fuming, time after recovery, and location of biological material on the recovery and analysis of DNA from post-blast pipe bomb fragments. *Journal of Forensic Sciences*, **54**(5), pp. 1059-1067.
- BLAKESLEY, R.W. and BOEZI, J.A., 1977. A new staining technique for proteins in polyacrylamide gels using coomassie brilliant blue G250. *Analytical Biochemistry*, **82**(2), pp. 580-582.
- BLEAY, S.M., SEARS, V.G., BANDEY, H.L., GIBSON, A.P., BOWMAN, V.J., DOWNHAM, R., FITZGERALD, L., CIUKSZA, T., RAMADANI, J. and SELWAY, C., 2012. *Fingerprint Source Book*. 1 edn. United Kingdom: Centre for Applied Science and Technology (CAST).
- BODZIAK, W., 1996. Use of leuco crystal violet to enhance shoe prints in blood. *Forensic Science International*, **82**(1), pp. 45-52.
- BOON, L.K., HITHAYA JEEVAN, N., PRIMULAPATHI, J.K., OTHMAN, M.I. and HIN, L.Y., 2006. Internal validation of the AmpF ℓ STR $^{\text{®}}$ Identifiler PCR $^{\text{®}}$ amplification kit on the ABI Prism $^{\text{®}}$ 3100 genetic analyzer for use in forensic casework at the Department of Chemistry, Malaysia. *International Congress Series*, **1288**, pp. 379-381.
- BOSSERS, L.C.A.M., ROUX, C., BELL, M. and MCDONAGH, A.M., 2011. Methods for the enhancement of fingermarks in blood. *Forensic Science International*, **210**(1-3), pp. 1-11.
- BOWDEN, A., FLEMING, R. and HARBISON, S., 2011. A method for DNA and RNA co-extraction for use on forensic samples using the Promega DNA IQ $^{\text{TM}}$ system. *Forensic Science International: Genetics*, **5**(1), pp. 64-68.
- BRIDGES, B., 1942. *Practical Fingerprinting*. 1 edn. New York, NY: Funk & Wagnalls.
- BRIGHT, J. and PETRICEVIC, S.F., 2004. Recovery of trace DNA and its application to DNA profiling of shoe insoles. *Forensic Science International*, **145**(1), pp. 7-12.

- BRINKMANN, B., KLINTSCHAR, M., NEUHUBER, F., HÜHNE, J. and ROLF, B., 1998. Mutation rate in human microsatellites: influence of the structure and length of the tandem repeat. *The American Journal of Human Genetics*, **62**(6), pp. 1408-1415.
- BUDOWLE, B., MORETTI, T., KEYS, K., KOONS, B. and SMERICK, J., 1997. Validation of the CTT STR Multiplex System. *Journal of Forensic Sciences*, **42**(4), pp. 701-707.
- BUDOWLE, B. and VAN DAAL, A., 2008. Forensically relevant SNP classes. *BioTechniques*, **44**(5), pp. 603-610.
- BUDOWLE, B., ALLARD, M.W., WILSON, M.R. and CHAKRABORTY, R., 2003. FORENSICS AND MITOCHONDRIAL DNA: Applications, Debates, and Foundations. *Annual Review of Genomics and Human Genetics*, **4**(1), pp. 119-141.
- BUDOWLE, B., MASIBAY, A., ANDERSON, S.J., BARNA, C., BIEGA, L., BRENNEKE, S., BROWN, B.L., CRAMER, J., DEGROOT, G.A., DOUGLAS, D., DUCEMAN, B., EASTMAN, A., GILES, R., HAMILL, J., HAASE, D.J., JANSSEN, D.W., KUPFERSCHMID, T.D., LAWTON, T., LEMIRE, C., LLEWELLYN, B., MORETTI, T., NEVES, J., PALASKI, C., SCHUELER, S., SGUEGLIA, J., SPRECHER, C., TOMSEY, C. and YET, D., 2001. STR primer concordance study. *Forensic Science International*, **124**(1), pp. 47-54.
- BUEL, E., WANG, G. and SCHWARTZ, M., 1995. PCR amplification of animal DNA with human X-Y amelogenin primers used in gender determination. *Journal of Forensic Sciences*, **40**(4), pp. 641-644.
- BURCKHARDT, J., 1994. Amplification of DNA from whole blood. *PCR methods and applications*, **3**(4), pp. 239-243.
- BUTLER, J. and REEDER, D., November 9, 2015, 2015-last update, Short Tandem Repeat DNA Internet DataBase [Homepage of National Institute for Standards and Technology], [Online]. Available: http://www.cstl.nist.gov/strbase/str_fact.htm [December 1, 2015].

- BUTLER, J.M., 2015. *Advanced Topics in Forensic DNA Typing: Interpretation*. 1 edn. Gaithersburg, Maryland: Elsevier.
- BUTLER, J.M., 2011. *Forensic DNA Typing: Methodology*. 1 edn. Gaithersburg, Maryland: Elsevier.
- BUTLER, J.M., 2006. Genetics and genomics of core short tandem repeat loci used in human identity testing. *Journal of Forensic Sciences*, **51**(2), pp. 253-265.
- BUTLER, J.M., 2005. *Forensic DNA Typing: Biology, Technology, and Genetics of STR Markers*. 2nd edn. New York: Elsevier Academic Press.
- BUTLER, J.M., BUEL, E., CRIVELLENTI, F. and MCCORD, B.R., 2004. Forensic DNA typing by capillary electrophoresis using the ABI Prism 310 and 3100 genetic analyzers for STR analysis. *Electrophoresis*, **25**(10-11), pp. 1397-1412.
- BUTLER, J.M., SHEN, Y. and MCCORD, B.R., 2003. The development of reduced size STR amplicons as tools for analysis of degraded DNA. *Journal of Forensic Sciences*, **48**(5), pp. 1054-1064.
- CAMDEN, S., January, 2009-last update, Obesity: an emerging concern for patients and nurses [Homepage of The Online Journal of Issues in Nursing], [Online]. Available: <http://www.nursingworld.org/MainMenuCategories/ANAMarketplace/ANAPeriodicals/OJIN/TableofContents/Vol142009/No1Jan09/Obesity-An-Emerging-Concern.aspx> [May 3, 2014].
- CHAKRABORTY, R., STIVERS, D., SU, B., ZHONG, Y. and BUDOWLE, B., 1999. *Electrophoresis*, (20), pp. 1682-1696.
- CHAMPOD, C., LENNARD, C., MARGOT, P. and STOILOVIC, M., 2004. *Fingerprints and other ridge skin impressions*. 1 edn. Boca Raton, Florida: CRC Press.
- COLLINS, J.R., STEPHENS, R.M., GOLD, B., LONG, B., DEAN, M. and BURT, S.K., 2003. An exhaustive DNA micro-satellite map of the human genome using high performance computing. *Genomics*, **82**(1), pp. 10-19.

COLLINS, P.J., HENNESSY, L.K., LEIBELT, C.S., ROBY, R.K., REEDER, D.J. and FOXALL, P.A., 2004. Developmental validation of a single-tube amplification of the 13 CODIS STR loci, D2S1338, D19S433, and amelogenin: the AmpF ℓ STR[®] Identifiler[®] PCR Amplification Kit. *Journal of Forensic Sciences*, **49**(6), pp. 1265-1277.

COMEY, C., KOONS, B., PRESLEY, K., SMERICK, J., SOBIERALSKI, C., STANLEY, D. and BAECHEL, F., 1994. DNA extraction strategies for amplified fragment length polymorphism analysis. *Journal of Forensic Sciences*, **39**(5), pp. 1254-1269.

COMPTÉ, N., BAILLY, B., DEBREUCKER, S., GORIELY, S. and PEPERSACK, T., 2015. Study of the association of total and differential white blood cell counts with geriatric conditions, cardio-vascular diseases, seric IL-6 levels and telomere length. *Experimental Gerontology*, **61**, pp. 105-112.

COTTER, S., 2001. *Hematology*. 1 edn. Jackson, Wyoming: Teton NewMedia.

COTTON, E.A., ALLSOP, R.F., GUEST, J.L., FRAZIER, R.R.E., KOUMI, P., CALLOW, I.P., SEAGER, A. and SPARKES, R.L., 2000. Validation of the AMPF ℓ STR[®] SGM Plus[®] system for use in forensic casework. *Forensic Science International*, **112**(2-3), pp. 151-161.

CULLEN, S., OTTO, A. and CHEETHAM, P., 2010. Chemical enhancement of bloody footwear impressions from buried substrates. *Journal of Forensic Identification*, **60**(1), pp. 45-86.

DALY, D.J., MURPHY, C. and MCDERMOTT, S.D., 2012. The transfer of touch DNA from hands to glass, fabric and wood. *Forensic Science International Genetics*, **6**(1), pp. 41-46.

DAVIS, C.P., KING, J.L., BUDOWLE, B., EISENBERG, A.J. and TURNBOUGH, M.A., 2012. Extraction platform evaluations: A comparison of Automate Express[™], EZ1[®] Advanced XL, and Maxwell[®] 16 Bench-top DNA extraction systems. *Legal Medicine*, **14**(1), pp. 36-39.

DEBRAUWERE, H., GENDREL, C.G., LECHAT, S. and DUTREIX, M., 1997. Differences and similarities between various tandem repeat sequences: minisatellites and microsatellites. *Biochimie*, **79**(9-10), pp. 577-586.

DEPARTMENT OF ENVIRONMENTAL SCIENCES, 2004. *Polymerase Chain Reaction (PCR)*. 1 edn. Toledo, Ohio: Laboratory for Environmental Pathogens Research, University of Toledo.

DILBECK, L., 2006. Use of bluestar forensic in lieu of luminol at crime scenes. *Journal of Forensic Identification*, **56**(5), pp. 706-720.

DIVNE, A. and ALLEN, M., 2005. A DNA microarray system for forensic SNP analysis. *Forensic Science International*, **154**(2-3), pp. 111-121.

DURRETT, R. and LIMIC, V., 2001. On the quantity and quality of single nucleotide polymorphisms in the human genome. *Stochastic Processes and their Applications*, **93**(1), pp. 1-24.

ECKERT, K. and KUNKEL, T., 1991. DNA polymerase fidelity and the polymerase chain reaction. *Genome Research*, **1**, pp. 17-24.

ELLEGREN, H., 2000. Heterogeneous mutation processes in human microsatellite DNA sequences. *Nature genetics*, **24**(4), pp. 400-402.

ELLEGREN, H., 2004. Microsatellites: simple sequences with complex evolution. *Nature Reviews Genetics*, **5**(6), pp. 435-445.

ENSENBERGER, M.G., THOMPSON, J., HILL, B., HOMICK, K., KEARNEY, V., MAYNTZ-PRESS, K.A., MAZUR, P., MCGUCKIAN, A., MYERS, J., RALEY, K., RALEY, S.G., ROTHOVE, R., WILSON, J., WIECZOREK, D., FULMER, P.M., STORTS, D.R. and KRENKE, B.E., 2010. Developmental validation of the PowerPlex[®] 16 HS System: An improved 16-locus fluorescent STR multiplex. *Forensic Science International: Genetics*, **4**(4), pp. 257-264.

EVIDENT, 2015. *Latent PRO- Fiberglass Brush*. ShopEvident. [Online]. Available: <https://www.shopevident.com/category/latent-fingerprints-1/latent-pro-8-fiberglass-brush> [December 1, 2015]

FARLEY, R. and ALBA, R., 2002. The New Second Generation in the United States. *International Migration Review*, **36**(3), pp. 669-701.

FARRUGIA, K., NICDAEID, N., SAVAGE, K. and BANDLEY, H., 2010. Chemical enhancement of footwear impressions in blood deposited on fabric-evaluating the use of alginate casting materials followed by chemical enhancement. *Science and Justice*, **50**(4), pp. 200-204.

FARRUGIA, K.J., BANDEY, H., SAVAGE, K. and NICDAÉID, N., 2013. Chemical enhancement of footwear impressions in blood on fabric — Part 3: Amino acid staining. *Science & Justice*, **53**(1), pp. 8-13.

FARRUGIA, K.J., SAVAGE, K.A., BANDEY, H. and NIC DAÉID, N., 2011. Chemical enhancement of footwear impressions in blood on fabric – Part 1: Protein stains. *Science & Justice*, **51**(3), pp. 99-109.

FOURNEY, R.M., BOWEN, K.L., FRÉGEAU, C.J. and LECLAIR, B., 2004. Systematic analysis of stutter percentages and allele peak height and peak area ratios at heterozygous STR loci for forensic casework and database samples. *Journal of Forensic Sciences*, **49**(5), pp. 1-13.

FOX, A., GITTO, M., HARBISON, S.A., FLEMING, R. and WIVELL, R., 2014. Exploring the recovery and detection of messenger RNA and DNA from enhanced fingermarks in blood. *Science & Justice*, **54**(3), pp. 192-198.

FRANK, W.E., LLEWELLYN, B.E., FISH, P.A., RIECH, A.K., MARCACCI, T.L., GANDOR, D.W., PARKER, D., CARTER, R.R. and THIBAUT, S.M., 2001. Validation of the AmpF ℓ STR Profiler Plus PCR amplification kit for use in forensic casework. *Journal of Forensic Sciences*, **46**(3), pp. 642-646.

FREGÉAU, C., BOWEN, K., LECLAIR, B., TRUDEL, I. and BISHOP, L., 2003. AmpF ℓ STR Profiler Plus short tandem repeat DNA analysis of casework samples, mixture samples, and nonhuman DNA samples amplified under reduced PCR volume conditions (25 μ l). *Journal of Forensic Sciences*, **48**(5), pp. 1014-1034.

FRÉGEAU, C.J., GERMAIN, O. and FOURNEY, R., 2000. Fingerprint enhancement revisited and the effects of blood enhancement chemicals on subsequent Profiler Plus TM fluorescent short tandem repeat DNA analysis of fresh and aged bloody fingerprints. *Journal of Forensic Sciences*, **45**(2), pp. 354-380.

FRÉGEAU, C.J., LETT, C.M. and FOURNEY, R.M., 2010. Validation of a DNA IQTM-based extraction method for TECAN robotic liquid handling workstations for processing casework. *Forensic Science International: Genetics*, **4**(5), pp. 292-304.

GAINES, M.L., WOJTKIEWICZ, P.W., VALENTINE, J.A. and BROWN, C.L., 2002. Reduced volume PCR amplification reactions using the AmpF ℓ STR Profiler Plus kit. *Journal of Forensic Sciences*, **47**(6), pp. 1224-1237.

GARDNER, R., 2012. *Practical Crime Scene Processing and Investigation*. 2 edn. Boca Raton, Florida: CRC Press.

GARNER, D.D., CANO, K.M., PEIMER, R.S. and YESHION, T.E., 1976. An evaluation of tetramethylbenzidine as a presumptive test for blood. *Journal of Forensic Sciences*, **21**(4), pp. 816-821.

GELFAND, D., STOFFEL, S., LAWYER, F. and SAIKI, R., 1989. *Purified thermostable enzyme*. US4889818 A edn. California, United States.

GILL, P., SPARKES, R. and KIMPTON, C., 1997. Development of guidelines to designate alleles using an STR multiplex system. *Forensic Science International*, **89**(3), pp. 185-197.

GILL, P., FEREDAY, L., MORLING, N. and SCHNEIDER, P.M., 2006. The evolution of DNA databases—recommendations for new European STR loci. *Forensic Science International*, **156**(2–3), pp. 242-244.

GINO, S. and OMEDEI, M., 2011. Effects of the most common methods for the enhancement of latent fingerprints on DNA extraction from forensic samples. *Forensic Science International: Genetics Supplement Series*, **3**(1), pp. e273-e274.

GOODWIN, W., LINACRE, A. and HADI, S., 2007. *An Introduction to Forensic Genetics*. 1 edn. West Sussex: Wiley.

GRAY, K., CROWLE, D. and SCOTT, P., 2014. Direct amplification of casework bloodstains using the Promega PowerPlex[®] 21 PCR Amplification System. *Forensic Science International: Genetics*, **12**, pp. 86-92.

GREENSPOON, S.A., MARCO A. SCARPETTA, M.A., DRAYTON, M.L. and TUREK, S.A., 1998. QIAamp spin columns as a for Forensic Casework. *Journal of Forensic Sciences*, **43**(5), pp. 1024-1030.

GRUBWIESER, P., THALER, A., KÖCHL, S., TEISSL, R., RABL, W. and PARSON, W., 2003. Systematic study on STR profiling on blood and saliva traces after visualization of fingerprint marks. *Journal of Forensic Sciences*, **48**(4), pp. 733-741.

GRUBWIESER, P., THALER, A., KOCHL, S., TEISSL, R., RABL, W. and PARSON, W., 2008. Systematic study on STR profiling on blood and saliva traces after visualization of fingerprints. *Journal of Forensic Sciences*, **48**(4), pp. 733-741.

GUBERNATOR, N., GUBERNATOR, K. and JAMES, C., 2015-last update, eMolecules. Available: <https://www.emolecules.com/> [March 13, 2015].

HANSON, E.K. and BALLANTYNE, J., 2005. Whole genome amplification strategy for forensic genetic analysis using single or few cell equivalents of genomic DNA. *Analytical Biochemistry*, **346**(2), pp. 246-257.

HAUZE, D.B., PETROVSKAIA, O., TAYLOR, B., JOULLIÉ, M.M., RAMOTOWSKI, R. and CANTU, A.A., 1998. 1,2-Indanediones: new reagents for visualizing the amino acid components of latent prints. *Journal of Forensic Sciences*, **48**(4), pp. 744-747.

HILL, C.R., DUEWER, D.L., KLINE, M.C., COBLE, M.D. and BUTLER, J.M., 2013. U.S. population data for 29 autosomal STR loci. *Forensic Science International: Genetics*, **7**, pp. e82-e83.

HILL, C.R., DUEWER, D.L., KLINE, M.C., SPRECHER, C.J., MCLAREN, R.S., RABBACH, D.R., KRENKE, B.E., ENSENBERGER, M.G., FULMER, P.M., STORTS, D.R. and BUTLER, J.M., 2011. Concordance and population studies along with stutter and peak height ratio analysis for the PowerPlex[®] ESX 17 and ESI 17 Systems. *Forensic Science International: Genetics*, **5**(4), pp. 269-275.

HINER, A.N., RAVEN, E.L., THORNELEY, R.N., GARCIA-CANOVAS, F. and RODRIGUEZ-LOPEZ, J.N., 2002. Mechanisms of compound I formation in heme peroxidases. *Journal of inorganic biochemistry*, **91**(1), pp. 27-34.

HOFFMAN, N.H. and FENGER, T., 2010. Validation of half-reaction amplification using Promega PowerPlex[®] 16. *Journal of Forensic Sciences*, **55**(4), pp. 1044-1049.

HOLLAND, M. and PARSONS, T., 1999. Mitochondrial DNA Sequences Analysis-Validation and Use for Forensic Casework. *Forensic Science Review*, **11**(21), pp. 22-50.

HOLT, C.L., BUONCRISTIANI, M., WALLIN, J.M., NGUYEN, T., LAZARUK, K.D. and WALSH, P.S., 2002. TWGDAM validation of AmpF ℓ STR PCR amplification kits for forensic DNA casework. *Journal of Forensic Sciences*, **47**(1), pp. 66-96.

INGRAM, V., November 1, 2007, 2007-last update, MIT Biology Hypertextbook. Available:<http://dwb4.unl.edu/chem/chem869k/chem869klinks/esg/www.mit.edu/esgbio/lm/nucleicacids/dna.html> [November 16, 2015].

INTEGRATED DNA TECHNOLOGIES, 2011-last update, The Polymerase Chain Reaction [Homepage of Integrated DNA Technologies], [Online]. Available: <http://www.idtdna.com/pages/docs/educational-resources/the-polymerase-chain-reaction.pdf> [June 17, 2015].

JAMES, S., KISH, P. and SUTTON, T., 2005. *Principles of Bloodstain Pattern Analysis: Theory and Practice*. 1 edn. Boca Raton, Florida: CRC Press.

- JASUJA, O.P. and SINGH, G., 2009. Development of latent fingermarks on thermal paper: Preliminary investigation into use of iodine fuming. *Forensic Science International*, **192**(1-3), pp. e11-e6.
- JEFFREYS, A., WILSON, A. and THEIN, S., 1985. Individual-specific 'fingerprint' of Human DNA. *Nature*, **316**, pp. 76-79.
- JEFFREYS, A.J., BROOKFIELD, J.F.Y. and SEMEONOFF, R., 1985. Positive identification of an immigration test-case using human DNA fingerprints. *Nature*, **317**(6040), pp. 818-819.
- JEFFREYS, A.J., WILSON, V. and THEIN, S.L., 1985. Hypervariable 'minisatellite' regions in human DNA. *Nature*, **314**(6006), pp. 67-73.
- JELLY, R., PATTON, E.L.T., LENNARD, C., LEWIS, S.W. and LIM (), K.F., 2009. The detection of latent fingermarks on porous surfaces using amino acid sensitive reagents: A review. *Analytica Chimica Acta*, **652**(1-2), pp. 128-142.
- JOBLING, M.A. and GILL, P., 2004. Encoded evidence: DNA in forensic analysis *Nature Reviews: Genetics*, **5**(10), pp. 739-751.
- KELLY, H., BRIGHT, J., CURRAN, J.M. and BUCKLETON, J., 2012. Modelling heterozygote balance in forensic DNA profiles. *Forensic Science International: Genetics*, **6**(6), pp. 729-734.
- KEMP, B., WINTERS, M., MONROE, C. and BARTA, J., 2014. How much DNA is lost? Measuring DNA loss of short tandem repeat length fragments targeted by the PowerPlex[®] 16 System using the Qiagen MinElute Purification Kit. *Human Biology*, **86**(4), pp. 313-329.
- KERMEKCHIEV, M.B., KIRILOVA, L.I., VAIL, E.E. and BARNES, W.M., 2009. Mutants of Taq DNA polymerase resistant to PCR inhibitors allow DNA amplification from whole blood and crude soil samples. *Nucleic acids research*, **37**(5), pp. e40.
- KLUG, W. and CUMMINGS, M., 2012. *Concepts of Genetics*. 10 edn. Upper Saddle River: Pearson Education.

KOTTE-MARCHANT, K. and DAVIS, B., eds, 2012. *Laboratory Hematology Practical*. 1 edn. Hoboken: Blackwell Publishing Ltd.

KRENKE, B.E., TEREBA, A., ANDERSON, S.J., BUEL, E., CULHANE, S., FINIS, C.J., TOMSEY, C.S., ZACHETTI, J.M., MASIBAY, A., RABBACH, D.R., AMIOTT, E.A. and SPRECHER, C.J., 2002. Validation of a 16-locus fluorescent multiplex system. *Journal of Forensic Sciences*, **47**(4), pp. 773-785.

KUCUKKAL, T., YANG, Y., CHAPMAN, S., CAO, W. and ALEXOV, E., 2014. Computational and experimental approaches to reveal the effects of single nucleotide polymorphisms with respect to disease diagnostics. *International Journal of Molecular Sciences*, **15**(6), pp. 9670-9717.

LAFOUNTAIN, M.J., SCHWARTZ, M.B., SVETE, P.A., WALKINSHAW, M.A. and BUEL, E., 2001. TWGDAM validation of the AmpF ℓ STR Profiler Plus and AmpF ℓ STR COfiler STR multiplex systems using capillary electrophoresis. *Journal of Forensic Sciences*, **46**(5), pp. 1191-1198.

LANDER, E.S., LINTON, L.M., BIRREN, B., NUSBAUM, C., ZODY, M.C., BALDWIN, J., DEVON, K., DEWAR, K., DOYLE, M., FITZHUGH, W., FUNKE, R., GAGE, D., HARRIS, K., HEAFORD, A., HOWLAND, J., KANN, L., LEHOCZKY, J., LEVINE, R., MCEWAN, P., MCKERNAN, K., MELDRIM, J., MESIROV, J.P., MIRANDA, C., MORRIS, W., NAYLOR, J., RAYMOND, C., ROSETTI, M., SANTOS, R., SHERIDAN, A., SOUGNEZ, C., STANGE-THOMANN, N., STOJANOVIC, N., SUBRAMANIAN, A., WYMAN, D., ROGERS, J., SULSTON, J., AINSCOUGH, R., BECK, S., BENTLEY, D., BURTON, J., CLEE, C., CARTER, N., COULSON, A., DEADMAN, R., DELOUKAS, P., DUNHAM, A., DUNHAM, I., DURBIN, R., FRENCH, L., GRAFHAM, D., GREGORY, S., HUBBARD, T., HUMPHRAY, S., HUNT, A., JONES, M., LLOYD, C., MCMURRAY, A., MATTHEWS, L., MERCER, S., MILNE, S., MULLIKIN, J.C., MUNGALL, A., PLUMB, R., ROSS, M., SHOWNKEEN, R., SIMS, S., WATERSTON, R.H., WILSON, R.K., HILLIER, L.W., MCPHERSON, J.D., MARRA, M.A., MARDIS, E.R., FULTON, L.A., CHINWALLA, A.T., PEPIN, K.H., GISH, W.R., CHISSOE, S.L., WENDL, M.C., DELEHAUNTY, K.D., MINER, T.L., DELEHAUNTY, A., KRAMER, J.B., COOK, L.L., FULTON, R.S., JOHNSON, D.L., MINX, P.J., CLIFTON, S.W., HAWKINS, T.,

BRANSCOMB, E., PREDKI, P., RICHARDSON, P., WENNING, S., SLEZAK, T., DOGGETT, N., CHENG, J., OLSEN, A., LUCAS, S., ELKIN, C., UBERBACHER, E., FRAZIER, M., GIBBS, R.A., MUZNY, D.M., SCHERER, S.E., BOUCK, J.B., SODERGREN, E.J., WORLEY, K.C., RIVES, C.M., GORRELL, J.H., METZKER, M.L., NAYLOR, S.L., KUCHERLAPATI, R.S., NELSON, D.L., WEINSTOCK, G.M., SAKAKI, Y., FUJIYAMA, A., HATTORI, M., YADA, T., TOYODA, A., ITOH, T., KAWAGOE, C., WATANABE, H., TOTOKI, Y., TAYLOR, T., WEISSENBACH, J., HEILIG, R., SAURIN, W., ARTIGUENAVE, F., BROTTIER, P., BRULS, T., PELLETIER, E., ROBERT, C., WINCKER, P., ROSENTHAL, A., PLATZER, M., NYAKATURA, G., TAUDIEN, S., RUMP, A., SMITH, D.R., DOUCETTE-STAMM, L., RUBENFIELD, M., WEINSTOCK, K., LEE, H.M., DUBOIS, J., YANG, H., YU, J., WANG, J., HUANG, G., GU, J., HOOD, L., ROWEN, L., MADAN, A., QIN, S., DAVIS, R.W., FEDERSPIEL, N.A., ABOLA, A.P., PROCTOR, M.J., ROE, B.A., CHEN, F., PAN, H., RAMSER, J., LEHRACH, H., REINHARDT, R., MCCOMBIE, W.R., DE LA BASTIDE, M., DEDHIA, N., BLÖCKER, H., HORNISCHER, K., NORDSIEK, G., AGARWALA, R., ARAVIND, L., BAILEY, J.A., BATEMAN, A., BATZOGLOU, S., BIRNEY, E., BORK, P., BROWN, D.G., BURGE, C.B., CERUTTI, L., CHEN, H., CHURCH, D., CLAMP, M., COPLEY, R.R., DOERKS, T., EDDY, S.R., EICHLER, E.E., FUREY, T.S., GALAGAN, J., GILBERT, J.G.R., HARMON, C., HAYASHIZAKI, Y., HAUSSLER, D., HERMJAKOB, H., HOKAMP, K., JANG, W., JOHNSON, L.S., JONES, T.A., KASIF, S., KASPRYZK, A., KENNEDY, S., KENT, W.J., KITTS, P., KOONIN, E.V., KORF, I., KULP, D., LANCET, D., LOWE, T.M., MCLYSAGHT, A., MIKKELSEN, T., MORAN, J.V., MULDER, N., POLLARA, V.J., PONTING, C.P., SCHULER, G., SCHULTZ, J., SLATER, G., SMIT, A.F.A., STUPKA, E., SZUSTAKOWKI, J., THIERRY-MIEG, D., THIERRY-MIEG, J., WAGNER, L., WALLIS, J., WHEELER, R., WILLIAMS, A., WOLF, Y.I., WOLFE, K.H., YANG, S., YEH, R., COLLINS, F., GUYER, M.S., PETERSON, J., FELSENFELD, A., WETTERSTRAND, K.A., MYERS, R.M., SCHMUTZ, J., DICKSON, M., GRIMWOOD, J., COX, D.R., OLSON, M.V., KAUL, R., RAYMOND, C., SHIMIZU, N., KAWASAKI, K., MINOSHIMA, S., EVANS, G.A., ATHANASIOU, M., SCHULTZ, R., PATRINOS, A. and MORGAN, M.J., 2001. Initial sequencing and analysis of the human genome. *Nature*, **409**(6822), pp. 860-921.

LANDERS, J., 1996. *Handbook of Capillary Electrophoresis*. 2 edn. Boca Raton, Florida: CRC Press.

LAURIN, N., DEMOORS, A. and FRÉGEAU, C., 2012. Performance of Identifiler[®] Direct and PowerPlex[®] 16 HS on the Applied Biosystems 3730 DNA Analyzer for processing biological samples archived on FTA cards. *Forensic Science International: Genetics*, **6**(5), pp. 621-629.

LAZARUK, K., WALSH, P.S., OAKS, F., GILBERT, D., ROSENBLUM, B.B., MENCHEN, S., SCHEIBLER, D., WENZ, H.M., HOLT, C. and WALLIN, J., 1998. Genotyping of forensic short tandem repeat (STR) systems based on sizing precision in a capillary electrophoresis instrument. *Electrophoresis*, **19**(1), pp. 86-93.

LEE, H. and GAENSSLEN, R., 2001. *Advances in Fingerprint Technology*. 2 edn. Boca Raton, Florida: CRC Press.

LEJA, D., June 12, 2010, 2010-last update, DNA Fingerprinting [Homepage of National Human Genome Research Institute], [Online]. Available: <https://www.genome.gov/dmd/img.cfm?node=Photos/Graphics&id=85150>[September 12, 2015].

LENNARD, C., 2001. The detection and enhancement of latent fingerprints, *13th INTERPOL Forensic Science Symposium, Lyon, France*, October 16-19, 2001 2001, Forensic Services, Australia Federal Police, pp. 1-14.

LENNARD, C., 2007. Fingerprint detection: current capabilities. *Australian Journal of Forensic Sciences*, **39**(2), pp. 55-71.

LENNARD, C., 2007. Fingerprint detection: future prospects. *Australian Journal of Forensic Sciences*, **39**(2), pp. 73-80.

LEVIN, B.C., CHENG, H. and REEDER, D.J., 1999. A Human Mitochondrial DNA Standard Reference Material for Quality Control in Forensic Identification, Medical Diagnosis, and Mutation Detection. *Genomics*, **55**(2), pp. 135-146.

LIN, B., TROMBLEY HALL, A., MCKAY ZOVANYI, A., CHRISTENSEN, D.R., KOEHLER, J.W. and DEVINS MINOGUE, T., 2013. Evaluation of inhibitor-resistant real-time PCR methods for diagnostics in clinical and environmental samples. *PLoS ONE*, **8**(9), pp. e73845.

LINACRE, A., PEKAREK, V., SWARAN, Y.C. and TOBE, S.S., 2010. Generation of DNA profiles from fabrics without DNA extraction. *Forensic Science International: Genetics*, **4**(2), pp. 137-141.

LINDNER, M., MANDREKAR, P.V., BESSETTI, J., NEWTON, C., MANKANI, B., KRUEGER, S. and KRUEGER, J., 2011. Improved performance for forensic casework: Extraction and isolation updates for the Maxwell[®] 16 instrument. *Forensic Science International: Genetics Supplement Series*, **3**(1), pp. e528-e529.

LOWE, A., MURRAY, C., WHITAKER, J., TULLY, G. and GILL, P., 2002. The propensity of individuals to deposit DNA and secondary transfer of low level DNA from individuals to inert surfaces. *Forensic Science International*, **129**(1), pp. 25-34.

LYGO, J.E., JOHNSON, P.E., HOLDAWAY, D.J., WOODROFFE, S., KIMPTON, C.P., GILL, P., WHITAKER, J.P. and CLAYTON, T.M., 1994. The validation of short tandem repeat (STR) loci for use in forensic casework. *International Journal of Legal Medicine*, **107**(2), pp. 77-89.

MANKEVICH, A., 2013-last update, Chemical Reagent Interactive Program [Homepage of Chesapeake Bay Division- International Association for Identification], [Online]. Available: <http://cbdiai.org/interactive-chemical-reagent-program> [July 30, 2012].

MARCHANT, B. and TAGUE, C., 2007. Developing fingerprints in blood: a comparison of several chemical techniques. *Journal of Forensic Identification*, **57**(1), pp. 76-93.

MASON, C., 2015-last update, Phenol-chloroform Extraction [Homepage of Weill Cornell Medical College], [Online]. Available: <http://physiology.med.cornell.edu/faculty/mason/lab/zumbo/files/PHENOL-CHLOROFORM.pdf> [February 22, 2015].

MATHEWS, C., VANHOLDE, K. and AHERN, K., 2000. *Biochemistry*. 3 edn. San Fransico, California: Benjamin Cummings.

MCCLINTOCK, J.T., 2014. *Forensic analysis of biological evidence: a laboratory guide for serological and DNA typing*. 1 edn. Boca Raton, Florida: CRC Press.

MCCUSKER, J., DAWSON, M.T., NOONE, D., GANNON, F. and SMITH, T., 1992. Improved method for direct PCR amplification from whole blood. *Nucleic Acids Research*, **20**(24), pp. 6747-6747.

MCNALLY, L., SHALER, R.C., BAIRD, M., BALAZS, I., DE FOREST, P. and KOBILINSKY, L., 1989. Evaluation of deoxyribonucleic acid (DNA) isolated from human bloodstains exposed to ultraviolet light, heat, humidity, and soil contamination. *Journal of Forensic Sciences*, **34**(5), pp. 1059-1069.

MEAKIN, G. and JAMIESON, A., 2013. DNA transfer: review and implications for casework. *Forensic Science International: Genetics*, **7**(4), pp. 434-443.

MERCIER, B., GAUCHER, C., FEUGEAS, O. and MAZURIER, C., 1990. Direct PCR from whole blood, without DNA extraction. *Nucleic Acids Research*, **18**(19), pp. 5908.

MEYERS, R., ed, 1995. *Molecular Biology and Biotechnology: A Comprehensive Desk Reference*. 1 edn. New York: VCH Publishers.

MILLER, A., 2013. Choosing the best fingerprint powder for your scene. *Evidence and Technology Magazine*, **11**(5), pp. 20-23.

MITSUHASHI, M., 1996. Technical report: Part 2. Basic requirements for designing optimal PCR primers. *Journal of Clinical Laboratory Analysis*, **10**(5), pp. 285-293.

MONTPETIT, S.A., FITCH, I.T. and O'DONNELL, P.T., 2005. A simple automated instrument for DNA extraction in forensic casework. *Journal of Forensic Sciences*, **50**(3), pp. 555-563.

MOORE, J., BLEAY, S.M., DEANS, J. and NICDAEID, N., 2008. Recovery of fingerprints from arson scenes: Part 2--fingerprints in blood. *Journal of Forensic Identification*, **58**(1), pp. 83-108.

- MORATA, P., QUEIPO-ORTUNO, M.I. and DE DIOS COLMENERO, J., 1998. Strategy for optimizing DNA amplification in a peripheral blood PCR assay used for diagnosis of human brucellosis. *Journal of clinical microbiology*, **36**(9), pp. 2443-2446.
- MORETTI, T.R., BAUMSTARK, A.L., DEFENBAUGH, D.A., KEYS, K.M., SMERICK, J.B. and BUDOWLE, B., 2001. Validation of short tandem repeats (STRs) for forensic usage: performance testing of fluorescent multiplex STR systems and analysis of authentic and simulated forensic samples. *Journal of Forensic Sciences*, **46**(3), pp. 647-660.
- MORF, N.V., SULZER, A., KRATZER, A. and BÄR, W., 2011. Internal validation of Tecan robots (Freedom EVO[®] 150 and 75) for PCR and capillary electrophoresis setup. *Forensic Science International: Genetics Supplement Series*, **3**(1), pp. e89-e90.
- MORIN, P.A., LUIKART, G., WAYNE, R.K. and THE SNP WORKSHOP GROUP, 2004. SNPs in ecology, evolution and conservation. *Trends in Ecology & Evolution*, **19**(4), pp. 208-216.
- MULERO, J.J., CHANG, C.W., LAGACE, R.E., WANG, D.Y., BAS, J.L., MCMAHON, T.P. and HENNESSY, L.K., 2008. Development and validation of the AmpF ℓ STR MiniFiler PCR amplification kit: a MiniSTR multiplex for the analysis of degraded and/or PCR inhibited DNA. *Journal of Forensic Sciences*, **53**(4), pp. 838-852.
- MULLIS, K., 1987. *Process of amplifying nucleic acid sequences*. 4,683,202 edn. United States.
- MULLIS, K. and FALOONA, F., 1987. Specific synthesis of DNA in vitro via polymerase-catalyzed chain reaction. *Methods in Enzymology*, **155**, pp. 335-350.
- MYERS, B., KING, J. and BUDOWLE, B., 2012. Evaluation and comparative analysis of direct amplification of STRs using PowerPlex[®] 18D and Identifiler[®] Direct systems. *Forensic Science International: Genetics*, **6**(5), pp. 640-645.
- NACHMAN, M.W. and CROWELL, S.L., 2000. Estimate of the mutation rate per nucleotide in humans. *Genetics*, **156**(1), pp. 297-304.

NADIR, E., MARGALIT, H., GALLILY, T. and BEN-SASSON, S.A., 1996. Microsatellite spreading in the human genome: evolutionary mechanisms and structural implications. *Proceedings of the National Academy of Sciences of the United States of America*, **93**(13), pp. 6470-6475.

NISHIMURA, N., NAKAYAMA, T., TONOIKE, H., KOJIMA, K. and KATO, S., 2000. Direct polymerase chain reaction from whole blood without DNA isolation. *Annals of Clinical Biochemistry*, **37** (Pt 5)(Pt 5), pp. 674-680.

NORLIN, S., NILSSON, M., HEDEN, P. and ALLEN, M., 2013. Evaluation of the impact of different visualization techniques on DNA in fingerprints. *Journal of Forensic Identification*, **63**(2), pp. 189-204.

OOSTDIK, K., ENSENBERGER, M., KRENKE, B.E., SPRECHER, C.J. and STORTS, D.R., 2011-last update, The PowerPlex[®] 18D System: A Direct-Amplification STR System with Reduced Thermal Cycling Time [Homepage of Promega Corporation Web site], [Online]. Available: <https://www.promega.com/resources/profiles-in-dna/2011/the-powerplex-18d-system-a-direct-amplification-str-system-with-reduced-thermal-cycling-time/?activeTab=0> [June 13, 2012].

OOSTDIK, K., FRENCH, J., YET, D., SMALLING, B., NOLDE, C., VALLONE, P.M., BUTTS, E.L.R., HILL, C.R., KLINE, M.C., RINTA, T., GEROW, A.M., ALLEN, S.R., HUBER, C.K., TESKE, J., KRENKE, B., ENSENBERGER, M., FULMER, P. and SPRECHER, C., 2013. Developmental validation of the PowerPlex[®] 18D System, a rapid STR multiplex for analysis of reference samples. *Forensic Science International: Genetics*, **7**(1), pp. 129-135.

PARK, S.J., KIM, J.Y., YANG, Y.G. and LEE, S.H., 2008. Direct STR amplification from whole blood and blood- or saliva-spotted FTA without DNA purification. *Journal of Forensic Sciences*, **53**(2), pp. 335-341.

PATEL, J., SHAIKN, M. and DARSHAN, M., 2014. Forensic Conception: DNA typing of FTA Spotted Samples. *Journal of Applied Biology and Biotechnology*, **2**(4), pp. 21-29.

PRASKA, N. and LANGENBURG, G., 2013. Reactions of latent prints exposed to blood. *Forensic Science International*, **224**(1–3), pp. 51-58.

PROMEGA CORPORATION, 2015. *Swab Solution Kit, Instructions for Use of Product (DC8271)*. 3 edn. Madison, Wisconsin: Promega Corporation.

PROMEGA CORPORATION, 2014. *PowerPlex[®] 16HS, Instructions for Use of Product (DC2100 & DC2101)*. 5 edn. Madison, Wisconsin: Promega Corporation.

PROMEGA CORPORATION, 2014. *PowerPlex[®] 18D, Instructions for Use of Product (DC1802 & DC1808)*. 3 edn. Madison, Wisconsin: Promega Corporation.

QIAGEN, 2011. *QIAamp DNA Mini Kit and QIAamp DNA Blood Mini Kit Handbook*. Qiagen.

QUINONES, I. and DANIEL, B., 2012. Cell free DNA as a component of forensic evidence recovered from touched surfaces. *Forensic science International: Genetics*, **6**(1), pp. 26-30.

RALSER, M., QUERFURTH, R., WARNATZ, H., LEHRACH, H., YASPO, M. and KROBITSCH, S., 2006. An efficient and economic enhancer mix for PCR. *Biochemical and biophysical research communications*, **347**(3), pp. 747-751.

RAYMOND, J., ROUX, C., DU PASQUIER, E., SUTTON, J. and LENNARD, C., 2004. Effect of common fingerprint detection techniques on the DNA typing of fingerprints deposited on different surfaces. *Journal of Forensic Identification*, **54**(1), pp. 22-44.

RAYMOND, J.J., VAN OORSCHOT, R.A., GUNN, P.R., WALSH, S.J. and ROUX, C., 2009. Trace evidence characteristics of DNA: A preliminary investigation of the persistence of DNA at crime scenes. *Forensic Science International: Genetics*, **4**(1), pp. 26-33.

REECE, J., URRY, L., CAIN, M., WASSERMAN, S., MINORSKY, P. and JACKSON, R., 2010. *Campbell Biology*. 9 edn. New York, NY: Pearson.

REEDER, D.J., 1999. Impact of DNA typing on standards and practice in the forensic community. *Archives of Pathology & Laboratory Medicine*, **123**(11), pp. 1063-1065.

- ROBERTSON, J.M. and WALSH-WELLER, J., 1998. An introduction to PCR primer design and optimization of amplification reactions. *Forensic DNA Profiling Protocols*. 1 edn. Methods in Molecular Biology, pp. 121-154.
- ROEWER, L., 2013. DNA fingerprinting in forensics: past, present, future. *Investigative Genetics*, **4**(1), pp. 22-2223-4-22.
- ROUX, C., GILL, K., SUTTON, J. and LENNARD, C., 1999. Further study to investigate the effect of fingerprint enhancement techniques on the DNA analysis of bloodstains. *Journal of Forensic Identification*, **49**(4), pp. 357-376.
- RUITBERG, C.M., REEDER, D.J. and BUTLER, J.M., 2001. STRBase: a short tandem repeat DNA database for the human identity testing community. *Nucleic Acids Research*, **29**(1), pp. 320-322.
- RUSSELL, P., 2010. *The History of Mexico: From Pre-Conquest to Present*. New York, NY: Routledge.
- SAFERSTEIN, R., 2005. *Forensic Science Handbook*. Upper Saddle River, NJ: Prentice Hall.
- SAIKI, R., SCHARF, S., FALOONA, F., MULLIS, K., HORN, G., ERLICH, H. and ARNHEIM, N., 1985. Enzymatic amplification of beta-globin genomic sequences and restriction site analysis for diagnosis of sickle cell anemia. *Science*, **230**(4732), pp. 1350-1354.
- SAIKI, R., GELFAND, D., STOFFEL, S., SCHARF, S., HIGUCHI, R., HORN, G., MULLIS, K. and ERLICH, H., 1988. Primer-directed enzymatic amplification of DNA with a thermostable DNA polymerase. *Science*, **239**(4839), pp. 487-491.
- SCHERCZINGER, C.A., BOURKE, M.T., LADD, C. and LEE, H.C., 1997. DNA extraction from liquid blood using QIAamp. *Journal of Forensic Sciences*, **42**(5), pp. 893-896.

SCHNOOR, M., VOSS, P., CULLEN, P., BÖKING, T., GALLA, H.J., GALINSKI, E.A. and LORKOWSKI, S., 2004. Characterization of the synthetic compatible solute homoectoine as a potent PCR enhancer. *Biochemical and Biophysical Research Communications*, **322**(3), pp. 867-872.

SCHULZ, M.M., WEHNER, H.-., REICHERT, W. and GRAW, M., 2004. Ninhydrin-dyed latent fingerprints as a DNA source in a murder case. *Journal of Clinical Forensic Medicine*, **11**(4), pp. 202-204.

SCOTT AND WHITE HOSPITAL, 03/11/2013, 03/11/2013-last update, Hemoglobin Variants [Homepage of ExitCare® Patient Information ©2014 ExitCare, LLC.], [Online]. Available: <http://www.sw.org/misc/health/Hemoglobin%20Variants.html> [02/05, 2015].

SEARS, V., BUTCHER, C. and FITZGERALD, L., 2005. Enhancement of fingerprints in blood part 3: reactive techniques, acid yellow 7, and process sequences. *Journal of Forensic Identification*, **55**(6), pp. 741-786.

SEARS, V., BUTCHER, C. and PRIZEMAN, T., 2001. Enhancement of fingerprints in blood-part2: protein dyes. *Journal of Forensic Identification*, **51**(1), pp. 28-38.

SEARS, V. and PRIZEMAN, T., 2000. Enhancement of fingerprints in blood part 1: The optimization of amido black. *Journal of Forensic Identification*, **50**(5), pp. 470-480.

SEWELL, J., QUINONES, I., AMES, C., MULTANEY, B., CURTIS, S., SEEBORUTH, H., MOORE, S. and DANIEL, B., 2008. Recovery of DNA and fingerprints from touched documents. *Forensic Science International: Genetics*, **2**(4), pp. 281-285.

SHEWALE, J. and LIU, R., eds, 2014. *Forensic DNA Analysis: Current Practices and Emerging Technologies*. Boca Raton, Florida: CRC Press.

SHRIVER, M.D., JIN, L., BOERWINKLE, E., DEKA, R., FERRELL, R.E. and CHAKRABORTY, R., 1995. A novel measure of genetic distance for highly polymorphic tandem repeat loci. *Molecular biology and evolution*, **12**(5), pp. 914-920.

SILVA, D.A., CAVALCANTI, P., FREITAS, H. and DE CARVALHO, E.F., 2013. High quality DNA from human remains obtained by using the Maxwell[®] 16 automated methodology. *Forensic Science International: Genetics Supplement Series*, **4**(1), pp. e248-e249.

SLATER, G.W., KENWARD, M., MCCORMICK, L.C. and GAUTHIER, M.G., 2003. The theory of DNA separation by capillary electrophoresis. *Current opinion in biotechnology*, **14**(1), pp. 58-64.

SODHI, G.S. and KAUR, J., 2001. Powder method for detecting latent fingerprints: a review. *Forensic Science International*, **120**(3), pp. 172-176.

SPATHIS, R. and LUM, J.K., 2008. An updated validation of Promega's PowerPlex[®] 16 System: high throughput databasing under reduced PCR volume conditions on Applied Biosystem's 96 capillary 3730xl DNA Analyzer. *Journal of Forensic Sciences*, **53**(6), pp. 1353-1357.

SPEAR, T., KHOSHKEBARI, N., CLARK, J. and MURPHY, M., 2002. Summary of experiments investigating the impact of fingerprint processing and fingerprint reagents on PCR-based DNA typing profiles, May 2002, California Association of Criminalistics News, pp. 1-6.

STANGEGAARD, M., FERRERO-MILIANI, L., BØRSTING, C., FRANK-HANSEN, R., HANSEN, A.J. and MORLING, N., 2011. Repeated extraction of DNA from FTA cards. *Forensic Science International: Genetics Supplement Series*, **3**(1), pp. e345-e346.

STANGEGAARD, M., FRØSLEV, T.G., FRANK-HANSEN, R., LAURSEN, S.S., JØRGENSEN, M., HANSEN, A.J. and MORLING, N., 2009. Automated extraction of DNA and PCR setup using a Tecan Freedom EVO[®] liquid handler. *Forensic Science International: Genetics Supplement Series*, **2**(1), pp. 74-76.

STEIN, C., KYECK, S.H. and HENSSGE, C., 1996. DNA typing of fingerprint reagent treated biological stains. *Journal of Forensic Sciences*, **41**(6), pp. 1012-1017.

STOILOVIC, M. and LENNARD, C., 2010. *Workshop manual: Fingerprint detection and enhancement*. 1 edn. Canberra: National Centre for Forensic Studies.

SWARAN, Y.C. and WELCH, L., 2012. A comparison between direct PCR and extraction to generate DNA profiles from samples retrieved from various substrates. *Forensic Science International: Genetics*, **6**(3), pp. 407-412.

SWEET, D., LORENTE, M., LORENTE, J.A., VALENZUELA, A. and VILLANUEVA, E., 1997. An improved method to recover saliva from human skin: the double swab technique. *Journal of Forensic Sciences*, **42**(2), pp. 320-322.

TACK, L.C., THOMAS, M. and REICH, K., 2007. Automated forensic DNA purification optimized for FTA card punches and Identifiler[®] STR-based PCR analysis. *Clinics in Laboratory Medicine*, **27**(1), pp. 183-191.

TAN, S.C. and YIAP, B.C., 2009. DNA, RNA, and protein extraction: the past and the present. *Journal of Biomedicine and Biotechnology*, **2009**(574398), pp. 1-10.

TEMPLETON, J., TAYLOR, D., HANDT, O., SKUZA, P. and LINACRE, A., 2015. Direct PCR improves the recovery of DNA from various substrates. *Journal of Forensic Sciences*, **60**(6), pp. 1558-1562.

THEEUWEN, A.B.E., VAN BARNEVELD, S., DROK, J.W., KEEREWEER, I., LIMBORGH, J.C.M., NABER, W.M. and VELDERS, T., 1998. Enhancement of footwear impressions in blood. *Forensic Science International*, **95**(2), pp. 133-151.

THERMO FISHER SCIENTIFIC, 2010. *Nucleic Acid*. 1 edn. Wilmington, Delaware: Thermo Fisher Scientific.

THERMO FISHER SCIENTIFIC, 2009. *NanoDrop 2000/2000c Spectrophotometer: User Manual*. 1 edn. Wilmington, Delaware: Thermo Fisher Scientific.

THERMO FISHER SCIENTIFIC, 2007. *Technical Support Bulletin: 260/280 and 260/230 Ratios NanoDrop ND-1000 and ND-8000 8-Sample Spectrophotometers*. 1 edn. Wilmington, Delaware: Thermo Fisher Scientific.

THOMAS, G.L., 1978; 2001. The physics of fingerprints and their detection. *Journal of Physics E: Scientific Instruments*, **11**(8), pp. 722-731.

THOMAS, G.L. and REYNOLDSON, T.E., 1975; 2001. Some observations on fingerprint deposits. *Journal of Physics D: Applied Physics*, **8**(6), pp. 724-729.

THOMAS, P. and FARRUGIA, K., 2013. An investigation into the enhancement of fingermarks in blood on paper with genipin and lawsone. *Science & Justice*, **53**(3), pp. 315-320.

TINDALL, K.R. and KUNKEL, T.A., 1988. Fidelity of DNA synthesis by the *Thermus aquaticus* DNA polymerase. *Biochemistry*, **27**(16), pp. 6008-6013.

TOBE, S.S., WATSON, N. and DAÉID, N.N., 2007. Evaluation of six presumptive tests for blood, their specificity, sensitivity, and effect on high molecular-weight DNA. *Journal of Forensic Sciences*, **52**(1), pp. 102-109.

TOZZO, P., GIULIODORI, A., RODRIGUEZ, D. and CAENAZZO, L., 2014. Effect of dactyloscopic powders on DNA profiling from enhanced fingerprints: results from an experimental study. *The American Journal of Forensic Medicine and Pathology*, **35**(1), pp. 68-72.

VALLONE, P., HILL, C. and BUTTS, L., 2011. Direct PCR amplification of STR loci: protocols and performance, September 3 2011, National Institute for Standards and Technology, pp. 1.

VALLONE, P.M. and BUTLER, J.M., 2004. AutoDimer: a screening tool for primer-dimer and hairpin structures. *BioTechniques*, **37**(2), pp. 226-231.

VALLONE, P.M., HILL, C.R. and BUTTS, E.L.R., 2011. Concordance study of direct PCR kits: PowerPlex[®] 18D and Identifiler[®] Direct. *Forensic Science International: Genetics Supplement Series*, **3**(1), pp. e353-e354.

VAN OORSCHOT, R. and JONES, M., 1997. DNA fingerprints from fingerprints. *Nature*, **387**, pp. 767.

VAN OORSCHOT, R.A., BALLANTYNE, K.N. and MITCHELL, R.J., 2010. Forensic trace DNA: a review. *Investigative Genetics*, **1**(1), pp. 14-2223-1-14.

VAN OORSCHOT, R.A.H., PHELAN, D.G., FURLONG, S., SCARFO, G.M., HOLDING, N.L. and CUMMINS, M.J., 2003. Are you collecting all the available DNA from touched objects?. *International Congress Series*, **1239**, pp. 803-807.

VANDENBERG, N., VAN OORSCHOT, R.A.H. and MITCHELL, R.J., 1997. An evaluation of selected DNA extraction strategies for short tandem repeat typing. *Electrophoresis*, **18**(9), pp. 1624-1626.

VANHOOFSTAT, D.E.O., DEFORCE, D.L.D., HUBERT DE PAUW, I.P. and VAN DEN EECKHOUT, E.G., 1999. DNA typing of fingerprints using capillary electrophoresis: effect of dactyloscopic powders. *Electrophoresis*, **20**(14), pp. 2870-2876.

VIRKLER, K. and LEDNEV, I.K., 2009. Analysis of body fluids for forensic purposes: from laboratory testing to non-destructive rapid confirmatory identification at a crime scene. *Forensic Science International*, **188**(1-3), pp. 1-17.

VOLKER, N., REINHARD, S. and HANSJÖRG, E., 1985. Clear background and highly sensitive protein staining with coomassie blue dyes in polyacrylamide gels: a systematic analysis. *Electrophoresis*, **6**(9), pp. 427-448.

WADE, D.C., 2002. Development of latent prints with titanium dioxide (TiO₂). *Journal of Forensic Identification*, **52**(5), pp. 551-559.

WALKER, C. and CRAM, I., 1990. DNA profiling and police powers. *Criminal Law Review*, pp. 479-493.

WALLACE-KUNKEL, C., LENNARD, C., STOILOVIC, M. and ROUX, C., 2007. Optimisation and evaluation of 1,2-indanedione for use as a fingermark reagent and its application to real samples. *Forensic Science International*, **168**(1), pp. 14-26.

WANG, D.Y., CHANG, C., LAGACÉ, R.E., OLDROYD, N.J. and HENNESSY, L.K., 2011. Development and validation of the AmpF ℓ STR[®] Identifier[®] Direct PCR amplification kit: a multiplex assay for the direct amplification of single-source samples. *Journal of Forensic Sciences*, **56**(4), pp. 835-845.

- WANG, D.Y., CHANG, C., OLDROYD, N.J. and HENNESSY, L.K., 2009. Direct amplification of STRs from blood or buccal cell samples. *Forensic Science International: Genetics Supplement Series*, **2**(1), pp. 113-114.
- WATSON, J. and CRICK, F., 1953. Molecular Structure of Nucleic Acids. *Nature*, **171**, pp. 737-738.
- WEBER, J.L. and WONG, C., 1993. Mutation of human short tandem repeats. *Human Molecular Genetics*, **2**(8), pp. 1123-1128.
- WEISNER, S., SPRINGER, E., SASSON, Y. and ALMOG, J., 2001. Chemical development of latent fingerprints: 1,2-indanedione has come of age. *Journal of Forensic Sciences*, **46**(5), pp. 1082-1084.
- WILSHIRE, B., 1996. Advances in fingerprint detection. *Endeavour*, **20**(1), pp. 12-15.
- WILSON, M.R., DIZINNO, J.A., POLANSKEY, D., REPLOGLE, J. and BUDOWLE, B., 1995. Validation of mitochondrial DNA sequencing for forensic casework analysis. *International Journal of Legal Medicine*, **108**(2), pp. 68-74.
- WIRSTAM, M., BLOMBERG, M. and SIEGBAHN, P., 1999. Reaction Mechanism of Compound I formation in heme peroxidases: a density functional theory study. *Journal of the American Chemical Society*, **121**(43), pp. 10178-10185.
- YAMAMOTO, S., FURUYA, H., TSUTSUI, K., UENO, S. and SATO, K., 2008. In situ observation of thermochromic behavior of binary mixtures of phenolic long-chain molecules and fluoran dye for rewritable paper application. *Crystal Growth & Design*, **8**(7), pp. 2256-2263.
- YANG, Y.G., KIM, J.Y., SONG, Y. and KIM, D., 2007. A novel buffer system, AnyDirect, can improve polymerase chain reaction from whole blood without DNA isolation. *Clinica Chimica Acta*, **380**(1-2), pp. 112-117.
- YANG, Y., KIM, J., SOH, M. and KIM, D., 2007. A simple and rapid gene amplification from arabidopsis leaves using AnyDirect System. *Journal of Biochemistry and Molecular Biology*, **40**(3), pp. 444-447.

ZHANG, Z., KERMEKCHIEV, M.B. and BARNES, W.M., 2010. Direct DNA amplification from crude clinical samples using a PCR enhancer cocktail and novel mutants of *Taq*. *The Journal of Molecular Diagnostics*, **12**(2), pp. 152-161.

ZOPPIS, S., MUCIACCIA, B., D'ALESSIO, A., ZIPARO, E., VECCHIOTTI, C. and FILIPPINI, A., 2014. DNA fingerprinting secondary transfer from different skin areas: morphological and genetic studies. *Forensic Science International: Genetics*, **11**, pp. 137-143.

Appendix

The following Appendices are found in this section:

- Appendix 1:** Materials and Equipment Used
- Appendix 2:** Reagent Preparation
- Appendix 3:** Raw Data/ Statistical Analysis Information
- Appendix 4:** Human DNA Profiles
- Appendix 5:** Partial Profiles Generated using PowerPlex[®] 16HS
- Appendix 6:** Consent Forms
- Appendix 7:** Quantitation (Concordance Study Samples)
- Appendix 8:** Summary of Loci
- Appendix 9:** Allele Frequency and Comparison Charts

Appendix 1: Material and Equipment Used

The following is a list of materials and equipment that were used during the project and their respective supplier. (A1.1)

Materials	Supplier
• 3500 Running Buffer, 10X	Applied Biosystems
• 3130 Running Buffer, 10X	Applied Biosystems
• Omni swabs	Whatman
• Laminate tile flooring (black and white)	Hampton Bay
<ul style="list-style-type: none"> • Fingerprint Powder <ul style="list-style-type: none"> - Standard black powder - Magnetic flake powder - Standard white powder 	K9 Forensics, UK
• Bleach	Domestos
• Raw Wood	Home Base
• Lead	Home Base
• Gypsum Board	Home Base
• Decon [®] 90	Appleton Woods
• DNA 2800M	Promega
• Acetate sheets	Grafix
• Wooden handle sterile swabs	
• Leucocrystal Violet	Evident, USA
• Ethanol (absolute)	Sigma Aldrich
• Ninhydrin	Sigma Aldrich
• Formamide	Applied Biosystem
• Microscope slides	Fisherbrand

Materials**Supplier**

- Promega® PowerPlex® 16hs™ kit, containing: Promega
 - Promega® PowerPlex® 16hs™ Reaction Mix
 - Promega® PowerPlex® 16hs™ Primer Mix
 - Promega® PowerPlex® 16hs™ Control DNA 2800M
 - Promega® PowerPlex® 16hs™ Allelic Ladder

- Promega® PowerPlex® 18d kit, containing: Promega
 - Promega® PowerPlex® 18d Reaction Mix
 - Promega® PowerPlex® 18d Primer Mix
 - Promega® PowerPlex® 18d Control DNA 2800M
 - Promega® PowerPlex® 18d Allelic Ladder

- Hi-Di Formamide Applied Biosystems

- Isopropanol Sigma Aldrich

- POP-6™ Polymer Applied Biosystems

- Amido Black 2x Solution Sigma Aldrich

- QIAamp® DNA Mini Kit, containing: Qiagen
 - QIAamp Mini Spin Columns
 - Buffer AL
 - Buffer AW 1
 - Buffer AW 2
 - Buffer AE

Equipment	Supplier
<ul style="list-style-type: none"> • ABI 3500 Genetic Analyzer set up with Data Collection and GeneMapper[®] ID-X. 	Applied Biosystems
<ul style="list-style-type: none"> • ABI 3130 Genetic Analyzer setup with Data Collection and GeneMapper[®] v2.0. 	Applied Biosystems
<ul style="list-style-type: none"> • Centrifuge 	Eppendorf
<ul style="list-style-type: none"> • 9700 Thermocycler 	Applied Biosystems
<ul style="list-style-type: none"> • Incubator 	Gallenkamp
<ul style="list-style-type: none"> • Microcentrifuge tubes (1.5 ml) 	ABgene
<ul style="list-style-type: none"> • Eclipse E200 Microscope 	Nikon
<ul style="list-style-type: none"> • PCR tubes (300µl) 	ABgene
<ul style="list-style-type: none"> • Pipettes (0.1-2 µl, 2-20 µl, 20-200 µl, 200-1000 µl) 	Nichipet EX

Appendix 2: Reagent Preparation

The following section describes the preparation of the reagents used during this project.

Preparation of Amido Black Solution

Amido Black Staining Solution 2X (Sigma-Aldrich®) was combined with deionized water to a final volume of 500 ml per the manufacturer's instructions. At the final volume the solution contained 0.1% (w/v) Amido Black, 25% (v/v) isopropanol, and 10% (v/v) acetic acid.

Phosphate-buffered Saline

A 10X solution of PBS was made by dissolving 80g of NaCl, 2.0g of KCl, 14.4g of Na₂HPO₄, 2.4g of KH₂PO₄ with 800ml distilled H₂O. The pH was then adjusted to 7.4 and the volume increased to 1L with additional distilled H₂O. For each experiment bottle of PBS 1X was made by diluting the 10X solution to 1:10.

Haematoxylin and Eosin Staining Reagents

Ehrlich's haematoxylin: Haematoxylin 6g; Absolute alcohol 300ml; Distilled water 300ml; Glycerol 300ml; Glacial acetic acid 30ml; Potassium alum- in excess

Dissolve haematoxylin in alcohol, and then add components in order. Add potash alum until a few crystals remain undissolved.

Acid Alcohol: 1ml conc HCl in 99ml 70% alcohol.

Alcoholic eosin: 0.5% eosin in 90% ethanol.

Scott's tap water: Sodium bicarbonate 3.5g; Magnesium sulphate 20g; Tap water 1000ml; Thymol crystal (preservative).

Appendix 3: Raw Data

This section addresses the information and outline of the data contained on the additional digital drive. It should be noted for the purposes of the data analysis ‘saliva’ refers to the epithelial cell samples and ‘stock’/’neat’ refers to the x1 dilutions as reported in the write-up.

All Chapters: Quantitation Data

Chapter 3: Sensitivity Study

- Minitab Project
 - *Data Sensitivity*
- Excel Spread sheets:
 - Blood Dilutions_16HS & Blood Dilutions_18D
 - Full vs. Half Reactions_16HS & Full vs. Half Reactions_18D
 - Saliva Dilutions_16HS & Saliva Dilutions_18D

Chapter 5: Evaluation of Epithelial Cell Samples Processed with Powder

- Minitab Project
 - *Data Powder*
- Excel Spread sheets:
 - Powder_16HS & Powder_18D

Chapter 6: Evaluation of Blood Samples Enhanced with Chemicals

- Minitab Projects
 - *Data Amido Black*
 - *Data LCV*
 - *Data Ninhydrin*
 - *Data Combined*
- Excel Spread sheets:
 - Amido Black_16HS & Amido Black_18D
 - LCV_16HS & LCV_18D
 - Ninhydrin_16HS & Ninhydrin_18D

Appendix 4: Genotypes of Human DNA

This section lists the known genotypes for profiles used in this project.

Table A4.1: Known genetic profiles used throughout the project.

	D 3 S 1 3 5 8	T H 0 1	D 2 1 S 1 1	D 1 8 S 5 1	P E N T A E	D 5 S 8 1 8	D 1 3 S 3 1 7	D 7 S 8 2 0	D 1 6 S 5 3 9	C S F 1 P O	P E N T A D	A M E L	V W A	D 8 S 1 1 7 9	T P O X	F G A	D 1 9 S 4 3 3	D 2 S 1 3 3 8
Sample																		
2800M	17,18	6,9.3	29,31.2	16,18	7,14	12	9,11	8,11	9,13	12	12,13	X,Y	16,19	14,15	11	20,23	13,14	22,25
A	15,18	9.3	30,32.2	15,19	11,13	10,13	8,11	9,10	11	9,12	9,10	X	17,18	11,16	11	22,24	13,14	19,21
B	17,18	7	30.2,32.2	14,19	7,17	11	11,13	8,10	11	10,11	12	X	14	12	11	22,24	15	17,25

Appendix 5: Partial Profiles Generated using Promega® PowerPlex® 16HS

The following section represents the status of the partial profiles generated by PowerPlex® 16HS for the Concordance Study (*Chapter 4*). (PP#= Partial profile# loci present). (A5.1)

<i>Sample</i>	<i>Status of Profile</i>	<i>1 of 2 Alleles</i>	<i>No Alleles</i>
23M	PP#12	D5, FGA	D18, CSF
26M	PP#12		D18, CSF, Penta E, D16
28M	PP#13	FGA	D18, CSF
29M	PP#7	D21, D16, D13, Penta D	D18, CSF, Penta E, FGA, TPOX
30M	PP#3		D18, D21, Penta E, CSF, D5, D13, D7, D16, Penta D, vWA, D8, FGA
32M	PP#2	D3, TH01, D5, D7	D18, D21, Penta E, CSF, D16, Penta D, vWA, D8, FGA
33M	PP#7	Penta E, Penta D, D16	D18, D21, D7, CSF, D8, FGA
35M	PP#8	D13, D16, Penta D	D18, CSF, FGA, Penta E
36M	PP#11	D18, Penta E, Penta D, FGA	CSF
37M	PP#8	D13, Penta D, TPOX, FGA	D18, Penta E, CSF, D16
39B	PP#12	D16, Penta E	D18, CSF
40B	PP#15	CSF	
41B	PP#5	Penta E, D13, Penta D, vWA, D8	D18, D5, D16, CSF, Amel, FGA
42B	PP#5	vWA, D13, Penta D, FGA	TH01, D18, Penta E, D16, CSF, TPOX, Amel
43B	PP#15	CSF	
44B	PP#15	CSF	
46B	PP#12	D16	D18, CSF, FGA
50B	PP#15	CSF	
5W	PP#14		D18, CSF
10W	PP#15		D18
11W	PP#13	Penta E	D18, CSF, D8
12W	PP#14		D18, CSF
14W	PP#14		D18, CSF

15W	PP#14		D18, CSF
17W	PP#14	D18, Penta E	
19W	PP#15	D18	
20W	PP#15		D18
28W	PP#14		D18, CSF
29W	PP#15	CSF	
31W	PP#14		D18, CSF
33W	PP#14		D18, CSF
35W	PP#14		D18, CSF
36W	PP#14	D18, CSF	
40W	PP#14	D18, CSF	
41W	PP#14	CSF	D18
42W	PP#15		CSF
48W	PP#14	D18, CSF	

Appendix 6: Consent Forms

As discussed in *Chapter 2*, prior to collecting any samples this project was approved through the Institutional Review Board at St. Edward's University and received ethical approval through the University of Central Lancashire. A risk assessment is also on file at the University of Central Lancashire. All samples obtained from individuals during the course of this research were collected following a written consent which was approved by both universities. Copies of both consent forms are located in this section: BUCCAL CONSENT, BLOOD CONSENT.

UNIVERSITY OF CENTRAL LANCASHIRE

CONSENT FORM

Title: Application and comprehensive evaluation of a new direct amplification system (PowerPlex® 18D) in forensic DNA profiling.

Researcher: Mrs. Casie Parish-Fisher MS– Department of Forensic & Investigative Science

Principal Investigator: Dr Sibte Hadi PhD

RESEARCHER'S STATEMENT

We are asking you to be in a research study. The purpose of this consent form is to give you the information you will need to understand about this study. Please read this form carefully. You may ask any questions about any sample you give and how it will be used, or anything else about the research or this form that is not clear. When all of your questions have been answered, you can decide if you want to voluntarily donate a sample to be used during this study or not. This process is called "informed consent".

PURPOSE AND PROCEDURE

As part of the study, we will be taking a buccal swab from you.

If you agree, we would like to keep samples of your swabs. The samples will be kept at the University of St. Edwards, Austin, Texas, USA and/or University of Central Lancashire, Preston, UK. The sample will be used for research. A copy of your form will be kept at one of the institutions listed above and can be seen upon request by contacting the principal investigator.

The research that is done with your samples will not be of any direct use to you and all information about your sample shall be anonymised. The results may be shared with collaborating institutions / companies but no personal data will be revealed.

THINGS TO THINK ABOUT

We will label your samples with a code that will indicate to us which ethnic origin you consider yourself to belong to. This will be asked when you provide the sample. This code will not be printed on your consent form. We will not keep any record that would link the code with any information that could identify you.

Sometimes DNA is used for genetic research (about diseases that are passed on in families). The sample that you donate **shall not** be used for any such research.

OTHER INFORMATION

Your sample will be kept until it is used up or destroyed. The samples will be used only for research. Your name will not be used in any published reports about this study.

QUESTIONS

If you have questions about this research or about this study, please contact one of the people listed on this form.

Principal Investigator: Dr. Sibte Hadi PhD– shadi@uclan.ac.uk

Signature of person obtaining consent

Date

Printed name of person obtaining consent

SUBJECT'S STATEMENT

I agree to allow the St. Edward's University and/or University of Central Lancashire to store my buccal swab sample for future research about developing new methods to study genetic polymorphism's & population study. I understand that no information can be given to me or anyone else about specific samples as there is no way of tracing them.

Your signature

Date

Your printed name

UNIVERSITY OF CENTRAL LANCASHIRE

CONSENT FORM

Title: Application and comprehensive evaluation of a new direct amplification system (PowerPlex® 18D) in forensic DNA profiling.

Researcher: Mrs. Casie Parish-Fisher MS– Department of Forensic & Investigative Science

Principal Investigator: Dr Sibte Hadi PhD

RESEARCHER'S STATEMENT

We are asking you to be in a research study. The purpose of this consent form is to give you the information you will need to understand about this study. Please read this form carefully. You may ask any questions about any sample you give and how it will be used, or anything else about the research or this form that is not clear. When all of your questions have been answered, you can decide if you want to voluntarily donate a sample to be used during this study or not. This process is called "informed consent".

PURPOSE AND PROCEDURE

As part of the study, we will be taking an anonymous fresh blood sample from you.

If you agree, we would like to keep blood samples obtained from you. The samples will be kept at the University of St. Edwards, Austin, Texas, USA/University of Central Lancashire, Preston, UK. The sample will be used for research. A copy of your form will be kept at one of the institutions listed above and can be seen upon request by contacting the principal investigator.

The research that is done with your samples will not be of any direct use and all information about the sample shall be anonymised. The results may be shared with collaborating institutions / companies but no personal data will be revealed.

THINGS TO THINK ABOUT

Sometimes DNA is used for genetic research (about diseases that are passed on in families). The sample **shall not** be used for any such research.

OTHER INFORMATION

The sample will be kept until it is used up or destroyed. The samples will be used only for research.

QUESTIONS

If you have questions about this research or about this study, please contact one of the people listed on this form.

Principal Investigator: Dr. Sibte Hadi PhD– shadi@uclan.ac.uk

Signature of person obtaining consent

Date

Printed name of person obtaining consent

SUBJECT'S STATEMENT

I agree to allow the University of Central Lancashire and/or St. Edward's University to use the blood sample research about developing new methods to study genetic polymorphism's & population study. I understand that no information can be given to us or anyone else about specific samples as there is no way of tracing them.

Your signature

Date

Your printed name

Appendix 7: NanoDrop[®] Results of Extracted Samples for the Concordance Study

The following section lists in table form the quantification values of each of the buccal swabs used during the concordance study (A7.1). These samples were extracted using PureLink™ Genomic DNA Purification kit (Invitrogen by Life Technologies) and were quantified on the NanoDrop 2000.

Mexican Sample ID#	Nucleic Acid Concentration (ng/μl)	260/280 Ratio
1M	8.8	1.76
2M	3.3	1.66
3M	8.5	1.62
4M	4.6	1.61
5M	7.8	1.85
6M	6.7	1.83
7M	2.3	1.61
8M	4.2	1.3
9M	2.8	1.76
10M	7.4	1.45
11M	5.6	1.64
12M	4.2	1.83
13M	4.1	1.44
14M	3	1.62
15M	4.6	1.58
16M	3.3	1.66
17M	3.8	1.79
18M	6.2	1.69
19M	4	1.52
20M	4.3	1.71
21M	5.1	1.42
22M	2.9	1.59
23M	1.8	1.86
24M	2.3	1.62
25M	4.3	1.42
26M	1.6	6.66
27M	1.1	1.98
28M	1.5	2.34
29M	1.0	4.61

30M	0.5	1.93
31M	1.0	1.76
32M	1.0	4.67
33M	1.7	1.69
34M	1.1	1.3
35M	1.5	1.56
36M	1.6	1.43
37M	1.5	1.55
38M	2.0	1.98
39M	2.5	1.87
40M	1.3	1.76
41M	3.1	1.8
42M	5.7	1.78
43M	1.2	5.87
44M	1.6	3.45
45M	2.0	4.88
46M	0.6	4.76
47M	1.6	2.0
48M	1.1	3.42
49M	1.2	1.89
50M	11.8	2.84

Black Sample ID#	Nucleic Acid Concentration (ng/μl)	260/280 Ratio
1B	-2.8	1.93
2B	7.7	1.82
3B	-1.2	0.96
4B	7	1.54
5B	1.5	1.25
6B	6.9	1.73
7B	9.5	1.76
8B	2.7	2.03
9B	5	1.7
10B	1.1	2.54
11B	1.6	1.56
12B	5.5	1.59
13B	5.7	1.55
14B	7.6	1.54
15B	4.9	1.78
16B	4.5	1.3
17B	9.7	1.52
18B	7	1.78
19B	5.5	1.7
20B	19.2	1.55
21B	13.1	1.65
22B	36	1.46
23B	4.7	2.0
24B	7.2	1.85
25B	8.6	2.25
26B	1.6	1.46
27B	1.8	1.99
28B	1	0.94
29B	1.2	1.87

30B	0.6	3.65
31B	1.4	1.44
32B	1.3	2.0
33B	0.9	1.54
34B	3	4.33
35B	4.9	2.52
36B	3.4	1.90
37B	0.6	1.81
38B	0.4	2.01
39B	1.1	2.11
40B	2.5	2.37
41B	1.5	2.89
42B	2.3	1.96
43B	1.3	1.45
44B	1.8	1.88
45B	0.8	1.23
46B	2.3	2.1
47B	1.4	1.34
48B	1.9	2.03
49B	3.9	4.87
50B	1.2	1.81

Caucasian Sample ID#	Nucleic Acid Concentration (ng/μl)	260/280 Ratio
1W	1.2	1.36
2W	1.8	2.35
3W	1.7	2.52
4W	2.2	1.90
5W	1.5	1.81
6W	1.8	2.21
7W	1.9	1.14
8W	5.9	4.37
9W	1.6	2.73
10W	2	1.81
11W	1.6	1.25
12W	2.2	1.85
13W	1.3	1.29
14W	1.2	2.33
15W	4.5	1.32
16W	1.3	1.26
17W	1.4	1.03
18W	2	1.62
19W	1.4	1.65
20W	1.2	1.89
21W	1.7	1.76
22W	2.1	1.81
23W	1.2	1.68
24W	3.2	5.87
25W	2.8	3.45
26W	0.6	1.37
27W	1.2	1.84
28W	1.8	1.45
29W	0.6	1.52

30W	1.8	1.88
31W	1	1.95
32W	1.6	2.11
33W	1.7	1.8
34W	2.2	1.74
35W	1.5	2.54
36W	0.7	2.56
37W	1.1	1.39
38W	1.9	1.75
39W	1.8	1.52
40W	0.8	1.71
41W	1.9	1.77
42W	4.9	1.81
43W	3.1	1.61
44W	1.1	1.25
45W	3.8	4.78
46W	0.5	3.22
47W	2.7	2.61
48W	0.5	2.81
49W	0.5	1.44
50W	2.7	3.97

Appendix 8: Summary of Loci in PowerPlex 16HS[®] and PowerPlex[®] 18D

A short summary of all the loci used in both kits for the course of this project (A8.1).

STR Loci ¹	Alleles	Chromosomal Location	Category; Repeat Motif	Description
D2S1338	10 to 31	2q35	Compound; TGCC/TTCC	Long arm of chromosome 2
D3S1358	6 to 26	3p21.31	Compound; TCTA/TCTG	Sort arm of chromosome 3
D5S818	4 to 29	5q23.2	Simple; AGAT	Long arm of chromosome 5
D7S820	5 to 16	7q21.11	Simple; GATA	Long arm of chromosome 7
D8S1179	6 to 20	8q24.13	Compound; TCTA/TCTG	Chromosome 8, primarily TCTA, TCTG enters for alleles larger than 13 repeats
D13S317	5 to 17	13q31.1	Simple; TATC	Long arm of chromosome 13
D16S539	4 to 17	16q24.1	Simple; GATA	Long arm of chromosome 16,
D18S51	5.3 to 40	18q21.33	Simple; AGAA	
D19S433	5.2 to 20	19q12	Compound; AAGG/TAGG	
D21S11	12 to 43.2	21q21.1	Complex; TCTA/TCTG	
FGA	12.2 to 51.2	4q31.3	Compound; CTTT/TTCC	Alpha fibrinogen, 3 rd Intron, long arm of chromosome 4
TH01	3 to 14	11p15.5;	Simple; TCAT	Tyrosine Hydroxylase, 1 st Intron, short arm of chromosome 11
vWA	10 to 25	12p13.31;	Compound; TCTA/TCTG	vonWillebrand Factor, 40 th Intron, short arm of chromosome 12
Penta E	5 to 32	15q26.2	Simple; AAAGA	Long arm of chromosome 15; polymorphic
Penta D	1.1 to 19	21q22.3	Simple; AAAGA	25 Mb from D21S11
TPOX	4 to 16	2p25.3	Simple; AATG	Thyroid peroxidase, 10 th Intron, short end on chromosome 2
CSFIPO	5 to 17	5q33.1	Simple; AGAT	c-fms proto-oncogene, long arm of chromosome 5, 6 th Intron

¹ D2S1338 and D19S433 are in **bold** to represent the 2 additional loci in PowerPlex[®] 18D.

Appendix 9: Allele Frequency and Comparison Charts

Although the population study could not be conducted due to low sample numbers and limited resources every effort was made to evaluate the data from a population perspective.

Tables A9.1 detail the allelic frequencies for each of the populations as described in *Chapter 2*.

Tables A9.2 look comparatively at the frequencies generated from the samples in this study and compare them to published allelic frequency data (Hill et al., 2013). The standard deviation between the data obtained in this study and published data are also noted for each allele and all loci.

TableA9.1: Caucasian Samples Allele Frequency Chart

<i>Allele</i>	CSF1PO	D2S1338	D3S1358	D5S818	D7S820	D8S1179	D13S317	D16S539
2								
3								
4								
5								
6								
7				0.010				0.010
8					0.130	0.030	0.100	0.020
9				0.040	0.250	0.010	0.070	0.080
9.3								
10	0.280			0.040	0.250	0.080	0.060	0.060
11	0.330			0.440	0.200	0.020	0.290	0.400
12	0.330			0.320	0.120	0.150	0.290	0.270
13	0.040		0.010	0.140	0.040	0.380	0.130	0.110
14	0.020	0.010	0.090	0.010	0.010	0.160	0.060	0.050
14.2								
15			0.230			0.110		
15.2								
16		0.030	0.320			0.050		
16.2								
17		0.220	0.190			0.010		
18		0.080	0.140					
19		0.160	0.020					
20		0.060						
21		0.030						
22		0.030						
23		0.130						
23.2								
24		0.130						
25		0.110						
25.2								
26		0.010						
<i>H(ob)</i>	0.680	0.820	0.840	0.700	0.800	0.780	0.740	0.780
<i>H(ex)</i>	0.724	0.885	0.789	0.888	0.816	0.816	0.786	0.754
<i>PD</i>	0.857	0.945	0.900	0.841	0.907	0.922	0.920	0.885
<i>PE</i>	0.398	0.637	0.675	0.428	0.599	0.562	0.493	0.562

TableA9.1: Caucasian Samples Allele Frequency Chart *continued*

<i>Allele</i>	D18S51	D19S433	D21S11	FGA	Penta D	Penta E	TH01	TPOX	vWA
7					0.010	0.190	0.160		
8						0.010	0.140	0.490	
9					0.290		0.200	0.140	
10	0.010				0.080	0.070		0.100	
11	0.010				0.130	0.130		0.220	
12	0.140	0.110			0.180	0.170		0.040	
13	0.180	0.210			0.210	0.100		0.010	
14	0.120	0.350			0.060	0.060			0.100
14.2		0.020							
15	0.160	0.190			0.040	0.070			0.130
15.2		0.090							
16	0.130	0.010				0.060			0.190
17	0.110					0.020			0.310
18	0.100			0.050		0.060			0.170
19	0.010			0.060					0.080
20	0.020			0.120		0.010			0.020
21				0.190		0.010			
22				0.200					
24	0.010			0.150					
25				0.050					
25.2			0.010						
26				0.020					
27			0.020						
28			0.090						
29			0.250						
30			0.260						
30.2			0.020						
31			0.040						
31.2			0.130						
32.2			0.130						
33.2			0.040						
34.2			0.010						
<i>H(ob)</i>	0.900	0.660	0.880	0.840	0.840	0.860	0.820	0.660	0.780
<i>H(ex)</i>	0.880	0.767	0.835	0.857	0.852	0.796	0.755	0.637	0.810
<i>PD</i>	0.950	0.914	0.931	0.946	0.910	0.946	0.905	0.851	0.929
<i>PE</i>	0.795	0.369	0.755	0.675	0.675	0.715	0.637	0.369	0.562

TableA9.1: African American Samples Allele Frequency Chart

<i>Allele</i>	<i>CSFIPO</i>	<i>D2S1338</i>	<i>D3S1358</i>	<i>D5S818</i>	<i>D7S820</i>	<i>D8S1179</i>	<i>D13S317</i>	<i>D16S539</i>
7	0.082							
8	0.051			0.060	0.210		0.031	0.020
9	0.051			0.010	0.130		0.020	0.224
9.3								
10	0.235			0.130	0.340		0.031	0.102
11	0.194			0.190	0.190	0.060	0.347	0.357
12	0.327			0.380	0.080	0.090	0.429	0.173
12.2								
13	0.041		0.020	0.190	0.020	0.220	0.122	0.102
13.2								
14	0.020	0.010	0.122	0.020	0.010	0.320	0.020	0.020
14.2								
15			0.276	0.010	0.010	0.220		
15.2								
16		0.041	0.286			0.060		
16.1								
16.2								
17		0.143	0.214	0.010	0.010	0.030		
18		0.071	0.061					
18.2								
19		0.143	0.020					
20		0.071						
21		0.092						
22		0.122						
23		0.143						
24		0.061						
25		0.051						
26		0.051						
<i>H(ob)</i>	0.857	0.837	0.735	0.780	0.780	0.880	0.653	0.796
<i>H(ex)</i>	0.776	0.893	0.744	0.757	0.775	0.803	0.702	0.795
<i>PD</i>	0.908	0.965	0.914	0.899	0.908	0.898	0.858	0.888
<i>PE</i>	0.709	0.669	0.484	0.562	0.562	0.755	0.359	0.591

TableA9.1: African American Samples Allele Frequency Chart *continued*

<i>Allele</i>	<i>D18S51</i>	<i>D19S433</i>	<i>D21S11</i>	<i>FGA</i>	<i>Penta D</i>	<i>Penta E</i>	<i>TH01</i>	<i>TPOX</i>	<i>vWA</i>
5					0.030	0.080	0.010		
6					0.010		0.120	0.080	
7					0.030	0.100	0.380	0.010	
8					0.100	0.180	0.260	0.410	
9					0.080	0.050	0.110	0.190	
10		0.020			0.100	0.050	0.010	0.070	
11	0.010	0.082			0.190	0.080		0.180	
12	0.061	0.153			0.200	0.080		0.040	
12.2		0.031							
13	0.061	0.224			0.100	0.090			0.030
13.2		0.071							
14	0.102	0.235				0.110			0.040
14.2		0.071							
15	0.143	0.020		0.010	0.010	0.080	0.010	0.010	0.230
15.2	0.010	0.051							
16	0.194	0.020				0.070			0.240
16.2		0.020							
17	0.143			0.020	0.010	0.030	0.010	0.010	0.150
18	0.122								0.170
19	0.051			0.060					0.100
20	0.071			0.070					0.020
21	0.031			0.140					0.010
24				0.170					
25				0.050					
26				0.060					
27			0.051	0.020					
28			0.184	0.030					
29			0.235	0.010					
30			0.194						
32			0.020						
36			0.010						
47.2				0.010					
<i>H(ob)</i>	0.837	0.918	0.776	0.880	0.920	0.900	0.720	0.740	0.820
<i>H(ex)</i>	0.885	0.854	0.845	0.876			0.736	0.764	0.813
<i>PD</i>	0.960	0.942	0.949	0.959	0.954	0.966	0.895	0.889	0.940
<i>PE</i>	0.669	0.833	0.554	0.755	0.836	0.795	0.460	0.493	0.637

TableA9.1: Mexican Samples Allele Frequency Chart

<i>Allele</i>	<i>CSFIPO</i>	<i>D2S1338</i>	<i>D3S1358</i>	<i>D5S818</i>	<i>D7S820</i>	<i>D8S1179</i>	<i>D13S317</i>	<i>D16S539</i>
7				0.040	0.010			
8					0.110	0.010	0.102	0.010
9	0.020			0.020	0.050	0.010	0.265	0.102
9.3								
10	0.224			0.080	0.340	0.100	0.112	0.153
10.2								
10.3					0.010			
11	0.378			0.500	0.230	0.030	0.214	0.235
12	0.316			0.180	0.190	0.140	0.235	0.276
12.2								
13	0.051			0.170	0.060	0.360	0.051	0.214
13.2								
14	0.010	0.020	0.120	0.010		0.240	0.020	0.010
14.2								
15		0.010	0.350			0.110		
15.2								
16		0.040	0.190					
16.1								
16.2								
17		0.150	0.240					
18		0.030	0.090					
19		0.110	0.010					
20		0.180						
21		0.010						
22		0.080						
23		0.240						
24		0.080						
25		0.050						
26								
27								
28								
35.2								
<i>H(ob)</i>	0.735	0.940	0.780	0.720	0.680	0.760	0.796	0.837
<i>H(ex)</i>	0.731	0.878	0.772	0.734	0.796	0.818	0.834	0.802
<i>PD</i>	0.842	0.938	0.897	0.859	0.906	0.897	0.921	0.905
<i>PE</i>	0.484	0.878	0.562	0.460	0.398	0.527	0.591	0.669

TableA9.1: Mexican Samples Allele Frequency Chart *continued*

<i>Allele</i>	<i>D19S433</i>	<i>D21S11</i>	<i>FGA</i>	<i>Penta D</i>	<i>Penta E</i>	<i>TH01</i>	<i>TPOX</i>	<i>vWA</i>
6				0.010	0.050			
8				0.010	0.100	0.340		
9				0.010	0.010	0.050	0.480	
9.3				0.180		0.130	0.100	
10						0.230	0.010	
10.2				0.230	0.060	0.030	0.040	
12			0.010	0.120	0.080		0.270	
12.2	0.100	0.010		0.120	0.190		0.100	
13	0.010	0.010						
13.2	0.230		0.010	0.240	0.090			
14	0.050							
14.2	0.290			0.080	0.060			0.120
15	0.030							
15.2	0.140				0.090			0.070
16	0.050							
16.1	0.050				0.040			0.350
18					0.050			0.270
19					0.040			0.160
20			0.070		0.030			0.030
21			0.080		0.040			
22			0.130		0.030			
23			0.130		0.030			
25			0.180		0.010			
26			0.120					
27		0.010	0.090					
28		0.050	0.020					
30		0.170						
30.2		0.220						
31		0.010						
31.2		0.030						
32		0.110						
35.2		0.040						
		0.010						
<i>H(ob)</i>	0.709	0.637	0.715	0.878	0.675	0.919	0.637	0.493
<i>H(ex)</i>	0.820	0.860	0.940	0.840	0.960	0.820	0.740	0.780
<i>PD</i>	0.775	0.847	0.880	.0709	.0637	0.787	0.881	0.814
<i>PE</i>	0.920	0.943	0.948	0.938	0.969	0.889	0.830	0.895

Table A9.2: Caucasian comparison chart.

Allele	CSF1PO			D13S317			D16S539		
	Promega	Parish	STDEV	Promega	Parish	STDEV	Promega	Parish	STDEV
2.2									
3.2									
4.0									
4.2									
5.0									
6.0									
6.3									
7.0								0.0100	
8.0	0.0055			0.1205	0.1000	0.0145	0.0180	0.0200	0.0014
8.1									
9.0	0.0139			0.0776	0.0700	0.0054	0.1066	0.0800	0.0188
9.1									
9.3									
10.0	0.2202	0.2800	0.0423	0.0471	0.0600	0.0091	0.0568	0.0600	0.0023
10.1									
10.2									
10.3									
11.0	0.3089	0.3300	0.0149	0.3255	0.2900	0.0251	0.3144	0.4000	0.0605
11.2									
11.3									
12.0	0.3601	0.3300	0.0213	0.2687	0.2900	0.0151	0.3144	0.2700	0.0314
12.2									
12.3									
13.0	0.0817	0.0400	0.0295	0.1163	0.1300	0.0097	0.1634	0.1100	0.0378
13.2									
13.3									
13.4									
14.0	0.0097	0.0200	0.0073	0.0429	0.0600	0.0121	0.0263	0.0500	0.0168
14.2									
14.3									
15.0				0.0014					
15.2									
15.3									
15.4									
16.0									
16.1									
16.2									
16.3									
17.0									
17.1									
17.2									

Table A9.2: Caucasian comparison chart. *continued*

Allele	D18S51			D2S1338			Penta_E		
	Promega	Parish	STDEV	Promega	Parish	STDEV	Promega	Parish	STDEV
5.0							0.0762	0.0400	0.0256
6.0									
7.0							0.1690	0.1900	0.0148
8.0							0.0139	0.0100	0.0028
9.0							0.0125		
9.3	0.0083								
10.0		0.0100					0.0859	0.0700	0.0112
10.3	0.0097								
11.0		0.0100					0.0873	0.1300	0.0302
11.2									
11.3	0.1136								
12.0		0.1400					0.1994	0.1700	0.0208
12.2									
12.3	0.1233								
13.0		0.1800					0.0859	0.1000	0.0100
13.4	0.1343								
14.0	0.0014	0.1200	0.0839		0.0100		0.0623	0.0600	0.0016
14.2									
14.3	0.1704								
15.0		0.1600		0.0014			0.0429	0.0700	0.0192
15.4	0.1468						0.0014		
16.0		0.1300		0.0374	0.0300	0.0052	0.0512	0.0600	0.0062
16.1	0.0014								
16.2									
16.3	0.1385								
17.0		0.1100		0.1856	0.2200	0.0243	0.0485	0.0200	0.0202
17.3	0.0776								
18.0		0.1000		0.0734	0.0800	0.0047	0.0332	0.0600	0.0190
18.3	0.0402								
19.0		0.0100		0.1205	0.1600	0.0279	0.0152		
19.4	0.0180								
20.0		0.0200		0.1565	0.0600	0.0682	0.0097	0.0100	0.0002
20.3	0.0097								
21.0				0.0374	0.0300	0.0052	0.0028	0.0100	0.0051
21.3	0.0069								
22.0				0.0346	0.0300	0.0033	0.0014		
23.0				0.1053	0.1300	0.0175			
24.0		0.0100		0.1150	0.1300	0.0106	0.0014		
25.0				0.1025	0.1100	0.0053			
25.2									
26.0				0.0305	0.0100	0.0145			

Table A9.2: Caucasian comparison chart. *continued*

Allele	D19S433			D22S1045			D8S1179		
	Promega	Parish	STDEV	Promega	Parish	STDEV	Promega	Parish	STDEV
5.0									
6.0									
6.3									
7.0									
8.0							0.0139	0.0300	0.0114
8.1									
9.0							0.0055	0.0100	0.0032
9.1									
9.3									
10.0	0.0014						0.1025	0.0800	0.0159
10.1									
10.2									
10.3									
11.0	0.0055			0.1399			0.0762	0.0200	0.0397
11.2									
11.3									
12.0	0.0706	0.1100	0.0279	0.0125			0.1676	0.1500	0.0124
12.2	0.0014								
12.3									
13.0	0.2548	0.2100	0.0317	0.0069			0.3296	0.3800	0.0356
13.2	0.0069								
13.3									
13.4									
14.0	0.3615	0.3500	0.0081	0.0568			0.1662	0.1600	0.0044
14.2	0.0235	0.0200	0.0025						
14.3									
15.0	0.1565	0.1900	0.0237	0.3213			0.1039	0.1100	0.0043
15.2	0.0360	0.0900	0.0382						
15.3									
15.4									
16.0	0.0568	0.0100	0.0331	0.3823			0.0332	0.0500	0.0119
16.1									
16.2	0.0152	0.0200	0.0034						
16.3									
17.0	0.0069			0.0748			0.0014	0.0100	0.0061
17.1									
17.2	0.0014								
17.3									
18.0				0.0055					
18.1									
18.2	0.0014								
18.3									

Table A9.2: Caucasian comparison chart. *continued*

Allele	D21S11			FGA		
	Promega	Parish	STDEV	Promega	Parish	STDEV
18.0				0.0249	0.0500	0.0177
19.0				0.0499	0.0600	0.0071
20.0				0.1233	0.1200	0.0023
21.0				0.1787	0.1900	0.0080
21.2				0.0055		
21.3						
22.0				0.2050	0.2000	0.0035
22.2				0.0125		
22.3						
23.0				0.1524	0.1400	0.0088
23.2				0.0028	0.0200	0.0122
23.3						
24.0				0.1343	0.1500	0.0111
24.2				0.0014		
24.3						
25.0				0.0789	0.0500	0.0204
25.2	0.0014	0.0100	0.0061			
26.0				0.0263	0.0200	0.0045
26.2						
27.0	0.0222	0.0200	0.0016	0.0042		
27.2						
27.3						
28.0	0.1593	0.0900	0.0490			
28.2						
28.3						
29.0	0.2022	0.2500	0.0338			
29.2	0.0028					
29.3						
30.0	0.2825	0.2600	0.0159			
30.2	0.0291	0.0200	0.0064			
30.3						
31.0	0.0720	0.0400	0.0226			
31.2	0.0983	0.1300	0.0224			
32.0	0.0055					
32.2	0.0900	0.1300	0.0283			
33.0	0.0014					
33.1						
33.2	0.0263	0.0400	0.0097			
34.0						
34.2	0.0042	0.0100	0.0041			
35.0	0.0014					
35.2	0.0014					

Table A9.2: Caucasian comparison chart. *continued*

Allele	D3S1358			vWA		
	Promega	Parish	STDEV	Promega	Parish	STDEV
11.0	0.0014					
11.2						
11.3						
12.0				0.0014		
12.2						
12.3						
13.0	0.0014	0.0100	0.0061	0.0014		
13.2						
13.3						
13.4						
14.0	0.1066	0.0900	0.0117	0.0928	0.1000	0.0051
14.2						
14.3						
15.0	0.2729	0.2300	0.0303	0.1053	0.1300	0.0175
15.2						
15.3						
15.4						
16.0	0.2382	0.3200	0.0578	0.2008	0.1900	0.0076
16.1						
16.2						
16.3						
17.0	0.2105	0.1900	0.0145	0.2839	0.3100	0.0185
17.1						
17.2						
17.3						
18.0	0.1510	0.1400	0.0078	0.2022	0.1700	0.0228
18.1						
18.2						
18.3						
19.0	0.0166	0.0200	0.0024	0.1039	0.0800	0.0169
19.1						
19.2						
19.3						
19.4						
20.0	0.0014			0.0069	0.0200	0.0093
20.1						
20.2						
20.3						
21.0				0.0014		
22.2						
22.3						
24.0						

Table A9.2: Caucasian comparison chart. *continued*

Allele	D5S818			D7S820			Penta_D		
	Promega	Parish	STDEV	Promega	Parish	STDEV	Promega	Parish	STDEV
2.2							0.0042		
3.2									
4.0									
4.2									
5.0									
6.0							0.0042		
6.3									
7.0	0.0028	0.0100	0.0051	0.0277			0.0042	0.0100	0.0041
8.0	0.0055			0.1440	0.1300	0.0099	0.0208		
8.1				0.0014					
9.0	0.0416	0.0400	0.0011	0.1676	0.2500	0.0583	0.2216	0.2900	0.0484
9.1									
9.3									
10.0	0.0554	0.0400	0.0109	0.2562	0.2500	0.0044	0.1150	0.0800	0.0247
10.1									
10.2									
10.3									
11.0	0.3560	0.4400	0.0594	0.2050	0.2000	0.0035	0.1260	0.1300	0.0028
11.2									
11.3									
12.0	0.3878	0.3200	0.0479	0.1593	0.1200	0.0278	0.2327	0.1800	0.0373
12.2									
12.3									
13.0	0.1427	0.1400	0.0019	0.0346	0.0400	0.0038	0.1967	0.2100	0.0094
13.2									
13.3									
13.4									
14.0	0.0069	0.0100	0.0022	0.0042	0.0100	0.0041	0.0609	0.0600	0.0006
14.2									
14.3									
15.0	0.0014						0.0097	0.0400	0.0214
15.2									
15.3									
15.4									
16.0							0.0028		
16.1									
16.2									
16.3									
17.0							0.0014		
17.1									
17.2									
17.3									

Table A9.2: Caucasian comparison chart. *continued*

Allele	TH01			TPOX		
	Promega	Parish	STDEV	Promega	Parish	STDEV
2.2						
3.2						
4.0						
4.2						
5.0	0.0014			0.0014		
6.0	0.2355	0.2400	0.0032	0.0014		
6.3						
7.0	0.1939	0.1600	0.0240			
8.0	0.0956	0.1400	0.0314	0.5249	0.4900	0.0247
8.1						
9.0	0.1191	0.2000	0.0572	0.1274	0.1400	0.0089
9.1						
9.3	0.3449	0.2600	0.0600			
10.0	0.0083			0.0499	0.1000	0.0354
10.1						
10.2						
10.3						
11.0	0.0014			0.2521	0.2200	0.0227
11.2						
11.3						
12.0				0.0416	0.0400	0.0011
12.2						
12.3						
13.0				0.0014	0.0100	0.0061
13.2						
13.3						
13.4						
14.0						
14.2						
14.3						
15.0						
15.2						
15.3						
15.4						
16.0						
16.1						
16.2						
16.3						
17.0						
17.1						
17.2						
17.3						

Table A9.2: African American comparison chart.

Allele	CSFIPO			D13S317			D16S539		
	Promega	Parish	STDEV	Promega	Parish	STDEV	Promega	Parish	STDEV
2.2									
3.2									
4.0									
4.2									
5.0							0.0015		
6.0									
6.3									
7.0	0.0556	0.0820	0.0187						
8.0	0.0556	0.0510	0.0033	0.0278	0.0310	0.0023	0.0322	0.0200	0.0086
8.1									
9.0	0.0395	0.0510	0.0081	0.0336	0.0200	0.0096	0.1827	0.2240	0.0292
9.1									
9.3									
10.0	0.2500	0.2350	0.0106	0.0307	0.0310	0.0002	0.1170	0.1020	0.0106
10.1									
10.2									
10.3									
11.0	0.2485	0.1940	0.0385	0.3099	0.2470	0.0445	0.3143	0.3570	0.0302
11.2									
11.3									
12.0	0.2953			0.4181	0.4290	0.0077	0.2047	0.1730	0.0224
12.2									
12.3									
13.0	0.0468	0.0310	0.0112	0.1404	0.1220	0.0130	0.1228	0.1020	0.0147
13.2									
13.3									
13.4									
14.0	0.0088	0.0200	0.0079	0.0395	0.0200	0.0138	0.0249	0.0200	0.0335
14.2									
14.3									
15.0									
15.2									
15.3									
15.4									
16.0									
16.1									
16.2									
16.3									
17.0									
17.1									
17.2									
17.3									

Table A9.2: African American comparison chart. *continued*

Allele	D18S51			D2S1338			Penta_E		
	Promega	Parish	STDEV	Promega	Parish	STDEV	Promega	Parish	STDEV
4.2									
5.0							0.0950	0.0800	0.0106
6.0							0.0015		
6.3									
7.0							0.1038	0.1000	0.0027
8.0							0.1667	0.1800	0.0094
8.1									
9.0	0.0029						0.0512	0.0500	0.0008
10.0	0.0044						0.0468	0.0500	0.0023
11.0	0.0015	0.0100	0.006				0.0643	0.0800	0.0111
11.2									
11.3									
12.0	0.0760	0.0610	0.0106				0.1287	0.0800	0.0344
12.2									
12.3									
13.0	0.0409	0.0610	0.0142				0.1038	0.0900	0.0098
13.2	0.0044								
14.0	0.0716	0.1020	0.0215		0.0100		0.0687	0.1100	0.0292
14.2									
14.3									
15.0	0.1652	0.1430	0.0157	0.0015			0.0556	0.0800	0.0173
15.2	0.0015	0.0100	0.006						
15.3									
15.4									
16.0	0.1711	0.1940	0.0162	0.0556	0.0410	0.0103	0.0409	0.0700	0.0206
17.0	0.1520	0.1430	0.0064	0.1009	0.1430	0.0298	0.0439	0.0300	0.0098
18.0	0.1213	0.1220	0.0005	0.0424	0.0710	0.0202	0.0161		
19.0	0.0994	0.0510	0.0342	0.1389	0.1430	0.0029	0.0073		
20.0	0.0629	0.0710	0.0057	0.1038	0.0710	0.0232	0.0044		
21.0	0.0102	0.0310	0.0147	0.1360	0.0920	0.0311			
21.2	0.0015								
21.3									
22.0	0.0073			0.1374	0.1220	0.0109			
22.2									
22.3									
23.0	0.0044			0.1038	0.1430	0.0277			
24.0	0.0015			0.0833	0.0610	0.0158			
25.0				0.0775	0.0510	0.0187			
25.2									
26.0				0.0146	0.0510	0.0257			
26.2									
27.0				0.0044					

Table A9.2: African American comparison chart. *continued*

Allele	D19S433			D8S1179		
	Promega	Parish	STDEV	Promega	Parish	STDEV
4.2						
5.0						
6.0						
6.3						
7.0						
8.0				0.0073		
8.1						
9.0				0.0044		
9.1						
9.3						
10.0	0.0102	0.0200	0.0069	0.0307		
10.1						
10.2						
10.3						
11.0	0.0629	0.0820	0.0135	0.0526	0.0600	0.0052
11.2						
11.3						
12.0	0.1228	0.1530	0.0214	0.1301	0.0900	0.0284
12.2	0.0365	0.0310	0.0039			
12.3						
13.0	0.2456	0.2240	0.0153	0.2193	0.2200	0.0005
13.2	0.0526	0.0710	0.0130			
13.3						
13.4						
14.0	0.2105	0.2350	0.0173	0.2939	0.3200	0.0185
14.2	0.0746	0.0710	0.0025			
14.3						
15.0	0.0804	0.0200	0.0427	0.1901	0.2200	0.0211
15.2	0.0614	0.0510	0.0074			
15.3						
15.4						
16.0	0.0044	0.0200	0.0110	0.0643	0.0600	0.0030
16.1						
16.2	0.0263	0.0200	0.0045			
16.3						
17.0				0.0044	0.0300	0.0181
17.1						
17.2	0.0088					
17.3						
18.0				0.0029		
18.1						
18.2	0.0029					

Table A9.2: African American comparison chart. *continued*

Allele	D21S11			FGA		
	Promega	Parish	STDEV	Promega	Parish	STDEV
16.2				0.0015		
17.0					0.0200	
17.2				0.0015		
18.0				0.0015		
18.2				0.0175	0.0200	0.0018
19.0				0.0512	0.0600	0.0062
19.2				0.0029		
20.0				0.0541	0.0700	0.0112
20.3						
21.0				0.1228	0.1400	0.0122
22.0				0.1988	0.2100	0.0079
22.2				0.0044		
22.3				0.0015		
23.0				0.1696	0.1200	0.0351
23.2				0.0015		
24.0				0.1330	0.1700	0.0262
25.0				0.1184	0.0500	0.0484
25.2				0.0015		
26.0	0.0015			0.0702	0.0600	0.0072
26.2						
27.0	0.0746	0.0510	0.0167	0.0234	0.0200	0.0024
27.2						
27.3						
28.0	0.2456	0.1840	0.0436	0.0146	0.0300	0.0109
29.0	0.2047	0.2350	0.0214	0.0058		
29.3	0.0015					
30.0	0.1696	0.1940	0.0173	0.0015		
30.2	0.0175	0.0200	0.0018	0.0015		
31.0	0.0789	0.1120	0.0234			
31.2	0.0512	0.1020	0.0359	0.0015		
32.0	0.0088	0.0200	0.0079			
32.2	0.0614	0.0200	0.0293			
33.0	0.0044					
33.1	0.0029					
33.2	0.0351					
34.0	0.0058					
35.0	0.0219	0.0510	0.0206			
35.2	0.0088	0.0100	0.0008			
36.0	0.0029					
37.0	0.0015					
38.0	0.0015					

Table A9.2: African American comparison chart. *continued*

Allele	D3S1358			vWA		
	Promega	Parish	STDEV	Promega	Parish	STDEV
10.3						
11.0				0.0029		
11.2						
11.3						
12.0	0.0044			0.0015		
12.2						
12.3						
13.0	0.0029	0.0200	0.0121	0.0088	0.0300	0.0150
13.2						
13.3						
13.4						
14.0	0.0906	0.1120	0.0151	0.0804	0.0400	0.0286
14.2						
14.3						
15.0	0.3085	0.2760	0.0230	0.1915	0.2300	0.0272
15.2	0.0015					
15.3						
15.4						
16.0	0.3187	0.2860	0.0231	0.2500	0.2400	0.0071
16.1						
16.2						
16.3						
17.0	0.2120	0.2140	0.0014	0.2354	0.1500	0.0604
17.1						
17.2						
17.3						
18.0	0.0570	0.0610	0.0028	0.1491	0.1700	0.0148
18.1						
18.2						
18.3						
19.0	0.0044	0.0200	0.0110	0.0629	0.1000	0.0262
19.3						
19.4						
20.0				0.0161	0.0200	0.0028
20.1						
20.2						
20.3						
21.0				0.0015	0.0100	0.0060
21.2						
21.3						
22.0					0.0100	
22.2						

Table A9.2: African American comparison chart. *continued*

Allele	D5S818			D7S820			Penta_D		
	Promega	Parish	STDEV	Promega	Parish	STDEV	Promega	Parish	STDEV
2.2							0.1140	0.1100	0.0028
3.2							0.0088	0.0300	0.0150
5.0							0.0439	0.0300	0.0098
6.0				0.0015			0.0102	0.0100	0.0001
6.3									
7.0	0.0015			0.0117			0.0439	0.0300	0.0098
8.0	0.0468	0.0600	0.0093	0.2281	0.2100	0.0128	0.1082	0.1000	0.0058
8.1									
9.0	0.0322	0.0100	0.0157	0.1155	0.1300	0.0103	0.1681	0.0800	0.0623
9.1									
9.3									
10.0	0.0731	0.1300	0.0402	0.3363	0.3400	0.0026	0.0994	0.1000	0.0004
10.1									
10.2									
10.3									
11.0	0.2339	0.1900	0.0310	0.2032	0.1900	0.0093	0.1798		
11.2									
11.3									
12.0	0.3699	0.3800	0.0071	0.0877	0.0800	0.0054	0.1082		
12.2									
12.3									
13.0	0.2237	0.1900	0.0238	0.0146	0.0200	0.0038	0.0833	0.1000	0.0118
13.2									
13.3									
13.4							0.0015		
14.0	0.0161	0.0020	0.0100	0.0015	0.0100	0.0060	0.0249		
14.2									
14.3									
15.0	0.0029	0.0100	0.0050		0.0100		0.0044	0.0100	0.0040
15.2									
15.3									
15.4									
16.0									
16.1									
16.2									
16.3									
17.0		0.0100			0.0100		0.0015	0.0100	0.0060
17.1									
17.2									
17.3									
18.0									
18.1									

Table A9.2: African American comparison chart. *continued*

Allele	TH01			TPOX		
	Promega	Parish	STDEV	Promega	Parish	STDEV
2.2						
3.2						
4.0						
4.2						
5.0	0.0044	0.0100	0.0040			
6.0	0.1316	0.1200	0.0082	0.0892	0.0800	0.0065
6.3						
7.0	0.4079	0.3800	0.0197	0.0175	0.0100	0.0053
8.0	0.1959	0.2600	0.0453	0.3670	0.4100	0.0304
8.1						
9.0	0.1594	0.1100	0.0349	0.1959	0.1900	0.0042
9.1						
9.3	0.0965	0.0900	0.0046			
10.0	0.0044	0.0100	0.0040	0.0863	0.0700	0.0115
10.1						
10.2						
10.3						
11.0				0.2164	0.1900	0.0187
11.2						
11.3						
12.0				0.0263	0.0400	0.0097
12.2						
12.3						
13.0				0.0015		
13.2						
13.3						
13.4						
14.0						
14.2						
14.3						
15.0		0.0100			0.0100	
15.2						
15.3						
15.4						
16.0						
16.1						
16.2						
16.3						
17.0		0.0100			0.0100	
17.1						
17.2						
17.3						

Table A9.2: Mexican comparison chart.

Allele	CSFIPO			D13S317			D16S539		
	Promega	Parish	STDEV	Promega	Parish	STDEV	Promega	Parish	STDEV
2.2									
3.2									
4.0									
4.2									
5.0									
6.0									
6.3									
7.0	0.0127								
8.0	0.0042			0.1102	0.1020	0.0058	0.0191	0.0100	0.0064
8.1									
9.0	0.0233	0.0200	0.0023	0.1653	0.2650	0.0705	0.1398	0.1020	0.0267
9.1									
9.3									
10.0	0.2373	0.2240	0.0094	0.0996	0.1120	0.0088	0.1504	0.1530	0.0018
10.1									
10.2									
10.3									
11.0	0.2797	0.3780	0.0695	0.2182	0.2140	0.0030	0.2648	0.2350	0.0211
11.2									
11.3									
12.0	0.3750	0.3160	0.0417	0.2352	0.2350	0.0001	0.2775	0.2760	0.0011
12.2									
12.3									
13.0	0.0593	0.0510	0.0059	0.1059	0.0510	0.0388	0.1335	0.2140	0.0569
13.2									
13.3									
13.4									
14.0	0.0064	0.0100	0.0025	0.0614	0.0200	0.0293	0.0127	0.0100	0.0019
14.2									
14.3									
15.0	0.0021			0.0042			0.0021		
15.2									
15.3									
15.4									
16.0									
16.1									
16.2									
16.3									
17.0									
17.1									
17.2									
17.3									

Table A9.2: Mexican comparison chart. *continued*

Allele	D18S51			D2S1338			Penta_E		
	Promega	Parish	STDEV	Promega	Parish	STDEV	Promega	Parish	STDEV
5.0							0.0360	0.0500	0.0099
6.0									
6.3									
7.0							0.1186	0.1000	0.0132
8.0							0.0254	0.0100	0.0109
8.1									
9.0							0.0169		
9.1									
9.3									
10.0	0.0021						0.0847	0.0600	0.0175
10.1									
10.2									
10.3									
11.0	0.0148	0.0200	0.0037				0.0742	0.0800	0.0041
11.2									
11.3									
12.0	0.1144	0.0510	0.0448				0.1737	0.1900	0.0115
12.2									
12.3									
13.0	0.1229	0.1730	0.0354				0.0932	0.0900	0.0023
14.0	0.1610	0.1020	0.0417		0.0200		0.0720	0.0600	0.0085
14.2	0.0021								
14.3									
15.0	0.1589	0.1730	0.0100		0.0100		0.0911	0.0900	0.0008
15.2									
15.4							0.0021		
16.0	0.1250	0.2140	0.0629	0.0297	0.0400	0.0073	0.0614	0.0400	0.0151
16.1		0.0100							
17.0	0.1250	0.0920	0.0233	0.1695	0.1500	0.0138	0.0551	0.0500	0.0036
18.0	0.0784	0.0410	0.0264	0.0805	0.0300	0.0357	0.0339	0.0400	0.0043
19.0	0.0466	0.0610	0.0102	0.1928	0.1100	0.0585	0.0212	0.0300	0.0062
20.0	0.0275	0.0100	0.0124	0.1271	0.1800	0.0374	0.0212	0.0400	0.0133
21.0	0.0085	0.0310	0.0159	0.0318	0.0100	0.0154	0.0064	0.0300	0.0167
22.0	0.0106	0.0100	0.0004	0.0572	0.0800	0.0161	0.0021	0.0300	0.0197
23.0				0.1398	0.2400	0.0709	0.0064		
24.0	0.0021			0.0763	0.0800	0.0026		0.0100	
24.2									
24.3									
25.0		0.0100		0.0784	0.0500	0.0201	0.0042		
25.2									
26.0				0.0169					
26.2									

Table A9.2: Mexican comparison chart. *continued*

Allele	D19S433			D22S1045			D8S1179		
	Promega	Parish	STDEV	Promega	Parish	STDEV	Promega	Parish	STDEV
6.3									
7.0									
8.0							0.0148	0.0100	0.0034
8.1									
9.0	0.0021						0.0064	0.0100	0.0025
9.1									
9.3									
10.0	0.0021			0.0148			0.0932	0.1000	0.0048
10.1									
10.2		0.0100							
10.3									
11.0	0.0148			0.0636			0.0530	0.0300	0.0163
11.2									
11.3									
12.0	0.0657	0.1000	0.0243	0.0127			0.1292	0.1400	0.0076
12.2	0.0127	0.0100	0.0019						
12.3									
13.0	0.2225	0.2300	0.0053	0.0085			0.2733	0.3600	0.0613
13.2	0.0445	0.0500	0.0039						
13.3									
13.4									
14.0	0.3538	0.2900	0.0451	0.0275			0.2627	0.2400	0.0161
14.2	0.0381	0.0300	0.0057						
14.3									
15.0	0.1356	0.1400	0.0031	0.4258			0.1292	0.1100	0.0136
15.2	0.0551	0.0500	0.0036						
15.3									
15.4									
16.0	0.0254	0.0500	0.0174	0.3496			0.0318		
16.1									
16.2	0.0275	0.0400	0.0088						
16.3									
17.0				0.0911			0.0042		
17.1									
17.2									
17.3									
18.0				0.0064			0.0021		
18.1									
18.2									
18.3									
19.0									
19.1									

Table A9.2: Mexican comparison chart. *continued*

Allele	D21S11			FGA		
	Promega	Parish	STDEV	Promega	Parish	STDEV
10.3						
11.0					0.0100	
12.0		0.0100				
12.2		0.0100				
13.0					0.0100	
17.0				0.0021		
18.0				0.0127		
19.0				0.0805	0.0700	0.0074
20.0				0.0847	0.0800	0.0033
21.0				0.1525	0.1300	0.0159
22.0				0.1653	0.1300	0.0250
22.2				0.0042		
22.3						
23.0				0.1208	0.1600	0.0277
23.2				0.0042		
23.3						
24.0				0.1419	0.1800	0.0269
24.2	0.0021					
24.3						
25.0				0.1186	0.1200	0.0010
25.2						
26.0		0.0100		0.0614	0.0200	0.0293
26.2	0.0021					
27.0	0.0275	0.0500	0.0159	0.0445		
28.0	0.0996	0.1500	0.0356	0.0021		
29.0	0.2076	0.1700	0.0266	0.0021		
29.2	0.0021					
29.3						
30.0	0.2733	0.2200	0.0377	0.0021		
30.2	0.0233	0.0100	0.0094			
30.3						
31.0	0.0763	0.0300	0.0327			
31.2	0.0996	0.1100	0.0074			
32.0	0.0169	0.0300	0.0093			
32.2	0.1271	0.1500	0.0162			
33.0	0.0042					
33.1	0.0021	0.0400	0.0268			
33.2	0.0339					
34.0	0.0021					
35.2		0.0100				
39.0	0.0005					
43.2				0.0005		

Table A9.2: Mexican comparison chart. *continued*

Allele	D3S1358			vWA		
	Promega	Parish	STDEV	Promega	Parish	STDEV
10.3						
11.0				0.0021		
13.0	0.0064					
13.2						
13.3						
13.4						
14.0	0.0784	0.1200	0.0294	0.0805	0.1200	0.0279
14.2						
14.3						
15.0	0.3220	0.3500	0.0198	0.1441	0.0700	0.0524
15.2						
15.3						
15.4						
16.0	0.2797	0.1900	0.0634	0.2839	0.3500	0.0467
16.1						
16.2						
16.3						
17.0	0.1843	0.2400	0.0394	0.2458	0.2700	0.0171
17.1						
17.2						
17.3						
18.0	0.1229	0.0900	0.0233	0.1801	0.1600	0.0142
18.1						
18.2						
18.3						
19.0	0.0042	0.0100	0.0041	0.0508	0.0300	0.0147
19.1						
19.2						
19.3						
19.4						
20.0	0.0021			0.0106		
20.1						
20.2						
20.3						
21.0				0.0021		
21.2						
21.3						
22.0						
22.2						
22.3						
23.0						
23.2						

Table A9.2: Mexican comparison chart. *continued*

Allele	D5S818			D7S820			Penta_D		
	Promega	Parish	STDEV	Promega	Parish	STDEV	Promega	Parish	STDEV
2.2							0.0169		
3.2							0.0021		
4.0									
4.2									
5.0							0.0064	0.0100	0.0025
6.0							0.0021		
6.3									
7.0	0.0339	0.0400	0.0043	0.0106	0.0100	0.0004	0.0021	0.0100	0.0056
8.0	0.0085			0.1208	0.1100	0.0076	0.0191	0.0100	0.0064
8.1									
9.0	0.0530	0.0200	0.0233	0.0911	0.0500	0.0291	0.2415	0.1800	0.0435
9.1									
9.3									
10.0	0.0572	0.0800	0.0161	0.3072	0.3400	0.0232	0.1568	0.2300	0.0518
10.1									
10.2									
10.3				0.0021	0.0100	0.0056			
11.0	0.3898	0.5000	0.0779	0.2775	0.2300	0.0336	0.1568	0.1200	0.0260
11.2									
11.3									
12.0	0.3390	0.1800	0.1124	0.1547	0.1900	0.0250	0.1631	0.1200	0.0305
12.2									
12.3									
13.0	0.1081	0.1700	0.0438	0.0360	0.0600	0.0170	0.1441	0.2400	0.0678
13.2									
13.3									
13.4									
14.0	0.0085	0.0100	0.0011				0.0720	0.0800	0.0057
14.2									
14.3									
15.0	0.0021						0.0106		
15.2									
15.3									
15.4									
16.0							0.0042		
16.1									
16.2									
16.3									
17.0							0.0021		
17.1									
17.2									
17.3									

Table A9.2: Mexican comparison chart. *continued*

Allele	TH01			TPOX		
	Promega	Parish	STDEV	Promega	Parish	STDEV
2.2						
3.2						
4.0						
4.2						
5.0						
6.0	0.2394	0.2200	0.0137	0.0085		
6.3						
7.0	0.2966	0.3400	0.0307	0.0064		
8.0	0.0911	0.0500	0.0291	0.4852	0.4800	0.0037
8.1						
9.0	0.1462	0.1300	0.0115	0.0932	0.1000	0.0048
9.1						
9.3	0.2182	0.2300	0.0083		0.0100	
10.0	0.0085	0.0300	0.0152	0.0487	0.0400	0.0062
10.1						
10.2						
10.3						
11.0				0.2542	0.2700	0.0112
11.2						
11.3						
12.0				0.1038	0.1000	0.0027
12.2						
12.3						
13.0						
13.2						
13.3						
13.4						
14.0						
14.2						
14.3						
15.0						
15.2						
15.3						
15.4						
16.0						
16.1						
16.2						
16.3						
17.0						
17.1						
17.2						
17.3						